Aus der Klinik für Dermatologie, Venerologie und Allergologie
Universitätsklinikum Mannheim der Medizinischen Fakultät Mannheim
der Ruprecht-Karls-Universität Heidelberg
(Direktor: Prof. Dr. med. S. Goerdt)

# *Molecular and Functional Characterization of P2Y12 Expression in Tumor-associated Macrophages*

**INAUGURALDISSERTATION**

zur Erlangung der Doktorwürde der
Naturwissenschaftlich-Mathematischen Gesamtfakultät
der Ruprecht-Karls-Universität Heidelberg

Vorgelegt von
**Loreen Kloss**

# DISSERTATION

submitted to the
Combined Faculty of Natural Sciences and Mathematics
of the Ruperto Carola University Heidelberg, Germany
for the degree of
Doctor of Natural Sciences

Presented by

Loreen Kloss, M.Sc.
Born in: Herrenberg, Germany

Oral examination: June 17th, 2019

# *Molecular and Functional Characterization of P2Y12 Expression in Tumor-associated Macrophages*

Referees:

Prof. Dr. rer. nat. Viktor Umansky

PD Dr. med. Astrid Schmieder

# Table of Contents

# Abstract

Macrophages are phagocytic cells of the innate immune system that exert important functions for immunological and homeostatic processes. They have a high plasticity and can quickly adapt to different environments. While Th1 cytokines induce a pro-inflammatory macrophage phenotype (M1), Th2 cytokines promote an anti-inflammatory one (M2). At tumor initiation a M1 phenotype is predominant, which then switches to a M2-like phenotype during tumor progression. These tumor-associated macrophages (TAM) promote tumor growth and metastasis by the secretion of growth factors, matrix metalloproteinases and immunosuppressive mediators such as arginase-1, IL-10 and TGF-ß. In many tumor entities including melanoma a high TAM infiltration correlates with a poor patient outcome. Thus, macrophages provide a promising therapeutic target for adjuvant tumor therapies. In the past our group identified several novel markers for TAM such as STABILIN-1 and LYVE-1. These markers can be induced *in vitro* by the treatment of peripheral blood monocytes (pBM) with M-CSF/dexamethasone/IL-4 (MDI). Microarray analysis of these *in vitro* generated M2-like macrophages identified the purinergic, G protein coupled receptor *P2Y12* as the highest up-regulated gene. So far, P2Y12 has been known to be expressed on microglia and platelets and is targeted therapeutically with clopidogrel, ticagrelor and prasugrel to treat thrombotic disorders. Since the expression of P2Y12 in TAM has not been described yet, the aim of this study was to characterize P2Y12 expression and its function in M2-like macrophages *in vitro* as well as in TAM *in vivo*. Since all commercially available antibodies failed to detect P2Y12 in transgenic P2Y12$^+$ U937 cells, we generated a peptide antibody against human P2Y12 and confirmed the expression of P2Y12 receptor in MDI-treated pBM as well as in CD68$^+$ and CD63$^+$ TAM of melanoma *in situ*. Like in the human system, *P2y12* can also be induced by the treatment of murine bone marrow-derived macrophages (BMDM) with MDI. We detected *P2y12* expression in CD11b$^+$ cells isolated from spleen, peritoneal fluid and subcutaneously transplanted B16F10 tumors of tumor-bearing mice. P2Y12 expression in murine TAM was confirmed by immunohistochemical staining of B16F10 tumors. Treatment of murine and human transgenic P2Y12$^+$ macrophage-like cell lines with the P2Y12 receptor agonist ADP increased the expression of several cytokines and chemokines (in the murine system CXCL2 and TNF-α and in the human system CXCL2, CXCL7 and IL-8), indicating an immunomodulatory role for the receptor. Analyzing signaling pathways underlying the induction of these cytokines, we detected ERK as well as Akt phosphorylation in ADP-treated P2Y12$^+$ U937 cells. Inhibition of these signaling pathways significantly impaired CXCL2, CXCL7 and IL-8 secretion. Since ADP acts as a chemoattractant for microglia cells, the migratory potential of P2Y12$^+$ macrophages was evaluated. We could show that ADP promotes the migration of human pBM$_{(MDI)}$ as well as murine P2Y12$^+$ Raw 264.7 cells in a transwell chamber. Pre-treatment with the P2Y12 antagonist PSB0739 abrogated the ADP-induced chemotaxis of P2Y12$^+$ cells. Since it is known that dying cells release nucleotides that act as find-me signals for phagocytic cells, we set up a co-culture experiment with P2Y12$^+$ Raw 264.7 cells and B16F1 melanoma cells, which we pre-treated with puromycin to induce cell death. Dying tumor cells promoted the migration of P2Y12$^+$ macrophages. Administration of the ATP/ADP cleaving enzyme apyrase to the dying tumor cells or treatment of P2Y12$^+$ Raw 264.7 cells with PSB0739 abrogated the

cell-death induced migration of P2Y12$^{+}$ macrophages. Taken together, our results indicate that P2Y12 is an important immunomodulatory macrophage receptor, which triggers migration of these cells towards ADP-rich tumor areas and is able to modulate the inflammatory environment upon ADP activation.

# Zusammenfassung

Makrophagen sind Zellen des angeborenen Immunsystems, die wichtige Funktionen für immunologische und homöostatische Prozesse ausüben. Die Phagozyten sind plastisch und können sich schnell an unterschiedliche Umgebungen anpassen. Während Th1 Zytokine einen pro-inflammatorischen Phänotyp induzieren (M1 Makrophagen), fördern Th2 Zytokine einen anti-inflammatorischen Phänotyp (M2 Makrophagen). Zu Beginn der Tumorentstehung dominiert ein M1 Phänotyp, welcher sich während des Tumorwachstums hin zu einem M2 Phänotyp entwickelt. Diese Tumor-assoziierten Makrophagen (TAM) fördern das Tumorwachstum und die Metastasierung indem sie Wachstumsfaktoren, Matrix-Metalloproteinasen und immunsuppressive Mediatoren wie beispielsweise Arginase-1, Interleukin-10 und TGF-ß sezernieren. In vielen Tumorentitäten, einschließlich dem Melanom, korreliert eine hohe TAM Infiltration mit einem schlechten Patienten Outcome. Daher eignen sich Makrophagen als vielversprechendes therapeutisches Target für adjuvante Tumortherapien. In der Vergangenheit identifizierte unsere Gruppe mehrere neue TAM Marker wie z. B. STABILIN-1 und LYVE-1. Diese Marker können durch Stimulation von humanen peripheren Blutmonozyten (pBMZ) mit M-CSF/Dexamethason/IL-4 (MDI) induziert werden. Eine Genexpressions-Analyse dieser *in vitro* generierten M2-ähnlichen Makrophagen identifizierte den purinergen, G-Protein gekoppelten Rezeptor *P2Y12* als das stärkste hochregulierte Gen. Bislang ist bekannt, dass P2Y12 von Mikrogliazellen und Thrombozyten exprimiert wird und das therapeutische Target für Medikamente wie Clopidogrel, Prasugrel und Ticagrelor ist, die zur Behandlung thrombotischer Erkrankungen verschrieben werden. Da die Expression von P2Y12 in TAM bislang nicht beschrieben wurde, ist das Ziel dieser Studie die Expression des Rezeptors sowie seine Funktion in M2-ähnlichen Makrophagen *in vitro* sowie in TAM *in vivo* umfassend zu charakterisieren. Da kein kommerziell erhältlicher Antikörper P2Y12 in transgenen $P2Y12^+$ U937 Zellen spezifisch nachweisen konnte, stellten wir einen Peptid-Antikörper gegen humanes P2Y12 her und bestätigten die Expression des Rezeptors in MDI-behandelten pBMZ sowie in $CD68^+$ und $CD163^+$ TAM des Melanoms *in situ*. Ähnlich wie im Menschen kann *P2y12* auch in der Maus durch die Stimulation von Knochenmarksmakrophagen mit MDI induziert werden. Wir detektierten *P2y12* auch in $CD11b^+$ myeloiden Zellen, welche aus der Milz, der Peritonealflüssigkeit sowie aus subkutan transplantierten B16F10 Tumoren von Tumor-tragenden Mäusen gewonnen wurden. Die P2Y12 Expression in murinen TAM wurde mit Hilfe von immunhistochemischen Färbungen von B16F10 Melanomen bestätigt. Eine Behandlung von murinen und humanen transgenen $P2Y12^+$ Zelllinien mit dem Rezeptor-Agonist ADP erhöhte die Expression einiger Zytokine und Chemokine (in der Maus CXCL2 und TNF-α und im Mensch CXCL2, CXCL7 und IL-8), was auf eine immunmodulatorische Rolle des Rezeptors hindeutet. Wir analysierten Signalwege, die dieser Zytokininduktion zugrunde liegen könnten und fanden eine verstärkte ERK und Akt Phosphorylierung in ADP-behandelten $P2Y12^+$ U937 Zellen. Eine Inhibierung dieser Signalwege verminderte die ADP-induzierte Sekretion von CXCL2, CXCL7 sowie IL-8. Da ADP als chemotaktisch wirksamer Botenstoff für Mikrogliazellen bekannt ist, untersuchten wir das migratorische Potential von $P2Y12^+$ Makrophagen. Wir konnten zeigen, dass ADP sowohl die Migration von humanen MDI-stimulierten pBMZ als auch von $P2Y12^+$ Raw 264.7 Zellen in einer

Transwell-Kammer fördert. Eine Vorbehandlung mit dem P2Y12 Antagonist PSB0739 wirkte hemmend auf die ADP-induzierte Chemotaxis der $P2Y12^+$ Zellen. Da bekannt ist, dass sterbende Zellen Nukleotide freisetzen, die als Aufspühr-Signale für Phagozyten fungieren, etablierten wir ein Co-Kultur Experiment mit $P2Y12^+$ Raw 264.7 Zellen und B16F1 Melanomzellen, welche wir mit Puromycin behandelten, um den Zelltod dieser Zellen zu induzieren. Die sterbenden Tumorzellen verstärkten die Migration der $P2Y12^+$ Makrophagen. Zugabe des ATP/ADP hydrolysierenden Enzyms Apyrase zu den sterbenden Tumorzellen oder Behandlung der $P2Y12^+$ Raw 264.7 Zellen mit PSB0739 verhinderten die Zelltod-induzierte Migration der $P2Y12^+$ Makrophagen. Zusammengefasst deuten unsere Ergebnisse darauf hin, dass P2Y12 ein wichtiger immunmodulatorischer Rezeptor ist, welcher die Migration von Makrophagen in Richtung ADP-reicher Tumorbereiche fördern und nach Aktivierung durch ADP die inflammatorische Umgebung modulieren kann.

# 1. Introduction

## 1.1 Macrophages

### 1.1.1 Origin and maintenance of macrophages

Macrophages are immune cells of the mononuclear phagocyte system comprising monocytes, macrophages and dendritic cells (DCs) [1]. They are found in all tissues where they exert tissue specific functions [2]. Macrophages differentiate from circulating monocytes. These cells derive from myeloid progenitor cells in the bone marrow which give rise to many other cell types such as granulocytes, DCs and mast cells (Figure 1) [3]. In mice, one distinguishes two major monocyte populations termed as inflammatory ($Gr^+/Ly6C^{high}$) and resident ($Gr1^-/Ly6C^{low}$) monocytes.
$Gr^+/Ly6C^{high}$ monocytes patrol between the blood and the bone marrow and give rise to $Gr1^-$ monocytes by loosing Ly6C expression [4, 5]. However, studies showed that the $Gr1^-$ subset is still present when $Gr1^+$ monocytes are depleted indicating that they develop independently of inflammatory monocytes [6-8]. Since $Gr1^+$ monocytes can differentiate to macrophages and DCs during infection they were termed as inflammatory. They are the first monocytes that enter the blood stream from the bone marrow and rapidly exit to give rise to distinct macrophage populations that can either activate or inhibit immune response [9, 10]. Long-lived tissue-specific macrophages such as intestinal macrophages can be replenished by patrolling $Gr1^+$ monocytes [11, 12]. Since $Gr1^-/Ly6C^{low}$ monocytes have a longer half-life and exist in the steady state as well as in inflamed tissue they were termed as resident monocytes [13]. They lack CCR2 and L-Selectin expression but have higher CX3CR1 and LFA-1 expression [14]. They seem to be involved in tissue repair and angiogenesis as they deposit collagens and express vascular endothelial growth factor (VEGF) [15]. In mice, both monocyte populations are equally distributed in the blood [14]. Since monocytes are a very heterogeneous population, it is still a matter of debate whether distinct tissue macrophages derive from specific monocyte populations in the blood. However, many tissue-specific macrophages do not origin from the bone marrow and thus are not monocyte-derived macrophages (MDM) [3]. Microglia, macrophages of the central nervous system (CNS), or Langerhans cells, DCs of the skin, for instance, do not originate from circulating monocytes but derive from yolk sac or fetal liver cells (Figure 1) [16-20]. Although some macrophage populations, e.g. of the kidney and lung, can be replenished by $Gr1^+$ monocytes, some of them including microglia are replaced by tissue-resident colony forming cells [21].

In humans one distinguishes three monocyte populations: $CD14^{++}CD16^-$ classical monocytes, $CD14^{++}$ $CD16^+$ intermediate monocytes and $CD14^+CD16^{++}$ non-classical monocytes [22]. Classical monocytes are characterized by high CCR2 and CD62L expression and are mainly involved in phagocytosis and the killing of pathogens by increased production of reactive oxygen species (ROS). They produce high amounts of IL-10 in response to LPS and are involved in angiogenesis and wound healing [14, 23]. $CD14^{++}CD16^+$ intermediate monocytes are also

termed inflammatory monocytes since their number is increased in inflammatory diseases. Furthermore, they produce higher amounts of IL-1ß and TNF-α in response to LPS. Gene expression analysis indicates that they are involved in antigen presentation and T cell activation [23]. $CD14^{+}CD16^{++}$ non-classical monocytes, also known as patrolling monocytes, are characterized by low CCR2 expression, low peroxidase activity, and high expression of CX3CR1 [24]. Like intermediate monocytes, they release IL-1ß and TNF-α in response to danger-associated molecular patterns (DAMPs) and pathogen-associated molecular patterns (PAMPs). They might be involved in autoimmune diseases including rheumatoid arthritis [25].

Since murine and human monocytes/macrophages differ in their phenotypes it remains challenging to transfer the knowledge obtained from mice studies to the human system.

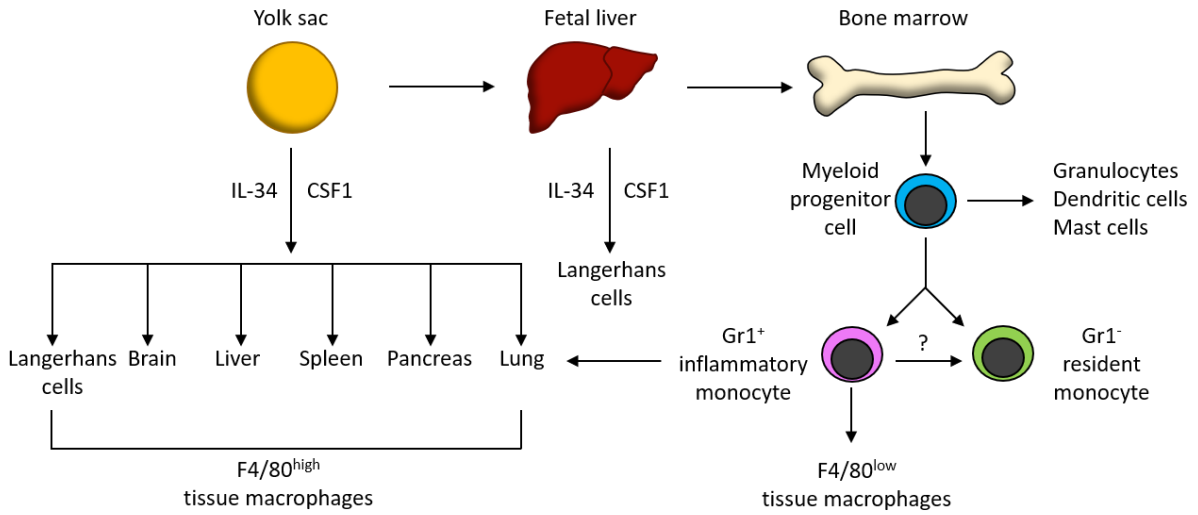


**Figure 1. Origin and differentiation of murine macrophages.** Macrophages originate from three different tissues: yolk sac, fetal liver and bone marrow. Monocyte-derived macrophages originate from the bone marrow and derive from myeloid progenitor cells which give rise to granulocytes, dendritic cells, mast cells and monocytes. The latter can be divided in $Gr1^{-}$ ($Ly6C^{-}$) resident monocytes and $Gr1^{+}$ ($Ly6C^{+}$) inflammatory monocytes which differentiate to $F4/80^{low}$ tissue macrophages. Many tissue macrophages including microglia originate from the yolk sac, while Langerhans cells of the skin derive from yolk sac and fetal liver cells. Figure adapted from Wynn et al. [3].

### 1.1.2 General and tissue-specific functions of macrophages

For a long time, the focus was set on the function of macrophages as immune effector cells that mediate host defense. As phagocytic cells of the innate immune system they are involved in the killing of bacteria and viruses through the production of ROS a process which is called respiratory burst [26]. Macrophages recognize PAMPs with special pattern recognition receptors (PRR) such as Toll-like receptors (TLRs) [27]. Being antigen presenting cells (APCs), they play a role in activating the adaptive immune response [28]. After ingestion of a pathogen, antigens are processed and presented on the surface of macrophages via MHC class II molecules to T cells which recognize the antigen with their T cell receptor (TCR). Besides

this interaction a secondary co-stimulatory signal is indispensable to provide an adequate immune response. Macrophages express several co-stimulatory molecules (e.g. B7.1/CD80 and B7.2/CD86) that are recognized by specific surface receptors (e.g. CD28) on T cells [29]. Through the secretion of interferon γ (IFN-γ), T cells promote the killing of engulfed bacteria and viruses by macrophages which in turn promote the proliferation of the T cells by secretion of the pro-inflammatory cytokine interleukin-12 (IL-12) [30]. There are also co-inhibitory molecules such as PD-L1 and PD-L2 that inhibit activation of T cells [31].

Besides their immunological function, macrophages exert important functions for homeostatic processes such as tissue remodeling, clearance of erythrocytes, apoptotic cells and cellular debris [3, 32]. This homeostatic clearance is mediated by scavenger receptors, phosphatidyl receptor, thrombospondin receptor, integrins and complement receptors [33, 34]. Furthermore, macrophages are the primary sensors for endogenous danger signals (e.g. heat shock proteins, nuclear proteins, or nucleotides) released by necrotic cells [35]. PRRs including TLRs and IL-1ß receptors recognize these molecules and mediate phagocytic clearance. Importantly, these mechanisms do not depend on the adaptive immune response or immune cell signaling [36]. Since maintenance of tissue integrity and homeostasis is important in almost all organs, macrophages are present in almost all tissues where they exert tissue-specific functions (Table 1).

Due to differential expression of transcription factors, tissue specific macrophages are heterogenous in their phenotypes as well as in their function and turnover [3]. In the bone, macrophages known as osteoclasts are crucial for bone resorption thereby regulating blood calcium levels [37]. Although bone formation is not altered in *Csf1*-null mice, hematopoiesis is impaired due to defect formation of the bone cavities [38]. In the brain, microglia controls brain development and maintenance of the brain structure. Neurons express CSF1 and IL-34 which are the major cytokines for differentiation and viability of microglia [39]. Microglia, in turn, regulate proliferation and survival of neurons after nerve injury. In *Csf1r*-null mice brain structure is disrupted resulting in defect neuronal processing [40]. In the lung, alveolar macrophages are responsible for toxin and pathogen removal [41]. In the spleen, three distinct macrophage populations can be distinguished based on their location within the tissue. Red pulp macrophages are important for the removal of erythrocytes and the recycling of iron. Both types of macrophages of the marginal zone, marginal zone macrophages (MZM) and marginal metallophilic macrophages (MMM) mediate uptake of apoptotic cells and pathogens. However, whereas MMM stimulate the adaptive immune response by type I IFN production, MZM have an immunosuppressive phenotype, for instance by expressing indolamine-2,3-dioxygenase (IDO) and IL-33 [42]. In adipose tissue, liver and pancreas, macrophages are important for metabolic homeostasis. They regulate lipolysis, insulin sensitivity and storage of nutrients [3]. In the kidney, mammary gland and pancreas, macrophages are important for tissue patterning and branching morphogenesis. Furthermore, they control stem cell function thereby regulating the growth of the ductal structure [38, 43]. In other organs such as the liver and intestine, modulation of stem cell function by macrophages is important for the regeneration after tissue damage [44, 45].

**Table 1. Macrophage populations and functions in different tissues**

| TISSUE | MACROPHAGE SUBSET | TISSUE-SPECIFIC FUNCTION |
|---|---|---|
| Bone | Osteoclast | Bone resorption<br>Hematopoiesis |
| CNS | Microglia | Neuronal patterning |
| Lung | Alveolar macrophage | Toxin and pathogen removal |
| Liver | Kupffer cell | Lipid metabolism |
| Spleen | Red pulp macrophage | Clearance of erythrocytes<br>Iron metabolism |
| Spleen | Marginal zone macrophage | Immunosuppression<br>Removal of apoptotic cells and pathogens |
| Spleen | Metallophilic macrophage | Activation of adaptive immune response<br>Uptake of pathogens and apoptotic cells |
| Adipose tissue | Adipose tissue macrophage | Adipogenesis<br>Insulin sensitivity |

Besides their morphological and functional heterogeneity, macrophages also differ in their transcriptomic and proteomic profile [3]. Although the heterogeneity of macrophage populations is immense, efforts have been made to classify macrophages according to their different phenotypes.

### 1.1.3 Macrophage polarization and activation

Macrophages are highly plastic cells, that can quickly adapt to different environments by changing their phenotypes. Many attempts have been made to classify macrophages according to their polarization. Mills and colleagues established a model that mirrors the Th1/Th2 dichotomy of T lymphocytes by dividing macrophages in pro-inflammatory, classically activated macrophages (M1) and anti-inflammatory, alternatively activated macrophages (M2) (Figure 2) [46]. M1 macrophages can be induced by Th1 cytokines such as IFN-γ, and by TNF-α or LPS. IFN-γ is mainly secreted by Th1 cells, $CD8^+$ T cells and NK cells whereas LPS comes from Gram-negative bacteria. TNF-α is produced by APC that are activated by a TLR ligand [32]. M1 macrophages secrete pro-inflammatory cytokines such as IL-12, IL-23 and TNF-α and express high levels of MHC class II molecules and the co-stimulatory molecules CD80 and CD68. Besides their increased endocytic functions, M1 macrophages are involved in the killing of intracellular pathogens and in stimulating an immune response. In the murine system, M1 macrophages also express inducible nitric oxide synthase (iNOS) which converts L-arginine to nitric oxide (NO) [47]. Due to the production of ROS they also exert tumoricidal functions. Martinez et al. envisaged a subclassification of M1 macrophages into classical activated macrophages (M1a) that are activated by IFN-γ and innate activated macrophages (M1b) that

are activated by PAMPS such as LPS. Although both populations produce high levels of the pro-inflammatory cytokines IL-1ß, IL-6 and TNF-α, innate activated macrophages don't show increased phagocytic activity and no increased IL-12 production [48]. In contrast to the pro-inflammatory M1 macrophages, M2 macrophages can be induced by Th2 cytokines such as IL-4, IL-13 as well as by IL-10 and glucocorticoids [49, 50]. M2 macrophages are involved in the killing of parasites and fungi, and in homeostatic processes such as matrix remodeling and tissue turnover. In addition, M2 macrophages support angiogenesis and wound healing. Through the secretion of anti-inflammatory mediators such as IL-10 and transforming growth factor-ß (TGF-ß) these macrophages play an important role in the counter-regulation of pro-inflammatory conditions. Typical M2 markers are scavenger receptors such as mannose receptor C-type 1 (MRC1/CD206), CD163 and STABILIN-1 [47]. Furthermore, M2 macrophages express high levels of arginase-1 thereby promoting immune suppression by impairing T cell response [51]. However, this M1/M2 macrophage classification model, which is based on *in vitro* studies, is an oversimplification of the *in vivo* situation where mixed and overlapping phenotypes co-exist.
Martinez and colleagues further subdivided the M2 population into M2a, M2b, M2c. In this model, M2a macrophages are induced by the typical Th2 cytokines IL-4 and IL-13, M2b by immune complexes plus LPS or IL-1ß and M2c by glucocorticoids, IL-10 and TGF-ß. In contrast to M2a cells, M2b cells express higher levels of the anti-inflammatory cytokine IL-10 but also secrete TNF-α, IL-1ß and IL-6 showing that these cells have no anti-inflammatory phenotype *per se*. M2c cells are a heterogenous population that is characterized by the down-regulation of pro-inflammatory cytokines, MHC class II as well as co-stimulatory molecules and an up-regulation of several scavenger receptors [48].
Mosser and colleagues classified macrophages according to their homeostatic activities: host defense (classically activated macrophages), wound healing (wound healing macrophages) and immune regulation (regulatory macrophages). They suggest that these macrophages shift their activation states thereby establishing macrophages with intermediate phenotypes. Tumor-associated macrophages, for instance, display features of both, wound healing macrophages and regulatory macrophages [32].

Since all these attempts to classify macrophages fail to display the real *in vivo* situation it is crucial to analyze macrophage subpopulations in different tissues in health and diseases. This should help to elucidate how the local microenvironment polarizes these macrophages and modulates their specific functions and how these macrophages contribute to the pathological condition and to disease progression.

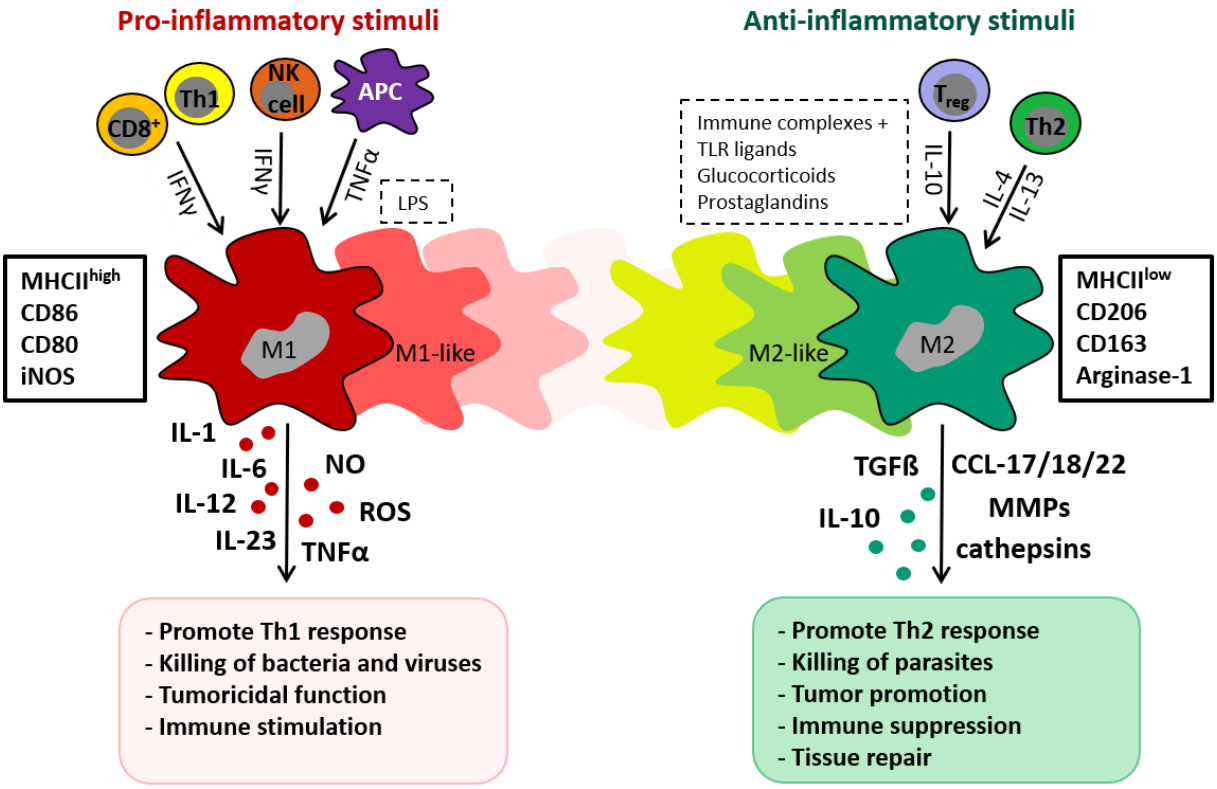


**Figure 2. M1/M2 model of macrophage classification.** Pro-inflammatory stimuli such as IFN-γ and TNF-α induce a M1 macrophage phenotype whereas anti-inflammatory stimuli such as IL-10, IL-4 and IL-13 induce a M2 phenotype. M1 macrophages express inducible nitric oxide synthase (iNOS) and the co-stimulatory molecules CD86 and CD80 and exert immune stimulatory functions by secreting pro-inflammatory cytokines including IL-1, IL-6 and IL-12. M2 macrophages express arginase-1 and the scavenger receptors CD206 and CD163 and mediate immunosuppression by the secretion of IL-10 and TGF-ß.

### 1.1.4 Macrophages in diseases

Macrophages play a crucial role in chronic inflammatory diseases such as atherosclerosis, obesity and cancer but also in allergies and wound healing [3, 52]. In many cases the balance between M1 and M2 macrophages is disrupted or shifted towards the one or other phenotype.

One example for a disease that is associated with a M2 macrophage phenotype is asthma [53]. In this allergic disorder Th2 lymphocytes, macrophages, mast cells and eosinophils are recruited to the lungs. Thus, in the local microenvironment high levels of the Th2-associated cytokines IL-4, IL-13 and IL-33 polarize macrophages to a M2-like phenotype [54]. These airway macrophages produce cytokines and chemokines that recruit more Th2 cells, basophils and eosinophils. This positive feedback loop worsens the symptoms of the IgE-mediated, allergic disease [55, 56].

Contrary, in autoimmune diseases such as inflammatory bowel disease, multiple sclerosis and rheumatoid arthritis most macrophages exhibit a proinflammatory phenotype by producing IL-12, IL-23 and TNF-α which are the key drivers of chronic inflammation [57]. M1-associated

cytokines (IL-1, IL-6 and IL-23) are also associated with the recruitment and expansion of Th17 cells. These cells secrete high levels of the cytokine IL-17 which mediates chronic inflammatory diseases such as psoriasis [58, 59]. Thus, targeting pro-inflammatory mediators or reprogramming of M1-polarized macrophages to an anti-inflammatory phenotype is beneficial for patients suffering from such disorders.

In line with this, M2-like macrophages can exert several protective roles, for example by counter-regulation of pro-inflammatory situations or by impairing T cell functions. Axon demyelination in the CNS is inhibited by IL-10 and TGF-ß producing macrophages since these immunosuppressive cytokines inhibit T cell activation or even increase apoptosis of effector T cells [60]. M1 macrophages can also be beneficial for the treatment of several diseases. ROS production by M1 macrophages protected mice from arthritis by impairing T cell function while M1-associated, pro-inflammatory cytokines promoted the killing of pathogenic commensal bacteria in Crohn's disease [61, 62].

The interplay between pro-and anti-inflammatory macrophages is very important in many pathological conditions such as wound healing. This multicellular process normally evolves in three steps: inflammation, tissue formation and maturation. Neutrophils are the first immune cells that are recruited to the injured tissue followed by the recruitment of monocyte-derived macrophages. By producing pro-inflammatory cytokines such as TNF-α, IL-6 as well as ROS these cells create an inflammatory environment [63, 64]. The induction of apoptosis in neutrophils and increased phagocytosis of these death cells by macrophages leads to an anti-inflammatory macrophage phenotype important for the resolution of inflammation and the transition to the tissue formation phase. In the final step of wound healing, macrophages exhibit a pro-angiogenic and pro-fibrotic phenotype characterized by the production of VEGF and TGF-ß [65, 66]. In chronic non-healing wounds this switch fails, and macrophages retain the pro-inflammatory phenotype [67].

Obesity is also associated with chronic inflammation. In obese humans, 40–50 % of all stromal cells of the white adipose tissue are macrophages compared to only about 10 % in the fat tissue of lean humans. Adipose tissue macrophages of non-obese individuals produce IL-10, whereas adipose tissue macrophages of obese humans produce high amounts of the pro-inflammatory cytokines IL-6, TNF-α, IL-1ß and CCL2 [68]. In lean adipose tissue there are high levels of the Th2 cytokine IL-4, which is a main inductor of M2 macrophages [69]. This switch from anti-inflammatory macrophages to classically activated macrophages is induced by stimuli such as TNF-α and free fatty acids that induce pro-inflammatory signaling pathways including NF-κB and JNK associated with insulin resistance and type 2 diabetes [70, 71].

A similar phenotypic switch in macrophage polarization is also observed during atherosclerosis which is a prerequisite for the development of cardiovascular diseases. During the development of atherosclerosis monocytes are recruited to the permeable arterial wall and differentiate into macrophages. Due to the uptake of lipoproteins macrophages become foam cells which express various inflammatory mediators such as IL-1, IL-6, TNF-α and CCL2 [72-74]. Free cholesterol triggers activation of inflammatory signaling pathways resulting in apoptotic cell death [75]. Impaired clearance of apoptotic macrophages by surrounding phagocytes is an important factor for the rupture of atherosclerotic plaques [52].

Not only obesity and atherosclerosis but also the development of cancer is associated with chronic inflammatory conditions. Tumors are complex organ-like structures that consist of

malignant cells, stromal cells and hematopoietic cells including macrophages [47]. Most neoplastic disease are caused by chronic infection, obesity, tobacco smoke, alcohol abuse or irradiation [76]. All these extrinsic factors are associated with chronic inflammation, which is one of the hallmarks of skin cancer described by Hanahan and Weinberg [77]. Furthermore, intrinsic factors like mutations of oncogenes such as *RET*, *RAS* or *MYC* result in the activation of signaling pathways inducing the expression of growth factors and pro-inflammatory mediators. Thus, it is not surprising that during tumor initiation macrophages display a pro-inflammatory phenotype [47]. The M1-associated cytokines TNF-α and IL-6 were shown to promote carcinogenesis [78, 79]. During tumor progression macrophages become tumor-educated and transit to a more M2-like phenotype. The underlying mechanisms of this M1 to M2 transition are poorly understood [47]. These tumor-associated macrophages (TAM) elicit various pro-tumoral functions as described in the following chapter.

## 1.2 Tumor-associated macrophages (TAM)

In many solid tumors TAM are the most abundant type of immune cells. Macrophages are recruited by the chemokines CCL2, CCL5, CXCL12 (SDF1) which are secreted by either the tumor cells themselves or by other inflammatory cells of the tumor microenvironment [80]. Although various studies show that mainly monocyte-derived macrophages contribute to the pool of TAM, the contribution of tissue-resident macrophages is still under investigation [52]. These TAM, which predominantly exhibit an anti-inflammatory M2-like phenotype, support tumor growth and progression through the secretion of growth factors, matrix metalloproteinases (MMPs), immunosuppressive mediators as well as pro-angiogenic molecules (Figure 3) [47]. In many tumor entities including melanoma or clear renal cell carcinoma the number of macrophages is a negative prognostic factor since it correlates inversely with patient outcome [81-83]. Thus, TAM provide an interesting target for adjuvant tumor therapies. Although a M2-like macrophage phenotype is predominant in most tumor entities, pro-inflammatory macrophages with tumoricidal functions are also present in the tumor microenvironment [84]. In some tumor entities such as colorectal and prostate cancer abundance of tumor infiltrated macrophages correlates with prolonged patient survival [85-87]. Thus, it is important to characterize macrophage subpopulations in different tumor entities and to identify markers that either function as prognostic markers or serve as potential therapeutic targets.

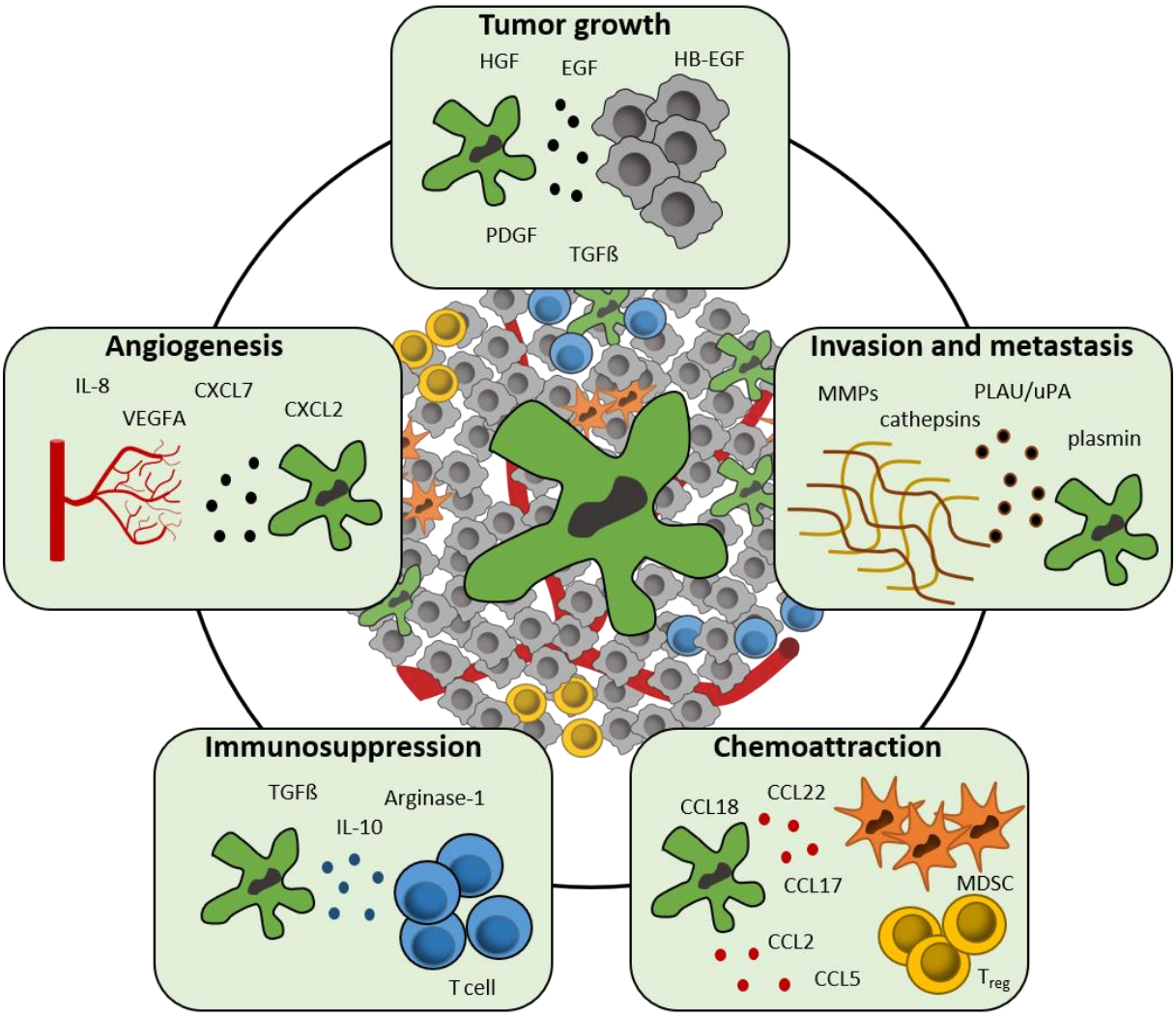


**Figure 3. TAM exert various pro-tumoral functions.** TAM support tumor growth and progression by production of various growth factors, matrix metalloproteinases (MMPs) and cathepsins. Through the secretion of chemokines (e.g. CCL17/18/22) TAM attract other immunosuppressive cells including myeloid-derived suppressor cells (MDSC) and regulatory T cells ($T_{regs}$) to the tumor microenvironment. TAM support immunosuppression and angiogenesis by the secretion of IL-10 and TGF-ß as well as pro-angiogenic mediators.

### 1.2.1 TAM promote tumor growth and metastasis

Various *in vitro* and *in vivo* studies showed that macrophages can stimulate the proliferation and invasion of tumor cells. TAM secrete several growth factors such as epidermal growth factor (EGF), hepatocyte growth factor (HGF), platelet-derived growth factor (PDGF) and TGF-ß that can directly promote primary tumor growth by activating signaling pathways responsible for cell cycle progression and survival [47, 88]. In turn, tumor cells secrete factors that attract and polarize macrophages, creating a positive paracrine loop. Breast cancer cells for instance can produce colony stimulating factor 1 (CSF1, also known as M-CSF) which is the major cytokine for macrophage recruitment, maintenance and survival. CSF1 induces EGF expression by macrophages, which promotes tumor cell invasion by stimulating proliferation

of endothelial cells (ECs) [89-92]. TAM also express various chemokines and chemokine receptors that are not only crucial for their recruitment to the tumor microenvironment but also mediate their tumor-promoting function [93]. Müller et al. showed that the CXCL12/CXCR4 axis promotes breast cancer invasion and metastasis *in vitro* and *in vivo* [94]. TAM-derived CCL18 was shown to promote breast cancer metastasis by mediating integrin rearrangements and supporting the binding of tumor cells to extracellular matrix (ECM) components [95]. CCL17 is associated with the progression of hepatocellular carcinoma and poor overall survival [96]. Under hypoxic conditions, the increased expression of hypoxia inducible factor 1α (HIF1α) and hypoxia inducible factor 1ß (HIF1ß) in macrophages results in transcription of growth factors such as VEGF, PDGF, HGF and EGF [97, 98]. Furthermore, MMPs such as MMP-2, MMP-7 and MMP-9 are induced resulting in increased tumor cell invasion and metastasis [99]. Not only MMPs but also other proteases such as cathepsins are frequently expressed by M2 macrophages [100]. These proteolytic enzymes do not only trigger matrix degradation, they also foster the release of membrane-bound growth factors such as heparin-binding EGF (HB-EGF), thereby supporting tumor cell invasion [101]. Recently, Gocheva et al. showed that TAM-derived cathepsin B and S are important for pancreatic tumor growth and invasiveness [102]. Another protease that is frequently expressed by TAM is urokinase/plasminogen activator (uPA/PLAU). uPA as well as its receptor uPAR (PLAUR) also play an important role in the metastatic process [103, 104]. uPA is a protease that converts plasminogen to plasmin. The latter cleaves various ECM components such as fibronectin and laminin and converts zymogens such as MMPs to their active form [101]. Various studies showed that uPA correlates with cancer progression and metastasis and therefore can be used as a prognostic biomarker [105-107]. Due to the molecular mechanisms described above, a high number of TAM correlates with increased tumor cell migration and invasion in many tumor entities [108].

### 1.2.2 TAM promote angiogenesis

Angiogenesis is a physiological process describing the formation of new blood vessels from already existing vasculature. It encompasses endothelial cell proliferation, migration, tube formation and vessel stabilization. In the context of tumor progression, angiogenesis is a prerequisite for the formation of metastases at distant organs. In numerous tissues including brain, breast and lung, TAM abundance is associated with increased angiogenesis and metastasis [109, 110]. The formation of blood vessels is a complex, multi-step process triggered by multiple pro-angiogenic stimuli. VEGF, one of the major mediators of angiogenesis, is strongly produced by M2-like TAM. Serum VEGF concentration correlates with increased metastasis and impaired patient survival in many tumor entities including gastric cancer and ovarian cancer [111, 112]. Various pro-inflammatory cytokines such as IL-6 can induce VEGF expression. CXCL12, one of the major monocyte-attracting chemokines, was shown to induce VEGF expression in macrophages via binding to CXCR4 [113]. Under hypoxic conditions HIF1α induces VEGF expression thereby enhancing the formation of new blood vessels [109]. Since VEGF is a main contributor to tumor angiogenesis, a lot of effort has been put in the development of therapeutic strategies targeting the VEGF pathway. In advanced

colorectal cancer, combination of chemotherapy with anti-VEGF antibodies (bevacizumab) is the first-line treatment strategy [114]. However, the clinical benefits are limited and often linked to resistance to therapy [115]. Importantly, an increased tumor growth upon anti-VEGF treatment was observed in several murine tumor models. Although the precise mechanisms are not fully elucidated, one possible explanation is the induction of *HIF1α* under hypoxic conditions, which is associated with increased invasiveness of tumor cells [116, 117]. Xu et al. reported increased serum concentration of CXCL12 after bevacizumab treatment associated with a rapid progression of rectal cancer indicating a link between CXCL12/CXCR4 axis and the VEGF pathway [118].

Not only CXCL12 but also other chemokines are important mediators of angiogenesis. CXC chemokines with an ELR-motif (CXCL1-3, CXCL5-CXCL8, CXCL12) promote angiogenesis whereas others (CXCL4, CXCL9-11) display angiostatic activities [119]. TAM secrete many of these pro-angiogenic chemokines while ECs express the corresponding receptors CXCR1, CXCR2 and CXCR4. Knockdown of the cytokine receptors CXCR1 and CXCR2 using shRNA inhibited EC proliferation, migration and other phenotypes crucial for angiogenesis [120]. CXCL7 was able to stimulate both tumor cell and EC proliferation and is a prognostic marker for patient survival in renal cell carcinoma. Administration of an anti-CXCL7 antibody significantly reduced tumor growth [121]. CXCL8 (IL-8), another pro-angiogenic cytokine secreted by TAM, is important for neovascularization and tumor progression [122].

Besides pro-angiogenic chemokines, macrophages also express Wnt molecules (e.g. Wnt5a) that can bind to Wnt receptors on ECs, regulating proliferation and migration of these cells *in vitro* [110]. TAM-derived Wnt5a can also act in an autocrine manner by stimulating the expression of other pro-angiogenic mediators such as IL-8 and IL-6 [123]. Furthermore, Wnt5a was shown to up-regulate expression of IL-6, IL-8 and CCL2 in ECs [124]. In TAM of breast and colon cancer, the expression of Wnt molecules is up-regulated during tumor progression [110].

Likewise, Notch signaling is important for vessel growth and maturation. Outtz et al. showed that Notch1 signaling in macrophages regulates retinal angiogenesis. Localization of macrophages as well as sprouting of ECs was altered in mice with *Notch1*-depleted myeloid cells indicating that communication between myeloid cells and ECs is mediated by Notch1 signaling [125].

Many TAM in the tumor microenvironment express the angiopoietin receptor TIE2. These so-called TIE2-expressing macrophages (TEM) are a pro-angiogenetic macrophage subpopulation. Angiopoietins are angiogenic molecules that are expressed by perivascular cells and bind to TIE1 and TIE2 tyrosine kinase receptors on ECs and macrophages [126, 127]. Ablation of TEM results in decreased angiogenesis, tumor growth and progression in several mouse models [128]. The abundance of TEM differs among tumor entities and TEM seem to accumulate after chemotherapy, radiotherapy and anti-angiogenic treatment to restore vessel integrity and rebuilt the vascular structure [129].

### 1.2.3 TAM support an immunosuppressive tumor microenvironment

M2-like TAM strongly express the anti-inflammatory cytokines IL-10 and TGF-ß [32, 130]. The latter triggers apoptosis of lymphocytes and favors the differentiation/induction of regulatory T cells ($T_{regs}$) [131, 132]. IL-10 was shown to inhibit the production of pro-inflammatory Th1 cytokines, antigen presentation by downregulation of MHC class II and co-stimulatory molecules and thus impairs anti-tumor immunity and facilitates tumor growth and progression [133]. Besides IL-10 and TGF-ß, TAM secrete various chemokines (CCL17, CCL18 and CCL22) that attract other immunosuppressive cells including $T_{regs}$ and myeloid-derived suppressor cells (MDSC) to the tumor microenvironment [47, 134, 135]. $T_{regs}$ inhibit effector T cells by expressing immunosuppressive molecules such as CD39 and CD73 [136-138]. The ectonucleotidases CD39 and CD73 cleave ATP to AMP and finally to the immunosuppressive molecule adenosine which inhibits effector T cell and NK cell function via binding to the adenosine receptors A2AR/A2BR [139]. Furthermore, adenosine was shown to increase the number as well as the immunosuppressive function of $T_{regs}$ and MDSC [140-142]. In the steady state, $T_{regs}$ prevent autoimmune diseases and are important for the tolerance of self-antigens [143, 144]. Besides macrophages, $T_{regs}$ are the main producers of the immunosuppressive cytokines TGF-ß and IL-10 [133]. Since IL-10 is an important stimulus for M2 polarization of macrophages, $T_{regs}$ orchestrate an immunosuppressive tumor microenvironment [145, 146]. In gastric cancer, the level of CCL17 and CCL22 positively correlates with $Foxp3^+$ $T_{regs}$ in the tumor microenvironment [147]. In line with this, CCL22 triggers infiltration of $T_{regs}$ and can be used as a negative prognostic marker for survival of breast cancer patients [148].
MDSC are immature myeloid cells that fail to terminally differentiate into mature granulocytes or monocytes/macrophages under pathological conditions such as chronic inflammation and cancer [149]. These immunosuppressive cells do not only inhibit cytotoxic T cell response but also affect the function of NK cells, macrophages and other myeloid cells. MDSCs express high levels of arginase-1 and produce ROS and NO thereby inhibiting T cell function. They also express PD-L1 which is an immunoinhibitory molecule for T cells [150, 151].
Like MDSC, TAM express high levels of arginase-1, which converts L-arginine to ornithine thereby withdrawing it for iNOS-mediated NO production. L-arginine is an amino acid that is crucial for intact T cell function enabling the expression of TCRζ chain [47, 149]. Thus, arginase-1 expression is linked to an impaired anti-tumor immune response. Rodriguez et al. showed that L-arginine depletion in a murine lung carcinoma model reduced CD3ζ chain expression and proliferation of antigen-specific T cells. Furthermore, inhibition of arginase-1 decreased tumor growth. High arginase-1 expression was found in tumor specimens of non-small cell lung cancer patients [152].

Since TAM are among the most abundant immune cells within the tumor stroma and exert various pro-tumorigenic functions as described above, several therapeutic strategies target these myeloid cells in different types of cancer.

### 1.2.4 TAM as therapeutic targets in cancer immunotherapy

In the last decade, immunotherapies such as cancer vaccines, adoptive T cell transfer and especially immune checkpoint inhibitors have been proven successful in enhancing anti-tumor immunity and thereby overall survival of patients in many immunogenic tumors such as renal cell carcinoma and melanoma. Therefore, inhibition and depletion of immunosuppressive cells is a promising therapeutic approach, especially when combined with other immunomodulatory strategies [153].

Three options exist to target TAM [154]:

1. Depletion of TAM
2. Reprogramming of TAM
3. Molecular targeting of TAM

*TAM depletion*
Since TAM mainly derive from monocytic progenitors of the bone marrow, deletion of TAM can be achieved by inhibiting their recruitment to the tumor microenvironment or by shorten their survival [153]. CSF1 (M-CSF) is one of the crucial cytokines for recruitment and differentiation of macrophages. Small molecule inhibitors or antibodies targeting CSF1R (e.g. PLX3397, PLX73086 and BLZ945) impaired macrophage survival and therefore decreased the number of infiltrating TAM in several studies [155-158]. Combination of anti-CSF1R with the immune checkpoint inhibitor anti-PD-1 decreased melanoma growth *in vivo* [159]. Furthermore, CSF1 blockade reversed resistance to chemotherapy in a breast cancer model [160]. Since monocyte-derived macrophages are mainly recruited via the CCL2-CCR2 axis, monoclonal antibodies against CCL2 and CCR2 are currently tested in clinical trials [161, 162].

*Reprogramming of TAM*
The second option is the reprogramming of TAM from an immunosuppressive, pro-tumoral phenotype to a pro-inflammatory, tumoricidal one.
The prostaglandin-synthetizing enzyme cyclooxygenase-2 (COX-2) is important for M1 to M2 transition and application of the COX-2 inhibitor celecoxib results in a decrease of M2 macrophages and increased IFN-γ levels in colon carcinoma [163].
The co-stimulatory molecule CD40 is expressed on APCs and binds to CD40 ligand (CD40L) on T cells providing the co-stimulatory signal for T cell response [164]. Agonistic CD40 antibodies induced the expression of IL-12 as well as MHC molecules, activated differentiation of T effector cells and inhibited tumor growth in several mouse models [165]. Combined treatment with anti-CSF1R and CD40 agonists repolarized macrophages prior to their deletion enabling an efficient T cell response [166, 167].
Since activation of transcription factors also determine whether macrophages display a M1 or M2 phenotype, targeting these signaling molecules is a promising tool for reprogramming macrophages [47]. Although increased NF-κB signaling favors the early steps of carcinogenesis aberrant NF-κB signaling via p50 homodimers results in reduced expression of pro-inflammatory mediators such as IL-12 and TNF-α in TAM during tumor progression. Thus, targeting p50 NF-κB induces a M1 macrophage phenotype and leads to tumor regression [168]. Depletion of phosphatidyl inositol 3 kinase γ (PI3Kγ) reduced the expression of TGF-ß,

IL-10 and arginase-1 in TAM of Lewis lung carcinoma (LLC) tumors and supported cytotoxic T cell response. Furthermore, the PI3Kγ inhibitor TG100-15 enhanced the response to anti-PD1 treatment and reduced growth of head and neck squamous carcinoma *in vivo* [169]. Administration of TLR7/8/9 agonists re-polarized macrophages to a pro-inflammatory, tumoricidal phenotype in several tumor models [170, 171]. Thus, imiquimod and other TLR agonists are either already established therapies or tested in clinical trials.

*Molecular targeting of TAM*
Molecular targeting of TAM molecules is another approach to inhibit their immunosuppressive phenotype. Two prominent examples are arginase-1 inhibitors or FcγR-blocking antibodies. Both strategies enhanced the efficacy of anti-PD1 treatment and suppressed tumor growth in different mouse models [172, 173].

All the described TAM-targeted therapies are especially successful in immunogenic tumors such as melanoma since these tumors are characterized by a high infiltration of immunosuppressive cells.

## 1.3 Malignant melanoma

### 1.3.1 Epidemiology, risk factors and pathophysiology

*Epidemiology*
Malignant melanoma is one of the most common tumors, but the incidence strongly varies between different countries. Without counting other types of skin cancer, melanoma was the 5$^{th}$ most common type of cancer in men and the 6$^{th}$ most common in women in the USA in 2017 [174]. Although melanoma is only the 4$^{th}$ most common type of skin cancer, it accounts for approximately 80 % of skin cancer related deaths [175]. One reason is the rapid development of metastases in lung, liver, brain and bone marrow which cause around 90 % of cancer-related deaths. The median age of diagnosis is 57 years indicating that melanoma mostly affects middle-aged individuals. Melanoma incidence is slightly higher in men but increased dramatically in both sexes during the last years [176].

*Risk factors*
Several environmental and genetic risk factors contribute to melanoma development. One of the major risk factors is ultraviolet (UV) light radiation. More than 80 % of melanoma cases can be linked to UV light exposure [177]. Interestingly, the patterns of sun light exposure determine the risk to develop melanoma. Studies showed that intense, intermitted exposure to UV light is a greater risk factor than chronic sun exposure [178, 179]. In line with this, the number of sunburns in childhood and adolescence positively correlates with melanoma incidence [180, 181]. UV radiation causes gene mutations, impairs cutaneous immunity and induces the production of ROS that further damage melanocytes and other cells [175]. One intrinsic mechanism that protects the skin against UV radiation is melanin production in melanocytes. α-melanocyte stimulating hormone (αMSH) and the melanocortin receptor 1

(MC1R) are the main players in melanin synthesis [182]. Thus, skin pigmentation and tanning type are determining factors for melanoma susceptibility [183]. Light-skinned and red-headed people often carry germ-line polymorphisms in the *MC1R* gene and therefore are at greater risk to develop melanoma [184-186]. This example shows that genetic susceptibility plays a crucial role in melanoma development. Besides UV radiation and genetic predisposition, immunosuppression is another risk factor for melanoma development. Studies have shown that immunocompromised patients such as organ transplant recipients, patients with HIV or lymphoproliferative diseases such as non-Hodgkin lymphoma or chronic lymphocytic leukaemia are at greater risk to develop melanoma, showing that the immune system plays a crucial role in melanoma biology [187]. Another risk factor is the number and type of melanocytic naevi [188-191].

*Pathophysiology*

Although 25 % of melanomas develop from a pre-existing naevus, most melanomas develop *de novo*, meaning that they derive from a newly formed melanocytic lesion. However, in both cases some genetic alterations (point mutations, gene amplification) are responsible for the malignant transformation of melanocytes to metastatic melanoma [174]. Thus, melanoma is characterized by a high mutational load. Since UVA and UVB cause C to T and G to T transitions, respectively, these point mutations are frequently found in melanoma [192, 193]. Activating mutations of oncogenes are also commonly detected in melanoma and are required for the initial steps of melanocytic transformation. Somatic mutations of *BRAF* and *NRAS* are associated with 50 % and 15 % of melanomas, respectively, resulting in constitutive activation of the ERK-MAPK signaling pathway [194]. Interestingly, *BRAF* mutations can not only be detected in primary and metastatic melanoma but also in benign naevi [195]. Mutant BRAF can induce cell senescence by inducing the expression of inhibitor of cyclin-dependent kinase 4a (*INK4A*), thereby abrogating malignant transformation [196]. Additional mutations, for instance in the telomerase reverse transcriptase (TERT) promoter, are required for melanoma progression [197]. Inactivating mutations of tumor-suppressor genes are responsible for the transition of malignant melanoma to invasive melanoma. The two tumor-suppressor genes p16/INK4A and p14/ARF, encoded by the *CDKN2A* locus, abrogate cell cycle progression by inhibiting cyclin-dependent kinases (CDK) [198]. Besides, loss-of-function mutations of the tumor-suppressor gene phosphatase and tensin homolog (*PTEN*) can be detected in 25–50 % of non-familial melanoma. PTEN inhibits PI3K/Akt signaling pathway which promotes cell survival by phosphorylation/inactivation of pro-apoptotic proteins such as Bcl-2 antagonist of cell death (BAD) [199]. *PTEN* and *TP53* mutations are associated with metastatic melanoma [174].

On the protein level, integrins and cadherins play a crucial role in the development of invasive and metastatic melanoma [175]. Both transmembrane proteins function as cell adhesion molecules. While cadherins provide cell-cell contacts, integrins support adhesion to the ECM. Increased αVß3 integrin expression during malignant transformation promotes the invasion of melanoma cells, for instance by up-regulating MMP-2 expression [200, 201]. Furthermore, αVß3 integrin promotes the survival of melanoma cells by inducing the expression of the anti-apoptotic protein Bcl-2 [202]. E-cadherin was shown to be involved in the adhesion of melanocytes to keratinocytes thereby controlling melanocytic cell growth [203]. Invasive

melanoma is characterized by the loss of E-cadherin and up-regulation of N-cadherin expression [204]. This down-regulation of E-cadherin is also linked to increased ß-catenin signaling [205]. Free intracellular ß-catenin acts as a co-transcription factor and induces the expression of genes that are responsible for proliferation, migration, and survival of melanoma cells. The translocation of ß-catenin to the nucleus is also induced by Wnt molecules that can be produced by melanoma cells [206]. Besides cyclin D1 and MMP-7, ß-catenin induces the expression of microphthalmia-associated transcription factor (*MITF*) [207]. Although MITF is essential for the differentiation and cell cycle arrest of normal melanocytes, melanoma cells evade these mechanisms [175]. By inducing Bcl-2 expression MITF can stimulate proliferation and survival of melanoma cells [208]. Increased copy numbers of a gene region containing the *MITF* locus were observed in melanoma, suggesting *MITF* as an oncogene. Indeed, MITF over-expression occurs mainly in melanomas with a poor prognosis [209].

Not only gene mutations and other tumor intrinsic factors but also tumor- or stroma-derived mediators such as growth factors, cytokines and chemokines promote melanoma growth and progression. Furthermore, environmental factors such as hypoxia, ECM components and particularly the immuno-microenvironment affect melanoma progression [174].

### 1.3.2 Melanoma immuno-microenvironment

Due to the high mutational load in melanoma, there is a high number of neoantigens that are presented to effector T cells [210]. Thus, melanoma is an immunogenic tumor with a strong infiltration of inflammatory cells such as T cells, B cells, NK cells, macrophages and other immune cells [211]. However, melanoma cells have developed various strategies to evade an anti-tumor immune response. Melanoma-induced immunosuppression is mediated by down-regulation of MHC class I molecules as well as tumor antigens, increased expression of immunoinhibitory receptors such as PD-L1, production of immunosuppressive cytokines (IL-10, TGF-ß) and the induction of immune tolerance. The melanoma-induced immune escape is accompanied and enhanced by the infiltration and activation of immunosuppressive cells in the tumor stroma. These cells include M2-like TAM, MDSC, $T_{regs}$, and tolerogenic/regulatory DCs [212].

TAM are the strongest immune cell population within the melanoma microenvironment and the presence of TAM negatively correlates with outcome of melanoma patients [82, 83, 211]. They exert various pro-tumorigenic and immunosuppressive functions as already described in chapter 2. Through the secretion of certain chemokines such as CCL22 M2-polarized TAM as well as melanoma cells attract other immunosuppressive cells including MDSC and $T_{regs}$ to the tumor microenvironment [213]. MDSC are immature myeloid cells that – under chronic inflammation – do not differentiate into macrophages, DCs or granulocytes. In humans, they can be divided into HLA-$DR^{-/low}$ $CD11b^{+}$ $CD14^{-}$ $CD15^{+}$ granulocytic/polymorphonuclear MDSC (PMN-MDSC) and HLA-$DR^{-/low}$ $CD11b^{+}$ $CD14^{+}$ $CD15^{-}$ monocytic MDSC (M-MDSC). MDSC share a lot of molecular characteristics with M2-like TAM. They both up-regulate PD-L1 thereby blocking T cell response. In addition, increased arginase-1 expression results in L-arginine

depletion thereby impairing TCRζ chain expression. MDSC further up-regulate iNOS expression and produce high amounts of NO and ROS, that either cause apoptosis of T cells or impair T cell function by nitration of the TCR [134, 135, 150]. Increased numbers of M-MDSC were detected in the peripheral blood of stage III-IV melanoma patients compared to healthy donors and this is associated with elevated levels of pro-inflammatory mediators such as IFN-γ and IL-1ß [149]. Other studies showed that the frequency of both M-MDSC and PMN-MDSC positively correlates with tumor burden [214, 215]. Furthermore, the number of circulating MDSC is associated with poor survival of melanoma patients and with decreased number of antigen-specific T cells [215]. MDSC also facilitate the differentiation of $CD4^+$ T cells into $CD4^+$ $CD25^+$ $T_{regs}$ that express high amounts of IL-10 and TGF-ß [216]. These immunosuppressive cytokines inhibit effector T cell and NK cell function. Several studies proofed the correlation between $T_{reg}$ abundance and melanoma progression [217]. Furthermore, a high count of $T_{regs}$ is associated with low levels of IL-2 or IL-12, which both promote anti-melanoma immunity [218]. Recently, a negative correlation between the presence of $T_{regs}$ and DCs was observed in advanced melanoma [217]. DCs are the most efficient APCs and like macrophages they show a high plasticity. Previously, they were divided into myeloid DCs (mDCs), exerting immune-stimulatory functions, and plasmacytoid DCs (pDCs) which are tolerogenic DCs [219]. In the melanoma microenvironment, DCs are polarized towards a tolerogenic phenotype, displaying impaired ability for antigen presentation. These DCs are induced by VEGF, IL-10, TGF-ß and IL-13 [220]. Defects in DC maturation as well as CD80 and CD86 expression were observed in melanoma [221]. Furthermore, melanoma cells can induce apoptosis of DCs (mainly pDCs), resulting in decreased IFN-α production and poor prognosis [222]. During melanoma progression there is a decrease in the number of both types of DCs. In stage IV melanoma, the number of mDCs inversely correlates with abundance of $T_{regs}$ [217, 221]. Decreased number of mature DCs were also observed in melanoma lesions of *Ret* transgenic mice, accompanied by increased numbers of MDSC [223].

Anti-melanoma immune response is mainly mediated by cytotoxic T cells and innate NK cells. Since tumor infiltrating lymphocytes (TIL) favor tumor regression, they are a predictive marker for good prognosis in patients with primary melanoma [224]. However, down-regulation of MHC class I molecules by tumor cells and T cell anergy, induced by the immunosuppressive melanoma microenvironment, impair an adequate T cell response [225].
NK cells are cytotoxic lymphocytes of the innate immune system that rapidly kill infected or malignant cells, either by lysis or by inducing apoptosis. Since NK cells can also destroy melanoma cells expressing low levels of MHC class I molecules, they are promising candidates to improve the anti-melanoma immunity. However, NK cell exhaustion or down-regulation of activating receptors was observed in melanoma patients. In addition, IFN-γ produced by NK cells was shown to induce IDO and prostaglandin E2 (PGE2) secretion by melanoma cells, which both can suppress the expression of activating receptors on NK cells [226-228]. Therefore, restoration of T cell and NK cell function as well as DC-based therapies (cancer vaccination) provide promising therapeutic tools to overcome melanoma-induced immune escape.

### 1.3.3 Melanoma immunotherapy

Since melanoma is a highly immunogenic tumor characterized by a strong infiltration of immune cells, efforts have been made to improve the anti-melanoma immune response [229]. In general, two signals are needed for an adequate T cell response (Figure 4). The first signal is the binding of the TCR to MHC I or MHC II on tumor cells and APCs, respectively. The second signal (co-stimulatory signal) is provided by binding of B7 molecules (B7.1 = CD80 and B7.2 = CD86), expressed on APCs, to CD28 on T cells or by CD40-CD40 ligand (CD40L) interactions. However, B7 molecules can also bind to CTLA-4 on T cells, providing a co-inhibitory signal for T cells. In addition, tumor cells and myeloid cells can express PD-L1 and PD-L2 which bind to PD-1 on T cells, transmitting an inhibitory signal [230]. This results in suppression of T cell proliferation and reduced effector T cell function. Under physiological conditions these inhibitory signals are important to prevent chronic inflammation [231]. However, in melanoma and other tumor entities such as renal cell carcinoma, a high expression of the inhibitory molecules PD-L1 and PD-L2 is associated with accelerated tumor growth and progression as well as with impaired overall survival [232, 233]. Thus, negative checkpoint inhibitors have been developed to block these co-inhibitory signals, thereby activating cytotoxic T cell response and promoting anti-tumor immunity. Ipilimumab, an anti-CTLA4 antibody, was the first drug that was approved for the treatment of metastatic melanoma in 2011 by the US Food and Drug Administration (FDA) [234]. In 2014, the two anti-PD1 antibodies pembrolizumab and nivolumab were approved by the FDA for the treatment of advanced melanoma [235, 236]. Later, they were also approved for the treatment of other tumor entities including renal cell carcinoma and non-small cell lung cancer. A combination of nivolumab and ipilimumab is now approved as a first-line treatment for advanced renal cell carcinoma and melanoma (https://www.drugs.com/history/keytruda.html https://www.drugs.com/history/opdivo.html). The next generation of immune checkpoint inhibitors, anti-PD-L1 antibodies (atezolizumab), are already approved for the treatment of advanced bladder cancer and specific types of lung cancer. Clinical trials using anti-PD-L1 antibodies for the treatment of melanoma are still ongoing.

Although immune checkpoint therapy is quite successful in melanoma, renal cell carcinoma or lung cancer, it is less efficient in non-immunogenic tumors such as breast or pancreatic cancer. One possible explanation for the resistance to checkpoint inhibitors is the low mutation rate in some tumor entities linked to a low number of neoantigens that are presented to $CD8^+$ T cells [210]. Furthermore, these tumors exhibit a low number of TIL while most T cells accumulate in the peritumoral stroma and only few infiltrate the tumor parenchyma [237, 238]. However, also in immunogenic tumors immunotherapy is still not satisfactory. Melanoma cells evade immune surveillance by down-regulation of MHC class I expression resulting in impaired antigen presentation and thus diminished anti-tumor immunity [239]. Furthermore, the presence of immunosuppressive cells within the tumor stroma limits effector T cell function [212]. Thus, combining immune checkpoint inhibitors with TAM-targeted therapies is a promising novel approach to fight against cancer [240]. Depletion of TAM by targeting CCR2 or CSF1R was shown to efficiently improve anti-tumor immune response mediated by immune checkpoint inhibitors [157, 161]. However, until now, there is only pre-clinical data available and clinical trials are still ongoing. Since research in this field is

still in the beginning, identifying targetable TAM molecules is of huge interest. In general, many molecules that can be targeted pharmaceutically are G protein coupled receptors (GPCR). Chemokine receptors and many purinergic receptors are GPCRs that are frequently expressed by immune cells present in the tumor microenvironment. Elucidating the function of these receptors on immunosuppressive cells such as TAM might help to identify novel therapeutic targets.

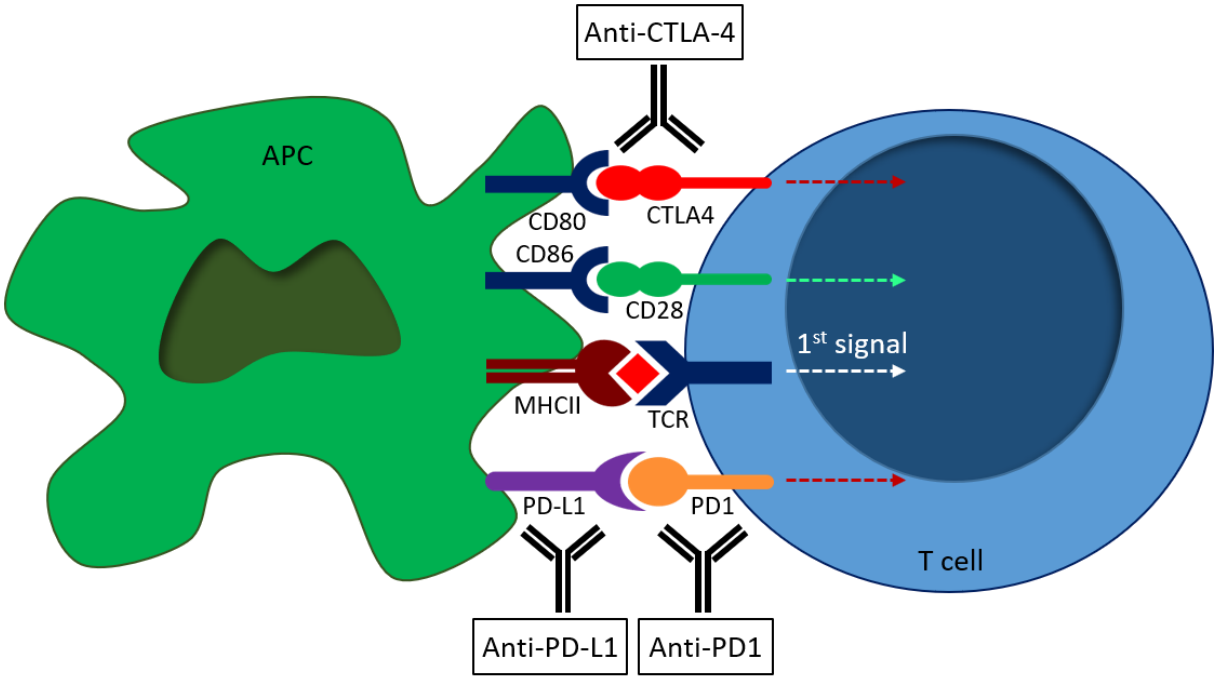


**Figure 4. Immune checkpoint inhibitors in melanoma.** Besides binding of the T cell receptor (TCR) to the MHCII – antigen complex, a second signal is required to activate T cells. The co-stimulatory molecules CD80 and CD86 induce T cell response by binding to CD28. If they bind to CTLA4 or when PD-L1 binds to PD1 the T cell response is inhibited. Checkpoint inhibitors including anti-CTLA-4, anti-PD1 and anti-PD-L1 antibodies target these immunoinhibitory receptors to improve anti-melanoma immune response.

## 1.4 Purinergic receptors

### 1.4.1 Classification and function

Purinergic receptors are expressed in nearly all mammalian tissues triggering distinct physiological processes including heart rate, muscle tonus, neuronal processing, nociception, bone homeostasis, immunity and inflammation. Purinergic receptors can be divided into P1 receptors, also known as adenosine receptors, and P2 receptors (Figure 5). Whereas P1 receptors are GPCRs activated by adenosine, P2 receptors are activated by nucleotides and can be further subdivided into P2X receptors which are ligand gated ion channels and P2Y receptors which are metabotropic GPCRs. P2X receptors are activated only by ATP while P2Y receptor are activated by diverse nucleotides. P2Y1, P2Y12 and P2Y13 are activated by ADP,

whereas ATP activates P2Y2 and P2Y11. UTP is the agonist for P2Y2 and P2Y4. P2Y6 is activated by UDP and UDP-glucose is the ligand for P2Y14. Interestingly, P2Y11 can interact with P2Y1 and is absent in rodents [241].

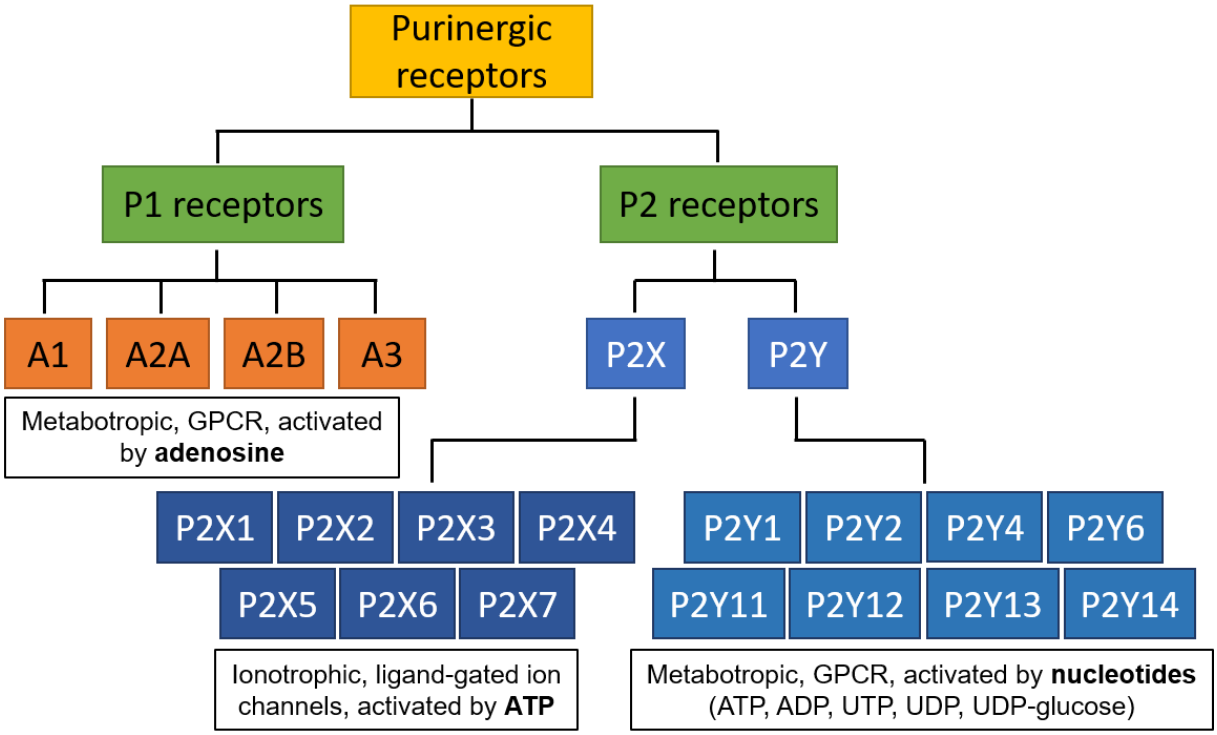


**Figure 5. Classification of purinergic receptors.** P1 receptors, also known as adenosine receptors, are activated by adenosine whereas P2 receptors are activated by nucleotides. There are 7 members of P2X family that are all activated by ATP and 8 members of the P2Y family with different substrate specificity.

Adenosine receptors can be further subdivided in 4 subtypes: A1, A2A A2B and A3. All these receptors exert different but partially overlapping functions. Adenosine receptors have a broad tissue distribution and are expressed almost ubiquitously throughout the body [242, 243]. Caffeine and other xanthine derivates such as theophylline are natural antagonist of adenosine receptors [244].

In the heart, adenosine receptors regulate heart rate and blood flow by triggering vasoconstriction [245]. In the CNS, they regulate release of neurotransmitters such as dopamine [246]. A2AR is also strongly expressed in lymphatic organs such as the spleen and thymus and is expressed on immune cells including lymphocytes and macrophages [247]. Like A2AR, A2BR plays an important role in innate immunity and inflammation. A3R is involved in chemotaxis of neutrophils and macrophages [248, 249]. In general, adenosine receptors mediate immunosuppression, thereby counteracting pro-inflammatory conditions and limiting tissue damage [250].

Like adenosine receptors P2X receptors are present in almost all tissues. Functional receptors consist of homotrimers or heterotrimers while each subunit consist of two transmembrane

domains. Extracellular binding of ATP binding results in conformational change of the receptor followed by opening of ion channels. Cations such as $Na^+$ and $Ca^+$ enter through these pores thereby depolarizing the cell membrane. In the heart, musculature or vasculature this results in contraction of cardiac muscle, skeletal muscle and smooth muscle cells, respectively. P2X receptors are also expressed in neurons and glial cells mediating synaptic transmission, signal integration and nociception. On immune cells they modulate activation, proliferation and apoptosis [251]. P2X1, P2X4 and P2X7 receptors, for instance, are expressed on leukocytes including T cells, macrophages and DCs. Besides being important for T cell activation, they trigger chemotaxis of myeloid cells [252]. P2X7 has a unique physiology since it has a low affinity for ATP and is only activated in highly inflamed tissue. Furthermore, it can build large pores by which endogenous ATP can be released [253].

P2Y receptors are GPCRs that signal via heterotrimeric G proteins. There are various subtypes of G proteins consisting of different alpha subunits that activate distinct signaling pathways P2Y1/2/4/6 and 11 are coupled to $G_{q/11}$ that activates phospholipase Cß (PLCß), resulting in increased intracellular calcium levels through the second messenger IP3. Besides $G_{q/11}$, P2Y11 couples to $G_s$ that activates adenylyl cyclase, triggering cAMP generation from ATP. P2Y12, P2Y13, and P2Y14 are coupled to $G_i$ proteins that inhibit adenylyl cyclase. The Gßγ subunit of the heterotrimeric G proteins can activate other effector enzymes such as PI3Kγ [241, 254]. Like other purinergic receptors, P2Y receptors are universally expressed and exert various functions throughout the body. They mediate platelet activation and aggregation, vasodilatation and chemotaxis of microglial cells as well as other immune cells [255, 256]. Like P2X receptors, they are involved in proliferation, migration and activation (e.g. cytokine production) of leukocytes thereby modulating immune responses [252].

### 1.4.2 Purinergic signaling regulates inflammation and immunity

During the last decade, various P1 and P2 receptors have been identified on immune cells indicating that they influence inflammation and immunity [252, 257]. In inflamed tissue, necrotic and apoptotic cells release high levels of ATP and other nucleotides which act as find-me or danger signals for phagocytic cells such as macrophages, neutrophils and DCs [258, 259]. Purinergic receptors on these myeloid cells are essential to sense the extracellular nucleotides. The purinergic receptor P2Y2 is important for the chemotaxis of neutrophils, eosinophils, DCs as well as monocytes [252, 260]. After recruitment to the site of inflammation they trigger phagocytic clearance of dead or dying cells [260]. Not only damaged or stressed cells can release nucleotides but also intact cells including leukocytes themselves. Controlled ATP release was first observed in neurons that release ATP via vesicles [261]. However, in the last years, several other mechanisms of ATP release were discovered. ATP can be released by connexin and pannexin hemichannels, voltage-dependent anion channels as well as by the purinergic receptor P2X7 itself [262]. Several types of immune cells including activated T cells or neutrophils were shown to release ATP via pannexin-1 hemichannels [263-266]. Interestingly, the released ATP does not only provide a paracrine signal for other immune cells but also signals in an autocrine manner. In neutrophils, chemotactic stimuli – IL-8 in humans

or fMLP in mice – induce ATP release, promoting chemotaxis of these cells by autocrine purinergic signaling via P2Y2 [267]. In macrophages, the complement component 5a (C5a) induces ATP release, creating a positive feedback loop by purinergic signaling via P2Y2 and P2Y12 [268]. In DCs, extracellular ATP promotes the migration of the cells by stimulating ATP release through pannexin-1 channels and autocrine purinergic signaling via P2X7 receptors [269]. These results indicate that autocrine purinergic signaling induced by extracellular stimuli or paracrine signals promotes the chemotaxis of myeloid cells. ATP does not only promote directed migration but also modulates maturation, activation and polarization of myeloid cells. In DCs, several purinergic receptors are involved in cell maturation [270]. P2Y11, for instance, was shown to be down-regulated upon differentiation of monocyte-derived DCs [271]. In macrophages, extracellular ATP triggers inflammation and innate immunity by activation of the NLRP3 inflammasome. Released ATP in response to DAMPS and PAMPs induces autocrine purinergic signaling via P2X7. This results in processing and release of IL-1ß and IL-18 from the inflammasome in a caspase-1 dependent manner. In P2X7 deficient mice, IL-1ß release upon LPS and ATP treatment is abrogated [272, 273]. T cells can also release ATP in response to extracellular signals or upon TCR activation. By autocrine signaling via P2X1, P2X4 and P2X7, ATP promotes IL-2 production and T cell proliferation [265, 274].

Extracellular ATP is rapidly metabolized by ectonucleotidases comprising four family members: the ectonucleoside triphosphate diphosphohydrolase (ENTPD) family, the ectonucleotide pyrophosphatase/phosphodiesterase (ENPP) family, alkaline phosphatase and ecto-5'-nucleotidase (CD73). ENTPD family members, including ENTPD1 (CD39), hydrolyze ATP or ADP to AMP while ENPPs cleave ATP to AMP and pyrophosphate. Alkaline phosphatases hydrolyze ATP, ADP and AMP to adenosine whereas CD73 only converts AMP to adenosine. Ectonucleotidases have a broad tissue distribution pattern and are expressed on several immune cells, including $T_{regs}$ and macrophages [275, 276]. In monocytes/macrophages adenosine reduced the secretion of the pro-inflammatory cytokines TNF-α, IL-6 and IL-8 and induced the expression of IL-10, revealing that adenosine is an immunosuppressive mediator [277, 278]. Thus, ectonucleotidases are important to resolve inflammatory conditions. The suppressive effect of the produced adenosine mainly occurs via A2A receptors, which are up-regulated during inflammation. In T cells and NK cells, A2AR signaling inhibits their cytotoxic function by suppressing IL-2 and IFN-γ expression [252]. In neutrophils, A2AR signaling is involved in limiting ATP-induced chemotaxis [279]. Thus, A2AR-deficient mice showed increased tissue damage and inflammation in several disease models [280]. Accordingly, *Entpd1*-deficient mice developed severe inflammation after tissue injury [281]. While A2AR is widely expressed by immune cells, the adenosine receptor A2BR is mainly expressed by macrophages and DCs [252]. Hamidzadeh and Mosser proposed that A2BR is involved in terminating pro-inflammatory response of M1 macrophages. They showed that TLR-stimulated macrophages release ATP through pannexin 1 channels. The extracellular ATP is rapidly cleaved by CD39 and CD73 which are both expressed on macrophages. The generated adenosine binds to A2AR and A2BR receptors and suppresses the expression of the pro-inflammatory cytokines IL-12 and TNF-α while increasing the expression of IL-10 [282]. Adenosine receptors were shown to be strongly up-regulated by TLR ligands, DAMPs and hypoxia [252]. A2BR-deficient macrophages secrete higher levels of pro-inflammatory cytokines but less immunosuppressive mediators [283]. Consequently, A2BR-deficient mice

showed severe inflammation after tissue injury. Interestingly, A2BR also contributes to angiogenesis and fibrosis by inducing VEGF and IL-6 expression [284, 285].

Besides signaling through P1 receptors, adenosine can be metabolized by adenosine deaminases (ADAs) that convert adenosine to inosine. ADAs are expressed on leukocytes and promote T cell response by the production of Th1 cytokines and stimulation of T cell proliferation [286, 287]. Besides being enzymatically converted, adenosine can also be up-taken by cells expressing specific nucleoside transporters. They were shown to be involved in the activation and proliferation of lymphocytes and macrophages [288, 289]. Thus, blocking adenosine uptake or conversion provides an additional therapeutic strategy for the treatment of chronic inflammatory diseases and autoimmune disorders. The application of adenosine receptor agonists for the treatment of rheumatoid arthritis is currently tested in clinical trials. In contrast, adenosine receptor antagonists might be helpful in diseases with increased A2BR signaling including chronic obstructive pulmonary disease (COPD) and asthma. Since adenosine promotes immunosuppression and limits anti-tumor immunity blockade of adenosine signaling might also be efficient in the tumor microenvironment [252, 290].

### 1.4.3 Purinergic receptors in the tumor microenvironment

Due to inflammation, necrosis and hypoxia there are high levels of ATP and adenosine in the tumor microenvironment. Both directly modulate tumor growth and progression as well as the activity and function of immune cells of the tumor microenvironment thereby affecting the anti-tumor immunity (Figure 6) [252]. Besides $T_{regs}$ and macrophages, tumor cells can express the ectonucleotidase CD73 that converts AMP to adenosine thereby creating an immunosuppressive tumor microenvironment. Ectonucleotidases were shown to be up-regulated under hypoxic conditions [291]. In several murine tumor models, deletion or blocking of CD73 reduced primary tumor growth and metastasis and restored $CD8^+$ T cell activity [292, 293]. In human breast cancer patients, CD73 expression is associated with poor outcome [294]. The generated adenosine exerts multiple functions on distinct immune cell populations in the tumor microenvironment. On the one hand, adenosine signaling via A2AR suppresses cytotoxic T cell response and NK cell activity and on the other hand adenosine enhances the immunosuppressive capacity of macrophages, MDSC and $T_{regs}$ [252]. A2AR-deficient myeloid cells exhibited reduced IL-10 expression resulting in reduced tumor growth and lung metastasis [295]. Although global A2AR deletion was shown to increase the number of TILs and decelerated tumor growth, specific deletion of A2AR in T cells can result in increased T cell exhaustion and apoptosis and thus enhanced tumor growth, indicating that A2AR regulates not only cytotoxicity but also survival of T cells [296]. Besides expressing A2AR, T cells express several P2 receptors, including P2X1, P2X4, P2X7 and P2Y12. Whereas adenosine receptors suppress the proliferation and cytotoxicity of T cells, ATP receptors activate NF-κB signaling and promote proliferation and cytotoxicity of T cells [252].

The balance between ATP and adenosine in the tumor microenvironment also determines macrophage polarization (Figure 6). Binding of ATP to P2 receptors (e.g. P2X7) on macrophages promotes a pro-inflammatory M1 phenotype by inducing the expression of pro-

inflammatory cytokines whereas adenosine triggers a M2 polarization of macrophages via A2AR [252]. Besides expressing IL-10 and TGF-ß, M2 macrophages express higher levels of CD39 and CD37 compared to M1 macrophages, thereby augmenting the immunosuppressive microenvironment [297].

As discussed previously, macrophages also express the adenosine receptor A2B. Besides reducing the expression of the proinflammatory cytokines TNF-α and IL-12, A2BR signaling induces the expression of the pro-angiogenic mediators VEGF and IL-6 [252, 282]. Since tumor cells themselves also express A2BR, blockade of A2BR can reduce tumor growth and metastases formation [298, 299]. Furthermore, tumor cells express P2X7 receptors that are involved in proliferation and P2X7 blockade reduced tumor growth. This pro-tumoral role of P2X7 is quite contradictory to the role of P2X7 in myeloid cells where P2X7 signaling induces IL-1ß secretion, activates $CD8^+$ T cells and is important for the chemotaxis of DCs [252]. P2X7-deficient mice exhibited decreased numbers of tumor-infiltrating inflammatory cells, while tumor growth and progression were significantly enhanced [300]. Cancer therapy including chemotherapy was shown to induce ATP release from damaged tumor cells [301]. This ATP can activate P2X7 receptors on DCs and macrophages resulting in IL-1ß production and increased anti-tumor immunity, for instance by activating IFN-γ-producing T cells [302]. Targeting adenosine receptors might be a promising approach to reduce tumor growth and progression. Due to the dual role of A2AR regarding T cell function and survival it might be more efficient to block A2BR signaling that mainly modulates myeloid cells in the tumor microenvironment [252].

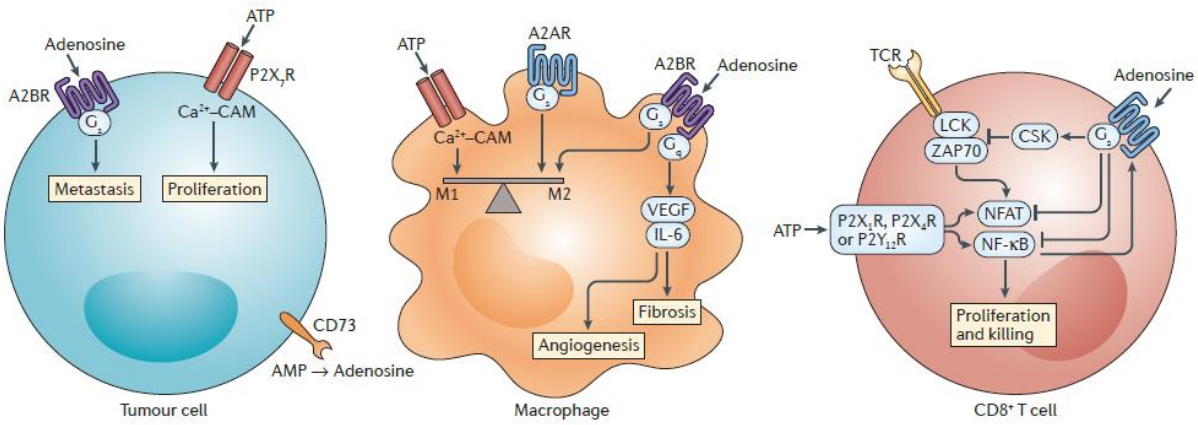


**Figure 6. Purinergic signaling in the tumor microenvironment.** Adenosine and ATP directly affect tumor cell proliferation and metastasis and modulate the function of macrophages and $CD8^+$ T cells. ATP induces M1 polarization of macrophages and promotes T cell proliferation and cytotoxicity by inducing NF-κB signaling via P2 receptors. Contrary, adenosine signaling via A2AR induces M2 polarization of macrophages, inhibits TCR signaling and thus cytotoxic T cell response. Adenosine binds to A2BR on tumor cells promoting metastasis. On macrophages A2BR signaling induces M2 polarization and promotes angiogenesis by the secretion of VEGF and IL-6. Figure adapted from Cekic and Linden [252].

## 1.5 The purinergic receptor P2Y12

### 1.5.1 Structure and signaling of P2Y12

Like other P2Y receptors, P2Y12 is a GPCR with 7 transmembrane domains. It has an extracellular N terminus, three extracellular loops, three intracellular loops and an intracellular C terminus. Two extracellular disulfide bridges are built by four cysteine residues. The human P2Y12 proteins contains 342 amino acids and there is an 83 % sequence homology between mouse and human [241]. The two existing N-linked glycosylation sites are important for signal transduction but not for ligand binding [303]. Among P2Y12 agonists the synthetic ADP analogue 2-methylthio-adenosine-5'-diphosphate (2-MeSADP) has the highest affinity, followed by ADP (Figure 7). Although P2Y12 was considered to be a selective ADP receptor, recent studies showed that ATP also activates P2Y12, but it is less potent and higher concentrations are needed to induce P2Y12 signaling [304]. Signal transduction of GPCRs is mediated via heterotrimeric G proteins consisting of the 3 subunit Gα, Gß and Gγ (Figure 7). There are several types of G proteins that activate different signaling molecules. Like P2Y13 and P2Y14, P2Y12 couples to $G_i$ proteins. Upon agonist binding there is a conformational change of the receptor resulting in exchange of G protein-bound GDP by GTP. Consequently, the Gα subunit dissociates from the Gßγ subunit and inhibits adenylyl cyclase resulting in reduced intracellular cAMP levels. The Gßγ subunit activates PI3K and its downstream effectors Akt and Rap1b (Figure 7) [241, 305, 306]. Thienopyridine compound such as clopidogrel and prasugrel are irreversible antagonist of the receptor. These prodrugs covalently bind to the receptor and must be metabolized in the liver to generate their active form. Ticagrelor is a reversible, competitive P2Y12 antagonist (Figure 7). It is an orally active compound and acts faster than the thienopyridine compounds [307, 308].
As described in the following chapters, P2Y12 is strongly expressed on platelets and in neuronal tissue, particularly in microglial cells. Recently, P2Y12 was also shown to be expressed by several leukocytes, including DCs and macrophages [308].

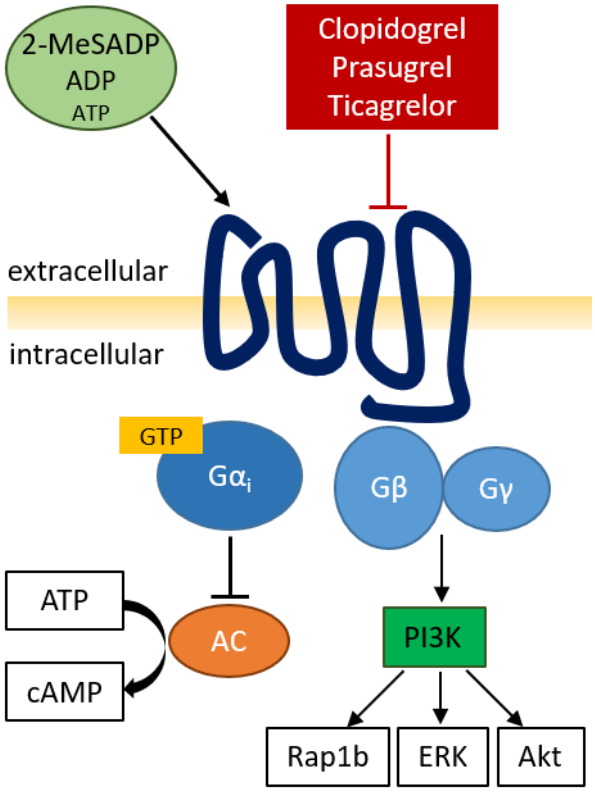


**Figure 7. P2Y12 signaling pathway.** The purinergic receptor P2Y12 is a GPCR with 7 transmembrane domains that bind 2-MeSADP, ADP and ATP with decreasing affinity. The clinically approved drugs clopidogrel, prasugrel and ticagrelor are P2Y12 antagonists. Signal transduction is mediated via heterotrimeric $G_i$ proteins. While the $G_i$ alpha subunit ($G\alpha_i$) inhibits adenylyl cyclase (AC) that converts ATP to cyclic AMP (cAMP) the Gßγ subunit activates effectors such as phosphatidyl-inositol-3 kinase (PI3K). PI3K induces downstream signaling via Akt, ERK and Rap1b.

### 1.5.2 P2Y12 expression in platelets

Platelets mediate hemostasis, a process that stops bleeding and initiates wound healing after tissue injury. During plug formation, platelets adhere to the endothelium and are activated by collagen resulting in the release of platelet granules containing ADP and thromboxane A2. This results in recruitment of more platelets and subsequent aggregation and thrombus formation [309]. Various receptors are involved in this process, including the purinergic ADP receptors P2Y1 and P2Y12 which together mediate platelet activation and aggregation [310]. ADP binding results in shape change and aggregation of platelets via activation of the αIIbβ3 integrin [311]. Compared to other agonists of platelet activation (thrombin, thromboxane A2, collagen) ADP is only a weak agonist of platelet aggregation. When strong agonists such a thrombin and collagen bind to platelets, ADP is released from platelet dense granules resulting in amplification of the platelet response [307, 308]. *P2Y12*-deficient mice showed reduced platelet activation and aggregation and thus increased bleeding [312, 313]. In the clinics, P2Y12 receptor antagonists such as clopidogrel and ticagrelor are used to treat or prevent thrombotic disorders [307, 308].

Besides hemostatic disorders, platelets also contribute to inflammation and chronic inflammatory diseases such as arthritis, atherosclerosis, allergic asthma and cancer. Platelets express various growth factors and surface molecules including PDGF, P-selectin, CD40 and CD40L which enable platelet-leukocyte interactions and activation of immune cells [314]. Thus, anti-platelet drugs might also target inflammatory actions mediated by platelets [315]. The P2Y12 antagonist clopidogrel was shown to reduce experimental transplant atherosclerosis in mice [316]. P2Y12 is also necessary for the leukotriene E4 (LTE4)-mediated pro-inflammatory actions in allergic asthma. Although the precise mechanisms are not clear yet, the authors hypothesized that P2Y12 associates with a co-receptor of the phylogenetically related cysteinyl leukotriene family [317]. Previously, Nonaka et al. showed that LTE4 can also bind to P2Y12 [318]. Platelets and their receptors also play a role in tumor progression and metastasis. Wang et al. reported reduced metastasis in *P2y12*$^{-/-}$ mice. P2Y12$^{+}$ platelets facilitated tumor extravasation by enabling platelet-tumor cell interactions. By increasing TGF-ß secretion, P2Y12$^{+}$ platelets also promoted an epithelial-mesenchymal transition of tumor cells, which is a key feature of the metastatic process [319]. Furthermore, Gebremeskel et al. showed that mice treated with the P2Y12 receptor antagonist ticagrelor exhibited less metastatic foci in the liver and lung after intravenous injection of B16 melanoma cells [320]. However, it is largely unclear whether all these effects are only linked to P2Y12 expression on platelets or also to its expression on other hematopoietic cells.

### 1.5.3 P2Y12 expression in microglia

Besides platelets, P2Y12 is also expressed in the CNS especially in microglial cells. These brain-resident macrophages are involved in almost all CNS pathologies. Brain injury or neuroinflammation are associated with the release of nucleotides and purinergic receptors function as sensor of these danger signals. Microglial cells express various P1 (adenosine) receptors and P2 receptors, which are responsible for process extension, migration, cytokine release and phagocytosis (Figure 8). Among P2 receptors, P2X4, P2X7, P2Y6 and P2Y12 are expressed by microglial cells [255]. While P2X7 was shown to be involved in proliferation and pro-inflammatory cytokine release, P2Y6 triggers phagocytosis of apoptotic neurons [321-323]. P2X4 is involved in migration after tissue injury and is strongly up-regulated during microglial activation [324]. In contrast to P2X4, P2Y12 is involved in branch extension and chemotaxis during early stages of microglial activation. Haynes et al. showed that P2Y12 is expressed on resting microglia and is down-regulated during late stages when microglial cells change their conformation to an amoeboid state. Furthermore, P2Y12 is down-regulated after microglial activation induced by LPS injection or experimental neural injury [325]. Haynes et al. revealed that P2Y12 deficiency delayed but did not completely abrogate activation and function of microglial cells [325]. This might be at least in part due to overlapping and redundant functions of purinergic receptors on microglial cells. Administration of the P2Y12 antagonist ticagrelor attenuated the number of infiltrating microglial cells and the expression of pro-inflammatory mediators such as IL-1, iNOS and CCL2 [326]. In an *ex vivo* study, the P2Y12 antagonist PSB0739 reduced the release of the chemokines CXCL1 and CCL2 form microglia cells [327]. Cytokines also modulate P2Y12 expression and function. TGF-ß increased

P2Y12 expression and the ADP-induced migration of microglial cells, whereas LPS-treated microglia showed reduced P2Y12 expression and migration towards ADP [328]. P2Y12 also plays a role in neuropathic pain. In a partial sciatic nerve ligation model used by Kobayashi et al. P2Y12 expression was up-regulated and administration of a P2Y12 antagonist inhibited the development of pain behaviour [329]. Besides on microglia, P2Y12 is also expressed on oligodendrocytes which are neuroglia cells that create the myelin sheaths around the axons of neurons [330]. Thus, P2Y12 might be involved in neurodegenerative or neuroinflammatory diseases including amyotrophic lateral sclerosis and multiple sclerosis (MS). In the brain of MS patients there is an inverse correlation between the number of demyelinated lesions and P2Y12 expression [331-333]. However, whether this P2Y12 down-regulation is a cause or consequence of the disorder, remains to be elucidated.

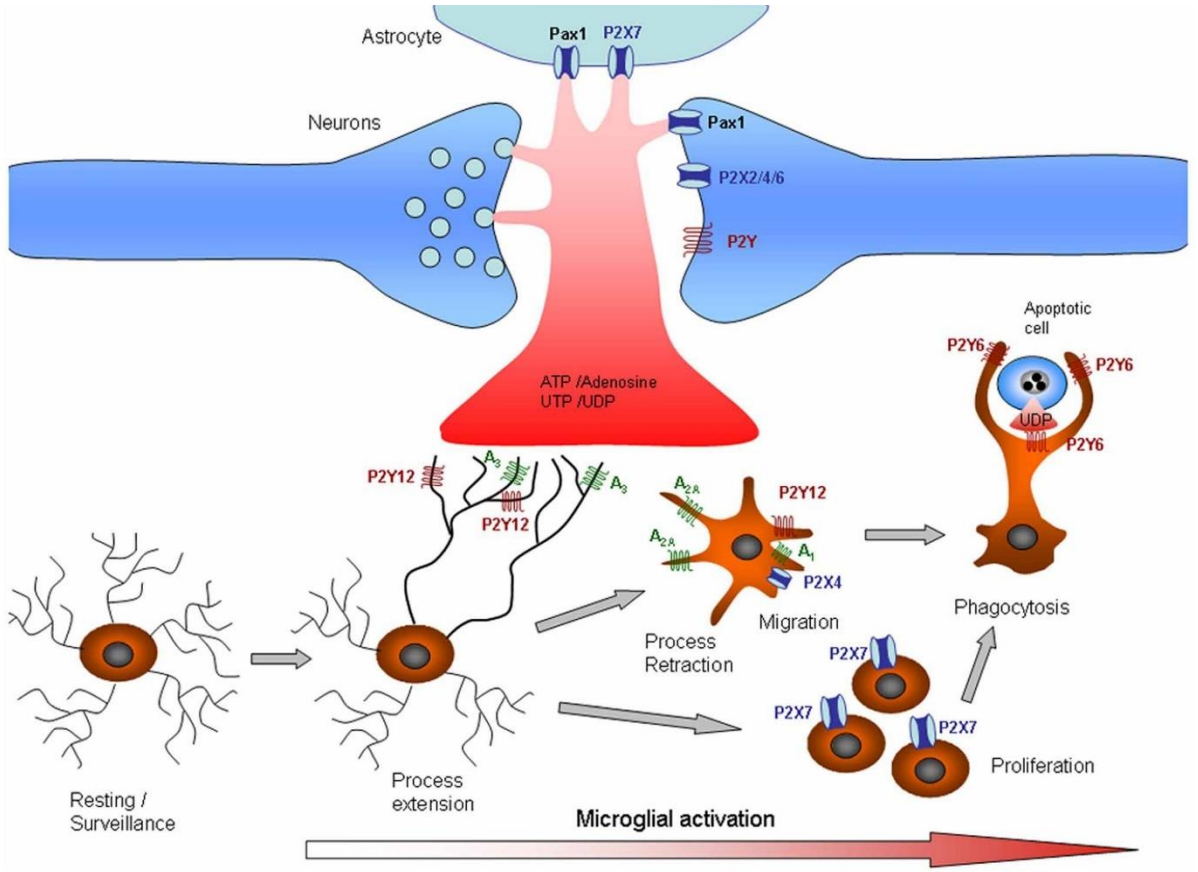


**Figure 8. Purinergic signaling during microglial activation.** Microglia express multiple P1 and P2 receptors. Purinergic receptor expression is strongly regulated during microglial activation. P2Y12 is expressed on resting microglia and is responsible for the sensing of nucleotides, branch extension and chemotaxis while P2X4 plays a role in migration during the late stages of microglial activation. A3 receptors are also involved in process extension and migration. Microglial activation is characterized by morphological changes that are associated with P2Y12 down-regulation and up-regulation of P2X4. Other P2 receptors mediate microglial proliferation (P2X7) and phagocytosis (P2Y6). Figure adapted from Domerq et al. [255].

### 1.5.4 P2Y12 expression in leukocytes

Previously, P2Y12 was found to be expressed on various leukocyte populations including lymphocytes, eosinophils, mast cells, DCs and macrophages [308]. Most of the studies detected P2Y12 expression on mRNA level and only few studies analyzed its cell type specific function. Furthermore, most of the conducted *in vivo* studies used P2Y12 antagonists such as clopidogrel and ticagrelor to investigate the effect of P2Y12 on inflammation and immunity. Diehl et al., for instance, showed that P2Y12 is expressed on leukocytes and that ADP-induced platelet aggregation correlates with leukocyte count. Treatment of patients suffering from coronary artery disease with clopidogrel abrogated leukocyte activation and their interaction with platelets resulting in diminished ADP-induced platelet aggregation [334]. Reduced platelet-leukocyte aggregates upon administration of P2Y12 antagonists were observed in several studies [335, 336]. Furthermore, clopidogrel reduced the risk of infections after surgery in ischemic stroke patients [337]. From these studies it is difficult to conclude whether the observed effects are only linked to P2Y12 expression on platelets or also to its expression on distinct leukocytes.

*Lymphocytes*
Wang et al. detected P2Y12 mRNA in human lymphocytes derived from the peripheral blood of healthy donors [338]. However, not much is known about its cell-type specific function. Interestingly, P2Y12 is involved in the differentiation of Th17 cells. *P2Y12*$^{-/-}$ mice or WT mice treated with P2Y12 antagonists exhibited reduced levels of IL-17 and Th17 cells in experimental autoimmune encephalomyelitis [339].

*Eosinophils*
P2Y12 expressed on eosinophils is involved in inflammatory conditions. Clopidogrel treatment reduced Th2 cytokine production and eosinophil infiltration after parasite infection *in vivo* [340]. Similarly, P2Y12 blockade reduced airway inflammation by decreasing the number of infiltrating eosinophils and reducing CCL5, IL-4 and IL-13 levels in a mouse model of allergic asthma [341].

*Mast cells*
P2Y12 expressed on blood-derived human mast cells might be involved in the resolution of inflammation since ATP and ADP limited the production of several pro-inflammatory cytokines and chemokines (e.g. TNF-α, CCL4, IL-8) in response to TLR2 ligands or leukotriene D4 (LTD4) [342]. Contrary, P2Y12 is crucial for LTE4-mediated mast cell activation, CCL4 and prostaglandin D2 (PGD2) production, and pulmonary inflammation [317]. These results suggest that P2Y12 on mast cells exerts opposing roles dependent on the presence of environmental stimuli or inflammatory mediators.

*Dendritic cells*
In DCs, P2Y12 modulates antigen presentation and T cell activation. Ben Addi et al. showed that P2Y12 is expressed on DCs stimulating endocytosis of antigens and activation of T cell response [343]. Treatment of DCs with the P2Y12 antagonist ticagrelor decreased the uptake of antigens and attenuated the activation of antigen-specific T cells [344]. Clopidogrel reduced

the number of infiltrating DCs in a mouse model of transplant atherosclerosis, suggesting that P2Y12 is also involved in the chemotaxis of DCs [316].

*Macrophages*

Lattin et al. showed that P2Y12 is expressed in murine bone marrow-derived macrophages (BMDM) as well as peritoneal macrophages on mRNA level [345]. While Isfort et al. confirmed P2Y12 protein expression in mouse peritoneal macrophages by Western blot analysis, Haynes et al. failed to detect P2Y12 protein expression in splenic macrophages [325, 346]. Although P2Y12 was shown to be expressed on several macrophage populations not much is known regarding its specific function in these cells. In several mouse models, the P2Y12 antagonist clopidogrel reduced the number of infiltrating macrophages [316, 347]. However, these clopidogrel-mediated effects were linked to an abolished platelet function since platelets are important mediators of inflammation. Recent evidence from one study suggests that clopidogrel and other P2Y12 antagonists might directly target $P2Y12^+$ macrophages. Kronlage et al. showed that autocrine P2Y12 signaling is important for chemotaxis of murine peritoneal macrophages in response to complement component C5a [268]. These results suggest that P2Y12 is involved in the migration of macrophages to the inflammatory site and that the reduced infiltration of macrophages upon clopidogrel treatment is caused by abrogated migratory function of $P2Y12^+$ macrophages. Regarding human macrophages, P2Y12 mRNA expression was reported in peripheral blood monocytes as well as in MDM differentiated *in vitro* [338, 348]. However, human alveolar macrophages were shown to lack P2Y12 mRNA expression [349]. Whether other tissue-resident macrophages express P2Y12 remains to be elucidated. To our knowledge no study detected P2Y12 protein expression, neither in MDM nor in tissue-resident macrophages, except microglia. One explanation for the lack of studies focusing on P2Y12 is the sparse availability of specific anti-hsP2Y12 antibodies. Thus, not much is known about the presence and function of $P2Y12^+$ macrophages in different tissues in health and disease. Especially the role of $P2Y12^+$ macrophages in the development and progression of chronic inflammatory diseases including cancer is largely unknown.

## 1.6 Aim of the study

TAM provide an interesting therapeutic target especially when combined with immune checkpoint inhibitors. Thus, it is crucial to identify novel TAM markers that can be targeted therapeutically. Previously, we could show that most of the classical TAM markers that are expressed *in vivo* need M-CSF/dexamethasone/IL-4 (MDI) for their induction in peripheral blood monocytes (pBM) *in vitro*. To identify other markers that might be expressed by TAM *in vivo*, we performed gene expression analysis of MDI-treated pBM. We identified the purinergic receptor *P2Y12* as the highest up-regulated gene. The aim of this doctoral thesis is to characterize P2Y12 expression and its function in TAM. The study focusses on the following:

**Generation and/or characterization of an antibody that specifically detects the human and murine P2Y12 protein *in vitro* and *in vivo***

We will generate a rabbit polyclonal anti-hsP2Y12 peptide antibody to detect the human P2Y12 protein in $pBM_{(MDI)}$ *in vitro* as well as in TAM *in vivo*. Specificity of this antibody will be validated using transgenic $P2Y12^+$ U937 cells. To detect P2Y12 in murine macrophages we will use a commercially available anti-P2Y12 antibody and test its specificity using transgenic $P2Y12^+$ Raw 264.7 cells.

**Characterization of P2Y12 expression in M2-like macrophages *in vitro***

We will use the self-generated anti-hsP2Y12 antibody to identify P2Y12 expression in M2-like macrophages *in vitro*. A time course experiment will reveal the kinetics of *P2Y12* induction. We will also test other combinations of pro- and anti-inflammatory cytokines and their impact on the induction of *P2Y12* expression. Finally, we will use small molecule inhibitors to analyze signaling pathways underlying the induction of *P2Y12*.

**Characterization of P2Y12 expression in TAM of melanoma *in vivo***

To verify P2Y12 expression on human TAM, we will stain melanoma sections with our self-generated anti-hsP2Y12 antibody. To analyze whether P2Y12 is expressed on $CD68^+$ M2-like macrophages in melanoma we will analyze the co-expression of P2Y12 and $CD163^+$ in TAM. In the murine system, we will stain B16F10 xenografts to analyze P2Y12 expression in TAM. We will confirm *P2y12* expression in *ex vivo* isolated $CD11b^+$ myeloid cells from B16F10 tumors, spleen and peritoneal fluid by qRT-PCR.

**Functional analysis of P2Y12 in transgenic cell lines and $pBM_{(MDI)}$ *in vitro***

To identify ADP-induced genes in macrophages, we will perform gene expression analysis of ADP-treated transgenic U937 cells. We will investigate ADP-induced downstream signaling pathways in $P2Y12^+$ cells. Using small molecule inhibitors, we will assess whether blockade of the signaling pathways will abrogate the expression of the ADP-induced genes. Since P2Y12 is an important chemotaxis receptor for microglia, we will investigate whether ADP also acts as a chemoattractant for $P2Y12^+$ macrophages triggering migration of these cells in a transwell chamber *in vitro*. Furthermore, we will assess whether dying tumor cells promote the migration of $P2Y12^+$ cells.

# 2. Materials

**Table 2. Chemicals and reagents**

| CHEMICAL / REAGENT | COMPANY |
|---|---|
| 0.5 M Tris (pH 6.8) | Bio-Rad |
| 1.5 M Tris (pH 8.8) | Bio-Rad |
| 10 x Tris Glycine Buffer (TGS) | Bio-Rad |
| 30 % Acrylamide mix | Bio-Rad |
| 2-MeSADP (ADP) | Tocris |
| 4-Aminophenylmercuric acetate (APMA) | Sigma Aldrich |
| β-Mercaptoethanol | Sigma Aldrich |
| Acetic Acid | Roth |
| Acetone | Roth |
| AEC Chromogen Substrate | Dako |
| Agarose | Sigma Aldrich |
| Akt inhibitor VIII | Calbiochem |
| Ammonium persulfate (APS) | Sigma Aldrich |
| Amphotericin B | Sigma Aldrich |
| Ampicillin | Sigma Aldrich |
| Antibody Diluent | Dako |
| Antigen Retrieval Solution pH 6 | Leica |
| Antigen Retrieval Solution pH 9 | Leica |
| Apyrase | Sigma Aldrich |
| Biocoll | Biochrom |
| Bovine Serum Albumin (BSA) | Sigma Aldrich |
| CD11b MicroBeads | Miltenyi |
| CD14 MicroBeads | Miltenyi |
| Cell Dissociation Solution non-enzymatic 1x | Sigma Aldrich |
| CFSE | Biolegend |
| CIAP | Fermentas |
| Collagenase IV | Genaxxon |
| Crystal violet | Roth |
| Dexamethasone | Sigma Aldrich |
| DFS-TAQ DNA Polymerase | Bioron |
| DH5 α competent *E. coli* | Invitrogen |
| DMSO | Sigma Aldrich |
| DNA Ladder | Thermo Fisher Scientific |
| DNase I | Fermentas |
| dNTP | Thermo Fisher Scientific |
| DPBS | Gibco |
| Dulbeccos's Modified Eagle Medium (DMEM) | Gibco |
| Earl's balanced salt solution (EBSS) | Gibco |
| EcoMount | Biocare Medical |
| Endothelial Cell Growth Medium (EGM) | Lonza |
| ERK inhibitor III | Calbiochem |
| Ethanol | Roth |

| CHEMICAL / REAGENT | COMPANY |
|---|---|
| Ethylenediaminetetraacetic acid (EDTA) | Sigma Aldrich |
| Faramount Aqueous Mounting Medium | Dako |
| Fc Block | BD Biosciences |
| Fetal Calf Serum (FCS) | Biochrom |
| Fluorescent Mounting Medium | Dako |
| Gelatin | Sigma Aldrich |
| Gentamycin | Sigma Aldrich |
| Heparin | Sigma Aldrich |
| Hydrogen peroxide ($H_2O_2$) | Merck |
| Interferon-γ (IFN-γ) | Invitrogen |
| Interleukin-4 | Peprotech |
| Interleukin-10 | Peprotech |
| Isopropanol | Roth |
| Ketamine 10 % | Medistar |
| Laemmli Buffer | Bio-Rad |
| Lipopolysaccharide (LPS) | Invitrogen |
| Luminata Forte Western HRP Substrate | Merck |
| Lysogeny broth (LB) Agar | Roth |
| Lysogeny broth (LB) Medium | Roth |
| Macrophage colony-stimulating factor (M-CSF) | Peprotech |
| Mayer's Haematoxylin | Merck |
| Medium 199 | Sigma Aldrich |
| Methanol | Sigma Aldrich |
| Mifepristone | Sigma Aldrich |
| Minimum Essential Medium Eagle | Sigma Aldrich |
| Mlu I | Thermo Fisher Scientific |
| Nancy 520 | Sigma Aldrich |
| NF-κB activation inhibitor | Calbiochem |
| Non-Essential Amino Acid (NEAA) | Biochrom |
| Oligo$(dT)_{18}$ Primer | Thermo Fisher Scientific |
| PageRuler Prestained Protein Ladder | Thermo Fisher Scientific |
| Paraformaldehyde (PFA) | Roth |
| Penicillin / Streptomycin | Biochrom |
| Percoll | GE Healthcare |
| Peroxidase Blocking Solution | Dako |
| Phosphate buffered saline (PBS) | Invitrogen |
| Phosphatase Inhibitor Cocktail | Roche |
| Protease Inhibitor Cocktail | Roche |
| PSB0739 | Tocris |
| Puromycin | Invitrogen |
| RiboLock RNase inhibitor | Thermo Fisher Scientific |
| RIPA Buffer | Sigma Aldrich |
| RNAscope® Hydrogen Peroxide Reagent | ACDbio |
| RNAscope® Protease Plus Reagent | ACDbio |
| RNAscope® Target Retrieval Reagent | ACDbio |
| Rompun 2 % | Bayer |
| Rotiophorese Buffer TAE | Roth |

| CHEMICAL / REAGENT | COMPANY |
|---|---|
| RPMI-1640 | Gibco |
| SB203580 p38 MAPK inhibitor | Calbiochem |
| Skim milk powder | Roth |
| SOC Medium | Invitrogen |
| Sodium dodecyl sulphate (SDS) | Bio-Rad |
| Sodium azide ($NaN_3$) | Sigma Aldrich |
| Sodium chloride (NaCl) | Sigma Aldrich |
| Sodium pyruvate ($C_3H_3NaO_3$) | Sigma Aldrich |
| SYBR® Green PCR Master Mix | Applied Biosystems |
| T4 DNA Ligase | Thermo Fisher Scientific |
| Tetramethylethylenediamine (TEMED) | GenAxxon |
| Transforming growth factor-β (TGF-β) | Peprotech |
| Tris / HCl | Sigma Aldrich |
| Triton X-100 | Sigma Aldrich |
| Trypsin / EDTA | Gibco |
| Tumor necrosis factor-α (TNF-α) | Peprotech |
| Tween 20 | Sigma Aldrich |
| Xba I | Thermo Fisher Scientific |
| X-treme Gene 9 DNA transfection reagent | Roche |
| X-VIVO | Lonza |
| Xylene | Roth |

**Table 3. Kits**

| KIT | COMPANY |
|---|---|
| BrdU Cell Proliferation Kit ELISA (colorimetric) | Abcam |
| DC™ Protein Assay | Bio Rad |
| GeneChip™ Human Gene 2.0 ST Array | Applied Biosystems |
| hROS Detection Kit | Cell Technology |
| Human CXCL2 DuoSet ELISA | R&D Systems |
| Human CXCL7 DuoSet ELISA | R&D Systems |
| Human IL-8 DuoSet ELISA | R&D Systems |
| innuPREP RNA Mini Kit | Analytik Jena |
| Intracellular Fixation & Permeabilization Buffer Set | eBioscience |
| KAPA HiFi HotStart PCR Kit | VWR / Peqlab |
| Maxima Reverse Transcriptase | Thermo Fisher Scientific |
| Mouse CCL4 DuoSet ELISA | R&D Systems |
| Mouse CXCL2 DuoSet ELISA | R&D Systems |
| Mouse TNF-α DuoSet ELISA | R&D Systems |
| Nitric Oxide Synthase Detection Kit | Cell Technology |
| Omnipure-OLS Purification Kit | Omni Life Science |
| Plasmid Midi Kit | Qiagen |
| Proteome Profiler Mouse Cytokine Array Kit, Panel A | R&D Systems |
| RNAscope® 2.5 HD Assay-Red | ACDbio |
| VECTOR NovaRED Peroxidase (HRP) Substrate Kit | Vector laboratories |

**Table 4. Instruments**

| INSTRUMENT | COMPANY |
|---|---|
| Axio VERT.A1 Microscope | Zeiss |
| Azure c400 | Azure Biosystems |
| Centrifuge 5417R | Eppendorf |
| Centrifuge 5810R | Eppendorf |
| Cryotome CM3050S | Leica |
| Cytospin 3 | Shandon |
| DS-U3 Digital Camera Control Unit | Nikon |
| FACS Canto™ II | BD Biosciences |
| Freezer MDF U743V | Sanyo |
| HeraSafe KS Laminar Flow | Thermo Fisher Scientific |
| Incubator Heracell L50 i | Thermo Fisher Scientific |
| Infinite M 200 Pro | Tecan |
| Kelvitron T | Heraeus |
| Microtome RM2065 | Leica |
| Mupid-One Electrophoresis Chamber | Biozym |
| Nanodrop 2000 | Thermo Fisher Scientific |
| pH Meter FG2 / EL2 | Mettler Toledo |
| PowerPac Basic | Bio-Rad |
| Quadro MACS™ Separator | Miltenyi |
| Rotator SB2 | Stuart |
| Shaker DRS12 | Peqlab |
| Stratagene Mx3005P | Agilent Technologies |
| TC20™ Automated Cell Counter | Bio-Rad |
| Thermoblock Thermomixer | Eppendorf |
| Thermocycler T100 | Bio-Rad |
| Trans-Blot Turbo Device | Bio-Rad |
| Upright motorized Microsope Eclipse Ni-E | Nikon |
| UV Systems N-90 m | Intas |
| Vortex Genie-2 | Scientific Industries |
| Water bath | Memmet |

**Table 5. Consumables**

| CONSUMABLE | COMPANY |
|---|---|
| 6-well plates | Greiner bio-one |
| 12-well plates | Greiner bio-one |
| 24-well plates | Greiner bio-one |
| 96-well plates | Greiner bio-one |
| Cell scraper | Greiner bio-one |
| Cell culture flask 25 $cm^2$ (T25) | Greiner bio-one |
| Cell culture flask 75 $cm^2$ (T75) | Greiner bio-one |
| Cell culture flask 175 $cm^2$ (T175) | Greiner bio-one |
| Cell strainer 100 µm | BD Falcon |
| Eppendorf Safe-Lock Tubes 0.5 mL | Eppendorf |
| Eppendorf Safe-Lock Tubes 1.5 mL | Eppendorf |
| Eppendorf Safe-Lock Tubes 2.0 mL | Eppendorf |
| Hyperfilm™ ECL | GE Healthcare |
| Immune-Blot PVDF Membrane | Bio-Rad |
| LS Columns | Miltenyi |
| MS Columns | Miltenyi |
| Transwell® polycarbonate membrane cell culture inserts (12 mm with 3 µm pore) | Corning |
| Transwell® polycarbonate membrane cell culture inserts (6.5 mm with 5 µm pore) | Corning |
| Vivaspin Columns (MWCO=100,000 PES) | Sartorius |

**Table 6. Software**

| |
|---|
| Adobe Photoshop 6.0 Software |
| FlowJo V 10.1 |
| GraphPad Prism 6.0 |
| Image J |
| MxPro Software |
| NIS-Elements Advanced software |
| Zeiss Software System |

**Table 7. Primers**

| PRIMER | TARGET SEQUENCE |
|---|---|
| Hs Arg1 fw | CGG AGA CCA CAG TTT GGC A |
| Hs Arg1 rev | TAC AGG GAG TCA CCC AGG AG |
| Hs CCL2 fw | GCT CAG CCA GAT GCA ATC AAT G |
| Hs CCL2 rev | GTG TCT GGG GAAA GCT AGG G |
| Hs CCL20 fw | GGA CAT AGC CCA AGA ACA GAA A |
| Hs CCL20 rev | GTC CAG TGA GGC ACA AAT TAG A |
| Hs CCL3L3 fw | CTG ACT ACT TTG AGA CGA GCA G |
| Hs CCL3L3 rev | GAC GTA TTT CTG GAC CCA CTC |
| Hs CXCL2 fw | CAC AGT GTG TGG TCA ACA TTT C |
| Hs CXCL2 rev | ACA GAG GGA AAC ACT GCA TAA T |
| Hs CXCL3 fw | GGA CAG CTG GAA AGG ACT TAA T |
| Hs CXCL3 rev | TCA GGA CTG AGC TAT GTT TGA TG |
| Hs CXCL7 fw | AAC TCC GCT GCA TGT GTA TAA |
| Hs CXCL7 rev | CCA TCC TTC AGT GTG GCT ATC |
| Hs FOSL1 fw | TGA TCC ACC CAA CCC TAT CT |
| Hs FOSL1 rev | AAT GGC CTG GTC CAA TCAC |
| Hs GAPDH fw | TGC ACC ACC AAC TGC TTA GC |
| Hs GAPDH rev | GGC ATG GAC TGT GGT CAT GA |
| Hs HB-EGF fw | GCT ACC TCT GAG AAG ACA CAA G |
| Hs HB-EGF rev | AAT TAT GGG AGG CCC AAT CC |
| Hs IL10 fw | ACA TCA AGG CGC ATG TGA AC |
| Hs IL10 rev | GCC ACC CTG ATG TCT CAG TT |
| Hs IL1ß fw | CTT CGA GGC ACA AGG CAC AA |
| Hs IL1ß rev | GGT GGT CGG AGA TTC GTA GC |
| Hs IL8 fw | CCT GAT TTC TGC AGC TCT GT |
| Hs IL8 rev | AAA CTT CTC CAC AAC CCT CTG |
| Hs jun fw | CCT GAT GTA CCT GAT GCT ATG G |
| Hs jun rev | CCT CCT GAA ACA TCG CAC TAT |
| Hs P2Y12 fw | CCA GGG TCA GAT TAC AAG AGC |
| Hs P2Y12 rev | GTT GTC GAC GGC TTG CAT TT |
| Hs P2Y12_Xba_fw | GCA TCT AGA CCA GAA TCA ACA GTT ATC AG |
| Hs P2Y12_Mlu_rev | GTA ACG CGT GCC ATT GGA GTC TCT TCA TTT GG |
| Hs ß-actin fw | GGC ACC ACA CCT TCT ACA ATG A |
| Hs ß-actin rev | TCT CCT TAA TGT CAC GCA CGA T |
| Hs TGFß fw | TAC CTG AAC CCG TGT TGC TC |
| Hs TGFß rev | CCG GTA GTG AAC CCG TTG AT |
| Hs TNF fw | AGC CCA TGT TGT AGC AAA CC |
| Hs TNF rev | CAG ACT CGG CAA AGT CGA GA |
| Mm P2Y12 fw | GAA CCA GGA CCA TGG ATG TGC |
| Mm P2Y12 rev | GTG TAC AGC AAT GGG AAG AGA ACC |
| Mm P2Y12_Xba_fw | TGC ATC TAG ACA CTC ATA TCC TTC AGA TT |
| Mm P2Y12_Mlu_rev | TGT AAC GCG TGC CAT TGG GGT CTC TTC GCT |
| Mm ß-actin fw | ACC CGC GAG CAC AGC TTC TTT |
| Mm ß-actin rev | CTT TGC ACA TGC CGG AGC CGT TG |

**Table 8. Primary antibodies**

| 1ST ANTIBODY | APPLICATION | DILUTION | COMPANY |
|---|---|---|---|
| anti-hsP2Y12 | WB<br>IHC (Ag retrieval pH 6) | 1/500<br>1/50 | Self-generated<br>(Peptide-specialties Lab) |
| anti-P2Y12 | WB<br>ICC/IHC | 1/1000<br>1/50 | Alomone<br>(APR-012) |
| Anti-Flag M2 | WB<br>ICC | 1/500<br>1/50 | Sigma-Aldrich<br>F1804 |
| anti-hsCD68 | IHC<br>(Ag retrieval pH 6) | 1/200 | Dako<br>(M087629-2) |
| anti-hsCD163 | IHC<br>(Ag retrieval pH 6) | 1/500 | Leica<br>(CD163-L-CE) |
| anti-GAPDH | WB | 1/2500 | Cell signaling Technology<br>(2118S) |
| anti-P-ERK1/2 | WB | 1/1000 | Cell signaling Technology<br>(4370S) |
| anti-ERK1/2 | WB | 1/1000 | Cell signaling Technology<br>(4695S) |
| anti-P-Akt | WB | 1/1000 | Cell signaling Technology<br>(9271S) |
| anti-Akt | WB | 1/1000 | Cell signaling Technology<br>(9272S) |

**Table 9. Secondary antibodies**

| 2ND ANTIBODY | APPLICATION | DILUTION | COMPANY |
|---|---|---|---|
| anti-mouse IgG HRP | IHC | undiluted | Dako<br>(K4005) |
| anti-rabbit IgG HRP | IHC | undiluted | Dako<br>(K4009) |
| anti-mouse IgG HRP | WB | 1/5000 | GE Healthcare<br>(NXA931V) |
| anti-rabbit IgG HRP | WB | 1/5000 | GE Healthcare<br>(NA934V) |
| anti-rabbit IgG DL-488 | IF | 1/400 | Dianova<br>(711-486-152) |
| anti-mouse IgG Cy3 | IF | 1/400 | Dianova<br>(712-165-153) |

**Table 10. Probes**

| PROBE | TARGET | ENTREZ GENE ID |
|---|---|---|
| Hs P2RY12 | 121–1283 | 64805 |
| Mm P2RY12 | 739–1854 | 70839 |

# 3. Methods

## 3.1 Cell culture methods

### 3.1.1 Cell lines

Cell lines were cultured in 75 $cm^2$ or 175 $cm^2$ cell culture flasks at 37 °C and an atmosphere of 5 % $CO_2$. Cell lines were regularly tested for mycoplasma contamination, and growth as well as morphology were controlled under an inverted microscope.

*Human cell lines*

U937

The monocytic U937 cells were purchased from ATCC. Cells were cultured in RPMI-1640 medium supplemented with 10 % fetal calf serum (FCS), 100 U Penicillin, as well as 100 µg/mL Streptomycin (Pen/Strep). Medium was replaced every two to three days by centrifugation of the suspension cells for 5 min at 300 g. Cells were split at a ratio of 1:10.

Human umbilical vein endothelial cells (HUVEC)

The cells were cultured in endothelial cell growth medium (EGM) mixed 1:2 with Medium 199, supplemented with 10 % FCS, 50 µg/mL gentamycin, 50 µg/mL heparin and 2.5 µg/mL amphotericin B. For sub-cultivation, adherent cells were washed twice with PBS and treated with Trypsin/EDTA for 5 min at 37 °C. To stop the reaction, complete medium was added and cells were centrifuged for 5 min at 300 g. Supernatant was discarded, and the pellet was resuspended in new culture medium. Cells were split with a ratio of 1:3.

*Murine cell lines*

Raw 264.7

The murine macrophage cell line Raw 264.7 was purchased from ATCC and cells were cultured in DMEM complete containing 10 % FCS and 100 U Penicillin and 100 µg/mL Streptomycin (DMEM complete). For sub-cultivation cells were washed with PBS, scraped off the plate and spun at 300 g for 5 min. Cells were split at a ratio of 1:10.

B16F1

This melanoma derived cell line was cultured in DMEM complete. For sub-cultivation the adherent cells were washed twice with PBS followed by treatment with Trypsin/EDTA for 5 min at 37 °C. Complete growth medium was used to stop the reaction. Cell suspension was centrifuged, cell pellet was resuspended in DMEM complete and cells were split with a ratio of 1:10.

B16F10

This melanoma derived cell line was used for *in vivo* tumor experiments and was cultured in DMEM complete. For sub-cultivation, B16F10 cells were treated as described for B16F1 cells. Prior to injection in C57BL/6 mice, adherent cells were washed twice with PBS, detached from the plates by treatment with cell dissociation buffer. Subsequently, cells were washed twice with PBS and cell concentration was adjusted to 10 x $10^6$ cells/mL.

### 3.1.2 Cryopreservation of cells

Cells were frozen in complete growth medium supplemented with 10 % DMSO and aliquoted into cryovials at a concentration of approximately 2 x $10^6$ cells/mL. The cryovials were placed in isopropanol-containing freezing boxes which were stored at -80 °C. For long-term storage, the cells were transferred to liquid nitrogen tanks.

The frozen cells were thawed quickly by placing the cryotubes in a 37 °C water bath for a few minutes. The cell suspension was added to 5 mL pre-warmed complete growth medium and cells were centrifuged at 300 g for 5 min. The supernatant was discarded, and the cell pellet was resuspended in fresh complete growth medium. Cells were seeded in cell culture flasks and the medium was renewed the other day.

### 3.1.3 Production of lentivirus for transduction of eukaryotic cell lines

For lentiviral transfection, HEK293/T17 producer cells were seeded in T175 $cm^2$ flasks and grown until 80 % confluency. Cells were transfected with the ADR6 vector carrying the *P2Y12* gene (section 3.3.1) and 3$^{rd}$ generation lentiviral plasmids (pMD2.G L1, pRSV rev L2, pMDLg / pRRE L3 and pCDNA3.1/p 35 E 71) using X-treme GENE 9 DNA transfection reagent. To promote plasmid uptake and thus transfection efficacy 100 mM natrium pyruvate was added to the DMEM complete medium. The next day medium was replaced by new culture medium supplemented with 10 mM natrium butyrate to stimulate the release of newly produced viruses. The following morning, medium was replaced by harvesting medium (DMEM + 1 % Pen/Strep) which, after 8 h of virus production was collected and filtered through a 0.22 µm filter to obtain sterile and cell-free supernatants containing lentiviruses. This harvesting step was repeated three times to obtain adequate virus amounts. Finally, harvesting media containing the viruses was concentrated using Vivaspin columns. Virus suspensions were aliquoted and stored at -80 °C.

### 3.1.4 Generation of transgenic cell lines

Lentiviruses (see section 3.1.3) were used for the transduction of the eukaryotic cell lines U937 and Raw 264.7. 1 x $10^6$ cells were seeded in 6 well plates in 10 mL complete growth medium. The following day, medium was renewed and 100 µL virus suspension was added dropwise. After 48 h of transduction, the medium was replaced by selection medium (complete growth medium + 2 µg/mL puromycin). Untreated cells were cultured in selection medium to determine puromycin concentration and time point when cells were dying. As soon as this happened, the surviving transduced cells were expanded in complete growth medium. The expression of the transgene *P2Y12* was verified by qRT-PCR, Western blot analysis and immunocytochemistry.

### 3.1.5 Isolation of $CD14^+$ cells from human peripheral blood

Buffy coat samples from healthy donors were obtained from German Red Cross Blood Donation Service, Baden-Württemberg. In the first step peripheral blood mononuclear cells (PBMCs) were isolated by density gradient centrifugation. Therefore, the buffy coats were diluted 1:1 with PBS, and 30 mL of the diluted blood was carefully layered over 15 mL Biocoll separation solution. The samples were centrifuged at 1200 g for 30 min without break. The mononuclear cells (monocytes, lymphocytes, some granulocytes) visible as a white ring just above the Biocoll layer were transferred to a new collection tube containing PBS. Cells were spun down at 300 g for 10 min and washed twice with PBS. To get rid of residual red blood cells and to further separate lymphocytes from monocytes another density gradient centrifugation step with Percoll was performed. Thus 15 mL Minimal essential eagle medium was mixed with 13.5 mL Percoll separating solution and 1.5 mL Earls Balanced Salt Solution and the gradient was achieved by centrifugation at 10,000 g for 10 min. 3 mL of the PBMC solution were layered slowly on top of the Percoll separation solution. After centrifugation at 1200 g for 30 min without breaks, the white layer of mostly monocytes was transferred to a new collection tube. Cells were washed two times with PBS. In the second step $CD14^+$ cells were isolated by magnetic-activated cell sorting (MACS). Therefore, cells were resuspended in MACS buffer (PBS containing 0.5 % BSA and 2 mM EDTA) labelled with CD14 MicroBeads and incubated for 15 min at 4 °C. Cells were washed once with MACS buffer and loaded on LS MACS columns which were used for positive selection of $CD14^+$ cells. After washing the columns three times with MACS buffer, the magnetically labeled cells were flushed out by inserting the plunger in the columns. Cells were spun down at 300 g for 10 min, washed once with PBS and resuspended in 10 mL X-VIVO medium. The cell concentration was determined by hematocytometer and cells were seeded at a concentration of 1 x $10^6$ cells/mL in 6 well plates. Cell were differentiated to macrophages using the following stimuli:

| STIMULI | CONCENTRATION |
|---|---|
| M-CSF | 100 ng/mL |
| Dexamethasone | 1 x $10^{-7}$ (1000 U/mL) |
| IL-4 | 10 ng/mL |
| LPS | 1 µg/mL |
| IFN-γ | 50 ng/mL |
| TNF-α | 10 ng/mL |
| IL-10 | 10 ng/mL |
| TGF-ß | 100 ng/mL |
| p38 MAPK inhibitor (SB203580) | 50 µM |
| NF-κB Inhibitor | 5 µM |
| Mifepristone | 100 nM |

## 3.2 *In vitro* Assays

### 3.2.1 BrdU Cell Proliferation Assay

1 x $10^4$ transgenic Raw 264.7 cells were seeded in 96 well plates. After cells became adherent, medium was replaced by DMEM complete containing 50 nM 2-Methylthio-adenosine-5'-diphosphate (ADP) and cells were incubated for 48 h. During the final 16 h, BrdU was added to the wells. Assay was performed according to the manufacturer's instructions (BrdU Cell Proliferation Kit ELISA (colorimetric)). Absorbance was read at 450 nm with a reference wavelength of 550 nm using a microplate reader.

### 3.2.2 Transwell migration assay with pBM

$CD14^+$ cells were isolated and differentiated as described before (section 3.1.5). After seven days of stimulation, MDI- and M-CSF-treated pBM were harvested by scraping the cells off the plate. Cell numbers were determined by hematocytometer and 2 x $10^5$ cells in X-VIVO medium were seeded in 6.5 mm transwell inserts of a 24 well plate with a pore size of 5 µm. X-VIVO medium supplemented with 50 nM ADP was used as a chemoattractant in the lower chamber of the transwell. After letting the cells migrate for 6 h at 37 °C medium was removed from the transwells, and remaining cells in the transwell insert were removed with a cotton swab. Transwells were washed once with PBS followed by fixation with 100 % methanol for 10 min. Subsequently, cells on the bottom of the transwell membrane were stained with 5 % crystal violet for 15 min and cells were washed once in PBS and once in $dH_2O$. Pictures of migrated cells were taken using an inverted microscope (Zeiss Axiovert). Crystal violet was then dissolved in methanol and quantified measuring the absorbance at 570 nm.

### 3.2.3 Transwell migration assay with transgenic Raw 264.7 cells

5 x $10^5$ transgenic Raw 264.7 cells were seeded in DMEM w/o FCS in the upper chamber of a 6.5 mm transwell insert with a 5 µm pore size. 50 nM ADP was used as a chemoattractant in the lower chamber. DMEM complete or DMEM w/o FCS were used as controls. In another set of experiments, Raw 264.7 cells were pre-treated with 10 µM of the P2Y12 specific antagonist PSB0739 prior to inducing cell migration with ADP-supplemented medium. Migration was assessed after 16 h at 37 °C as described before (section 3.2.2).

For migration experiments with conditioned medium (CM) of transgenic Raw cells. 1 x $10^6$ $P2Y12^+$ Raw cells and empty vector (EV) cells were seeded in 6 well plates. The following day, cells were washes once with PBS and cultured in DMEM w/o FCS or in DMEM w/o FCS supplemented with 50 nM ADP for 24 h. CM was harvested, and supernatants were centrifuged at 1000 g for 10 min to obtain cell-free supernatants. 700 µL of the CM (with or without 1 U/mL apyrase) was used as a chemoattractant in the lower chamber of a transwell. Number of migrated cells was determined after 6 h of migration as described in section 3.2.2.

For migration experiments with dying tumor cells 2 x $10^4$ B16F1 melanoma cells were seeded in 24 well plates. The following day, cell death was induced with 2 µg/mL puromycin for 24 h. Cell death was assessed by morphological changes observed using an inverted microscope. Transwell inserts loaded with 5 x $10^5$ transgenic Raw 264.7 cells in 100 µL DMEM were added to the 24 well plate containing the puromycin-treated B16F1 cells. Untreated B16F1 cells and complete growth medium served as controls. For several experiments 1 U/mL apyrase was added to the puromycin-treated B16F1 cells or transgenic Raw 264.7 cells were pre-treated with 10 µM of the P2Y12 antagonist PSB0739. Migration was assessed after 6 h as described in section 3.2.2.

### 3.2.4 Adhesion of U937 to HUVECs

Wells of a 12 well plate were coated with 500 µL 0.1 % gelatin in PBS and the plate was incubated for 1 h at 37 °C. Wells were washed twice with PBS and 2 x $10^5$ HUVECs were seeded and grown for 24–48 h until they formed a monolayer. To activate the cells, they were stimulated with 10 ng/mL TNF-α for 16 h. Meanwhile, transgenic U937 cells were seeded at 1 x $10^6$ cells/well in 6 well plates and treated with 50 nM ADP for 24 h. The following day, U937 cells were harvested, washed twice and counted by hematocytometer. 1 x $10^6$ cells were resuspended in 100 µL of a 5 µM CFSE solution and incubated for 20 min at RT. The staining was quenched by addition of 1 mL RPMI complete medium. Cells were centrifuged and resuspended in 1 mL RPMI complete. 500 µL cells suspension (≙ 5 x $10^5$ cells) were added to the wells containing the endothelial monolayer. Cells were incubated for 1 h at 37 °C. Non-adherent cells were removed by washing the plate two times with PBS. Cells were lysed with 500 µL RIPA lysis buffer, incubated for 5 min at RT with shaking and fluorescence intensity at 480/520 nm was measured using a microplate reader.

### 3.2.5 U937 Transmigration Assay

1 x $10^5$ HUVECs were seeded in inserts of a 12 mm transwell plate (3 µm pore size) and grown for 24–48 h until they formed a monolayer. Subsequently, cells were treated with 10 ng/mL TNF-α for 16 h. Meanwhile, transgenic U937 cells were seeded at 1 x $10^6$ cells/well in 6 well plates and treated with 50 nM ADP for 24 h. Untreated cells served as a control. U937 cells were harvested, washed twice with PBS, and concentration was adjusted to 2.5 x $10^6$ cells/mL. 200 µL of the cell suspension was added to the transwell insert containing the endothelial monolayer. 1 mL medium w/o FCS was added to the lower chamber of the transwell plate. Plates were incubated for 6 h at 37 °C. Medium in the lower well containing transmigrated U937 cells was collected, centrifuged and pellet was resuspended in 200 µL PBS. Cells were counted by flow cytometry (number of events was recorded for 40 s using medium flow rate).

## 3.3 Molecular biology

### 3.3.1 Cloning of hsP2Y12 and mmP2Y12

HsP2Y12 and mmP2Y12 were cloned in an ADR6 expression vector containing the eukaryotic promoter sequence of EF1α, a multiple cloning site (MCS) with a Flag tag, an internal ribosomal entry site (IRES), a puromycin resistance as a selection marker, and red fluorescent protein (RFP) as a reporter gene to identify successfully cloned genes.
As a first step cDNA of mmP2Y12 (clone IRAVp968D0977D) and hsP2Y12 (clone IRAUp969F0383D) was amplified with primers that add the restriction sites for the restriction enzymes Xba I and Mlu I (Table 7). The PCR was performed with κ-HiFi HotStart DNA Polymerase according to the manufacturer's instructions:

| COMPONENT | VOLUME |
|---|---|
| 5 x κ-HiFi Buffer | 10 µL |
| 10 mM dNTP | 1.5 µL |
| Forward Primer (10 µM) | 1.5 µL |
| Reverse Primer (10 µM) | 1.5 µL |
| κ-Polymerase (1 U/µL) | 1 µL |
| cDNA | 1 ng |
| Nuclease-free water | to 50 µL |

PCR was performed using the following thermocycler settings:

| STEP | TEMPERATURE | TIME | CYCLE |
|---|---|---|---|
| Hot Start | 95 °C | 3 min | 1 |
| Denaturation | 98 °C | 20 s | 18 or 22 |
| Annealing | $T_m$ of primer (60–75 °C) | 15 s | |
| Elongation | 72 °C | 60 s | |
| Final extension | 72 °C | 5 min | 1 |

The PCR product was purified using the Omnipure-OLS Purification Kit. The PCR product and the vector construct were digested with the restriction enzymes Xba I and Mlu I for 1.5 h at 37 °C. After 1 h, the enzyme CIAP was added to the vector DNA but not to the DNA of the PCR product (insert). CIAP prevents re-ligation of the linearized vector by removing the 5' phosphate group. DNA was purified again, and ligation of vector and insert was performed using the enzyme $T_4$ DNA ligase either for 1 h at RT or overnight at 4 °C.

| COMPONENT | VOLUME |
|---|---|
| Vector DNA | 20–100 ng |
| Insert DNA | 3:1 molar ratio over vector |
| 10 x $T_4$ Ligase Buffer | 2 µL |
| $T_4$ DNA Ligase (5 U/µL) | 0.2 µL |
| Nuclease-free water | to 20 µL |

For heat shock transformation, 50 µL of DH5 α competent *E. coli* were thawed on ice, mixed with 3 µL of the ligated vector and incubated on ice for 10 min. Heat shock transformation was performed at 42 °C for 45 s, followed by cooling the bacteria quickly on ice and addition of 500 µL SOC medium. After shaking the bacteria suspension for 1 h at 37 °C and 800 rpm, approximately 500 µL was seeded on LB agar plates containing 100 µg/mL ampicillin. Plates were incubated overnight at 37 °C. Several colonies were picked and transferred to conical flasks containing LB medium plus ampicillin. Bacteria were shaken overnight at 37 °C. Bacteria suspension was centrifuged, and plasmid DNA was purified using QIAGEN Plasmid Midi Kit according to the manufacturer's instruction. Finally, the DNA pellet was resolved in nuclease-free water, and the DNA concentration was determined using Nanodrop. The sequencing of the plasmid was performed by LGC Genomics GmbH (Berlin).

### 3.3.2 RNA isolation and cDNA synthesis

After cells were harvested and washed once in PBS, the cell suspension was spun down and the supernatant was discarded. The cell pellets were used for RNA isolation by using the innuPREP RNA Mini Kit according to the manufacturer's protocol. RNA was eluted in a volume of 40 µL RNase free water. RNA concentration of the samples was determined using the photometer Nanodrop 2000. The RNA was directly used for cDNA synthesis or stored at -80 °C.

cDNA synthesis was performed using Maxima Reverse Transcriptase according to the manufacturer's protocol:

| | |
|---|---|
| RNA | 1 µg |
| Oligo dT Primer | 1 µL (100 pmol) |
| dNTP Mix (10 mM) | 1 µL |
| Nuclease-free water | to 14.5 µL |

The premix was incubated for 5 min at 65 °C and quickly chilled on ice prior to addition of the following components:

| | |
|---|---|
| 5 x RT Buffer | 4 µL |
| RiboLock RNase Inhibitor | 0.5 µL (20 U) |
| Maxima Reverse Transcriptase | 1 µL (200 U) |

Reverse transcription was performed at 50 °C for 30 min followed by heat-induced inactivation of the enzyme for 5 min at 85 °C. cDNA samples were stored at -20 °C.

### 3.3.3 Polymerase chain reaction (PCR)

For PCR, cDNA was diluted 1:10 in dd$H_2O$ and the following reaction mix was prepared:

| | |
|---|---|
| 10 x Complete Buffer | 1.2 µL |
| dNTP (2 mM) | 0.6 µL |
| Forward Primer (10 µM) | 0.5 µL |
| Reverse Primer (10 µM) | 0.5 µL |
| DFS-TAQ DNA Polymerase | 0.1 µL |
| cDNA (1:10) | 1 µL |
| dd$H_2O$ | 6.1 µL |

The cycling conditions were as follows:

| TEMPERATURE | TIME | REPEATS |
|---|---|---|
| 95 °C | 3 min | 1x |
| 95 °C | 30 s | 34x |
| 60 °C (adjusted to primer) | 30 s | |
| 72 °C | 45 s | |
| 72 °C | 5 min | 1x |
| 4 °C | ∞ | 1x |

PCR products were loaded on 1–2 % agarose gels containing 10 % Nancy-520, a fluorescent stain for double-stranded DNA. Agarose electrophoresis was performed at 100 V for 30 min. DNA bands were visualized using Azur c400.

### 3.3.4 Quantitative Real-time PCR (qRT-PCR)

Template cDNA was diluted 1:50 in dd$H_2O$, mixed with primers and SYBR® Green PCR Master Mix containing the fluorescent dye, dNTPs, DNA Polymerase and buffer.

| | |
|---|---|
| cDNA (1:50) | 10 µL |
| Forward Primer (2 µM) | 3.5 µL |
| Reverse Primer (2 µM) | 3.5 µL |
| SYBR® Green PCR Master Mix | 17 µL |

10 µL of each sample was pipetted in triplicates on a 96 well qRT-PCR plate. The housekeeping gene ß-actin was used for normalization of the template amount. The PCR was run under standard conditions with an MX3000P sequence detection system (Stratagene).

### 3.3.5 Microarrays

Transgenic U937 cells were seeded at a concentration of 1 x $10^6$ cells/mL and stimulated with 50 nM ADP for 4 h and 24 h, respectively. Cells were harvested, washed twice with PBS and total RNA was isolated as described before. Concentration was adjusted to 100 ng/µL. 1 µg RNA was used for each microarray. Technical triplicates were performed for each sample. Microarrays (GeneChip™ Human Gene 2.0 ST Array) were run and analyzed at the Affymetrix core facility of the UMM.

### 3.3.6 In situ hybridization

In situ hybridization was performed using the RNAScope 2.5 HD Detection Kit for FFPE tissue. Paraffin sections (4 µm) were baked for 1 h at 60 °C. To deparaffinize the sections, they were rinsed in xylene two times for 5 min and then in 100 % ethanol twice for 1 min. Finally, the sections were air dried for 5–15 min at RT. 5 drops of hydrogen peroxide solution were applied to each section for 10 min at RT. Slides were washed twice in $dH_2O$ for 1 min. Antigen retrieval was performed by boiling the slides in 1 x antigen retrieval solution for 15 min. Section were washed shortly in $dH_2O$, followed by 100 % ethanol. After air drying the slides, a barrier was created with a hydrophobic barrier pen. Slides were air dried overnight at RT. The following day, 5 drops of Protease Plus were added to the slides and incubated for 30 min at 40 °C. Slides were washed twice in $dH_2O$. The probes were hybridized two hours at 40 °C followed by hybridization of the amplifiers as indicated in the manufacturer's instructions. Signal was detected by applying 100 µL of a 1:60 mixture of RED-B and RED-A for 10 min at RT. Slides were washed three times in $dH_2O$ followed by counterstaining with 50 % hematoxylin for 90 s. After rinsing the slides in $dH_2O$, they were placed in 0.02 % ammonia water for 10 s and washed again in $dH_2O$ three times. Finally, slides were dried at 60 °C for 15 min and mounted using EcoMount. Tissue sections were examined under a bright field microscope.

## 3.4 Biochemical methods

### 3.4.1 Generation of an anti-human P2Y12 antibody

A polyclonal antibody against human P2Y12 was generated in rabbit, targeting the peptide sequence SQDNRKKEQDGGDPNEETPM referring to amino acid 323 to 342 of the C-terminus (sequence ID NP_073625.1). The synthetized peptide coupled to a KLH carrier protein was

used as an immunogen in a commercial process (Peptide Specialty Laboratories GmbH, Heidelberg). The anti-hsP2Y12 antibody was purified by affinity chromatography using a specific peptide column provided by the company. The antibody specificity was validated by immunocytochemical stainings and Western blot analysis of generated transgenic U937 cells.

### 3.4.2 Cell lysates and protein determination

Cells were harvested and washed twice with PBS. Cell pellets were resuspended in RIPA lysis buffer containing protease and phosphatase inhibitors. The samples were incubated on ice for 20 min and centrifuged at 14,000 g for 10 min at 4 °C to remove cellular debris. The supernatant was transferred to a new collection tube. Protein concentration was determined by the colorimetric DC™ Protein Assay, which is based on the Lowry assay. A bovine serum albumin (BSA) dilution series ranging from 10 mg/mL to 0.16 mg/mL was prepared to create a standard curve.

### 3.4.3 SDS-PAGE

10 % polyacrylamide gels were prepared just prior to use.

*Resolving gel*

| | |
|---|---|
| $dH_2O$ | 5.9 mL |
| 30 % Acrylamide | 5.0 mL |
| 1.5 M Tris, pH = 8.8 | 3.8 mL |
| 10 % SDS | 0.15 mL |
| 10 % APS | 0.15 mL |
| TEMED | 6 µL |

After casting the resolving gel, it was covered with isopropanol to avoid drying. After polymerization, isopropanol was removed, the gel was washed with $dH_2O$ and the stacking gel was added followed by insertion of a comb.

*Stacking gel*

| | |
|---|---|
| $dH_2O$ | 1.72 mL |
| 30 % Acrylamide | 0.50 mL |
| 0.5 M Tris, pH = 6.8 | 0.76 mL |
| 10 % SDS | 0.03 mL |
| 10 % APS | 0.03 mL |
| TEMED | 3 µL |

After 20 min of gel polymerization samples were loaded. Protein samples were mixed with Laemmli buffer containing β-mercaptoethanol and SDS to denaturate tertiary and secondary

structure. The samples were boiled at 95 °C for 5 min. The SDS gels were placed in electrophoresis chambers which were filled with TGS buffer. Of each sample 40 µg protein was loaded on the gels. 6 µL pre-stained protein ladder was used for the assignment of protein size. Electrophoresis was performed at 20 mA for approximately 2 h.

### 3.4.4 Western blot analysis (WB)

After electrophoresis, the proteins in the gels were transferred horizontally to PVDF membranes. Semi-dry blotting was performed for 35 min at 0.45 A (max. 25 V) in the Trans-Blot Turbo device. Subsequently, the membranes were blocked in 5 % skimmed milk powder for 1 h at RT. The membranes were then incubated with primary antibodies diluted in 5 % milk powder overnight at 4 °C. The following day, the membranes were washed three times for 10 min with PBS and incubated with a horse-radish-peroxidase (HRP)-conjugated secondary antibody diluted in 5 % milk powder for 1 h at RT. After washing again three times for 10 min with PBS, the membranes were incubated with Luminata Forte Western HRP Substrate for 3 min. Chemiluminescence was detected using Azur c400.

### 3.4.5 Enzyme-linked immunosorbent Assay (ELISA)

1 x $10^6$ transgenic Raw 264.7 and U937 cells were seeded in 2 mL complete growth medium in 6 well plates and stimulated with 50 nM ADP for 24 h. Cell supernatants were collected and centrifuged at 1000 g for 10 min to obtain cell free supernatants. All ELISAs were performed according to the manufacturer's instructions. 100 µL of cell supernatant was used in each experiment and all standards and samples were read in duplicates. Optical density (OD) was measured at 450 nm using TECAN microplate reader.

### 3.4.6 Proteome Profiler Mouse Cytokine Array

The proteome Profiler Mouse Cytokine Array is a membrane-based antibody array that allows the detection of 40 different mouse cytokines and chemokines. Transgenic Raw 264.7 cells were seeded at a concentration of 1 x $10^6$ cells/mL and stimulated with 50 nM ADP for 24 h. Cell supernatants were collected and centrifuged at 1000 g to obtain cell-free conditioned media. 500 µL cell supernatant was used to incubate each membrane. The assay was performed according to the manufacturer's instructions. Chemiluminescent signal was detected using Azure c400.

### 3.4.7 Immunocytochemistry (ICC)

Transgenic Raw 264.7 cells were grown to 80 % confluency on coverslips whereas U937 cells were centrifuged onto glass slides as cytospins. The coverslips or cytospins were washed thoroughly with PBS, fixed with 2 % PFA for 10 min and permeabilized with 0.5 % Triton X-100 in PBS for 15 min. After fixation with 4 % PFA for 10 min, the cells were washed two times with PBS and once with 0.01 % Tween 20 in PBS (PBST). Fixed cells were treated with Peroxidase Blocking Solution for 10 min at RT to block intrinsic peroxidase. After washing the slides or coverslips two times in PBS and once in PBST, cells were treated with 2 % BSA in PBS for 20 min at RT to prevent unspecific staining. Cells were incubated with the desired primary antibodies diluted in Antibody Diluent for either 2 h at RT or overnight at 4 °C. Cells were washed again and incubated with the appropriate HRP conjugated secondary antibody diluted in Antibody Diluent for 1 h at RT. After washing three times a described before, samples were incubated with the ready-to-use AEC chromogen substrate for 5–10 min. The samples were rinsed in $dH_2O$ and counterstained in 10 % hematoxylin for 8 min. After rinsing in $H_2O$ for several minutes, slides and cytospins were embedded in Faramount aqueous mounting media. Pictures were taken using the Nikon Eclipse NI microscope and the NIS-Elements Advanced software (Nikon). Images were adjusted with Adobe Photoshop 6.0 software.

### 3.4.8 Immunohistochemistry (IHC)

Cryo-sections (7 µm) of murine B16F10 tumors were air-dried overnight, fixation was performed with ice-cold acetone for 10 min at RT and sections were washed three times in PBS.

Paraffin sections (1 µm) of human tissue samples were dried overnight at 60 °C. To deparaffinize the sections, they were rinsed in xylene three times for 4 min and then rehydrated in a decreasing alcohol series ranging from 100–70 % ethanol for 3 min each. Finally, the sections were washed twice with $dH_2O$ for 3 min. For antigen retrieval the sections were incubated at 95 °C for 20 min either in pre-heated citrate buffer (pH 6) or EDTA buffer (pH 9). Sections were cooled down in the buffer for 30 min at RT followed by washing once in $dH_2O$ and once in PBS.

Circles were drawn around the tissue sections using a DAKO pen and specimens were treated with Peroxidase Blocking Solution for 10 min at RT. After washing slides two times in PBS and once in PBST, samples were incubated with 2 % BSA in PBS for 20 min. Subsequently, tissue samples were incubated with the desired primary antibody diluted in Antibody Diluent either for 2 h at RT or overnight at 4 °C. After washing again three times as described before, the appropriate HRP-labelled secondary antibody diluted in Antibody Diluent was applied to the tissue specimens for 1 h at RT. Washing was conducted and samples were incubated with the AEC substrate for up to 10 min. Slides were washed in $dH_2O$ and counterstaining was performed using 10 % hematoxylin. After rinsing in $H_2O$ for several minutes, tissue sections were embedded in Faramount aqueous mounting media. Pictures were taken using the Nikon

Eclipse NI microscope and the NIS-Elements Advanced software (Nikon). Images were adjusted with Adobe Photoshop 6.0 software.

### 3.4.9 Immunofluorescence (IF)

Paraffin sections (1 µm) of human melanomas were prepared as described before (section 3.4.8). Circles were drawn around the tissue sections using a DAKO pen and samples were blocked with 5 % donkey serum in PBS for 20 min at RT. Subsequently, tissue samples were incubated with the desired primary antibody diluted in 1 % donkey serum in PBS overnight at 4 °C. After washing three times in PBS the appropriate fluorochrome-labelled secondary antibody diluted in Antibody Diluent was applied to the tissue specimens for 45 min at RT. Washing was conducted and tissue sections were embedded in Fluorescent mounting medium. Pictures were taken using the Nikon Eclipse NI microscope and the NIS-Elements Advanced software (Nikon). Images were adjusted with Adobe Photoshop 6.0 software.

### 3.4.10 Sequential staining

Paraffin sections (1 µm) of human melanoma samples were prepared as described before (section 3.4.8). Circles were drawn around the tissue sections using a DAKO pen and samples were blocked in 5 % skimmed milk powder in PBS for 20 min. Subsequently, tissue samples were incubated with the desired primary antibody diluted in antibody diluent either for 2 h at RT or overnight at 4 °C. After washing three times with PBS, the samples were incubated with Peroxidase Blocking Solution for 8 min at RT. The specimens were washed again three times with PBS followed by incubation with the appropriate HRP labelled secondary antibody diluted in Antibody Diluent for 1 h at RT. Washing was conducted as described before and samples were incubated with the HRP substrate VECTOR NovaRED Peroxidase solution for up to 10 min. Slides were washed in $dH_2O$ for 5 min and counterstaining was performed using 10 % hematoxylin. After rinsing in $H_2O$ for several minutes, tissue sections were embedded in Faramount aqueous mounting media. After pictures were taken with the Nikon Eclipse NI microscope, the slides were placed in PBS to allow the coverslips to detach overnight. Specimens were destained in stripping buffer (2 % SDS, 62.5 mM Tris-HCL (pH 7.5), 0.8 % ß-mercaptoethanol) for 1 h at 50 °C. Samples were washed two times in $dH_2O$ and once in PBS and were used again to stain another antigen of interest.

### 3.4.11 Fluorescence-activated cell sorting (FACS)

For surface staining, cells were harvested, washed in PBS and resuspended in 100 µL FACS surface buffer. The samples were incubated with 1.0 µL Fc block per 1 x $10^6$ cells for 10 min and stained with the fluorochrome conjugated antibody for 20 min at room temperature in

the dark. After washing two times with FACS surface buffer, cells were resuspended in 200 µL FACS surface buffer (10 % BSA + 0.05 % $NaN_3$ in PBS) and analyzed by flow cytometry using FACS-Canto™ II. Data analysis was conducted using FlowJo V 10.1 software. For intracellular staining, the Intracellular Fixation & Permeabilization Buffer Set was used. Cells were harvested, washed in PBS and fixed in 100 µL IC Fixation buffer for 20 min at RT. Cells were washed two times with 1 x Permeabilization Buffer and cell pellet was resuspended in 100 µL 1 x Permeabilization Buffer and directly conjugated primary antibodies were added and incubated for 20 min at RT in the dark. After washing two times with 1 x Permeabilization Buffer, the cells were resuspended in 200 µL FACS buffer. Samples were analyzed by flow cytometry.
For detection of reactive oxygen species (ROS) the hROS Detection Kit was used. pBMs were harvested, washed once in PBS and incubated with the probe Hydroxyphenyl fluorescein (HPF) for 30 min at 37 °C in the dark. In the presence of ROS, the probe is converted to a fluorescent dye. Cells were washed twice with PBS, resuspended in 200 µL PBS and analyzed by FACS. For nitric oxide synthase (NOS) detection, the NOS Detection Kit was used. pBMs were washed once in PBS and incubated with the probe DAF-2DA for 30 min at 4 °C. In the presence of NOS, the probe is converted to a fluorescent dye. Cells were washed twice with PBS, resuspended in 200 µL PBS and analyzed by flow cytometry.

## 3.5 Mouse experiments

### 3.5.1 Mice

C57BL/6 were purchased from The Jackson Laboratory. Mice were housed under specific pathogen-free conditions at the animal facility at the UMM, Mannheim. All animal experiments were approved by the animal ethics committee (Regierungspräsidium Karlsruhe, Az: 35-9185.81/G-42/14).

### 3.5.2 B16F10 melanoma model

10–12-week-old female C57BL/6 mice were anesthetized by intraperitoneal injection of 150 µL of a 10 % Ketamine/Rompun (20 mg/mL) mixture. 1 x $10^6$ B16F10 cells were injected subcutaneously in the right flank of C57BL/6 mice. Mice were sacrificed after 10–14 days or when the tumors reached a diameter of 1.5 cm. Tumors were harvested and either directly processed further for isolation of $CD11b^+$ cells or immediately shock frosted in liquid nitrogen, followed by storage at -80 °C to perform IHC of cryosections.

### 3.5.3 Isolation of murine macrophages

Tumor-bearing mice were sacrificed 14 days after B16F10 cell injection or when the tumors reached a diameter of 1.5 cm. Peritoneal macrophages were isolated by injection of 10 mL ice cold PBS through the peritoneal wall flowed by aspiration of the fluid from the peritoneal cavity. Tumor and spleen were harvested and homogenized by squeezing through a 100 µm cell strainer. Collection tubes were filled up with ice cold PBS and samples were centrifuged at 300 g for 10 min. Spleen and intraperitoneal fluid were not enzymatically digested but directly used for MACS sorting. The tumor cell pellet was resuspended in 10 mL RPMI containing collagenase IV (190 U/mL) and DNAse I (500 U/mL). Tumor digestion was performed at 37 °C for 1 h, followed by washing once with PBS. Cell numbers were determined by hematocytometer and the cell pellets (tumors, spleen, intraperitoneal fluid) were resuspended in the appropriate amount of MACS buffer and CD11b MicroBeads according to the manufacturer's instructions. Magnetic labelling of the cells was performed at 4 °C for 20 min. Collection tubes were filled up with 10 mL MACS buffer, centrifuged at 300 g for 10 min and cell pellets were resuspended in 1 mL MACS buffer. Cell suspensions were loaded on MS columns and cell sorting was performed as described in section 3.1.5. After washing the cells once in PBS, the pellet was directly used for RNA isolation.

### 3.5.4 Generation of bone marrow-derived macrophages (BMDM)

Bone marrow cells of C57BL/6 mice were isolated by flushing of femur and tibia with PBS. Cells were seeded at a concentration of 1 x $10^6$ cells/mL in DMEM complete supplemented with 30 ng/mL M-CSF and incubated at 37 °C and 7.5 % $CO_2$ for 4 days. Subsequently, cell culture medium was replaced by DMEM complete containing 30 ng/mL M-CSF plus different pro- and anti-inflammatory stimuli as indicated. Cells were incubated for three additional days.

| STIMULI | CONCENTRATION |
|---|---|
| M-CSF | 30 ng/mL |
| IL-4 | 10 ng/mL |
| Dexamethasone | 5 x $10^{-7}$ M |
| IFN-γ | 10 ng/mL |
| LPS | 1 µg/mL |

## 3.6 Statistical analysis

Data was analyzed using GraphPad Prism 6.0 software. Statistical significance was calculated by using standard Student's t-test or by one-way ANOVA and Bonferroni as a post-test. The level of significance is indicated by asterisks (*** ≤ 0.001; ** ≤ 0.01 and * ≤ 0.05). Data is expressed as mean. Error bars depict standard error of mean (SEM) of each experiment. All experiments were performed at least in triplicates.

# 4. Results

## 4.1 Characterization of P2Y12 expression in human pBM *in vitro*

### 4.1.1 *P2Y12* is strongly induced in MDI-treated pBM

Our group aims to identify signaling pathways involved in the recruitment, expansion and differentiation of human TAM in melanoma. Since the whole melanoma is needed for diagnostic purposes and thus cannot be used for research applications such as *ex vivo* isolation of TAM, we had to generate an *in vitro* model that mirrors the TAM situation *in vivo*. We could show that many typical human TAM markers such as STABILIN-1 and LYVE-1 that are expressed *in vivo* need M-CSF/dexamethasone/IL-4 (MDI) for their induction in human peripheral blood monocytes (pBM) *in vitro* [350]. To identify possible novel therapeutic targets in human TAM, we performed microarray analysis of our *in vitro* generated M2-like macrophages ($pBM_{(MDI)}$). We found the purinergic receptor *P2Y12* as one of the highest up-regulated genes in MDI- versus M-CSF-treated pBM. Various other prominent macrophage receptors such as *LYVE1*, *ADORA3*, *CLEC10A* were also significantly up-regulated in $pBM_{(MDI)}$ (Table 11). Since P2Y12 is a G protein coupled receptor (GPCR) that has not yet been described in TAM and is the target of clinically-approved oral anti-coagulation therapies (clopidogrel, prasugrel and ticagrelor), we further focused on the characterization of this molecule.

**Table 11. Microarray analysis of MDI-treated pBM.** $CD14^+$ pBM were isolated from the blood of three healthy donors and stimulated for 7 days with M-CSF or M-CSF/dexamethasone/IL-4 (MDI). Microarray analysis was performed and the fold change of MDI vs. M-CSF-treated pBM was calculated.

| GENE SYMBOL | GENE NAME | FOLD CHANGE |
|---|---|---|
| *P2RY12* | purinergic receptor P2Y, G-protein coupled, 12 | 44.4 |
| *P2RY14* | purinergic receptor P2Y, G-protein coupled, 14 | 40.8 |
| *CCL13* | chemokine (C-C motif) ligand 13 | 33.9 |
| *F13A1* | coagulation factor XIII, A1 polypeptide | 31.6 |
| *FCER2* | Fc fragment of IgE, low affinity II, receptor for (CD23) | 30.8 |
| *PDK4* | pyruvate dehydrogenase kinase, isozyme 4 | 28.8 |
| *GLDN* | gliomedin | 22.9 |
| *ADORA3* | adenosine A3 receptor | 21.3 |
| *CD200R1* | CD200 receptor 1 | 20.1 |
| *LYVE1* | lymphatic vessel endothelial hyaluronan receptor 1 | 15.0 |
| *DAAM2* | dishevelled associated activator of morphogenesis 2 | 14.5 |
| *EPS8* | epidermal growth factor receptor pathway substrate 8 | 12.1 |
| *SESN1* | sestrin 1 | 12.0 |
| *SEP3* | septin 3 | 11.7 |
| *MAOA* | monoamine oxidase A | 11.3 |
| *CD209* | CD209 molecule | 11.2 |
| *FGL2* | fibrinogen-like 2 | 10.2 |

| GENE SYMBOL | GENE NAME | FOLD CHANGE |
|---|---|---|
| *SHMT1* | serine hydroxymethyltransferase 1 (soluble) | 9.5 |
| *MTSS1* | metastasis suppressor 1 | 9.1 |
| *SOCS1* | suppressor of cytokine signaling 1 | 9.1 |
| *HRH1* | histamine receptor H1 | 9.0 |
| *KCNJ2* | potassium inwardly-rectifying channel, subfamily J, member 2 | 8.7 |
| *MYC* | v-myc myelocytomatosis viral oncogene homolog (avian) | 8.4 |
| *SUCNR1* | succinate receptor 1 | 8.3 |
| *IL17RB* | interleukin 17 receptor B | 8.2 |
| *SCN9A* | sodium channel, voltage-gated, type IX, alpha subunit | 8.2 |
| *TGFBR3* | transforming growth factor, beta receptor III | 7.9 |
| *FLT3* | fms-related tyrosine kinase 3 | 7.8 |
| *GGT5* | gamma-glutamyltransferase 5 | 7.7 |
| *MS4A6E* | membrane-spanning 4-domains, subfamily A, member 6E | 7.4 |
| *GCNT1* | glucosaminyl (N-acetyl) transferase 1, core 2 | 6.9 |
| *SLAMF1* | signaling lymphocytic activation molecule family member 1 | 6.6 |
| *CLEC10A* | C-type lectin domain family 10, member A | 6.6 |

### 4.1.2 MDI induces a M2-like macrophage phenotype in pBM

Since we found P2Y12 to be up-regulated in MDI-treated pBM we wanted to know whether our *in vitro* generated macrophages exhibit a M2 phenotype. The scavenger receptor CD163 as well as mannose receptor C-type 1 (CD206) are commonly used to identify human M2 macrophages [351]. We isolated $CD14^+$ pBM from the blood of healthy donors, differentiated them with MDI and M-CSF for 7 days and analyzed the expression of macrophage markers, chemokine receptors as well as ectonucleotidases by FACS analysis. We found that CD206, CD163 as well as CD73, which generates the immunosuppressive mediator adenosine, were significantly up-regulated whereas the cytokine receptors CCR2 and CXCR4 were significantly down-regulated in MDI-treated pBM. Expression of the ATP-hydrolyzing enzyme CD39 did not significantly differ between M-CSF and MDI-treated pBM. There was also no significant difference regarding the expression of the MHC class II surface receptor human leukocyte antigen (HLA-DR), CD11b and CD14 (Figure 9).

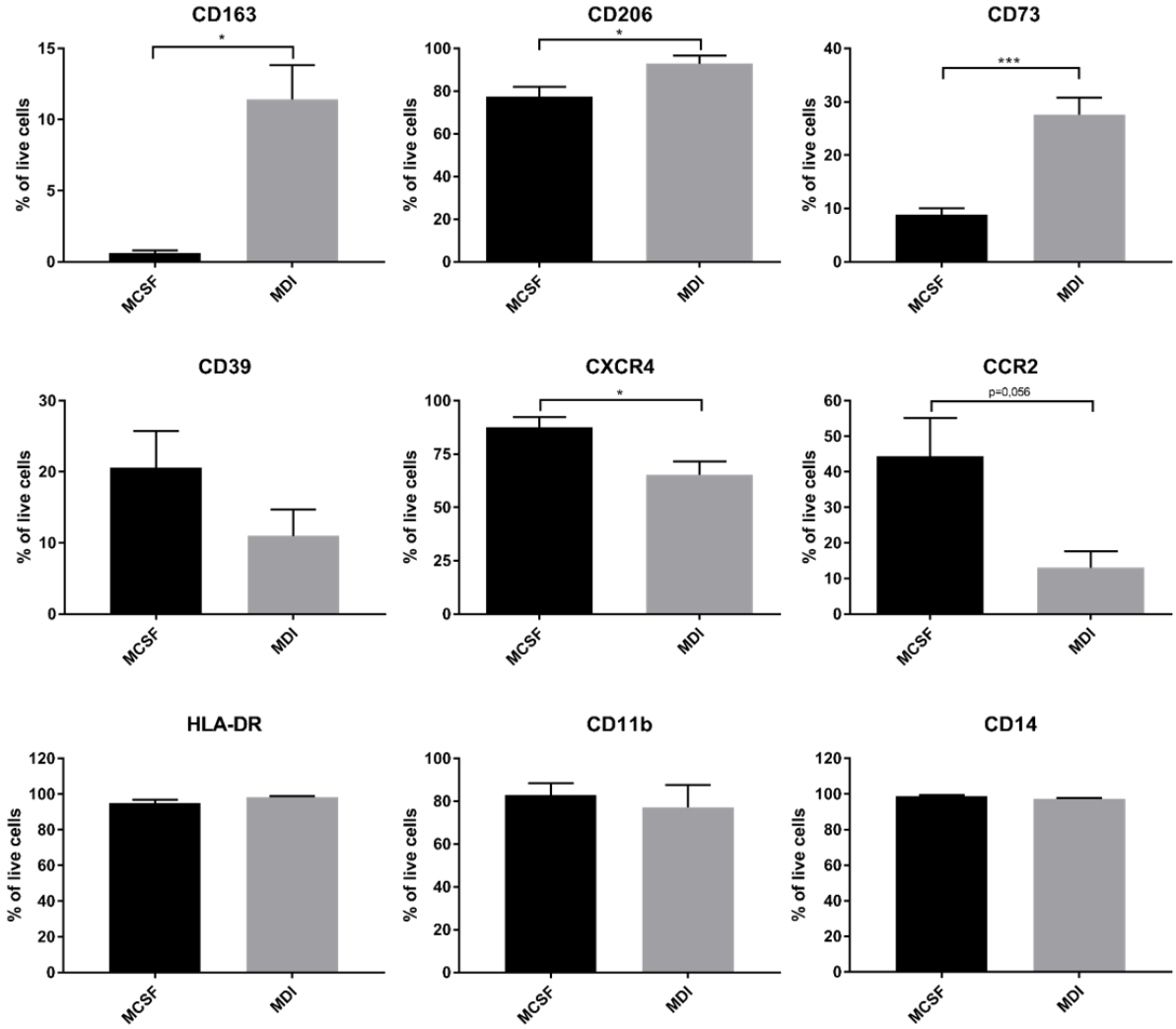


**Figure 9. Characterization of MDI-treated pBM by FACS.** pBM were stimulated for 7 days with M-CSF or MDI and the expression of macrophage markers, chemokine receptors as well as ectonucleotidases was analyzed by FACS. Live cells were gated on FSC/SSC and the percentage of positive cells was calculated from live cells (n=3).

Besides their characteristic surface marker profile, M2 macrophages are also known to express high levels of anti-inflammatory cytokines and low levels of pro-inflammatory cytokines [48]. We stimulated pBM for 7 days with MDI and assessed gene expression of various cytokines and other mediators by qRT-PCR. We detected an up-regulation of the anti-inflammatory and immunosuppressive cytokines TGF-ß and IL-10 as well as arginase-1 in $pBM_{(MDI)}$ compared to $pBM_{(MCSF)}$. In contrast, pro-inflammatory cytokines associated with a M1 phenotype such as TNF-α and IL-1ß as well as the chemokine CCL2 were significantly down-regulated in $pBM_{(MDI)}$ compared to $pBM_{(MCSF)}$ (Figure 10 a). Levels of pro-inflammatory cytokines in the cell supernatants of pBM were determined by ELISA. We detected significantly reduced concentrations of TNF-α and IL-1ß in the supernatants of MDI-treated pBM (Figure 10 b).

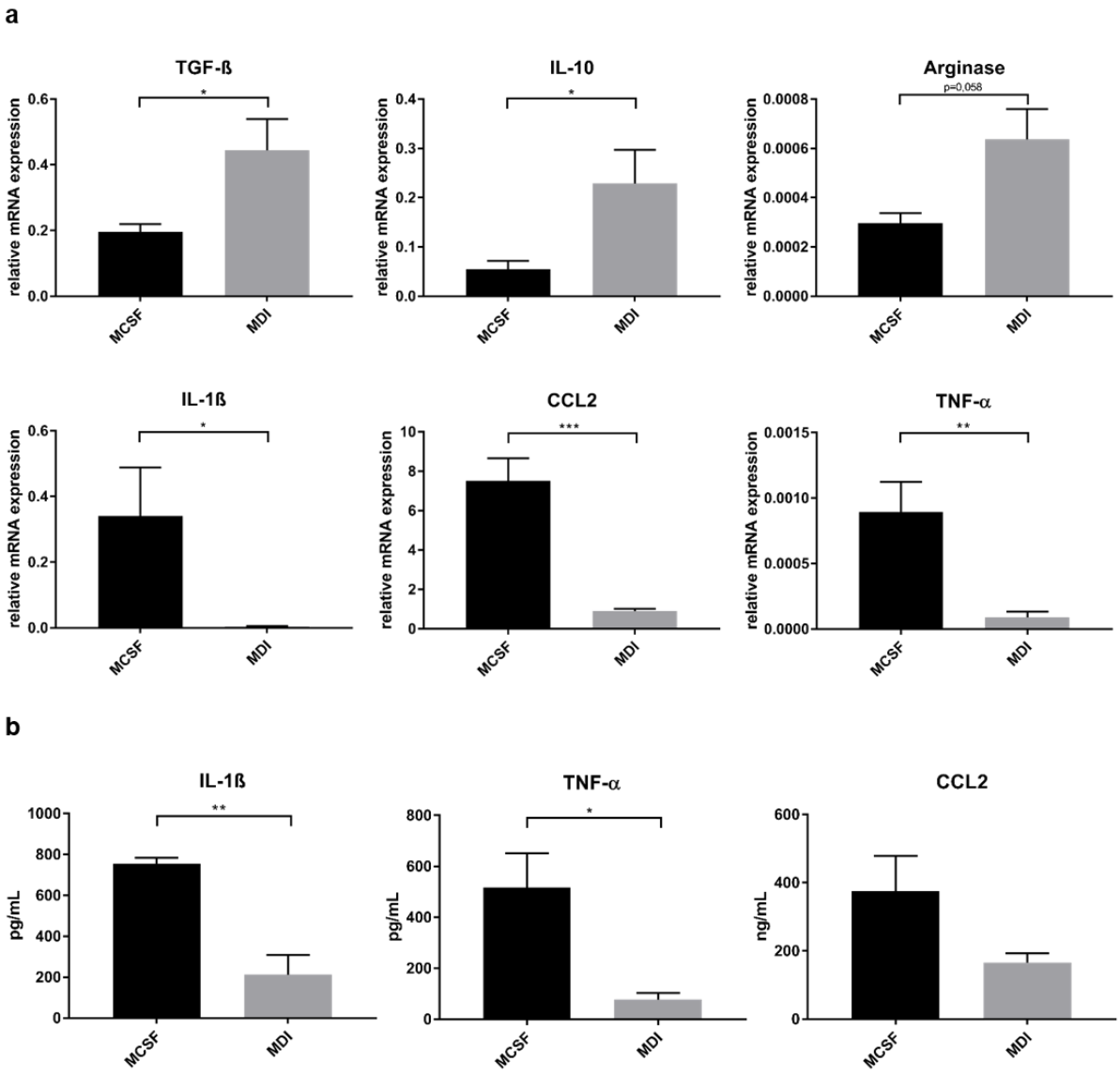


**Figure 10. pBM$_{(MDI)}$ express higher levels of anti-inflammatory and lower levels of pro-inflammatory cytokines.** (a) pBM were stimulated with M-CSF or MDI for 7 days and the expression of pro- and anti-inflammatory mediators was analyzed by qRT-PCR (n=6). (b) Cell supernatants of pBM treated with M-CSF or MDI for 7 days were collected, and the concentration of the indicated mediators was determined by ELISA (n=4).

Whereas in M2-like TAM arginase-1 is mainly responsible for L-arginine depletion, pro-inflammatory M1 macrophages deplete L-arginine via iNOS activation to produce NO. Furthermore, M1 macrophages show a high ROS production, which is important for the killing of bacteria and viruses [48]. We assessed the production of ROS as well as the expression of NOS in pBM by FACS analysis. Whereas pBM$_{(MDI)}$ produce significantly lower levels of ROS compared to pBM$_{(MCSF)}$, there was no significant difference regarding the percentage of NOS-expressing cells (Figure 11).

Taken together, our results indicate that treatment of pBM with MDI results in a M2-like macrophage phenotype based on their marker expression and cytokine profile.

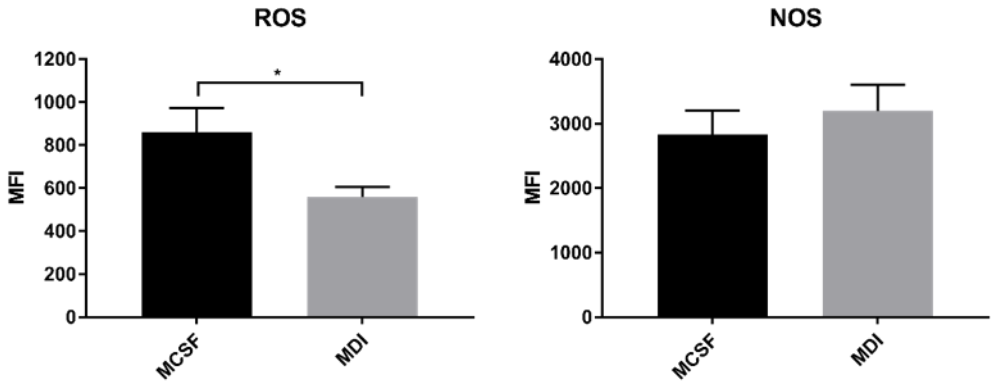


**Figure 11. ROS production is impaired in pBM$_{(MDI)}$.** pBM were stimulated for 7 days with M-CSF or MDI. Presence of reactive oxygen species (ROS) and nitric oxide synthase (NOS) was detected by loading the cells with the probes HPF and DAF-2, respectively. The median fluorescence intensity (MFI) of ROS and NOS producing cells was analyzed by FACS (n=8).

### 4.1.3 Generation of an anti-P2Y12 peptide antibody and characterization of its specificity in transgenic U937 cells

Since we detected an up-regulation of P2Y12 in pBM$_{(MDI)}$ by gene expression analysis, we next aimed at verifying P2Y12 expression in MDI-treated pBM on protein level. A rabbit polyclonal anti-hsP2Y12 peptide antibody against the C-terminal peptide sequence SQDNRKKEQDGGDPNEETPM was generated (Figure 12 a) as none of the commercially available anti-hsP2Y12 antibodies proofed specific. Our anti-hsP2Y12 antibody unambiguously detected P2Y12 in self-generated transgenic U937 cells, that stably express *P2Y12* on mRNA level (Figure 12 b), by Western blot analysis (Figure 12 c), Immunocytochemistry (Figure 12 d) as well as by FACS analysis (Figure 12 e). Since the transgene *P2Y12* is tagged with a Flag tag we used an anti-Flag M2 antibody to confirm P2Y12-Flag expression on protein level (Figure 12 c–f). In the Western blot analysis, we detected a specific band at a molecular weight of 43 kDa in P2Y12$^+$ U937 cells, whereas empty vector (EV) cells did not show this band. FACS analysis also revealed that P2Y12 and Flag are over-expressed in P2Y12$^+$ U937 cells. However, 40 % of all EV cells were P2Y12 positive, while only around 10 % were positive for the Flag tag (Figure 12 e). Immunofluorescence revealed co-expression of P2Y12 and Flag in P2Y12$^+$ U937 cells, whereas EV cells neither showed P2Y12 nor Flag expression (Figure 12 f).

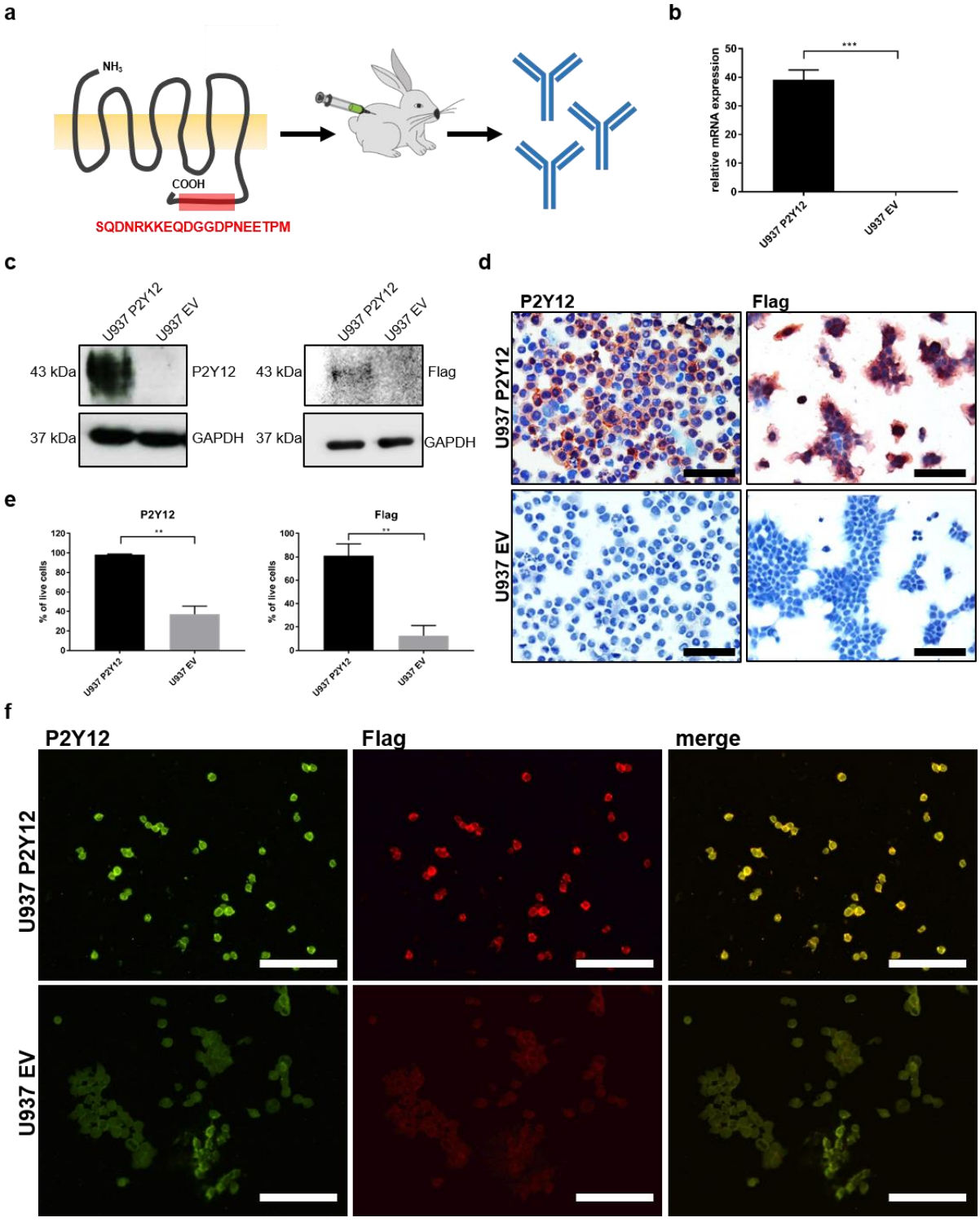


**Figure 12. Validation of an anti-hsP2Y12 peptide antibody using transgenic U937 cells.** (a) A polyclonal anti-hsP2Y12 antibody targeting the intracellular, C-terminal sequence SQDNRKKEQDGGDPNEETPM was generated by immunization of a rabbit with the synthesized peptide. (b) P2Y12 mRNA expression in transgenic U937 cells was assessed by qRT-PCR (n=4). (c–f) P2Y12 and Flag expression of transgenic U937 cells were assessed by Western blot analysis (c), immunocytochemistry (d), FACS analysis (e) and immunofluorescence (f) using the self-generated rabbit anti-hsP2Y12 antibody and an anti-Flag M2 antibody, respectively. Scale bar = 100 µm.

### 4.1.4 P2Y12 is expressed in MDI-treated pBM and its induction can be inhibited with mifepristone

qRT-PCR analysis corroborated the microarray result showing that MDI strongly induces *P2Y12* mRNA in *in vitro* stimulated pBM whereas M-CSF leads to no induction (Figure 13 a). Western blot analysis with the self-generated anti-hsP2Y12 antibody confirmed P2Y12 expression on protein level in 4 different donors (Figure 13 b). The induction of *P2Y12* expression was time dependent reaching the highest mRNA expression level after 5 days of stimulation whereas protein expression was even stronger after 7 days of MDI treatment (Figure 13 c–d).

We next determined whether other anti- or pro-inflammatory cytokines can induce P2Y12 expression in pBM. Treatment of pBM with IL-4 or dexamethasone alone as well as with LPS, TNF-α or TNF-α + IFN-γ did not induce *P2Y12* expression on mRNA level, while IFN-γ alone showed a slightly *P2Y12* induction (Figure 13 e). However, on protein level, P2Y12 expression was not detectable in IFN-γ-treated pBM (Figure 13 f). Besides IL-4/dexamethasone, no other tested anti-inflammatory cytokines (IL-10 and TGF-β) induced P2Y12 expression on the protein level (Figure 13 f).

Treatment of pBM with the glucocorticoid receptor inhibitor mifepristone significantly abrogated the MDI-induced *P2Y12* expression on mRNA level (Figure 13 g). Treatment with other signaling pathway inhibitors such as a NF-κB inhibitor or a p38 MAPK inhibitor did not significantly alter *P2Y12* induction (Figure 13 h).

Taken together, our results indicate that *P2Y12* can only be induced by the combined treatment of pBM with MDI and its expression can be inhibited with the GC receptor inhibitor mifepristone.

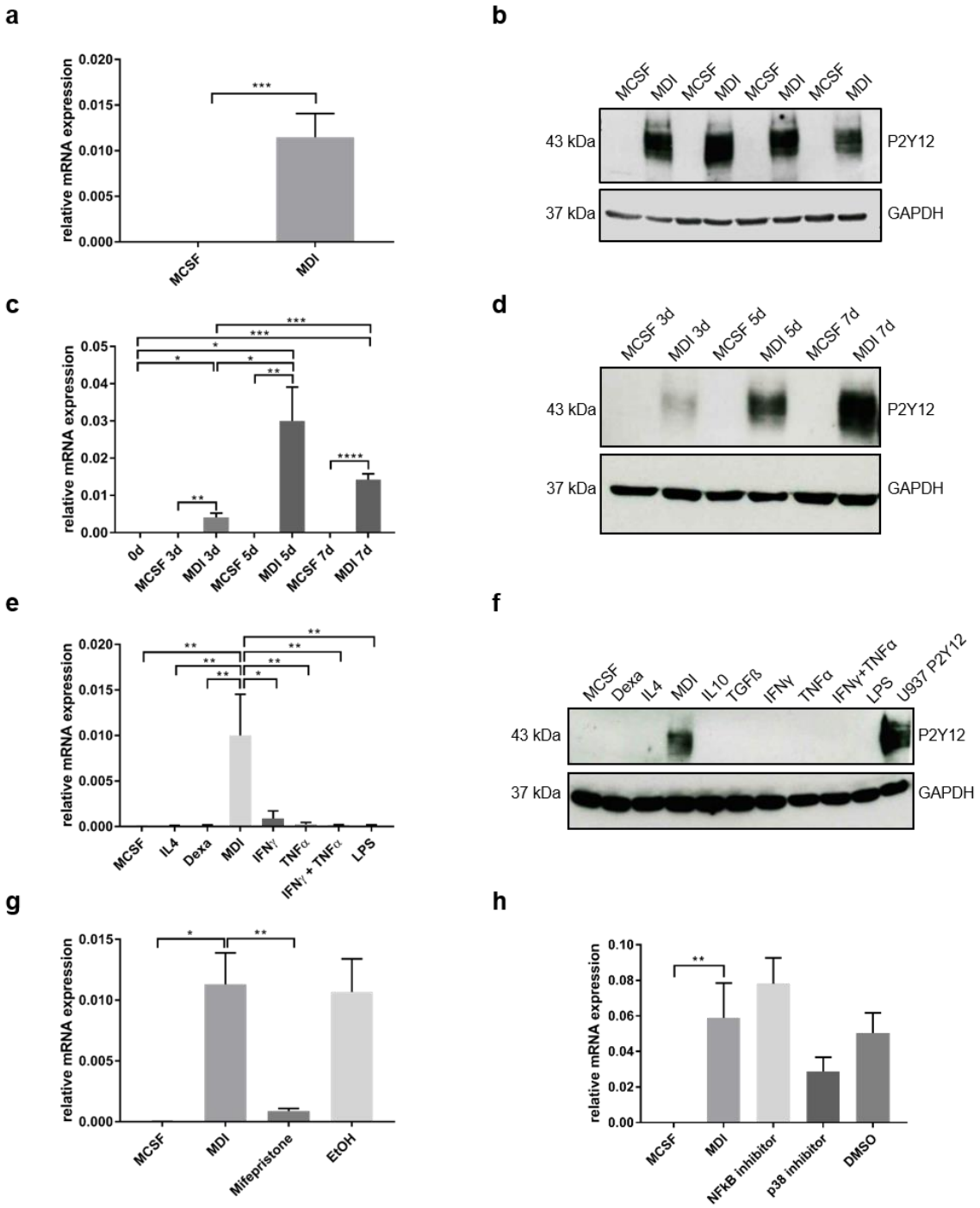


**Figure 13. P2Y12 expression is induced in MDI-treated pBM.** (a–b) P2Y12 expression in pBM treated with MDI or M-CSF for 7 days was analyzed by qRT-PCR (a) and Western blot analysis (b) (n=11). (c–d) Time dependent induction of P2Y12 expression after 3 days, 5 days and 7 days was analyzed by qRT-PCR (c) and Western blot analysis (d) (n=6). (e–f) P2Y12 expression was assessed after treatment of pBM with M-CSF alone or M-CSF plus the indicated pro-and anti-inflammatory cytokines for 7 days by qRT-PCR (e) or Western blot analysis (f) (n=7). For all experiments one representative Western blot is depicted. (g) *P2Y12* induction in pBM treated with M-CSF, MDI or MDI plus mifepristone for 7 days was assessed by qRT-PCR. Cells treated with equivalent concentrations of ethanol (EtOH) were used as control (n=4). (h) *P2Y12* expression in pBM treated with M-CSF, MDI, MDI plus NF-κB inhibitor or MDI plus p38 MAPK inhibitor was assessed by qRT-PCR. Cells treated with equivalent concentrations of dimethyl sulfoxide (DMSO) were used as control (n=8).

## 4.2 Characterization of P2Y12 expression in human macrophages *in vivo*

### 4.2.1 P2Y12 is expressed in microglia cells and splenic macrophages

Since it has been described that P2Y12 is expressed by microglia cells *in vivo*, we stained human glioblastoma sections immunohistochemically to verify specificity of our self-generated anti-hsP2Y12 antibody in formalin-fixed paraffin embedded (FFPE) tissue. We found P2Y12 strongly expressed in a subpopulation of $CD68^+$ brain-resident macrophages (Figure 14 a). In situ hybridization of glioblastoma tissue also revealed *P2Y12* mRNA expression in microglia cells (Figure 14 b).

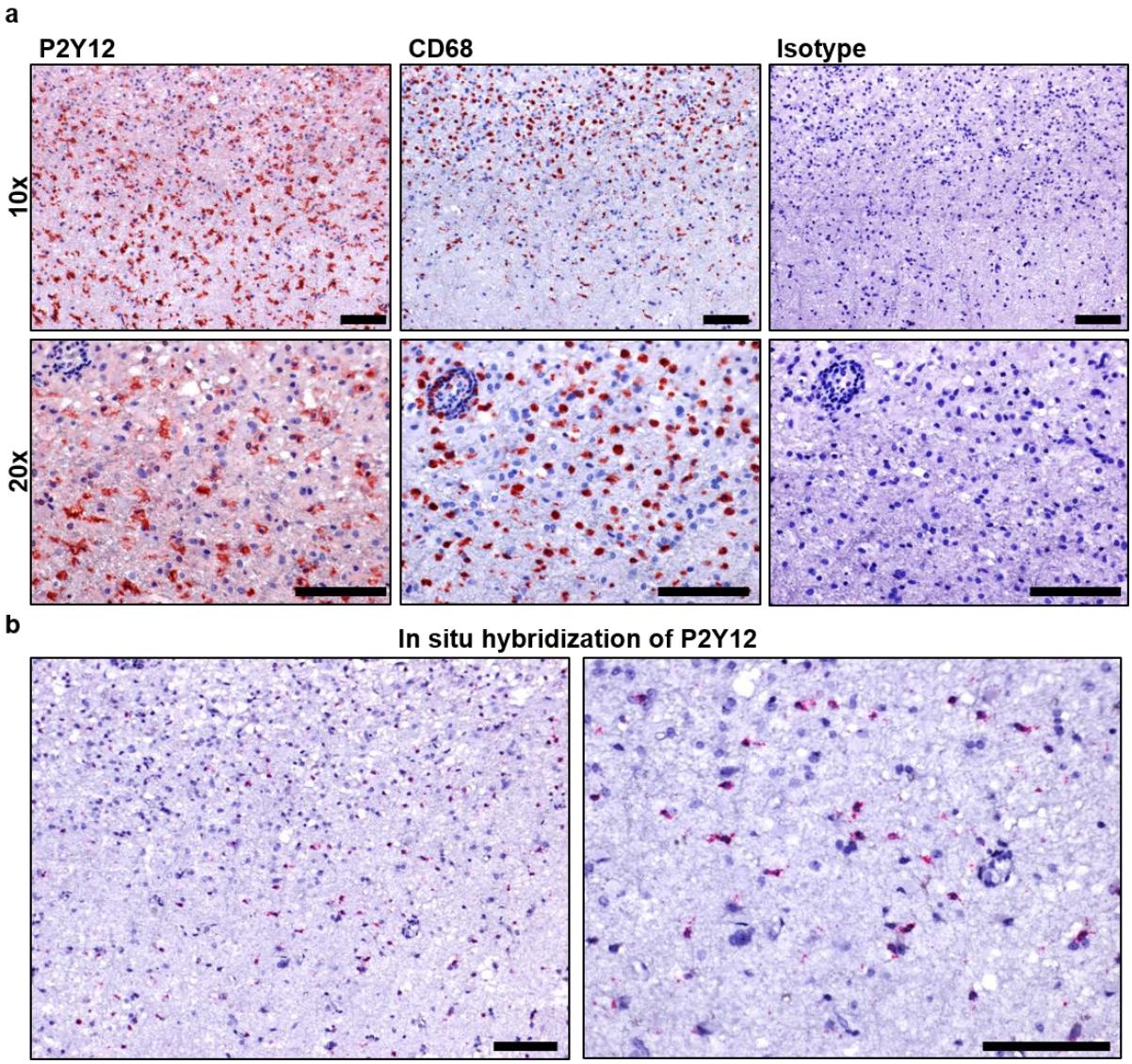


**Figure 14. Identification of $P2Y12^+$ cells in human glioblastoma.** (a) Immunohistochemical staining of a human glioblastoma using anti-hsP2Y12, anti-hsCD68 and isotype control of the anti-hsP2Y12 antibody (rabbit IgG). One representative picture is shown for each staining and magnification. Scale bar = 100 µm. (b) In situ hybridization of *P2Y12* mRNA in human glioblastoma. One representative picture is shown. Scale bar = 100 µm.

To investigate whether P2Y12 is also expressed by other tissue macrophages, we stained human spleen sections with the self-generated anti-hsP2Y12 antibody. P2Y12 was strongly expressed in the spleen. Like in human glioblastoma, not all $CD68^+$ splenic macrophages co-expressed P2Y12. $CD68^+$ $P2Y12^+$ macrophages were mostly found in the marginal zone of the splenic follicles and not so much in the germinal center and in the red pulp (Figure 15).

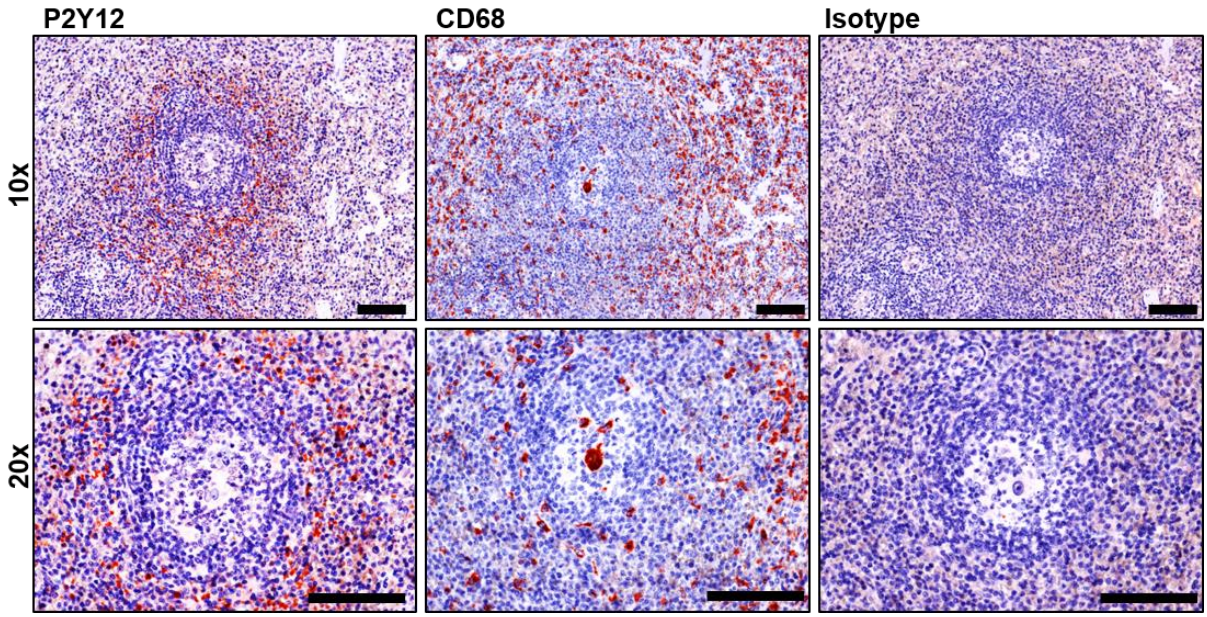


**Figure 15. Identification of $P2Y12^+$ cells in human spleen.** Immunohistochemistry of human spleen sections using anti-hsP2Y12, anti-hsCD68 and the respective isotype control of the anti-hsP2Y12 antibody (rabbit IgG). One representative picture is shown for each staining. Scale bar = 100 µm.

### 4.2.2 P2Y12 is expressed in human TAM of melanoma

Since our self-generated antibody proofed specific, we analyzed the expression of P2Y12 in human TAM of melanoma *in situ*. By immunohistochemistry we detected P2Y12 expression on a subset of $CD68^+$ macrophages in human primary melanoma (Figure 16 a). $P2Y12^+$ macrophages were mainly situated at the tumor periphery. In addition, we found P2Y12 not only expressed in macrophages of the primary tumor but also in skin metastatic lesions of melanoma (Figure 16 b). To detect *P2Y12* mRNA expression in TAM of metastatic melanoma, we performed in situ hybridization. *P2Y12* mRNA was identified in human skin metastases (Figure 16 c).

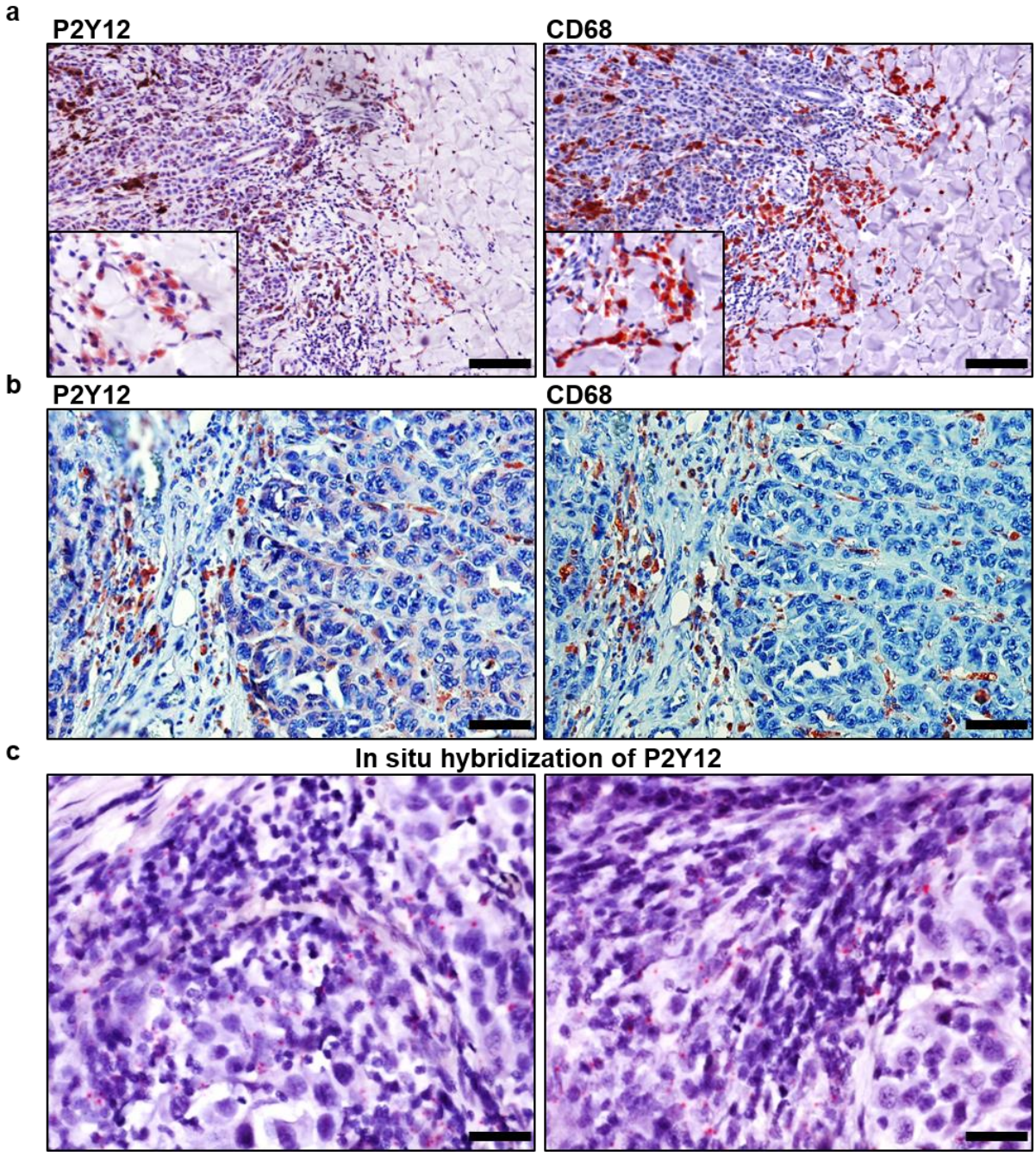


**Figure 16. Identification of P2Y12$^{+}$ macrophages in human melanoma.** (a) Serial immunohistochemical staining of a human primary melanoma using anti-hsP2Y12 and anti-hsCD68 antibodies. One representative picture is shown for each staining. Scale bar = 100 µm. (b) Immunohistochemistry of a skin metastases using anti-hsP2Y12 and anti-hsCD68 antibodies. One representative picture is shown for each staining. Scale bar = 50 µm. (c) In situ hybridization of melanoma skin metastases using a P2Y12-specific probe. Small red dots indicate *P2Y12* mRNA. Two representative pictures are shown. Scale bar = 25 µm.

To specifically detect P2Y12 in CD68$^+$/CD163$^+$ macrophages in melanoma, we established a sequential staining protocol which allows staining of the same slide consecutively with three different antibodies (anti-P2Y12, anti-CD68 and anti-CD163). We found P2Y12 to be co-expressed on a subpopulation of CD68$^+$ and CD163$^+$ cells in human primary melanoma (Figure 17 a). Immunofluorescent stainings confirmed this co-expression in TAM within the tumor tissue (Figure 17 b).

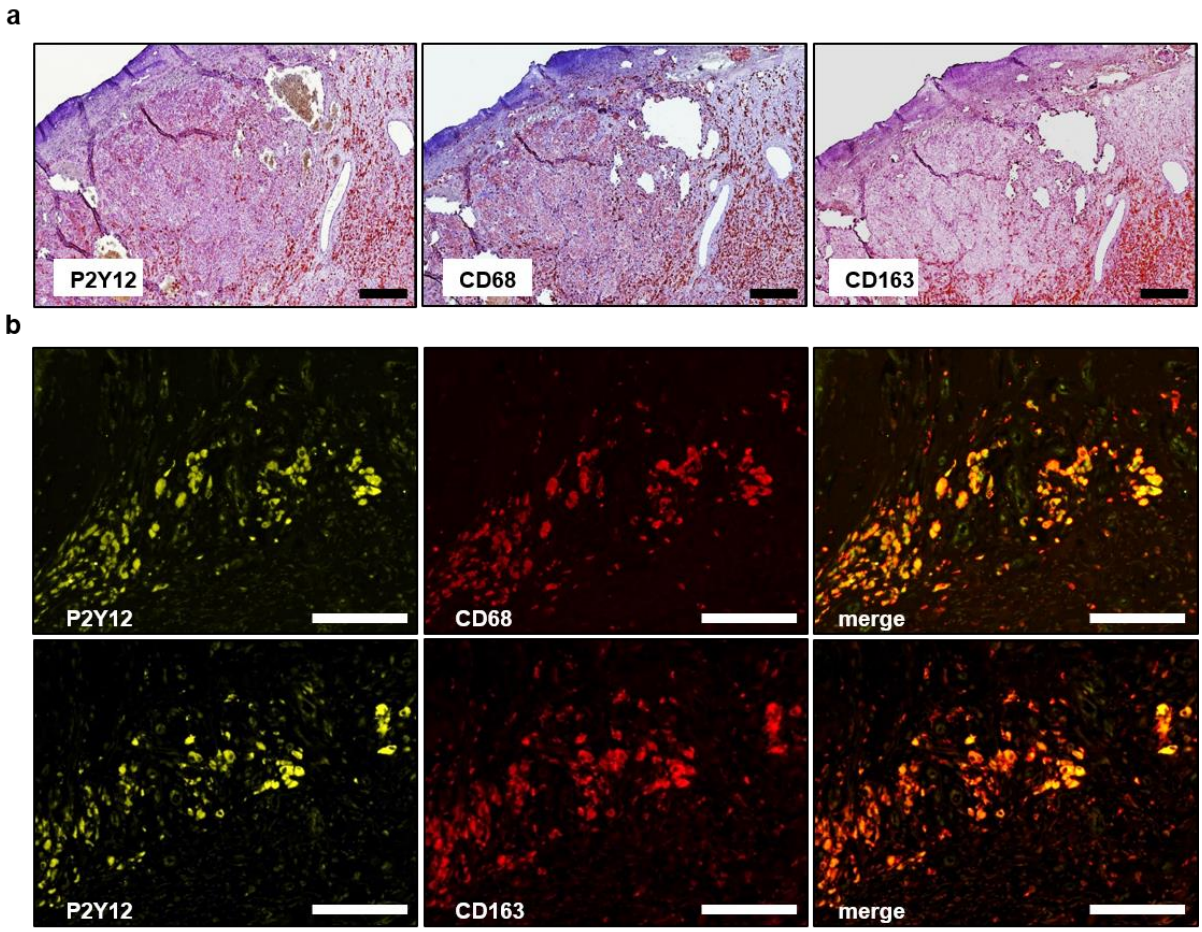


**Figure 17. P2Y12 is co-expressed in CD68$^+$ and CD163$^+$ macrophages.** (a) Sequential staining of a human melanoma section using anti-P2Y12, anti-CD68 and anti-CD163 antibodies. (b) Immunofluorescent double staining of primary melanoma using anti-P2Y12 (green) / anti-CD68 (red) and anti-P2Y12 (green) / anti-CD163 (red) antibodies. One representative picture is shown for each staining. Scale bar = 100 µm.

After identification of P2Y12$^+$ macrophages in primary as well as metastatic melanoma, we analyzed P2Y12 expression in melanocytic naevi. Immunohistochemical stainings did not reveal P2Y12 expression in human naevi, though CD68$^+$ macrophages were present in the tissue (Figure 18 a). To visualize *P2Y12* mRNA in melanocytic naevi, we performed in situ hybridization with a P2Y12-specific probe. Likewise, we could not detect *P2Y12* mRNA expression in naevi sections (Figure 18 b).

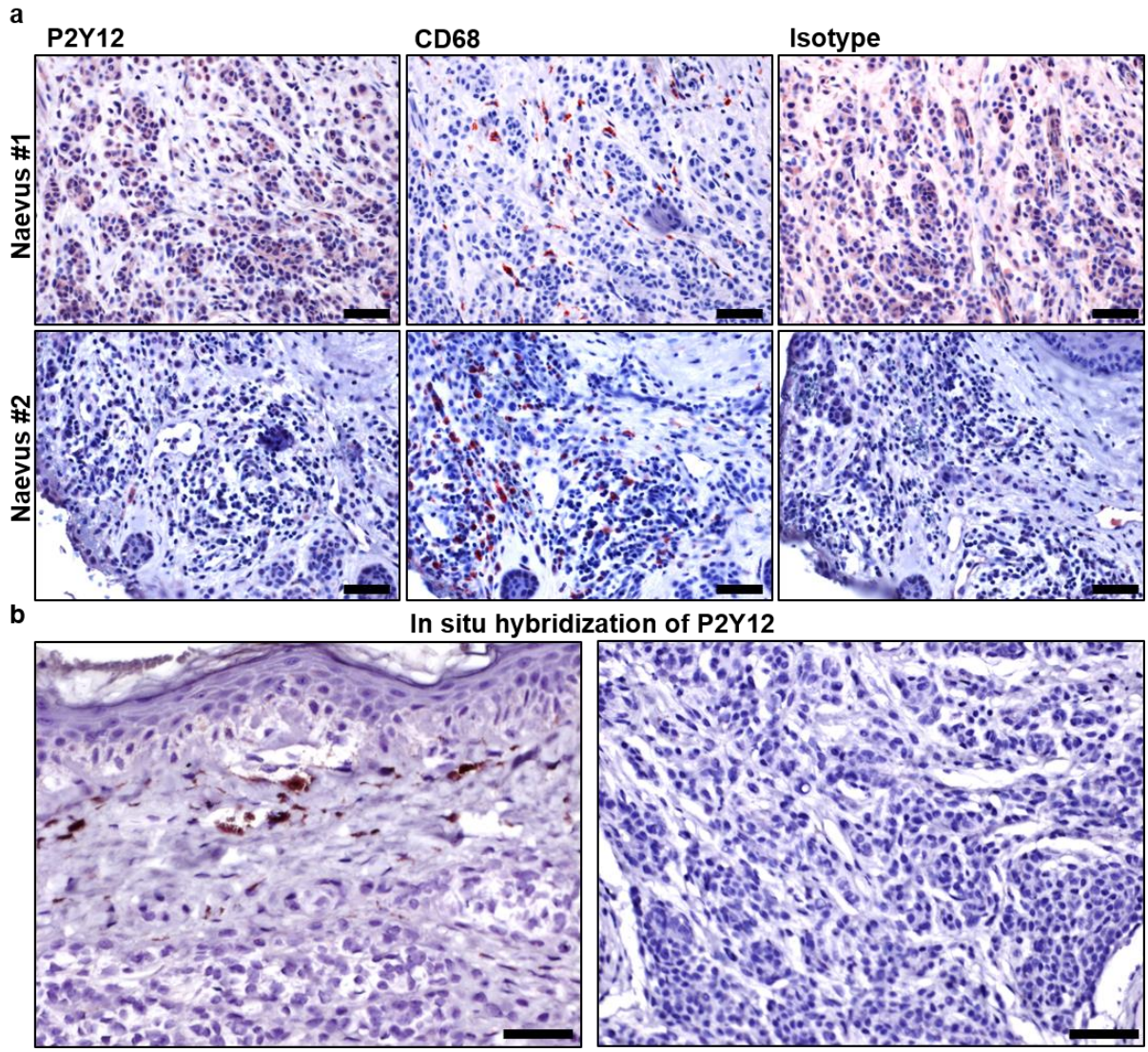


**Figure 18. P2Y12 is not expressed in melanocytic naevi.** (a) Immunohistochemical staining of human naevi using anti-hsP2Y12 and anti-hsCD68 antibodies as well as isotype control of the anti-hsP2Y12 antibody (rabbit IgG). Two representative pictures are shown. Scale bar = 100 µm. (b) In situ hybridization of *P2Y12* mRNA in human melanocytic naevi. Two representative pictures are shown. Scale bar = 50 µm.

## 4.3 Characterization of P2Y12 expression in murine macrophages

### 4.3.1 Validation of the specificity of a commercial anti-P2Y12 antibody using transgenic Raw 264.7 cells

Since we could show that P2Y12 is expressed in human TAM as well as in splenic and brain macrophages, we hypothesized that the purinergic receptor is also expressed in murine macrophages. To detect murine P2Y12, we first validated the specificity of a commercially available anti-P2Y12 antibody using transgenic P2Y12$^{+}$ Raw 264.7 cells that stably overexpress *P2y12*. qRT-PCR confirmed mRNA over-expression, and Western blot analysis as well as immunocytochemical staining verified protein over-expression in transgenic P2Y12$^{+}$ Raw 264.7 cells (Figure 19).

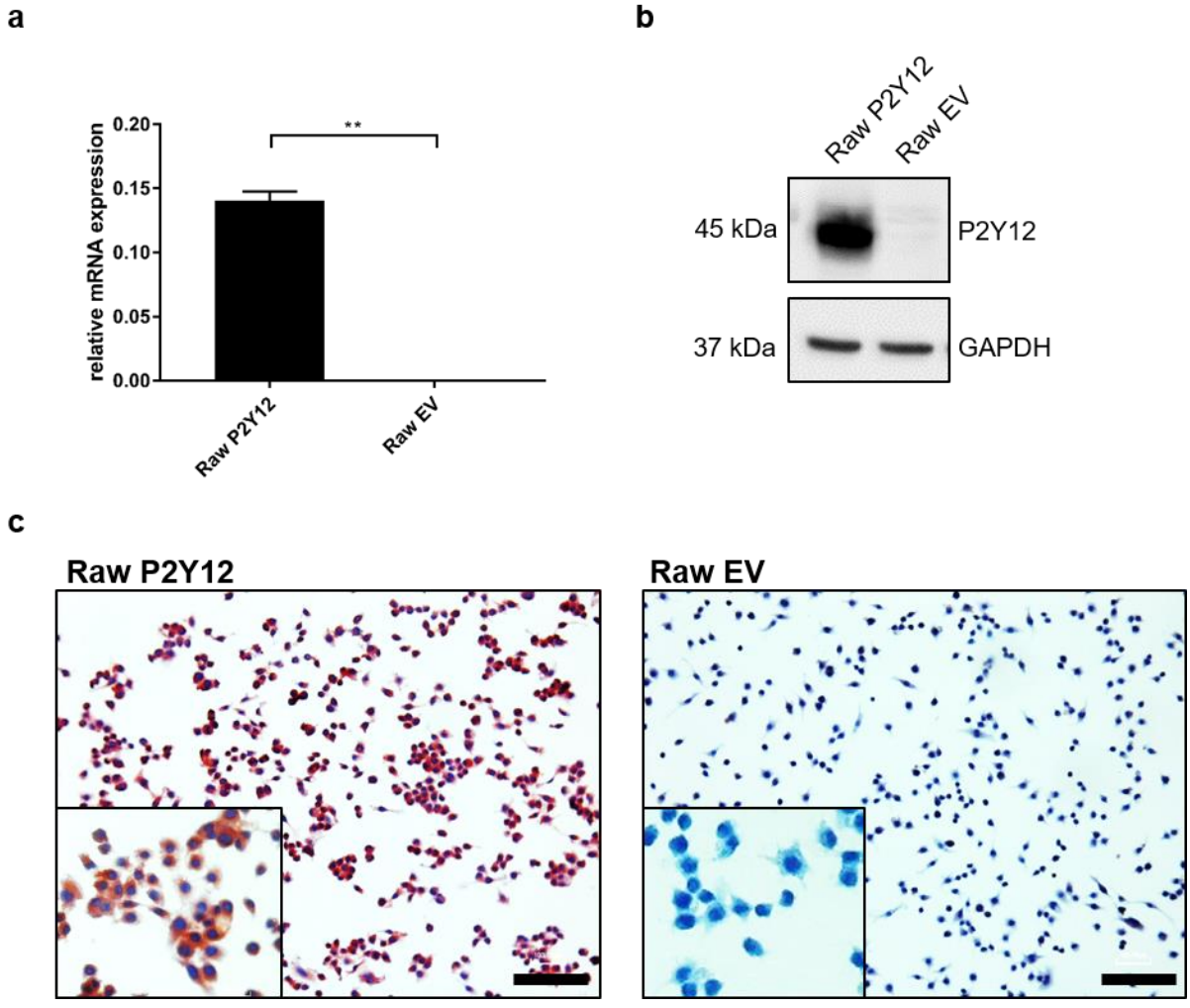


**Figure 19. Characterization of a commercially available anti-P2Y12 antibody in transgenic Raw 264.7 cells.** (a) qRT-PCR analysis of *P2y12* mRNA in transgenic Raw 264.7 cells (n=3). (b) Western blot analysis of transgenic Raw 264.7 cells using an anti-P2Y12 antibody. (c) Transgenic Raw 264.7 cells were immunocytochemically stained using an anti-P2Y12 antibody. One representative picture is shown. Scale bar = 50 µm.

### 4.3.2 P2Y12 is induced in bone marrow-derived macrophages by MDI and is expressed in murine macrophages *in vivo*

We further characterized P2Y12 expression in murine macrophages *in vitro* and *in vivo*. First, we investigated whether similar stimulations as used in the human system can induce *P2y12* also in *in vitro* generated murine BMDM. *P2y12* mRNA was significantly induced in BMDM by MDI compared to M-CSF + IFN-γ and M-CSF + LPS but not compared to M-CSF treatment. Compared to M-CSF-treated BMDM there was a significant down-regulation of *P2y12* mRNA in M-CSF + LPS treated BMDM (Figure 20 a)

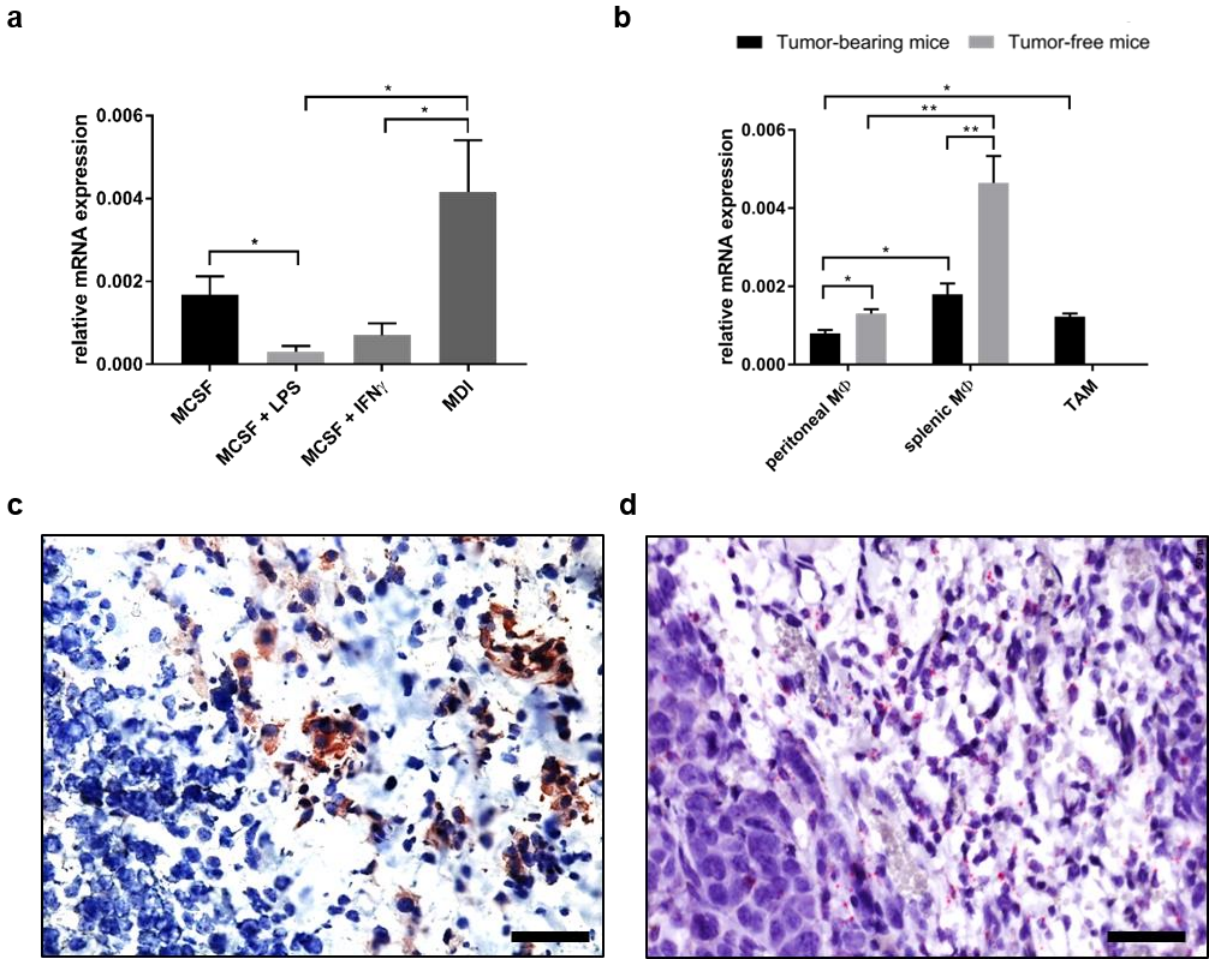


**Figure 20. P2Y12 is induced in MDI-treated BMDM *in vitro* and is expressed by murine macrophages *in vivo*.** (a) qRT-PCR analysis of *P2y12* expression in BMDM stimulated with the indicated cytokines (n=4). (b) $CD11b^+$ cells were isolated from the peritoneal fluid, spleen and from subcutaneously grown B16F10 tumors by MACS technology. *P2y12* expression was assessed by qRT-PCR analysis (n=4). (c) Immunohistochemical staining of a murine B16F10 tumor using an anti-P2Y12 antibody. One representative picture is shown. Scale bar = 50 µm. (d) In situ hybridization of *P2y12* mRNA in a B16F10 tumor. One representative picture is shown. Scale bar = 50 µm.

To investigate *P2y12* expression in murine TAM *ex vivo*, we isolated $CD11b^+$ cells from subcutaneously grown B16F10 tumors. In addition, *P2y12* expression was analyzed in peritoneal as well as splenic macrophages from tumor-bearing as well as tumor-free mice. *P2y12* was expressed by TAM as well as by peritoneal and splenic macrophages. Interestingly, *P2y12* expression in splenic and peritoneal macrophages was significantly higher in tumor-free mice compared to tumor-bearing mice (Figure 20 b).
Immunohistochemical stainings of B16F10 tumors with an anti-P2Y12 Ab revealed that P2Y12 was mainly expressed in macrophages situated in the tumor periphery (Figure 20 c). To confirm *P2y12* mRNA expression in B16F10 tumors, we performed in situ hybridization. Comparable to our protein data, we detected *P2y12* mRNA in the periphery of B16F10 tumors (Figure 20 d).

## 4.4 Functional characterization of P2Y12$^+$ macrophages

### 4.4.1 Gene expression analysis of ADP-treated P2Y12$^+$ U937 cells

To identify genes that are up-regulated by the P2Y12 receptor agonist 2-Methylthio-adenosine-5'-diphosphate (ADP) in transgenic U937 cells, we performed microarray analysis after two time points (4 h and 24 h) of ADP stimulation. We identified several genes up-regulated in ADP-treated P2Y12$^+$ U937 cells (P2Y12 ADP) compared to untreated P2Y12$^+$ U937 cells (P2Y12 CTRL) that are associated with cell motility migration and invasion. Among these genes were the matrix metalloproteinases *MMP7* and *MMP14*, urokinase/plasminogen activator (*PLAU*), urokinase/plasminogen activator receptor (*PLAUR*), the plasminogen activator inhibitors *SERPINE1* and *SERPINB2* as well as heparanase (*HPSE*) (Figure 21). These genes were not significantly up-regulated in ADP-treated EV cells (EV ADP) compared to untreated EV U937 cells (EV CTRL) (Figure 21 and Table 12). The highest up-regulated gene in P2Y12 ADP compared to P2Y12 CTRL was the chemokine *CXCL8* (IL-8), followed by the chemokine *CXCL7* (*PPBP*, pro-platelet basic protein) (Table 12). We identified several other chemokines (*CCL3L3, CXCL3, CCL20, CXCL2*), cytokines (*IL-1ß, TGF-ß3, TNFSF15, TNFSF8*) and growth factors (*HB-EGF*) up-regulated in P2Y12 ADP compared to P2Y12 CTRL (Table 12 and Figure 22). Interestingly, *CXCL7*, *CXCL8* as well as *TGF-ß3* were also induced in EV ADP compared to EV CTRL, but the fold change (FC) was much lower than in P2Y12 ADP (Table 12).

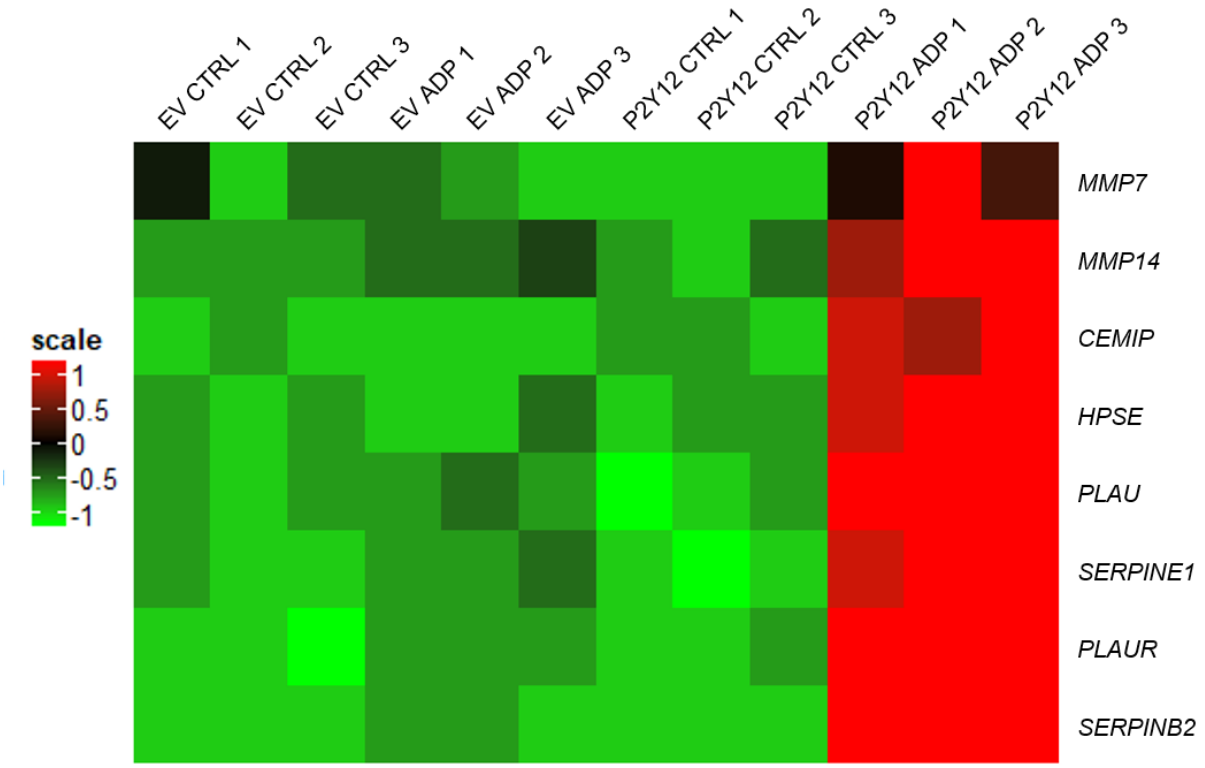


**Figure 21. Heatmap showing a selection of genes associated with cell motility, invasion and migration up-regulated by ADP in P2Y12$^+$ U937 cells after 4 h.**

**Table 12. Gene expression analysis of transgenic U937 cells showing up-regulated genes after 4 h of ADP stimulation.**

| GENE SYMBOL | GENE NAME | FC P2Y12 ADP vs. P2Y12 CTRL | FC EV ADP vs. EV CTRL |
|---|---|---|---|
| ***CXCL8*** | chemokine (C-X-C motif) ligand 8 | 62.8 | 2.0 |
| ***PPBP*** | pro-platelet basic protein (CXCL7) | 60.0 | 1.3 |
| ***IL1B*** | interleukin 1, beta | 31.3 | ns |
| *TRAC* | T cell receptor alpha constant | 27.7 | ns |
| *TM4SF1* | transmembrane 4 L six family member 1 | 27.2 | 4.9 |
| *DCSTAMP* | dendrocyte expressed seven transmembrane protein | 17.9 | 3.1 |
| *KIAA0226L* | KIAA0226-like | 13.7 | 1.6 |
| ***SERPINE1*** | serpin peptidase inhibitor, clade E | 13.5 | ns |
| *USP53* | ubiquitin specific peptidase 53 | 12.5 | ns |
| *SHC4* | SHC (Src homology 2 domain containing) family member 4 | 11.7 | ns |
| ***TGFB3*** | transforming growth factor, beta 3 | 11.5 | 1.8 |
| *HAVCR2* | hepatitis A virus cellular receptor 2 | 10.8 | 2.3 |
| *BCL2A1* | BCL2-related protein A1 | 9.2 | 1.5 |
| *GLIPR1* | GLI pathogenesis-related 1 | 9.1 | 2.1 |
| ***TNFSF15*** | tumor necrosis factor (ligand) superfamily member 15 | 8.9 | ns |
| ***CCL3L3*** | chemokine (C-C motif) ligand 3-like 3 | 8.6 | ns |
| ***CXCL3*** | chemokine (C-X-C motif) ligand 3 | 8.4 | ns |
| ***SERPINB2*** | serpin peptidase inhibitor, clade B | 8.4 | ns |
| *PHLDA1* | pleckstrin homology-like domain, family | 7.9 | ns |
| *LUCAT1* | lung cancer associated transcript 1 | 7.4 | ns |
| *TGFBI* | transforming growth factor, beta-induced | 6.3 | ns |
| *TRAF1* | TNF receptor-associated factor 1 | 6.1 | ns |
| *MGAM* | maltase-glucoamylase | 6.0 | ns |
| *MAML2* | mastermind-like transcriptional coactivator | 5.7 | ns |
| ***PLAUR*** | plasminogen activator, urokinase receptor | 5.4 | ns |
| *TMEM158* | transmembrane protein 158 | 5.2 | ns |
| *DLGAP1-AS2* | DLGAP1 antisense RNA 2 | 4.9 | ns |
| ***PLAU*** | plasminogen activator, urokinase | 4.9 | ns |
| *MACC1* | metastasis associated in colon cancer 1 | 4.7 | ns |
| *MAFB* | v-maf avian musculoaponeurotic fibrosarcoma | 4.6 | ns |
| *NT5E* | 5'-nucleotidase, ecto (CD73) | 4.4 | ns |
| *DUSP16* | dual specificity phosphatase 16 | 4.4 | ns |
| ***CCL20*** | chemokine (C-C motif) ligand 20 | 4.3 | ns |

Among the genes that were down-regulated by ADP in P2Y12$^{+}$ U937 cells compared to P2Y12 CTRL were the chemokine receptors *CXCR4* and *CCR2* (Table 13 and Figure 22). Furthermore, ADP suppressed the expression of the purinergic receptor *P2RY8* in P2Y12 ADP compared to P2Y12 CTRL. These genes were not significantly down-regulated in EV ADP compared to EV CTRL (Table 13).

**Table 13. Gene expression analysis of transgenic U937 cells showing down-regulated genes after 4 h of ADP stimulation.**

| GENE SYMBOL | GENE NAME | FC P2Y12 ADP vs. P2Y12 CTRL | FC EV ADP vs. EV CTRL |
|---|---|---|---|
| *KIT* | v-kit Hardy-Zuckerman 4 feline sarcoma v | 0.2 | ns |
| *BTLA* | B and T lymphocyte associated | 0.2 | ns |
| *MYB* | v-myb avian myeloblastosis viral oncogene | 0.3 | ns |
| *FGL2* | fibrinogen-like 2 | 0.3 | ns |
| *CXorf21* | chromosome X open reading frame 21 | 0.3 | ns |
| ***CXCR4*** | chemokine (C-X-C motif) receptor 4 | 0.3 | ns |
| *KBTBD7* | kelch repeat and BTB (POZ) domain | 0.3 | ns |
| *BCL11A* | B-cell CLL/lymphoma 11A | 0.3 | ns |
| *MIR223* | microRNA 223 | 0.3 | ns |
| ***CCR2*** | chemokine (C-C motif) receptor 2 | 0.4 | ns |
| *JMY* | junction mediating and regulatory protein | 0.4 | ns |
| *CD34* | CD34 molecule | 0.4 | ns |
| *NR1D2* | nuclear receptor subfamily 1, group D | 0.4 | ns |
| *RAP1GAP2* | RAP1 GTPase activating protein 2 | 0.4 | ns |
| *ZMYM3* | zinc finger, MYM-type 3 | 0.4 | ns |
| *LOC102723703* | uncharacterized LOC102723703 | 0.4 | ns |
| *FLJ42627* | uncharacterized LOC645644 | 0.4 | ns |
| *ZBTB12* | zinc finger and BTB domain containing 12 | 0.4 | ns |
| *PHLPP1* | PH domain and leucine rich repeat protein | 0.4 | ns |
| *FAM117B* | family with sequence similarity 117, member B | 0.4 | ns |
| ***P2RY8*** | purinergic receptor P2Y, G-protein coupled, 8 | 0.4 | ns |
| *DTX4* | deltex 4, E3 ubiquitin ligase | 0.4 | ns |
| *TFAP4* | transcription factor AP-4 | 0.4 | ns |
| *FUT7* | fucosyltransferase 7 (alpha (1,3) fucosyltransferase) | 0.4 | ns |
| *KANK2* | KN motif and ankyrin repeat domains 2 | 0.4 | ns |
| *NCF1C* | neutrophil cytosolic factor 1C pseudogene | 0.5 | ns |
| *TRIM71* | tripartite motif containing 71 | 0.5 | ns |
| *KCTD21-AS1* | KCTD21 antisense RNA 1 | 0.5 | ns |
| *DBP* | D site of albumin promoter | 0.5 | ns |
| *ASB13* | ankyrin repeat and SOCS box containing 13 | 0.5 | ns |
| *PARP8* | poly (ADP-ribose) polymerase family, member 8 | 0.5 | ns |
| *CNOT6L* | CCR4-NOT transcription complex, subunit 6 like | 0.5 | ns |
| *HSH2D* | hematopoietic SH2 domain containing protein | 0.5 | ns |

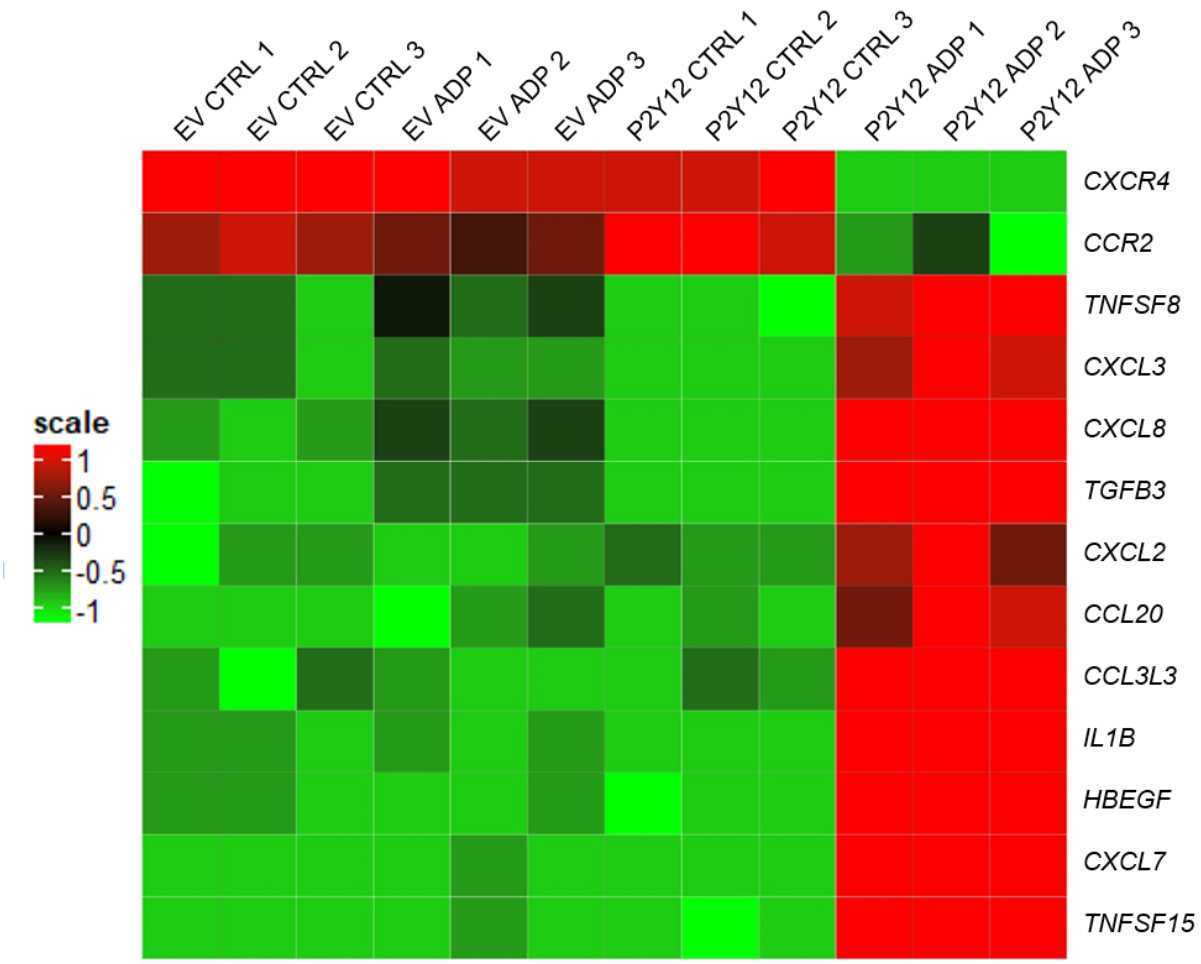


**Figure 22. Heatmap showing a selection of chemokines, cytokines, growth factors and chemokine receptors up-regulated and down-regulated by ADP in P2Y12$^+$ U937 cells after 4 h.**

After 24 h of ADP stimulation, the chemokine *CXCL7* was still strongly induced in P2Y12 ADP compared to P2Y12 CTRL (Table 14). Furthermore, the microglia marker *GPR34* as well as the macrophage markers *MRC1* (CD206) and *CD68* were up-regulated upon ADP treatment of P2Y12$^+$ U937 cells. Additional surface molecules that were found to be up-regulated in P2Y12 ADP versus P2Y12 CTRL were the tetraspanins *CD82* and *TSPAN7* as well as *CD52* and *CD34*. These genes were not induced in EV ADP compared to EV CTRL (Table 14 and Figure 23). Among the genes that were significantly down-regulated in P2Y12 ADP versus P2Y12 CTRL were *SERPINE2*, *CD48* and the adhesion receptor *ADGRA3* (Table 15).

**Table 14. Gene expression analysis of transgenic U937 cells showing up-regulated genes after 24 h of ADP stimulation.**

| GENE SYMBOL | GENE NAME | FC P2Y12 ADP vs. P2Y12 CTRL | FC EV ADP vs. EV CTRL |
|---|---|---|---|
| ***PPBP*** | pro-platelet basic protein (CXCL7) | 25.2 | ns |
| *IFI44L* | interferon-induced protein 44-like | 8.2 | ns |
| *OAS2* | 2'-5'-oligoadenylate synthetase 2 | 6.9 | ns |
| ***CD82*** | CD82 molecule | 4.7 | ns |
| *OAS3* | 2'-5'-oligoadenylate synthetase 3 | 4.1 | ns |
| *IFI6* | interferon, alpha-inducible protein 6 | 3.8 | ns |
| *ISG15* | ISG15 ubiquitin-like modifier | 3.7 | ns |
| *OAS1* | 2'-5'-oligoadenylate synthetase 1 | 3.6 | ns |
| ***CD34*** | CD34 molecule | 3.6 | ns |
| ***GPR34*** | G protein-coupled receptor 34 | 3.4 | ns |
| ***MRC1*** | mannose receptor, C type 1 | 3.4 | ns |
| ***TSPAN7*** | tetraspanin 7 | 3.1 | ns |
| *DDX60* | DEAD (Asp-Glu-Ala-Asp) box polypeptide 60 | 3.0 | ns |
| *XAF1* | XIAP associated factor 1 | 3.0 | ns |
| *HERC6* | HECT and RLD domain containing E3 ubiquitin | 2.7 | ns |
| *IFIT3* | interferon-induced protein with tetratricopeptide | 2.7 | ns |
| *IRF9* | interferon regulatory factor 9 | 2.6 | ns |
| *IFIT1* | interferon-induced protein with tetratricopeptide | 2.6 | ns |
| *CLNK* | cytokine-dependent hematopoietic cell linker | 2.5 | ns |
| *SAMD9L* | sterile alpha motif domain containing 9-like | 2.5 | ns |
| ***CD52*** | CD52 molecule | 2.4 | ns |
| *SAMD9* | sterile alpha motif domain containing 9 | 2.4 | ns |
| *SIGLEC17P* | sialic acid binding Ig-like lectin 17, pseudogene | 2.4 | ns |
| *IFI27* | interferon, alpha-inducible protein 27 | 2.4 | ns |
| *ADAM28* | ADAM metallopeptidase domain 28 | 2.4 | ns |
| *BTLA* | B and T lymphocyte associated protein | 2.4 | ns |
| *UBA7* | ubiquitin-like modifier activating enzyme 7 | 2.3 | ns |
| ***CD68*** | CD68 molecule | 2.3 | ns |
| *GSN* | gelsolin | 2.2 | ns |
| *MILR1* | mast cell immunoglobulin-like receptor 1 | 2.2 | ns |
| *SP110* | SP110 nuclear body protein | 2.1 | ns |
| *RNASE6* | ribonuclease, RNase A family, K6 | 2.1 | ns |
| *S100A10* | S100 calcium binding protein A10 | 2.0 | ns |

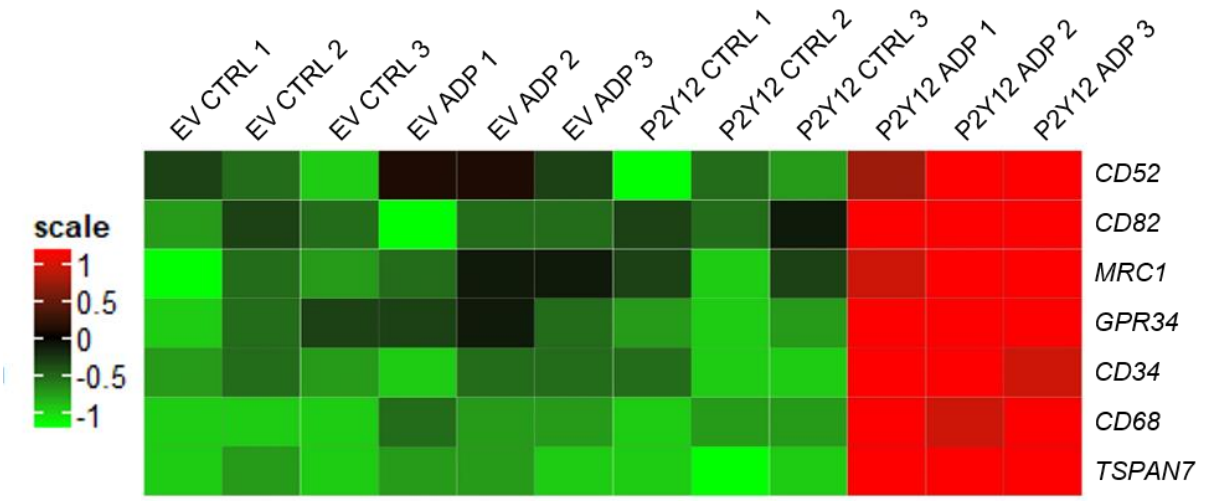


**Figure 23. Heatmap showing a selection of surface molecules and receptors up-regulated in P2Y12$^{+}$ U937 cells after 24 h of ADP treatment.**

**Table 15. Gene expression analysis of transgenic U937 cells showing down-regulated genes after 24 h of ADP stimulation.**

| GENE SYMBOL | GENE NAME | FC P2Y12 ADP vs. P2Y12 CTRL | FC EV ADP vs. EV CTRL |
|---|---|---|---|
| *AKR1C3* | aldo-keto reductase family 1, member C3 | 0.48 | ns |
| *CSAD* | cysteine sulfinic acid decarboxylase | 0.60 | ns |
| *CTH* | cystathionine gamma-lyase | 0.66 | ns |
| *CHAC1* | glutathione-specific gamma-glutamylcyclotransferase 1 | 0.68 | ns |
| *PAXIP1-AS1* | PAXIP1 antisense RNA 1 (head to head) | 0.69 | ns |
| *DDIT4* | DNA-damage-inducible transcript 4 | 0.69 | ns |
| *GPT2* | glutamic pyruvate transaminase 2 | 0.69 | ns |
| *DANCR* | differentiation antagonizing non-protein coding RNA | 0.70 | ns |
| *QPCTL* | glutaminyl-peptide cyclotransferase-like | 0.70 | ns |
| *MYT1* | myelin transcription factor 1 | 0.70 | ns |
| *NME1* | NME/NM23 nucleoside diphosphate kinase 1 | 0.71 | ns |
| *TUBE1* | tubulin, epsilon 1 | 0.72 | ns |
| *SNHG10* | small nucleolar RNA host gene 10 | 0.72 | ns |
| ***SERPINE2*** | serpin peptidase inhibitor, clade E | 0.72 | ns |
| *PWAR5* | Prader Willi/Angelman region RNA 5 | 0.73 | ns |
| *FBXL13* | F-box and leucine-rich repeat protein 13 | 0.73 | ns |
| *IPO4* | importin 4 | 0.73 | ns |
| *GCLM* | glutamate-cysteine ligase, modifier subunit | 0.74 | ns |
| *TRBV10-2* | T cell receptor beta variable 10-2 | 0.74 | ns |
| *METTL2A* | methyltransferase like 2A | 0.75 | ns |
| *HID1* | HID1 domain containing | 0.75 | ns |
| ***CD48*** | CD48 molecule | 0.76 | ns |
| *PSMD3* | proteasome 26S subunit, non-ATPase 3 | 0.76 | ns |
| *CKMT2-AS1* | CKMT2 antisense RNA 1 | 0.77 | ns |
| ***ADGRA3*** | adhesion G protein-coupled receptor A3 | 0.77 | ns |
| *ANKRD39* | ankyrin repeat domain 39 | 0.77 | ns |

Since it is known that P2Y12 is an important immunomodulatory receptor in microglia cells, we focused on cytokines and chemokines induced by ADP in P2Y12$^{+}$ U937 cells. We confirmed expression of the highest up-regulated cytokines and chemokines (*IL-8, CXCL7, CXCL2, IL-1ß, CCL3L3, CXCL3, HB-EGF, CCL20* and *TGF-ß3*) in P2Y12 ADP by qRT-PCR (Figure 24).

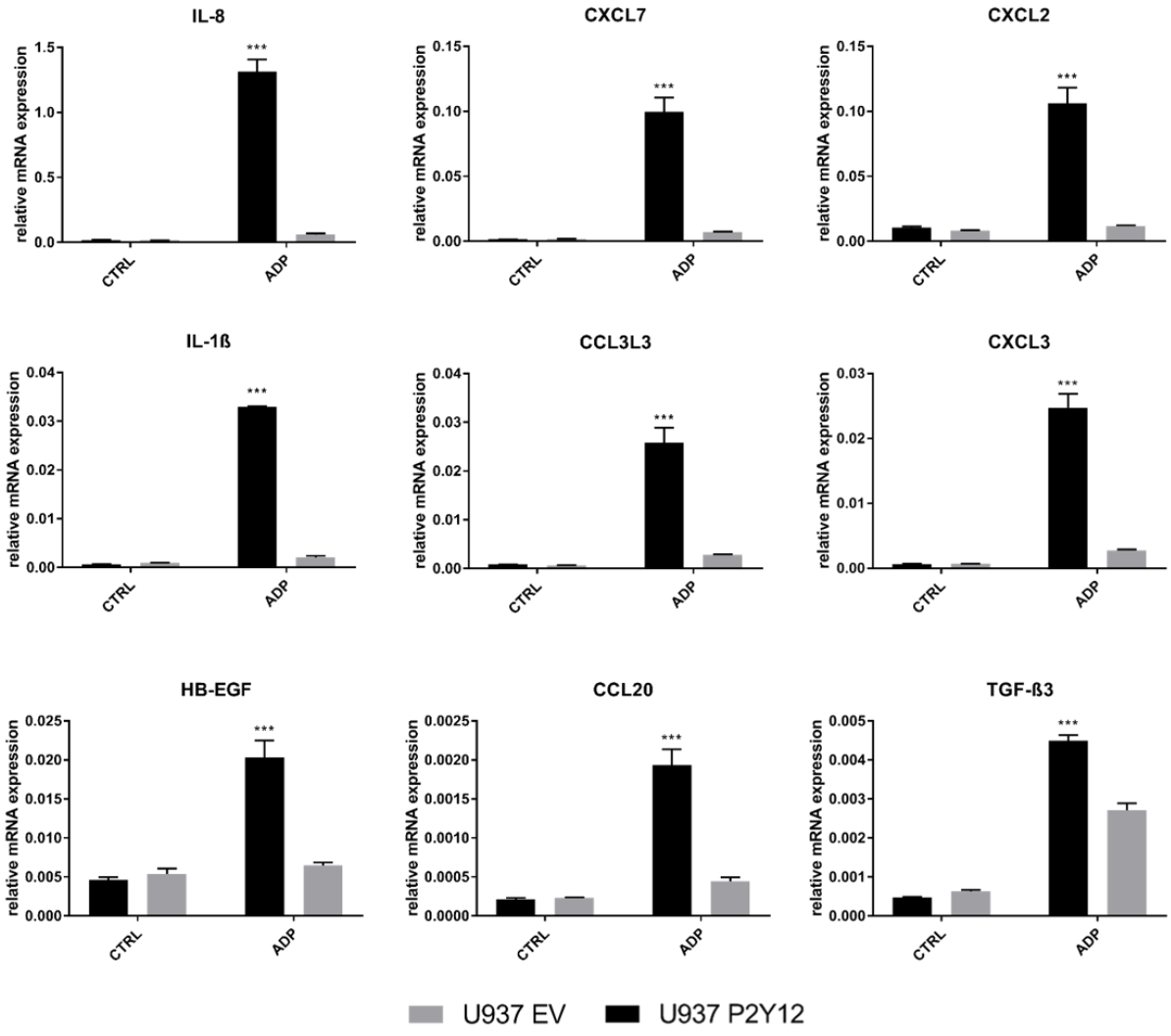


**Figure 24. Validation of microarray data by qRT-PCR focusing on cytokines and chemokines.** Transgenic U937 cells were treated with 50 nM ADP for 4 h and gene expression of the indicated cytokines and chemokines was assessed by qRT-PCR (n=3).

### 4.4.2 Cytokine and chemokine expression in ADP-treated pBM$_{(MDI)}$

In order to analyze whether the same genes that were up-regulated in ADP-treated P2Y12$^{+}$ U937 cells are also induced in P2Y12-expressing MDI-treated pBM upon ADP stimulation, we isolated human pBM and stimulated them for 7 days with MDI followed by ADP treatment for the indicated time points. Except for *TGF-ß*, which was not induced by ADP, and *CXCL2*, which was suppressed by ADP, all analyzed cytokines and chemokines that were induced in ADP-treated P2Y12$^{+}$ U937 cells were also found to be up-regulated in ADP-stimulated pBM$_{(MDI)}$ when compared to unstimulated pBM$_{(MDI)}$ (Figure 25). In contrast to P2Y12$^{+}$ U937 cells, up-regulation of most analyzed mRNAs occurred after 1–2 h in MDI-treated pBM and reached basal levels already after 4 h stimulation with ADP. Induction of *CXCL7*, which was one of the highest up-regulated genes in ADP-treated P2Y12$^{+}$ U937 cells, was not significantly up-regulated in ADP-treated pBM$_{(MDI)}$ (Figure 25).

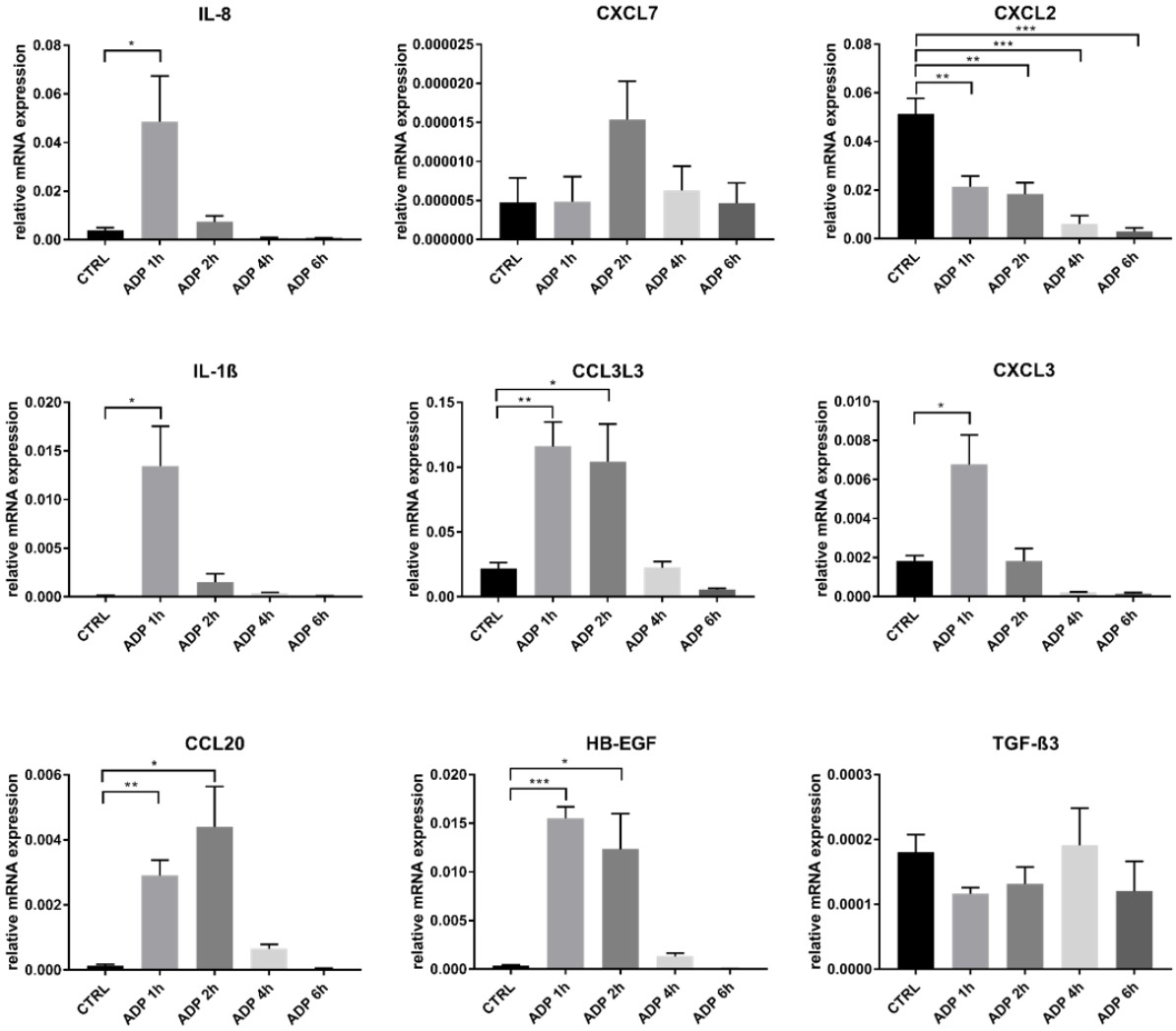


**Figure 25. Cytokine and chemokine mRNA expression is also induced in ADP-treated pBM$_{(MDI)}$.** CD14$^{+}$ pBM were isolated from the blood of healthy donors and stimulated with MDI for 7 days followed by treatment with 50 nM ADP for the indicated time points. Gene expression of the indicated cytokines and chemokines was assessed by qRT-PCR (n=4).

Since we detected induction of the pro-inflammatory cytokine *IL-1ß* in ADP-treated $pBM_{(MDI)}$ we analyzed other typical cytokines associated with a pro-inflammatory and anti-inflammatory macrophage phenotype. We showed before that expression of *TNF-α* and *CCL2* is significantly down-regulated in $pBM_{(MDI)}$ compared to $pBM_{(M\text{-}CSF)}$ whereas the expression of *IL-10* and *TGF-ß* is induced upon MDI-treatment (Figure 10). We now assessed the expression of these mediators after treatment of $pBM_{(MDI)}$ with 50 nM ADP for 30 min, 1 h, 2 h and 4 h. ADP induced the expression of the pro-inflammatory cytokine *TNF-α* and the chemokine *CCL2* whereas it suppressed the expression of the anti-inflammatory and immunosuppressive cytokines *TGF-ß* and *IL-10* (Figure 26). These data suggest that ADP reprograms macrophages towards a pro-inflammatory phenotype.

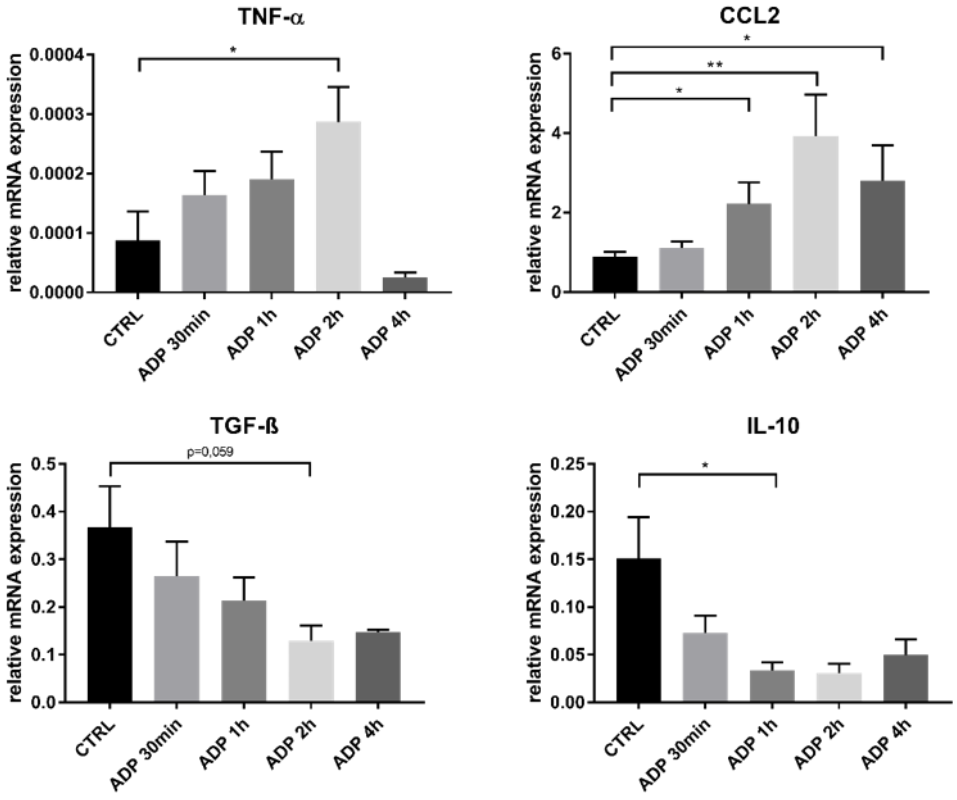


**Figure 26. ADP up-regulates pro-inflammatory mediators in MDI-treated pBM.** $CD14^+$ pBM were treated with MDI for 7 days followed by stimulation with 50 nM ADP for the indicated time points. Gene expression of the indicated cytokines and chemokines was assessed by qRT-PCR (n=4).

### 4.4.3 ADP-induced chemokine secretion in P2Y12$^+$ U937 cells can be inhibited by the specific P2Y12 antagonist PSB0739

To assess whether cytokine secretion is also enhanced by ADP in P2Y12$^+$ U937 cells, we analyzed concentrations of IL-8 (CXCL8), CXCL7 and CXCL2 in the cell supernatants of ADP-treated P2Y12$^+$ U937 cells by ELISA. Indeed, ADP treatment promoted the secretion of all three chemokines. CXCL7 levels in the cell supernatant of P2Y12 ADP were highest (511 pg/mL), followed by IL-8 (454 pg/mL) and CXCL2 (14 pg/mL) (Figure 27 a). When P2Y12$^+$ U937 cells were pre-treated with the P2Y12 specific antagonist PSB0739 prior to stimulation with ADP, chemokine secretion was significantly reduced (Figure 27 b).

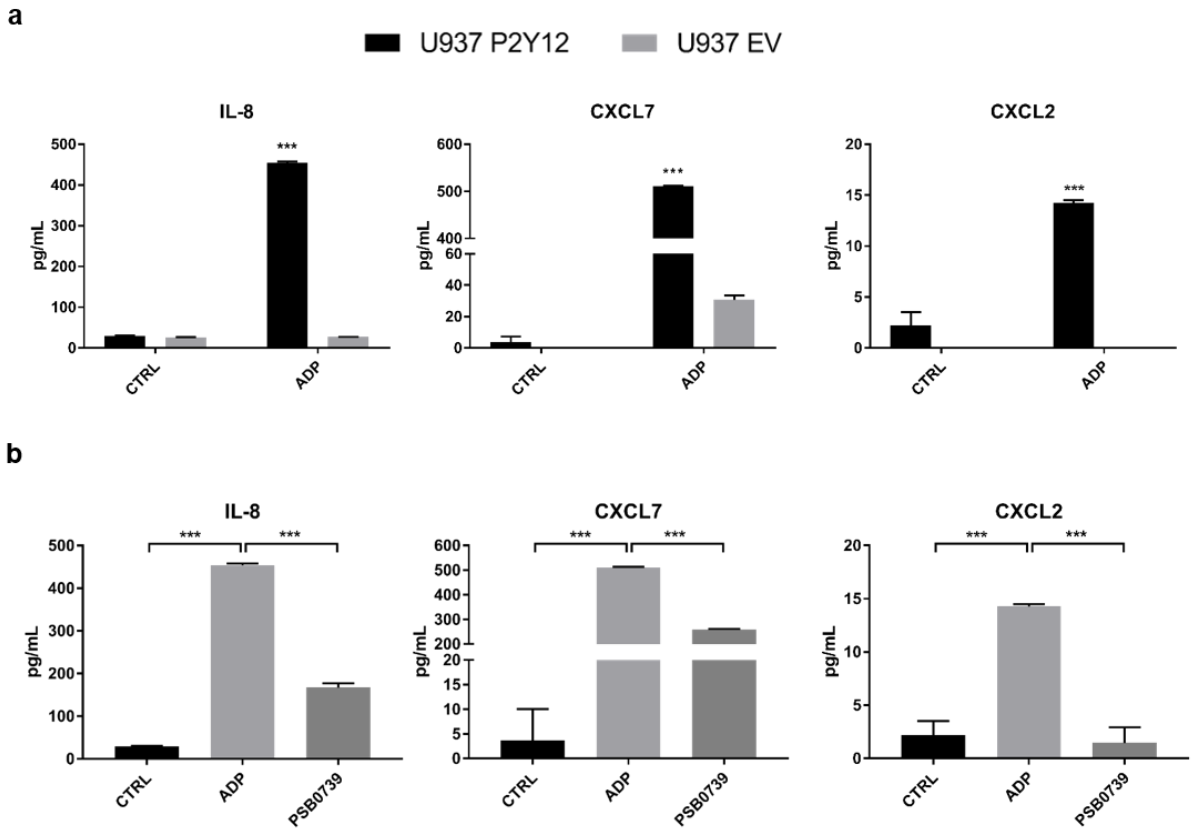


**Figure 27. Chemokine secretion is induced in P2Y12$^+$ U937 cells and can be inhibited with the P2Y12 antagonist PSB0739.** (a) 2 x $10^6$ transgenic U937 cells were treated with 50 nM ADP for 24 h. Cell supernatants were harvested, and chemokine concentrations were assessed by ELISA (n=3). (b) 2 x $10^6$ P2Y12$^+$ U937 cells were pre-treated with 10 µM PSB0739 for 30 min prior to stimulation with 50 nM ADP for 24 h. Chemokine concentrations in the cell supernatants were determined by ELISA (n=3).

We next assessed whether chemokine secretion is also induced in pBM$_{(MDI)}$ upon ADP treatment. Thus, we isolated CD14$^+$ pBM from the blood of healthy donors and stimulated the cells for 7 days with MDI to induce P2Y12 expression. Subsequently, cells were treated with 50 nM ADP for 24 h and presence of IL-8, CXCL2 and CXCL7 in the cell supernatants was

analyzed by ELISA. In contrast to P2Y12$^{+}$ U937 cells, ADP-treated pBM$_{(MDI)}$ did not show an enhanced CXCL2 or CXCL7 release and only a slightly but not significant increase of IL-8 secretion (Figure 28). Since we showed that pro-inflammatory cytokine expression is induced in ADP-treated pBM$_{(MDI)}$, we also assessed the release of IL-1ß and TNF-α. Also here, secretion of these cytokines was not enhanced in pBM$_{(MDI)}$ upon ADP stimulation (data not shown).

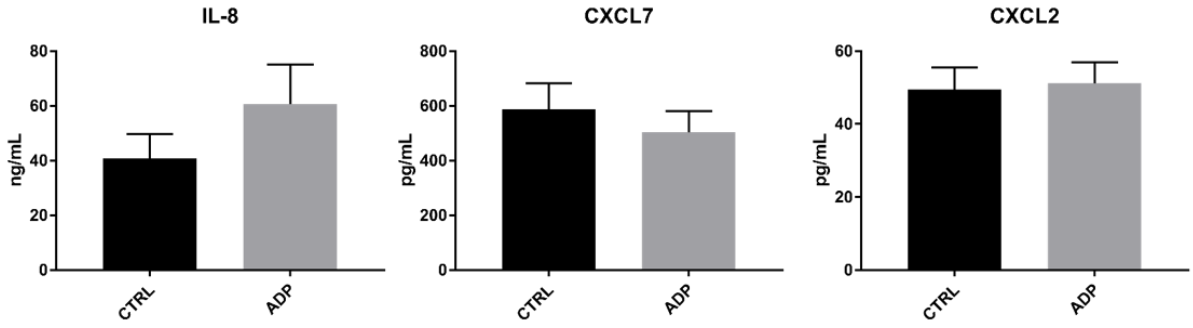


**Figure 28. Chemokine secretion is not enhanced in ADP-treated pBM$_{(MDI)}$.** CD14$^{+}$ pBM were treated with MDI for 7 days, followed by stimulation with 50 nM ADP for 24 h. Concentrations of the indicated chemokines in the cell supernatant were assessed by ELISA (n=4).

### 4.4.4 Analysis of P2Y12 downstream signaling pathways in macrophages

Aiming at analyzing signaling pathways that might lead to the induction of the found ADP/P2Y12-dependent cytokines in macrophages, we stimulated transgenic U937 cells with 50 nM ADP for 5, 15 and 30 min and performed Western blot analysis. We detected ERK1/2 as well as Akt phosphorylation after ADP treatment of P2Y12$^{+}$ U937 cells whereas these signaling pathways were only weakly induced in ADP-treated EV cells. While ERK1/2 phosphorylation was strongly induced after 5 min of ADP treatment, Akt phosphorylation was induced after 5 min as well as after 30 min (Figure 29 a) in P2Y12$^{+}$ U937 cells. Furthermore, ADP induced the expression of the transcription factor subunits *FOSL1* and *JUN*, suggesting that the transcription factor AP-1 might be a key activator of the transcription of the chemokines (Figure 29 b). Expression of *FOSL1* and *JUN* was significantly reduced when P2Y12$^{+}$ U937 cells were pre-treated with an Akt inhibitor prior to ADP stimulation. Pre-treatment with an ERK inhibitor only slightly decreased expression of both transcription factor subunits (Figure 29 c).

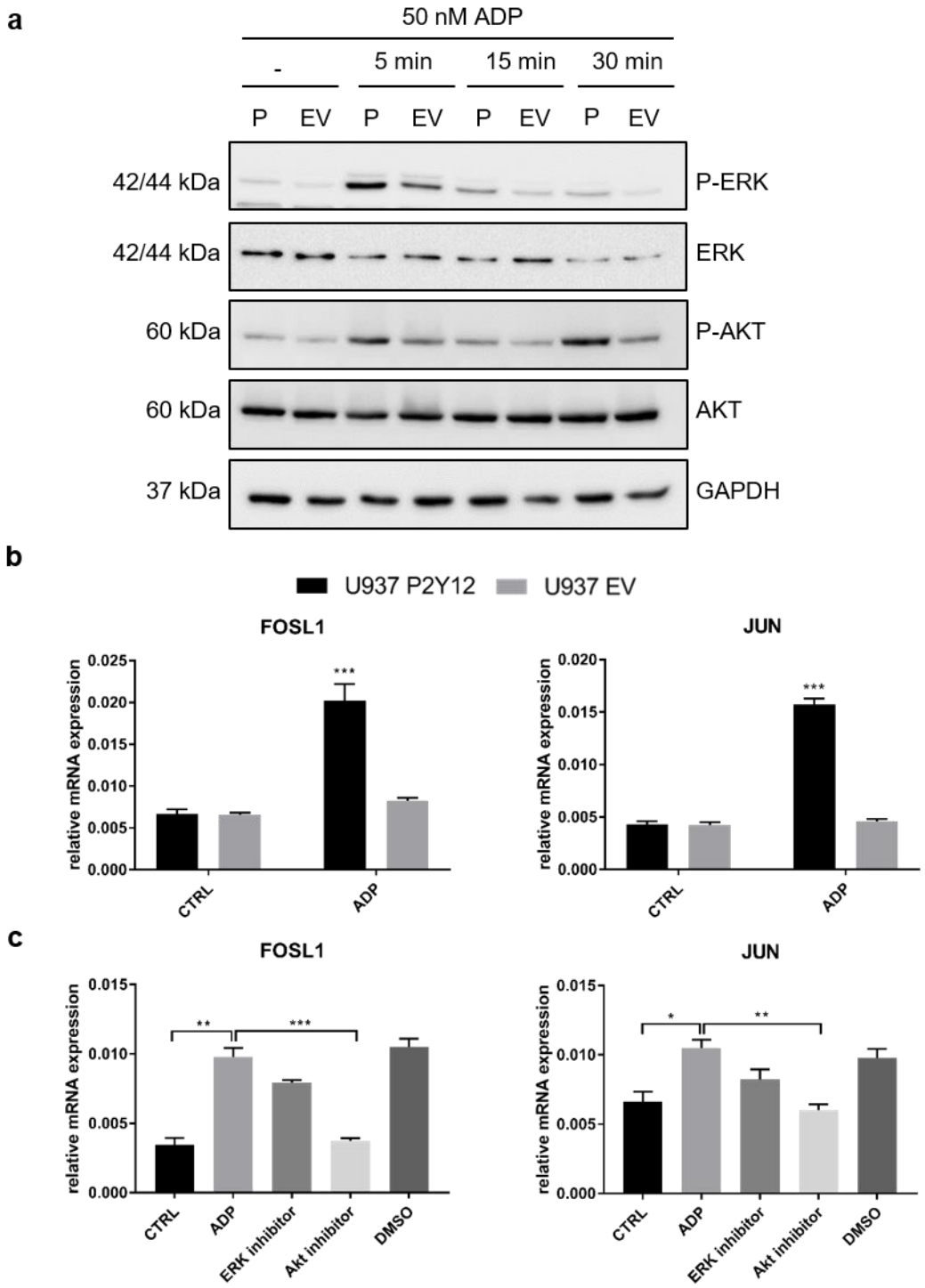


**Figure 29. ADP promotes AKT and ERK phosphorylation and induces the expression of the transcription factors *JUN* and *FOSL1* in P2Y12$^+$ U937 cells.** (a) 2 x $10^6$ transgenic U937 cells (P = P2Y12$^+$ U937 cells, EV = empty vector U937 cells) were treated with 50 nM ADP for the indicated time points and Western blot analysis was performed using anti-P-ERK1/2, anti-ERK1/2, anti-P-Akt and anti-Akt antibodies. (b) 2 x $10^6$ transgenic U937 cells were treated with ADP for 4 h and expression of *JUN* and *FOSL1* was assessed by qRT-PCR (n=3). (c) 2 x $10^6$ P2Y12$^+$ U937 cells were pre-treated with 1 µM ERK inhibitor or 1 µM Akt inhibitor for 30 min prior to stimulation with 50 nM ADP for 4 h. *JUN* and *FOSL1* expression was assessed by qRT-PCR. Cells treated with equivalent concentrations of DMSO were used as control (n=3).

To test the hypothesis that ADP induces chemokine expression via Akt and/or ERK signaling, we treated transgenic P2Y12$^{+}$ U937 cells with specific Akt and ERK inhibitors for 30 min, followed by stimulation with ADP for 24 h. We analyzed concentration of the ADP-induced chemokines CXCL2, CXCL7 as well as IL-8 in the cell supernatants by ELISA. Secretion of all three chemokines was significantly reduced upon ERK and Akt inhibition (Figure 30). While pre-treatment of P2Y12$^{+}$ cells with an ERK inhibitor only weakly reduced chemokine secretion, Akt inhibition was more effective in inhibiting ADP-induced chemokine release. A combined treatment with Akt and ERK inhibitors strongly reduced ADP-induced CXCL2, CXCL7 and IL-8 secretion. While CXCL2 and CXCL7 concentration in the cell supernatants nearly reached levels of the unstimulated control, IL-8 release could only be reduced by 50 % upon combined treatment with ERK and Akt inhibitors (Figure 30).

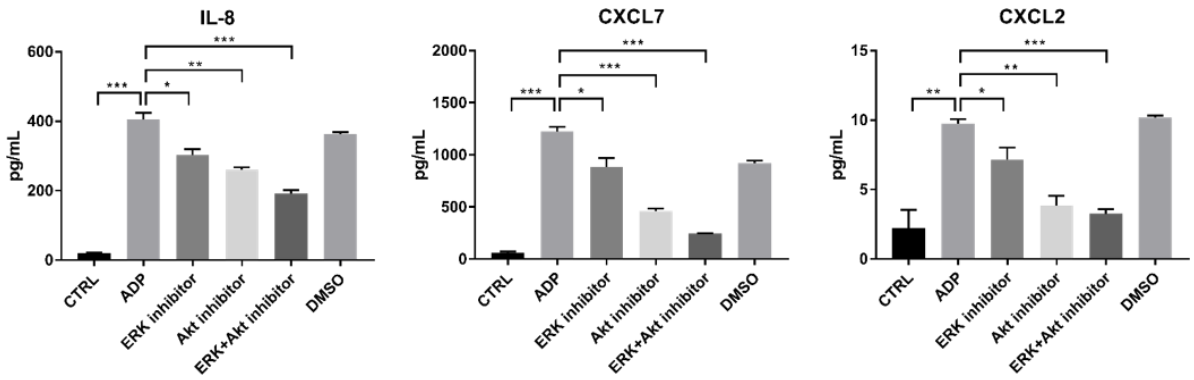


**Figure 30. ADP-induced chemokine secretion can be inhibited with ERK and Akt inhibitors.** 2 x 10$^{6}$ P2Y12$^{+}$ U937 cells were seeded in 6 well plates and pre-treated with 1 µM ERK inhibitor, 1 µM Akt inhibitor or combination of both for 30 min prior to stimulation with 50 nM ADP for 24 h. Cell supernatants were collected, and chemokine concentrations were determined by ELISA. Cells treated with equivalent concentrations of DMSO were used as control (n=3).

To test whether the same signaling pathways that are activated in P2Y12$^{+}$ U937 are also induced in MDI-treated pBM upon ADP stimulation, we isolated CD14$^{+}$ pBM from the blood of healthy donors and treated the cells for 7 days with MDI. Subsequently, cells were treated with ADP for 5, 15 and 30 min and ERK1/2 as well as Akt phosphorylation were assessed by Western blot analysis. Like in P2Y12$^{+}$ U937 cells, ADP induced ERK1/2 phosphorylation in pBM$_{(MDI)}$ after 5 min of ADP treatment (Figure 31 a). Interestingly, Akt phosphorylation was not detected in ADP-treated pBM$_{(MDI)}$ (Figure 31 a). Nevertheless, expression of the AP-1 transcription factor subunits *JUN* and *FOSL1* was induced in pBM$_{(MDI)}$ after 2–4 h of ADP treatment (Figure 31 b).

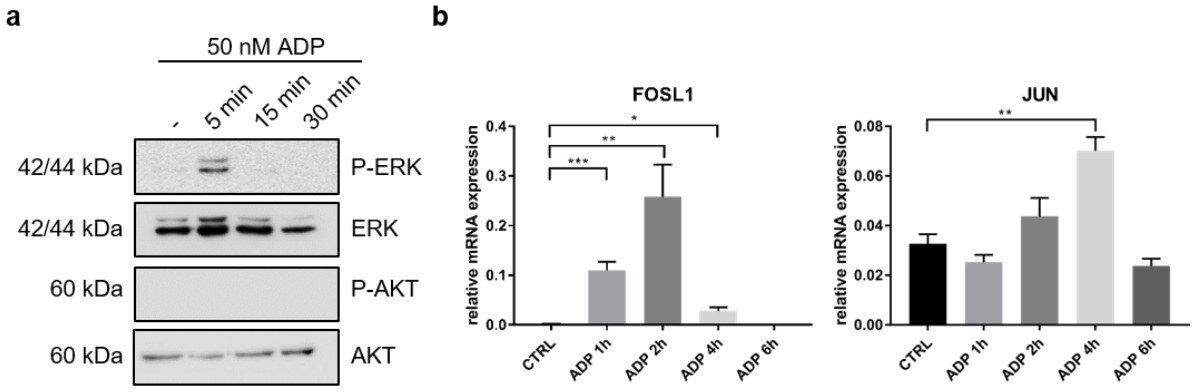


**Figure 31. ADP induces ERK phosphorylation and expression of *FOSL1* and *JUN* in pBM$_{(MDI)}$.** 3 x $10^6$ CD14$^+$ pBM were seeded in 6 well plates and stimulated with MDI for 7 days. Subsequently, cells were treated with 50 nM ADP for the indicated time points and ERK1/2 as well as Akt phosphorylation was analyzed by Western blot analysis. Stainings with anti-ERK1/2 and anti-Akt antibodies served as loading controls. One representative Western blot is shown for each antibody (n=4). (b) pBM$_{(MDI)}$ were treated with 50 nM ADP for the indicated time points and expression of *JUN* and *FOSL1* was assessed by qRT-PCR (n=4).

To investigate whether ADP induces cytokine expression in pBM$_{(MDI)}$ via the ERK signaling pathway, we pre-treated pBM$_{(MDI)}$ with a specific ERK inhibitor prior to stimulation with ADP and assessed cytokine expression by qRT-PCR. ERK inhibition did not reduce ADP-induced expression of *IL-8, IL-1ß* or *TNF-α* (Figure 32). The P2Y12 antagonist PSB0739 completely abrogated *TNF-α* expression, while *IL-8* and *IL-1ß* expression were significantly reduced but did not reach the basal levels of the unstimulated control (Figure 32). These data suggest that ADP might also activate other purinergic receptors and signaling pathways.

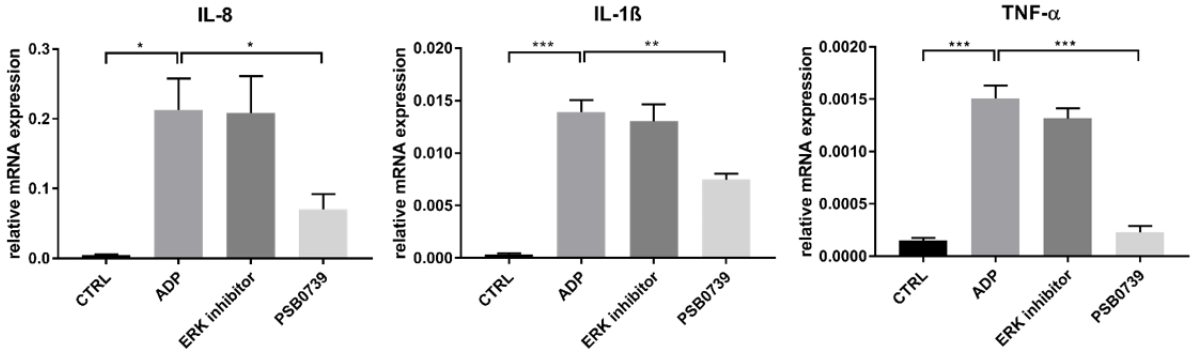


**Figure 32. The P2Y12 antagonist PSB0739 but not the ERK inhibitor reduces cytokine expression in pBM$_{(MDI)}$.** 3 x $10^6$ CD14$^+$ pBM were stimulated with MDI for 7 days. Cells were pre-treated with 1 µM ERK inhibitor or 10 µM PSB0739 for 30 min prior to stimulation with 50 nM ADP for 1 h. Gene expression of the indicated cytokines was assessed by qRT-PCR (n=4).

### 4.4.5 ADP promotes the migration of MDI-treated pBM

It is well known that nucleotides such as ATP released by dying cells act as find-me signals for purinergic receptors. Since P2Y12 is expressed on microglia cells triggering migration of these cells to the site of inflammation, we investigated whether ADP might also act as a chemoattractant for P2Y12$^+$ macrophages. We set up a transwell migration assay and seeded 2 x $10^5$ M-CSF and MDI-treated pBM in the inserts of a transwell plate. 50 nM ADP were added to the medium in the lower chamber and migration was assessed after 6 h. ADP significantly promoted the migration of MDI-treated pBM whereas it was no chemoattractant for M-CSF-treated pBM (Figure 33).

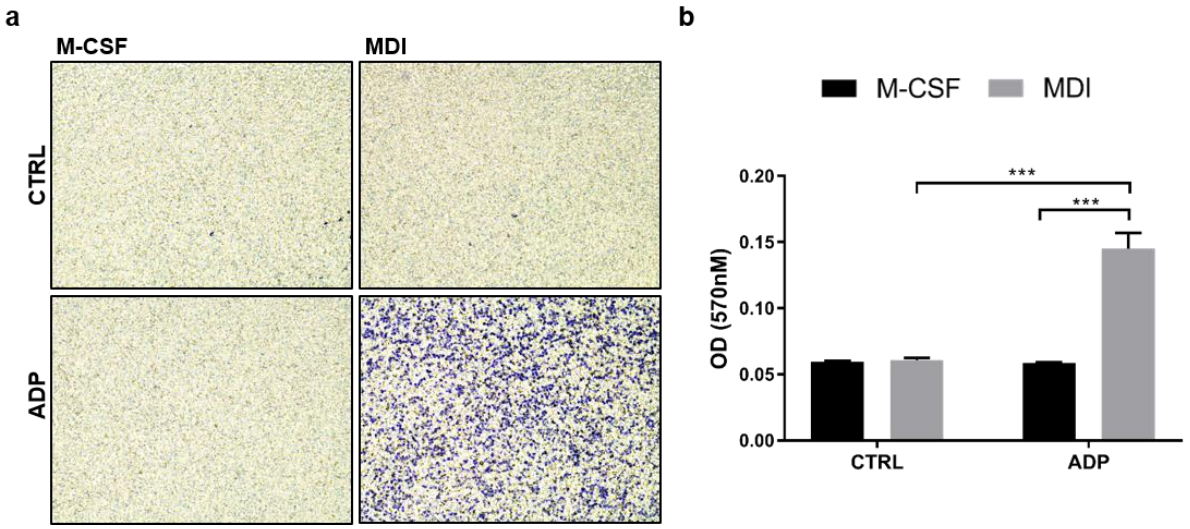


**Figure 33. ADP promotes the migration of MDI-treated pBM in a transwell chamber assay.** pBM were treated with M-CSF or MDI for 7 days, harvested, and 2 x $10^5$ cells were seeded in the insert of a transwell chamber with a 5 µm pore size. 50 nM ADP was added to X-VIVO medium in the lower chamber. Migration was assessed after 6 h by fixing the cells at the bottom of the transwell membrane with methanol followed by staining with crystal violet. (a) Pictures of the stained migrated cells at the bottom of the transwell membrane were taken using an inverted microscope. (b) Crystal violet was resolved with 100 % methanol and absorbance at 570 nm was measured by microplate reader (n=3).

### 4.4.6 ADP promotes the migration of P2Y12$^+$ Raw 264.7 cells

We next used transgenic Raw 264.7 cells as another model to investigate the ADP-induced migration of P2Y12$^+$ macrophages. Like in MDI-treated pBM that express the purinergic receptor P2Y12, ADP also acted as a chemoattractant for P2Y12$^+$ Raw 264.7 cells by promoting the migration of these cells in a transwell chamber assay (Figure 34 a–b). Interestingly, also medium without FCS significantly induced the migration of P2Y12$^+$ cells. Addition of ADP to the medium w/o FCS significantly enhanced the migration of P2Y12$^+$ Raw 264.7 cells. These

results indicate that under serum starvation cells might release nucleotides that trigger the migratory ability of P2Y12$^+$ macrophages in an autocrine manner. To exclude that ADP promotes the proliferation of P2Y12$^+$ cells, we performed a BrdU assay showing that the proliferation was not affected by ADP treatment for 48 h (Figure 34 c).

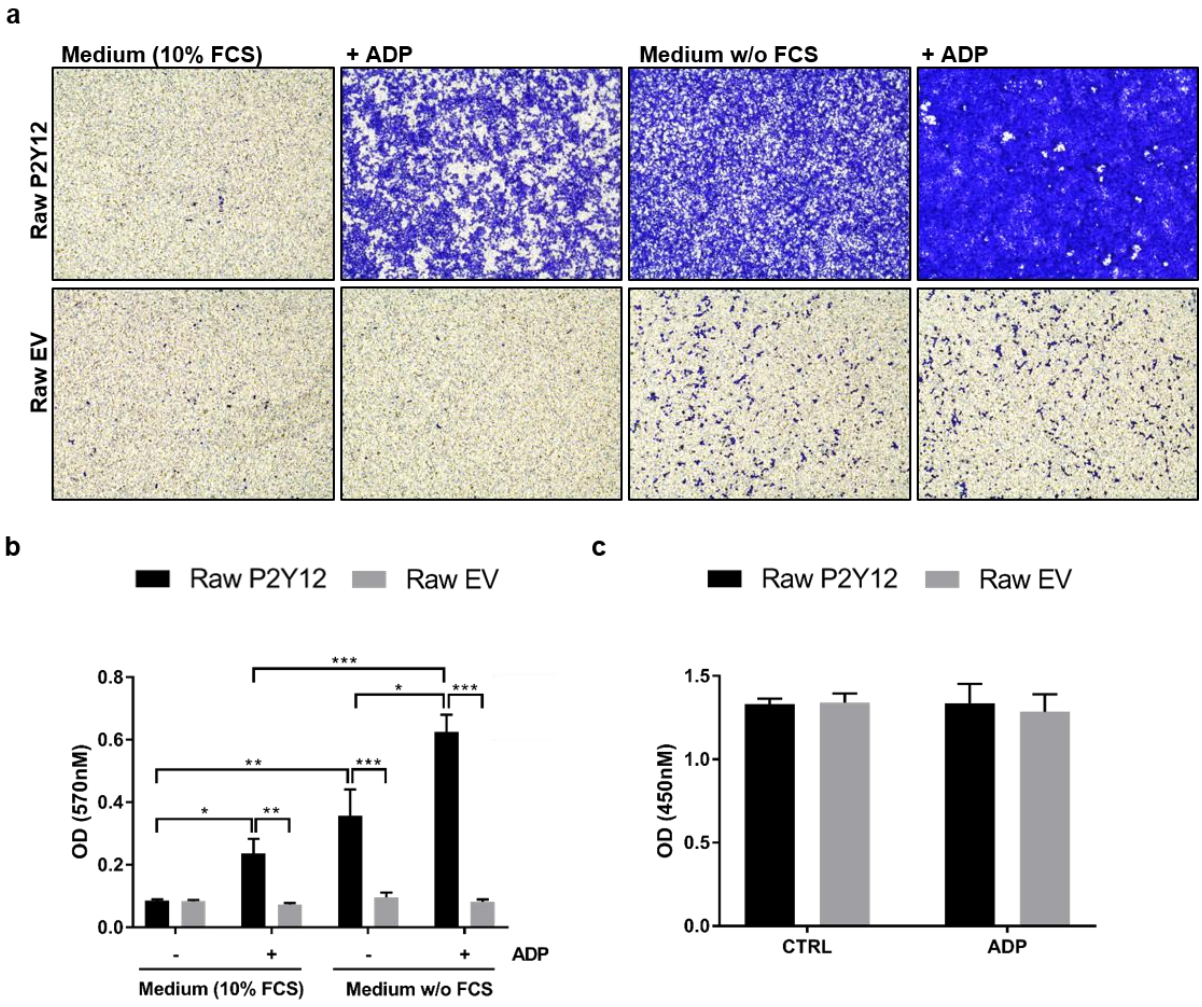


**Figure 34. ADP promotes the migration of P2Y12$^+$ Raw 264.7 cells in a transwell chamber assay.** (a-b) 5 x $10^5$ cells were seeded in a transwell insert with a 5 µm pore size. 50 nM ADP was added to the medium in the lower chamber. Migration was assessed after 16 h by fixing the cells at the bottom of the transwell membrane with methanol followed by staining with crystal violet. (a) Pictures of the stained migrated cells at the bottom of the transwell membrane were taken using an inverted microscope. (b) Crystal violet was then resolved with 100 % methanol and absorbance at 570 nm was measured by microplate reader (n=3). (c) 1 x $10^4$ transgenic Raw cells were seeded in 96 well plate and treated with 50 nM ADP for 48 h. Proliferation was assessed by BrdU assay (n=3).

In the next experiment, transgenic Raw 264.7 cells were pre-treated with the specific P2Y12 antagonist PSB0739 und migration towards ADP was assessed after 16 h. Blockade of the P2Y12 receptor significantly abrogated the ADP-induced chemotaxis of P2Y12$^+$ Raw 264.7 cells. Furthermore, when P2Y12$^+$ cells were treated with PSB0739 their migratory ability towards medium w/o FCS was significantly reduced (Figure 35).

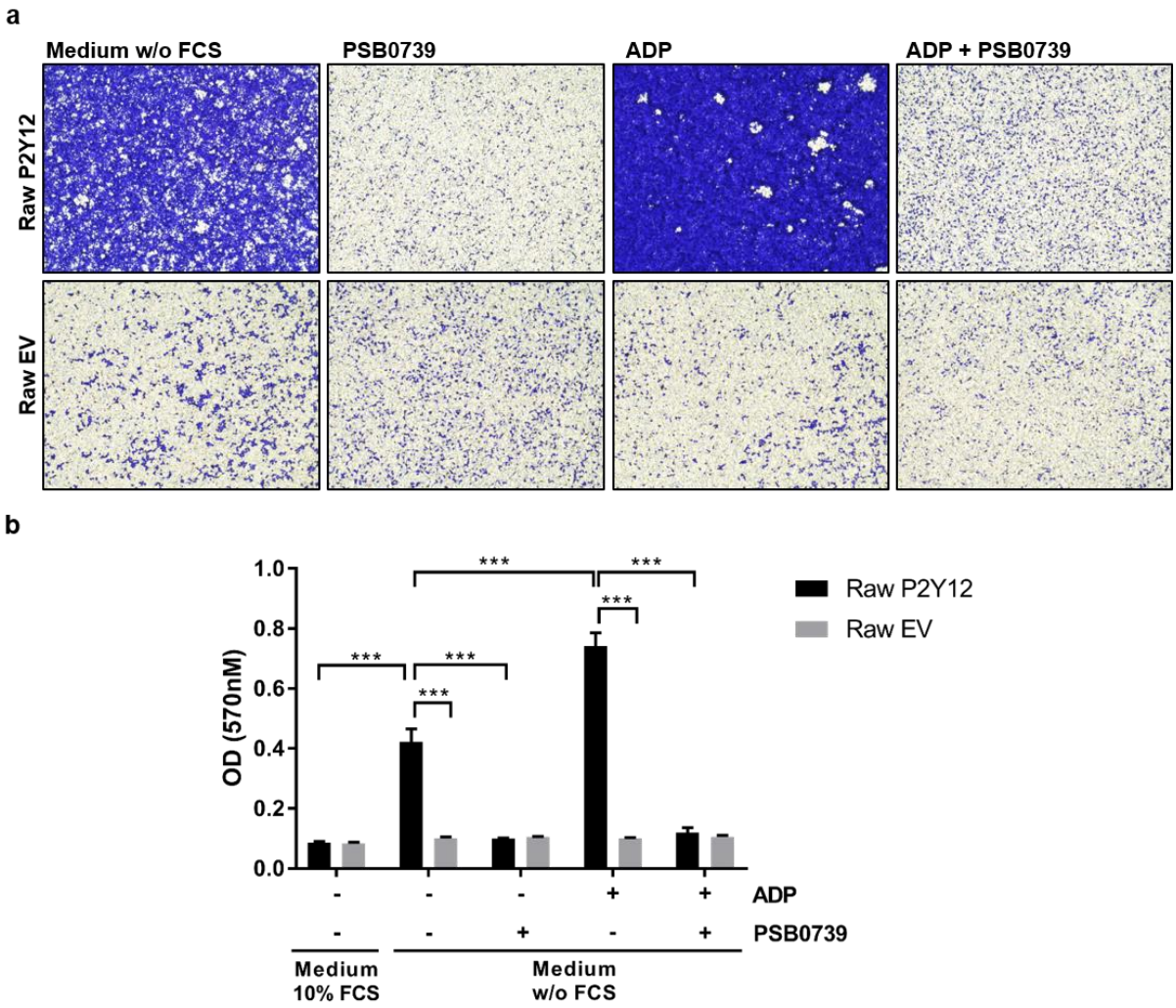


**Figure 35. P2Y12 blockade inhibits the migration of P2Y12$^+$ Raw 264.7 cells.** 5 x $10^5$ cells were seeded in 6.5 mm transwell insert with a 5 µm pore size. 10 µM P2Y12 antagonist PSB0739 and/or 50 nM ADP were added to DMEM w/o FCS in the lower chamber. Migration was assessed after 16 h by fixing the cells at the bottom of the transwell membrane with methanol followed by staining with crystal violet. (a) Pictures of the migrated cells at the bottom of the transwell membrane were taken using an inverted microscope. (b) Intercalated crystal violet was then resolved with 100 % methanol and absorbance at 570 nm was measured by microplate reader (n=3).

To test the hypothesis that upon serum starvation cells release nucleotides that trigger migration of these cells, we supplemented the DMEM w/o FCS in the lower chamber of the transwell inserts with apyrase which is an ATP/ADP-hydrolyzing enzyme. Apyrase completely abrogated the enhanced migration of P2Y12$^+$ cells towards medium w/o FCS (Figure 36 a–b). To strengthen these results, we produced conditioned medium (CM) from transgenic Raw 264.7 cells by culturing the cells in DMEM w/o FCS with or without 50 nM ADP for 24 h. The cell supernatants were then used as chemoattractants to assess the migration of transgenic Raw 264.7 cells. The CM of both cell lines, P2Y12$^+$ and EV cells, significantly promoted the migration of P2Y12$^+$ Raw 264.7 cells compared to EV cells, suggesting that the cell supernatants contain nucleotides that trigger the migration of P2Y12$^+$ macrophages.

Interestingly, the ADP-CM did not significantly enhance the migration of P2Y12$^+$ Raw 264.7 cells when compared to the CM of untreated P2Y12$^+$ cells (Figure 36 c). When apyrase was added to the CM of untreated P2Y12$^+$ cells and EV cells, the migration of P2Y12$^+$ Raw cells was significantly reduced (Figure 36 d). Taken together, these results suggest that serum-starved cells release nucleotides that trigger migration of P2Y12$^+$ macrophages in an autocrine manner.

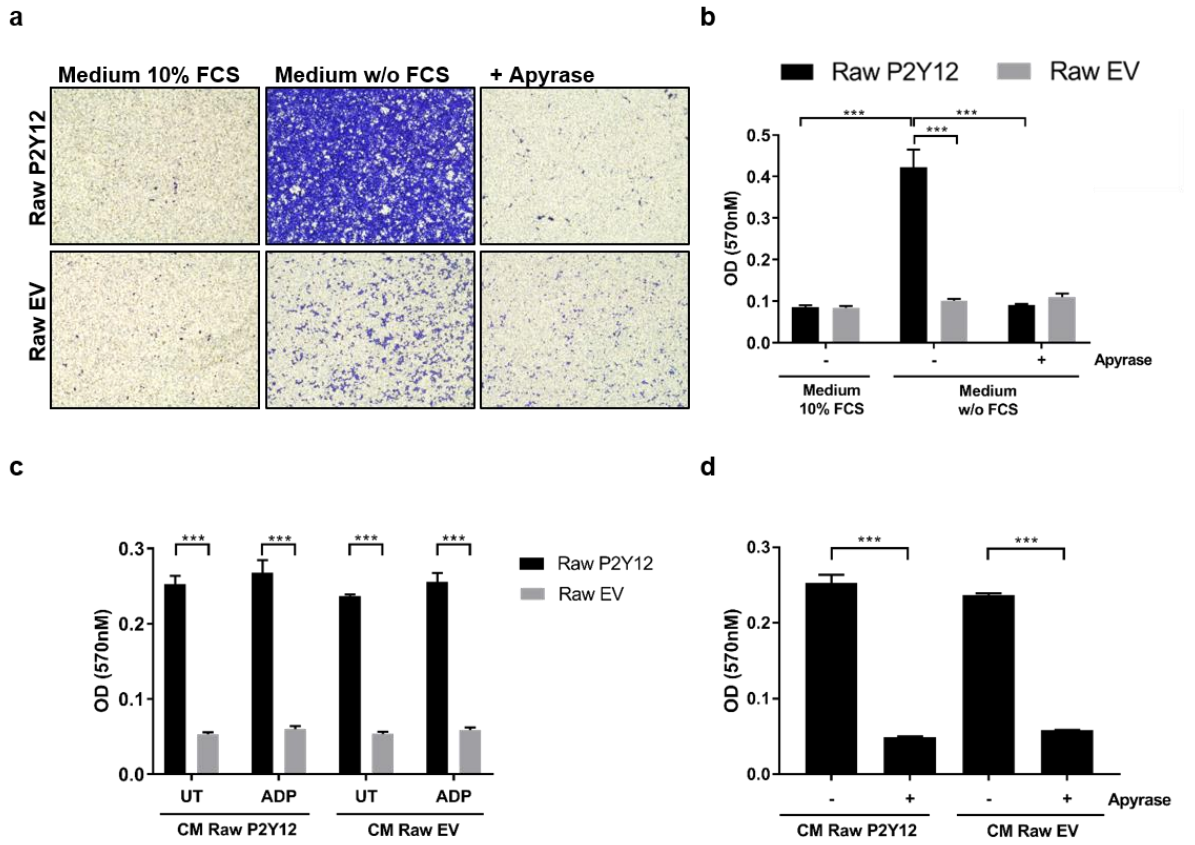


**Figure 36. Nucleotides released by serum-starved cells trigger migration of P2Y12$^+$ Raw 264.7 cells in an autocrine manner.** 5 x $10^5$ transgenic Raw 264.7 cells were seeded in 6.5 mm transwell insert with 5 µm pore size. (a–b) 1 U/mL apyrase was added to DMEM w/o FCS in the lower chamber. Migration was assessed after 16 h by fixing the cells at the bottom of the transwell membrane with methanol followed by staining with crystal violet. (a) Pictures of the migrated cells at the bottom of the transwell membrane were taken using an inverted microscope. (b) Intercalated crystal violet was then resolved with 100 % methanol and absorbance at 570 nm was measured by microplate reader (n=3). (c) Transgenic Raw 264.7 cells were seeded in DMEM w/o FCS and treated with 50 nM ADP for 24 h. The CM of ADP-treated and untreated (UT) cells was harvested and used as chemoattractant in the lower chamber of a transwell plate. (d) CM of untreated transgenic Raw 264.7 cells was supplemented with 1 U/mL apyrase. (c–d) Migration was assessed after 6 h by fixation of the migrated cells with methanol followed by staining with crystal violet. Intercalated crystal violet was then resolved with 100 % methanol and absorbance at 570 nm was measured by microplate reader (n=3).

### 4.4.7 Cell death induces the migration of P2Y12$^+$ Raw 264.7 cells

Since it is known that dying cells release nucleotides that act as find-me signals for phagocytic cells expressing purinergic receptors, we set up a transwell co-culture experiment with P2Y12$^+$ Raw 264.7 cells and B16F1 melanoma cells, which we pre-treated with 2 µg/mL puromycin to induce cell death. Since the transgenic Raw 264.7 cells contain a puromycin resistance they were not affected by the treatment. Compared to untreated B16F1 cells, puromycin-treated B16F1 cells in the lower transwell chamber significantly promoted the migration of P2Y12$^+$ cells (Figure 37). The migration of EV cells towards dying B16F1 cells was only minimally induced and was a lot weaker compared to P2Y12$^+$ macrophages (Figure 37 a).

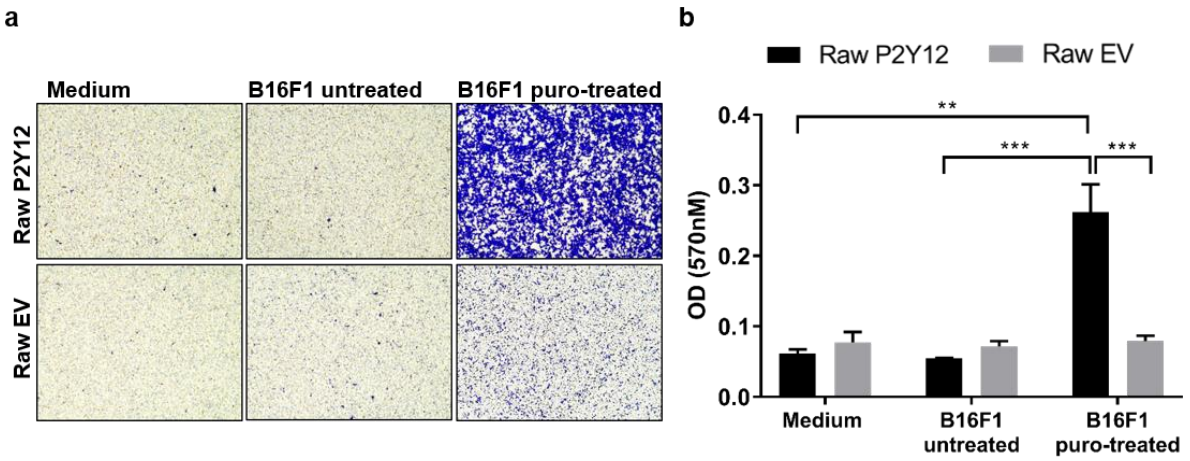


**Figure 37. Dying B16F1 cells promote the migration of P2Y12$^+$ Raw 264.7 cells in a transwell chamber assay.** 2 x $10^4$ B16F1 cells were seeded in 24 well plates. Cells were treated with 2 µg/mL puromycin for 24 h to induce cell death. Untreated B16F1 cells and medium without cells served as controls. 5 x $10^5$ transgenic Raw 264.7 cells were seeded in 6.5 mm transwell inserts with a pore size of 5 µm. Transwell inserts were then placed in the 24 well plate containing the puromycin-treated B16F1 cells. Migration was assessed after 6 h by fixation of the migrated cells with methanol followed by staining with crystal violet. (a) Pictures of the migrated cells at the bottom of the transwell membrane were taken using an inverted microscope. (b) Intercalated crystal violet was then resolved with 100 % methanol and absorbance at 570 nm was measured by microplate reader (n=3).

To test whether nucleotides are responsible for the induced migration of P2Y12$^+$ Raw 264.7 cells towards dying tumor cells, we added apyrase to the culture medium of the puromycin-treated B16F1 cells. Addition of the ATP/ADP-hydrolyzing enzyme apyrase significantly reduced the migration of P2Y12$^+$ Raw cells. Furthermore, pre-treatment of P2Y12$^+$ Raw 264.7 cells with the P2Y12 antagonist PSB0739 significantly reduced the migration towards dying B16F1 cells (Figure 38). We therefore assume that dying cells release nucleotides that act as a find-me signal for P2Y12$^+$ macrophages.

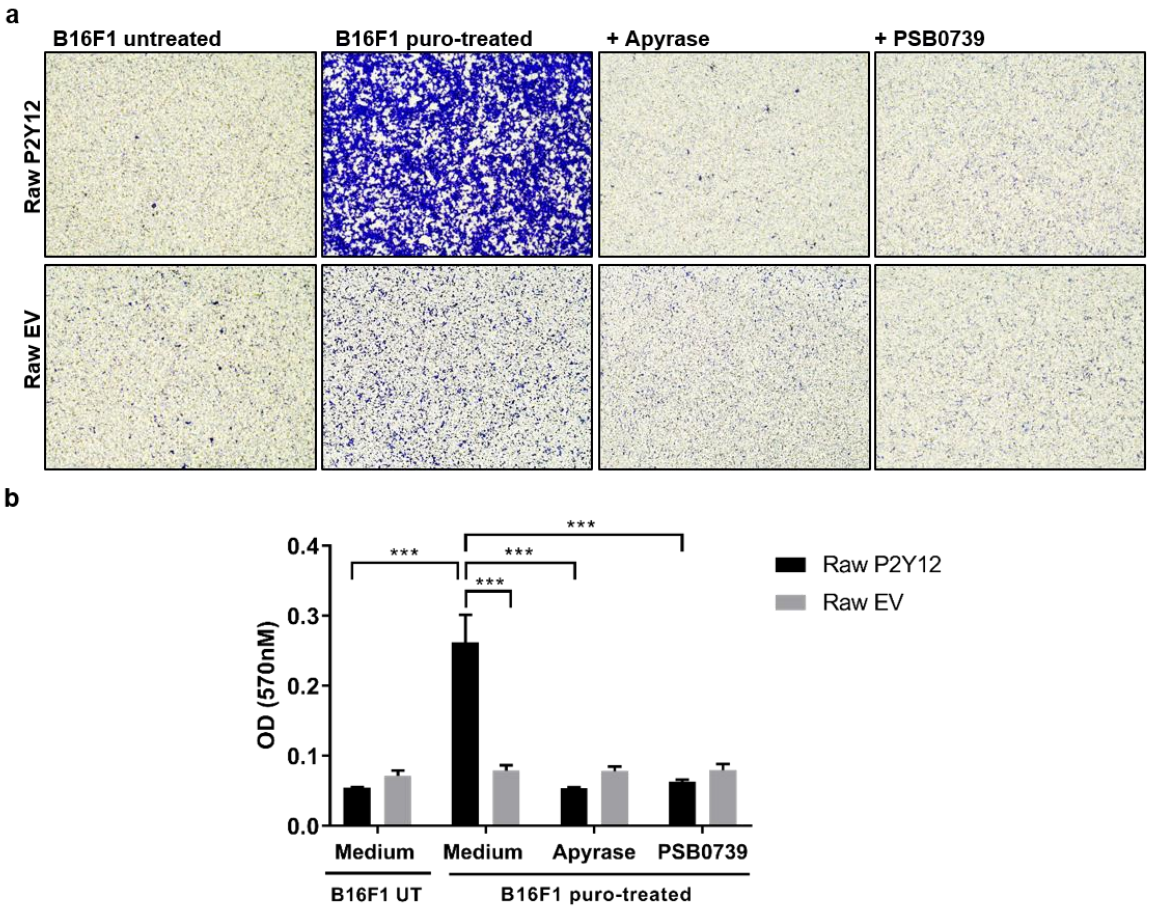


**Figure 38. Addition of apyrase or P2Y12 antagonist to dying B16F1 cells abrogates the cell death-induced migration of P2Y12⁺ Raw 264.7 cells.** 2 x $10^4$ B16F1 cells were seeded in 24 well plates. Cells were treated with 2 µg/mL puromycin (puro) for 24 h to induce cell death. Untreated (UT) B16F1 cells served as control. 1 U/mL apyrase or 10 µM PSB0739 (P2Y12 antagonist) were added to the dying B16F1 cells. 5 x $10^5$ transgenic Raw 264.7 cells were seeded in 6.5 mm transwell inserts with a pore size of 5 µm. Transwell inserts were then placed in the 24 well plate containing the puro-treated B16F1 cells. Migration was assessed after 6 h by fixation of the migrated cells with methanol followed by staining with crystal violet. (a) Pictures of the migrated cells at the bottom of the transwell membrane were taken using an inverted microscope. (b) Intercalated crystal violet was then resolved with 100 % methanol and absorbance at 570 nm was measured by microplate reader (n=3).

### 4.4.8 ADP induces cytokine secretion in P2Y12⁺ Raw 264.7 cells

We showed that ADP induces chemokine secretion in human P2Y12⁺ U937 cells (Figure 27). To assess whether chemokine secretion is also induced in the murine system, we treated transgenic Raw 264.7 cells with 50 nM ADP for 24 h and performed a cytokine array, being able to analyze 40 different cytokines and chemokines in the supernatant of ADP-treated and untreated P2Y12⁺ Raw 264.7 cells. We found an up-regulation of CXCL2, CCL4 and TNF-α secretion in ADP-treated P2Y12⁺ Raw 264.7 cells compared to untreated cells (Figure 39 a). To

proof these results, we performed ELISAs and analyzed the concentration of the three up-regulated cytokines in the cell supernatants. While we could not detect an increase in CCL4 secretion in ADP-treated P2Y12$^+$ Raw 264.7 cells, we verified a significantly enhanced TNF-α secretion and a tendency towards an increased CXCL2 secretion in ADP-treated P2Y12$^+$ cells compared to untreated P2Y12$^+$ cells and ADP-treated EV cells (Figure 39 b).

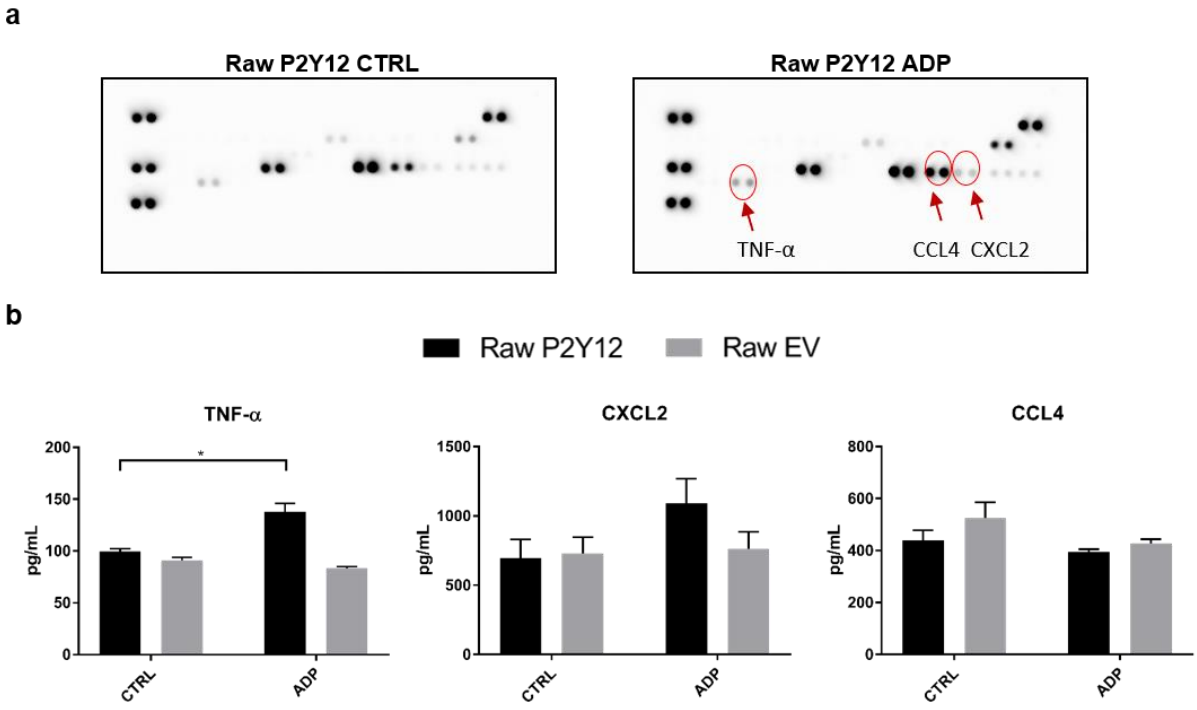


**Figure 39. ADP induces TNF-α secretion in P2Y12$^+$ Raw 264.7 cells.** (a) 1 x 10$^6$ P2Y12$^+$ Raw cells were seeded in 6 well plates and treated with 50 nM ADP for 24 h. The cell supernatants were harvested and 500 µL were used to analyse the presence of 40 different cytokines and chemokines by mouse proteome profiler cytokine array. (b) 1 x 10$^6$ transgenic Raw cells were seeded in 6 well plates and treated with 50 nM ADP for 24 h. The concentration of the indicated cytokines and chemokines in the cell supernatants was assessed by ELISA (n=3).

### 4.4.9 P2Y12 facilitates the adhesion and transmigration of U937 cells

In our previous results we showed that ADP/P2Y12 triggers migration of macrophages. Since Since others revealed that P2Y12 is an important adhesion receptor for platelets, facilitating platelet-tumor cell interactions and adhesion to endothelial cells [319, 320], we aimed at investigating whether P2Y12 supports the adhesion of monocytes to ECs and/or whether P2Y12 enhances the leukocyte-endothelial transmigration. For the adhesion assay we seeded HUVECs in gelatin-coated 12 well plates. CFSE-labelled, ADP-treated and untreated transgenic U937 cells were added to the endothelial monolayer. P2Y12$^+$ U937 cells displayed a stronger adherence to HUVECs than EV cells. Interestingly, the adherence of ADP-treated P2Y12$^+$ U937

cells was markedly reduced when compared to untreated P2Y12$^+$ cells whereas in EV cells ADP treatment had no effect on the adhesion of the cells (Figure 40 a). Next, we assessed whether transmigration is also supported by the P2Y12 receptor. We seeded HUVECs in transwell inserts and added transgenic U937 cells to the endothelial monolayer. The number of transmigrated cells was determined after 6 h by counting the cells in the lower well of the transwell chamber by flow cytometry. P2Y12$^+$ U937 cells showed the strongest transmigration, whereas the migratory ability was markedly reduced when P2Y12$^+$ U937 cells were pre-treated with ADP for 24 h. In total, only very few EV cells migrated through the HUVEC monolayer (Figure 40 b).

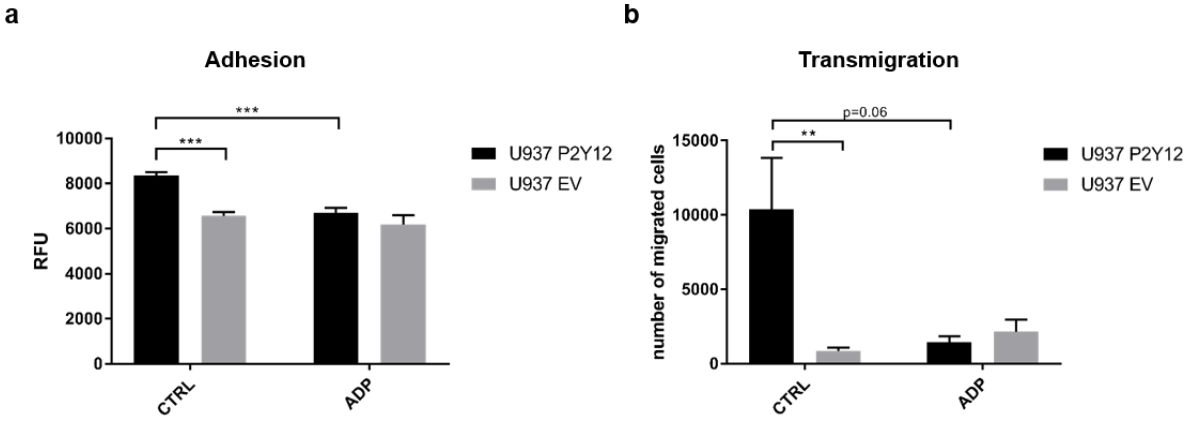


**Figure 40. P2Y12 promotes endothelial adhesion and transmigration of U937 cells.** (a) 2 x $10^5$ HUVECs were seeded in gelatin-coated 12 well plates and grown until they form a monolayer. Transgenic U937 cells were seeded in 6 well plates and treated with 50 nM ADP for 24 h. 5 x $10^5$ U937 cells were labelled with CFSE and added to the endothelial monolayer. Adherence was assessed after 1 h by lysis of the adherent cells and measuring fluorescence intensity at 480/520 nm by microplate reader (n=6). (b) 1 x $10^5$ HUVECs were seeded in 12 mm transwell inserts and grown until they form a monolayer. Transgenic U937 cells were seeded in 6 well plates and treated with 50 nM ADP for 24 h. 5 x $10^5$ transgenic U937 cells were added to the transwell inserts containing the HUVEC monolayer. After 6 h, the number of transmigrated cells present in the lower chamber of the transwell was assessed by flow cytometry (n=3).

# 5. Discussion

## 5.1 Characterization of P2Y12 expression in human macrophages

### 5.1.1 Characterization of P2Y12$^{+}$ macrophages *in vitro*

Recently, we identified Lyve-1, Slamf9 and Ms4a8a as novel TAM markers [350, 352, 353]. Besides being expressed in human or murine TAM of melanoma *in situ*, expression of Lyve-1 and Ms4a8a can be induced by the treatment of pBM or BMDM with M-CSF/dexamethasone/IL-4 (MDI) [350, 353, 354]. To identify other markers that might be relevant in TAM *in vivo* we performed gene expression analysis of MDI-treated pBM.
The purinergic receptor *P2Y12* was strongly up-regulated in pBM$_{(MDI)}$ compared to pBM$_{(M\text{-}CSF)}$. This ADP receptor is expressed on platelets and microglia but has not yet been described to be expressed on human TAM. We verified *P2Y12* mRNA expression in pBM$_{(MDI)}$ by qRT-PCR. Accordingly, Martinez et al. showed that P2Y12 is up-regulated in M2-polarized macrophages (M-CSF + IL-4-differentiated pBM) when compared to M1-polarized macrophages (M-CSF + IFN-γ + LPS-differentiated pBM), M-CSF-differentiated macrophages or monocytes [348]. Interestingly, P2Y12 was shown to be up-regulated in M2-polarized microglia, differentiated *ex vivo* with M-CSF, IL-4 and IL-13 [355]. Hohenhaus et al. showed that *P2Y12* is up-regulated in GM-CSF-differentiated MDM when compared to monocytes or M-CSF-differentiated MDM [356]. Since GM-CSF is a stimulus that generates a M1-like macrophage phenotype [357], it remains to be elucidated whether P2Y12 is also expressed on pro-inflammatory macrophages. In our hands, *P2Y12* expression was slightly higher in IFN-γ-treated pBM compared to only M-CSF-treated pBM but the highest expression was induced by MDI. Although several studies detected *P2Y12* in MDM on mRNA level, none of these studies detected P2Y12 expression on protein level probably due to the unavailability of specific antibodies in the human system. Since we also failed to specifically detect P2Y12 in pBM$_{(MDI)}$ with commercially available antibodies, we generated a rabbit anti-hsP2Y12 peptide antibody targeting the C-terminal, intracellular peptide sequence SQDNRKKEQDGGDPNEETPM. Specificity of this antibody was validated using transgenic P2Y12$^{+}$ U937 cells. We detected P2Y12 over-expression in P2Y12$^{+}$ U937 cells compared to EV cells by Western blot analysis, FACS, immunocytochemistry and immunofluorescence. We used this antibody to verify P2Y12 expression also in pBM$_{(MDI)}$ by Western blot analysis. Other combinations of pro-and anti-inflammatory cytokines failed to induce a detectable protein expression of P2Y12. In microglial cells it has been described, that *P2Y12* expression is up-regulated by the anti-inflammatory cytokine TGF-ß while pro-inflammatory stimuli such as LPS suppress *P2Y12* induction [328]. We could not detect P2Y12 expression in TGF-ß-treated pBM. As microglial cells have another origin and constitutively express P2Y12, its expression might be differently regulated as in MDM.

Besides P2Y12, our microarray analysis identified up-regulation of other purinergic receptors in pBM$_{(MDI)}$ among them *P2Y14*. This receptor belongs to the same phylogenetic family as

P2Y12. While the ADP receptor P2Y12 is mainly expressed on microglia cells and platelets, P2Y14 binds UDP-glucose and is involved in mast cell degranulation as well as neutrophil chemotaxis. Lacey et al. revealed that *P2Y14* is up-regulated in GM-CSF-treated human monocytes compared to M-CSF-stimulated monocytes [358]. Lattin et al. found that *P2y14* is expressed in murine peritoneal macrophages and is up-regulated upon LPS treatment. However, P2Y14 is also expressed on other murine leukocyte populations, suggesting that this purinergic receptor is almost ubiquitously expressed on immune cells at least in mice [345]. Further studies are needed to elucidate whether P2Y14 elicits distinct functions on these cells and whether it is also expressed on human and murine TAM.
Interestingly, we not only detected over-expression of P2Y12 and P2Y14 but also up-regulation of the purinergic receptors *P2Y1* and *P2Y13* in $pBM_{(MDI)}$. Like P2Y12, they are ADP receptors [241]. In platelets co-signaling of P2Y1 and P2Y12 is involved in platelet activation and aggregation [310]. P2Y13 mRNA was detected in $CD14^+$ monocytes, MDM, and $CD33^+$ myeloid cells [338]. In line with our results, Martinez et al. showed that *P2Y12*, *P2Y13* and *P2Y14* are up-regulated in IL-4-differentiated pBM compared to M-CSF-treated pBM [348]. Interestingly, they also found over-expression of the purinergic receptors *P2Y8* and *P2Y11* which we could not detect in our *in vitro* generated $pBM_{(MDI)}$. The function of purinergic receptors in macrophages and especially in TAM has not yet been elucidated and needs further studies. Besides purinergic receptors, we also identified up-regulation of several classical M2 markers including *ADORA3*, *LYVE1* and *CD163* in $pBM_{(MDI)}$ compared to $pBM_{(M\text{-}CSF)}$. Most of these surface molecules have previously been linked to a M2 macrophage phenotype and are also expressed in TAM *in vivo* [47, 350, 359, 360].

To verify that our *in vitro* generated macrophages resemble an anti-inflammatory M2-like phenotype, we further characterized $pBM_{(MDI)}$ regarding their marker profile, cytokine expression and cytokine secretion by FACS, qRT-PCR and ELISA, respectively. We could show that MDI-treated pBM display increased CD206 and CD163 expression while the expression of the cytokine receptors CXCR4 and CCR2 is down-regulated. CD206 and CD163 are typical M2-associated macrophage markers which are frequently used to detect M2-like TAM in human tumors *in situ*. Presence of $CD206^+$ and/or $CD163^+$ TAM correlates with tumor burden and poor prognosis in various tumor entities [351]. Furthermore, we showed that the ectonucleotidase CD73 is significantly up-regulated in $pBM_{(MDI)}$ compared to $pBM_{(M\text{-}CSF)}$. CD73 converts AMP to adenosine which is an important immunosuppressive mediator. In the tumor microenvironment, adenosine impairs proliferation and cytotoxicity of T cells and triggers M2 polarization of macrophages. Thus, depletion of CD73 or targeting adenosine receptors promotes an anti-tumor immunity thereby impairing tumor growth and progression [293, 295, 296, 299]. Zanin et al. showed that murine M2-polarized peritoneal macrophages exhibit increased expression of the ectonucleotidases CD39 and CD73 thereby converting ATP to AMP and finally to adenosine [297]. Besides surface molecules and receptors, cytokine and chemokine expression also differ between M1 and M2 macrophages [48]. We detected increased expression of IL-10 and TGF-ß in $pBM_{(MDI)}$ whereas expression and secretion of the pro-inflammatory mediators TNF-α, IL-1ß and CCL-2 was reduced. M2-like TAM and other immunosuppressive cells of the tumor microenvironment (e.g. $T_{regs}$, MDSC) express high levels of the ant-inflammatory cytokines IL-10 and TGF-ß. They impair anti-tumor immunity by inhibiting T cell response, favoring the differentiation of immunosuppressive cells and

reducing the production of pro-inflammatory cytokines thereby promoting tumor growth and progression [361, 362].

### 5.1.2 Signaling pathways underlying the induction of P2Y12 expression

Next, we investigated signaling pathways underlying the induction of P2Y12 expression. Since P2Y12 is induced by the combined treatment of pBM with dexamethasone and IL-4, we treated pBM with the glucocorticoid receptor inhibitor mifepristone and with a p38 MAPK inhibitor upon differentiation with MDI. The p38 MAPK signaling pathway is activated by different stimuli including cytokines, growth factors, stress and UV [363]. IL-4 was shown to induce p38 MAPK signaling in alternatively activated macrophages. Jiménez-Garcia et al. revealed that p38 inhibition blocked the IL-4-induced phosphorylation of STAT6, suggesting that p38 is up-stream of STAT6 signaling [364]. We showed that p38 inhibitor only slightly reduced *P2Y12* induction in $pBM_{(MDI)}$. Similar to our results, Kobayashi et al. showed that in contrast to other purinergic receptors, *P2Y12* expression in microglia cannot be suppressed by the p38 MAPK inhibitor SB203580 [365]. Interestingly, Bhattacharyya et al. showed that dexamethasone inhibits the p38 MAPK signaling pathway [366]. This could explain why inhibition of p38 MAPK had no significant effect on *P2Y12* induction in $pBM_{(MDI)}$. Although we showed that dexamethasone alone is not sufficient to induce *P2Y12* expression in pBM, the glucocorticoid receptor inhibitor mifepristone significantly suppressed *P2Y12* induction upon MDI treatment. These results indicate that glucocorticoid signaling is indispensable for P2Y12 induction. Glucocorticoids mediate immunosuppression and thus are frequently used to treat inflammatory diseases. Almost all cell types including macrophages express glucocorticoid receptors (GR) that acts as transcription factors by binding to glucocorticoid response elements (GRE). The promoter region of the *P2Y12* gene has a GRE which might be responsible for the transcription of P2Y12 after dexamethasone stimulation, but this needs further studies. In general, glucocorticoids repress the transcription of pro-inflammatory cytokines (e.g. IL-2) and inhibit the production of eicosanoids (prostaglandins, leukotrienes) which are important mediators of inflammation [367]. Dexamethasone was shown to induce an immunosuppressive M2 macrophage phenotype in various *in vitro* studies [368]. In the last decades, researchers found that glucocorticoid synthesis also occurs in the skin. During inflammation in the skin or upon exposure to inflammatory stimuli including UV irradiation, cutaneous glucocorticoid synthesis is up-regulated [369]. Thus, it is possible that local glucocorticoid synthesis in the skin polarizes macrophages to an anti-inflammatory M2 phenotype.

We also investigated whether NF-κB signaling is responsible for *P2Y12* induction in MDI-treated pBM. In thrombin-treated smooth muscle cells, NF-kB was shown to bind to the P2Y12 promoter, suggesting that thrombin increases P2Y12 expression via activation of NF-κB [370]. In pBM, inhibition of NF-κB signaling did not suppress *P2Y12* induction. Since NF-κB is an important pro-inflammatory signaling pathway and TNF-α or LPS did not induce *P2Y12* expression in pBM, it is not surprising that P2Y12 induction cannot be inhibited with the NF-κB inhibitor.

### 5.1.3 Characterization of P2Y12$^+$ macrophages *in vivo*

Since we detected P2Y12 in MDI-treated pBM *in vitro*, we aimed at investigating whether P2Y12 is also expressed in human TAM of melanoma. To verify specificity of our self-generated anti-hsP2Y12 antibody for the application in immunohistochemistry, we first stained human glioblastoma sections and specifically detected P2Y12 in microglia cells. Several studies have described the expression of P2Y12 on resting microglia. In these cells P2Y12 is involved in sensing of nucleotides and chemotaxis during tissue damage [325]. Since microglia cells origin from the yolk sac it is not clear whether monocyte-derived tissue macrophages also express P2Y12. Moore et al. detected P2Y12 expression in microglia, but failed to detect P2Y12 protein expression in *in vitro* generated MDM [355]. TAM mainly consist of MDM that origin from the bone marrow or spleen [371]. To detect P2Y12 in TAM, we analyzed human melanoma sections. We established a sequential staining protocol to specifically detect P2Y12 in CD68$^+$ and CD163$^+$ macrophages. While CD68 is frequently used to detect myeloid cells in general [372, 373], CD163 is a specific marker for mature macrophages [374]. Various studies have shown that the presence of CD163$^+$ macrophages correlates with tumor burden and poor overall survival in many tumor entities including melanoma [351]. Indeed, we found co-expression of P2Y12, CD68 and CD163 in primary melanoma sections, as well as melanoma metastases. We confirmed existence of P2Y12$^+$ CD163$^+$ macrophages by immunofluorescence. Not all CD68$^+$ macrophages were positive for P2Y12, indicating that the purinergic receptor is only expressed on a distinct macrophage subpopulation. Furthermore, P2Y12 expression was also detected on CD68$^-$ cells, which might be platelets or other immune cells as P2Y12 was found to be expressed also on *ex vivo* isolated mast cells and eosinophils [340, 342]. Although we found CD68$^+$ cells in melanocytic naevi, we failed to detect P2Y12 expression by in situ hybridization and immunohistochemistry indicating that the ADP receptor is either up-regulated by specific stimuli in the tumor microenvironment or P2Y12$^+$ cells are recruited to the tumor site. Since we found P2Y12$^+$ macrophages in the spleen, it is possible that these macrophages are also recruited during tumor progression.

## 5.2 Characterization of P2Y12 expression in murine macrophages

We aimed at investigating whether P2Y12 is also expressed in murine macrophages. It is well accepted that there are differences between human and murine M2-polarized macrophages. Murine M2 macrophages express Ym1 (Chi3l3) and Fizz1 and which are not expressed by human M2 macrophages [375, 376]. However, there are also markers including CD163 and CD206 that are shared by human and murine TAM. Previously, our group could show that several M2 macrophage markers can be induced *in vitro* in murine BMDM by dexamethasone treatment [353, 354]. To analyze whether we can induce *P2y12* expression in these cells, we isolated BMDM and stimulated them with M-CSF for 3 days, followed by stimulation with different pro- and anti-inflammatory cytokines for 4 days. Like in human pBM, strongest *P2y12* induction was observed upon MDI treatment. However, *P2y12* expression could also be detected in M-CSF treated BMDM. In line with our results, Barbera-Cremades et al. showed

that *P2y12* is up-regulated in murine BMDM during M-CSF differentiation [377]. We also revealed a much weaker *P2y12* expression in LPS or IFN-γ-differentiated M1 macrophages. Consistently, Lattin et al. showed that *P2y12* is down-regulated in BMDM by LPS [345]. In contrast to our results, Zanin et al. showed that purinergic receptors including *P2y12* are not differentially expressed between murine M1 and M2-polarized peritoneal macrophages. However, instead of differentiating BMDM with M-CSF prior to stimulation with pro and anti-inflammatory cytokines they used murine peritoneal macrophages and treated them with IL-4 and LPS to generate M2 and M1 macrophages, respectively [297].

Although several studies investigated *P2y12* induction in murine BMDM or peritoneal macrophages, none of these studies focused on P2Y12 expression in tissue-resident macrophages. To analyze *P2y12* expression in macrophages, we isolated CD11b$^+$ myeloid cells from the spleen, peritoneal fluid and from B16F10 tumors of tumor-bearing mice and from the spleen and peritoneal fluid of tumor-free C57BL/6 mice and assessed *P2y12* expression by qRT-PCR. Highest *P2y12* expression was detected in splenic macrophages. Here, *P2y12* expression was significantly higher in tumor-free mice compared to tumor-bearing hosts, which could indicate that P2Y12$^+$ splenic macrophages are recruited to the tumor site in tumor-bearing mice. *P2y12* expression in CD11b$^+$ cells from B16F10 tumors was comparable to that in splenic macrophages of tumor-bearing mice. Lowest *P2y12* expression was observed in macrophages of the peritoneal cavity. Consistent with our results, Zanin et al. also reported low *P2y12* mRNA expression in peritoneal macrophages [297]. Since we detected *P2y12* on mRNA level, we aimed at investigating whether the P2Y12 protein is also expressed by TAM of subcutaneously transplanted B16F10 tumors. We analyzed specificity of a commercially available anti-P2Y12 antibody by using transgenic P2Y12$^+$ Raw 264.7 cells and confirmed P2Y12 over-expression by Western blot analysis as well as immunocytochemistry. We stained murine B16F10 melanomas with this antibody and found P2Y12 expression in murine TAM. These P2Y12$^+$ TAM were located mainly at the tumor border. This is not surprising since B16 tumors are poorly infiltrated by immune cells, including macrophages, compared to other highly immunogenic tumor models such as CT26 colon carcinoma or 4T1 breast carcinoma [378]. We verified *P2y12* expression in murine B16F10 tumors by in situ hybridization confirming that P2Y12$^+$ macrophages are located at the tumor border. To our knowledge, we are the first to describe P2Y12 protein expression in murine TAM *in situ*.

## 5.3 Functional characterization of P2Y12$^+$ macrophages

### 5.3.1 Gene expression analysis of P2Y12$^+$ U937 cells

We went on characterizing the function of P2Y12$^+$ macrophages. First, we aimed at identifying the ADP-induced genes in transgenic P2Y12$^+$ U937 cells. Thus, we treated the cells for 4 h and 24 h with ADP and performed gene expression analysis. Interestingly, after 4 h of stimulation, we found up-regulation of various chemokines and pro-inflammatory cytokines in ADP-treated P2Y12$^+$ U937 cells (P2Y12 ADP) compared to untreated P2Y12$^+$ U937 cells

(P2Y12 CTRL). The highest up-regulated genes were the chemokines *CXCL8* (IL-8) and *CXCL7*. P2Y12 ADP also exhibited up-regulation of several other chemokines including *CCL3L3*, *CXCL3*, *CCL20* as well as *CXCL2*. Besides chemokines, ADP induced growth factors and cytokines including *IL1B*, *TGFB3*, *TNFSF15* and *HBEGF* in P2Y12$^+$ U937 cells. Also in microglial cells, ADP has been shown to induce the release of various cytokines and chemokines in a P2Y12-dependent manner. Tozaki-Saitoh et al. showed that CCL3 is induced in ADP-treated microglia [379]. In addition, the P2Y12 antagonist ticagrelor reduced IL-1ß and CCL2 expression in the brain, suggesting that ADP induces the expression of inflammatory cytokines and chemokines via P2Y12 [326].

We confirmed the increased expression of pro-inflammatory cytokines and chemokines in ADP-treated P2Y12$^+$ U937 cells by qRT-PCR. Interestingly, we found up-regulation of the same genes – except *CXCL2* – in ADP-treated pBM$_{(MDI)}$ expressing P2Y12. To investigate whether ADP polarizes macrophages towards a pro-inflammatory phenotype, we analyzed the expression of typical M1 and M2-associated cytokines in ADP-treated pBM$_{(MDI)}$ by qRT-PCR. Whereas ADP induced the expression of *TNF-α*, the expression of the anti-inflammatory and immunosuppressive cytokines *IL-10* and *TGF-ß* was significantly down-regulated in ADP-treated pBM$_{(MDI)}$. These results suggest that ADP reprograms macrophages towards a pro-inflammatory phenotype.

However, we also detected one immunosuppressive cytokine, namely *TGF-ß3*, up-regulated in ADP-treated P2Y12$^+$ U937 cells compared to P2Y12 CTRL. Although TGF-ß is released by M2 macrophages and is involved in wound healing and immunosuppression, the distinct role of different TGF-ß isoforms remains largely unclear [361, 380]. Interestingly, platelets also release TGF-ß in response to ADP treatment [319, 381]. Wang et al. reported impaired TGF-ß1 secretion from ADP-treated platelets of *P2y12*-deficient mice, resulting in reduced epithelial to mesenchymal transition (EMT) of tumor cells and thus reduced invasiveness *in vitro*. Subsequently, *P2y12*-deficient mice exhibited decreased metastasis [319]. Whether TGF-ß3 released from ADP-treated P2Y12$^+$ macrophages also induces EMT of tumor cells remains to be elucidated.

We also detected up-regulation of the growth factor *HB-EGF* in ADP-treated P2Y12$^+$ U937 cells. HB-EGF is released by M2 macrophages and induces proliferation of tumor cells *in vitro* [382, 383]. HB-EGF expression is strongly up-regulated in PBMC from ovarian cancer patients compared to healthy individuals [384]. Since HB-EGF is a membrane-bound growth factor it must be enzymatically cleaved to be released and to induce paracrine signaling. In the tumor microenvironment, soluble HB-EGF binds to EGFR on tumor cells, thereby promoting tumor growth [385]. Carroll et al. showed that the matrix metalloproteinase MMP-9 cleaves HB-EGF [384]. We did not detect over-expression of *MMP9* but significantly increased expression of *MMP14* and *MMP7* in P2Y12 ADP compared to P2Y12 CTRL. They were both shown to promote the cleavage of HB-EGF [386-388]. MMP-14 (MT1-MMP) is a membrane-bound MMP that is frequently associated with cancer cell invasion and metastasis [389].

Besides MMPs, we also detected up-regulation of several other genes in P2Y12 ADP compared to P2Y12 CTRL that are associated with cell motility, migration and invasion. One example is the matrix remodeling enzyme heparanase that is involved in tumor cell invasion and metastasis [390]. We also detected up-regulation of urokinase/plasminogen activator (uPA, *PLAU*) and urokinase/plasminogen activator receptor (uPAR, *PLAUR*) in ADP-treated P2Y12$^+$

U937 cells. They are involved in the generation of plasmin which mediates fibrinolysis but also degradation of the ECM and thus is associated with tumor invasion and metastasis [391]. uPA and uPAR are frequently associated with a M2 macrophage phenotype [104, 392]. uPA/uPAR-mediated signaling induces TGF-ß and IL-4 expression, thereby supporting polarization of macrophages [393]. Interestingly, plasminogen activator inhibitor-1 (PAI-1, *SERPINE1*) and plasminogen activator inhibitor-2 (PAI-2, *SERPINB2*), which inhibit uPA-mediated plasminogen activation, were also strongly up-regulated in P2Y12 ADP compared to P2Y12 CTRL. Although they seem to reduce tumor cell invasion and metastasis, pro-tumoral and anti-inflammatory roles were also reported. PAI-2 is up-regulate during inflammation and seems to limit Th1-associated cytokine release [394]. PAI-1 was reported to elicit pro-angiogenic function and thus promotes tumor progression. Furthermore, it seems to be involved in the recruitment and M2-polarization of macrophages [395]. Interestingly, some of these genes we found up-regulated in ADP-treated P2Y12$^+$ U937 cells, for instance PAI-1 and PAI-2, are also induced in tumor cells that are co-cultured with platelets. Since activated platelets release ADP and tumor cells might express purinergic receptors it is possible that the same genes that are up-regulated by ADP in P2Y12$^+$ macrophages are also induced in tumor cells co-incubated with platelets [396, 397].

Interestingly, ADP up-regulated the ectonucleotidase *CD73* in P2Y12$^+$ U937 cells. Since CD73 converts AMP to the immunosuppressive mediator adenosine, it is crucial for limiting inflammatory conditions [136]. Previously, increased *CD73* expression was associated with M2-polarized macrophages [297]. We also detected increased levels of CD73 in P2Y12 expressing pBM$_{(MDI)}$ suggesting that ADP signaling via P2Y12 might up-regulate *CD73*. Different stimuli (e.g. chemokines) can induce ATP release also from intact cells. Extracellular ATP can either signal in an autocrine manner or can be rapidly cleaved by ectonucleotidases including CD39 [252]. Since pBM$_{(MDI)}$ also express CD39 on protein level, which converts ATP to ADP and AMP, it is possible that the generated ADP induces *CD73* expression via P2Y12.

We also identified suppressed genes in P2Y12$^+$ U937 cells after ADP treatment for 4 h. Interestingly, the purinergic receptor *P2RY8* is significantly down-regulated in ADP-treated P2Y12$^+$ U937 cells. Since P2RY8 was previously seen as a non-mammalian nucleotide receptor, not much is known about its function [398]. However, two studies analyzed its expression in promyelocytic cell lines. *P2RY8* is strongly expressed by undifferentiated monocytic U937 cells as well as HL60 cells and is down-regulated in PMA-differentiated HL60 cells displaying a monocytic/macrophage-like phenotype. In general, the authors showed that most purinergic receptors exhibit dynamic expression patterns during myeloid cell differentiation. While P2Y2 was suggested to be involved in monocyte-to-macrophage differentiation, P2Y11 seems to play a role in granulocytic differentiation of HL60 cells as well as in the maturation of monocyte-derived DCs [399, 400].
The chemokine receptors *CCR2* and *CXCR4* are also significantly down-regulated in ADP-treated P2Y12$^+$ U937 cells. They are both strongly expressed on monocytes and are down-regulated during differentiation to macrophages [401]. Phillips et al. showed that CCR2 is expressed by THP1 monocytes but is down-regulated in THP-1-derived macrophages [402]. Creery et al. suggested that M2 macrophages express lower levels of CXCR4, since the Th2 cytokines IL-4 and IL-13 inhibit the expression of CXCR4 [403]. Indeed, we also detected

decreased CCR2 and CXCR4 levels in P2Y12-expressing $pBM_{(MDI)}$ compared to $pBM_{(MCSF)}$. These results suggest that ADP-induced signaling via P2Y12 promotes monocyte-to-macrophage differentiation by down-regulation of several chemokine receptors as well as the purinergic receptor *P2RY8*.

To identify late response genes, we performed microarray analysis of $P2Y12^+$ U937 cells treated for 24 h with ADP. Like after 4 h of ADP treatment, *CXCL7* was still strongly up-regulated in P2Y12 ADP compared to P2Y12 CTRL. Induction of other genes was much weaker. Interestingly, many surface molecules were up-regulated, including the general macrophage marker *CD68* and the M2 marker *MRC1* (CD206). The two tetraspanins *CD82* and *TSPAN7* were also significantly up-regulated in P2Y12 ADP after 24 h. Tetraspanins are cell surface molecules with 4 transmembrane domains which are involved in cell growth, motility and adhesion. Interestingly, *CD82* was shown to be up-regulated during monocyte differentiation, also in PMA-differentiated U937 cells [404-406]. Different cytokines including IL-1ß but also the Th2-associated cytokines IL-4 and IL-13 induce the expression of *CD82* [406]. Besides being a differentiation marker not much is known regarding the function of CD82 in macrophages. However, CD82 was reported to be expressed on T cells and DCs. In the latter cell population CD82 inhibits cell motility by modulating actin polymerization and RhoA signaling. On several hematopoietic cells, CD82 regulates clustering and adhesiveness of adhesion molecules (e.g. $\alpha_4ß_1$ integrins, LFA-1) and thus is involved in cell-cell or cell-ECM adhesion [407]. Like CD82, TSPAN7 also mediates organization and rearrangement of the cytoskeleton [408].
These results reinforce our hypothesis that ADP signaling promotes the differentiation of monocytic $P2Y12^+$ U937 cells towards macrophages. Moreover, ADP treatment might affect the adhesion of $P2Y12^+$ macrophages either to ECs or to components of the ECM thereby regulating cell motility and (trans)migration.

Interestingly, *GPR34*, which phylogenetically belongs to the P2Y12-like receptor group, was significantly up-regulated in ADP-treated $P2Y12^+$ U937 cells. GPR34 is expressed on several immune cells including myeloid cells. For a long time GPR34 was an orphan receptor until in 2006 lyso-phosphatidylserine (lysoPS) was uncovered as an endogenous agonist of the receptor [409]. LysoPS promotes various immunological function including mast cell degranulation, macrophage engulfment of apoptotic cells and suppression of T cell proliferation [410, 411]. *Gpr34*-deficient mice showed impaired immune response after bacterial infection accompanied by increased bacterial load, fewer infiltration of inflammatory cells and elevated levels of several cytokines including IL-4, TNF-α and IFN-γ [412]. Like P2Y12, GPR34 is highly expressed in $P2Y12^+$ microglia. Preissler et al. revealed impaired phagocytosis of *Gpr34*-deficient microglia while motility was not affected. [413]. Contrary, P2Y12 is involved in chemotaxis but does not play a role in phagocytosis [325]. Whether GPR34 is also expressed on other tissue-specific macrophages including TAM remains to be elucidated.

### 5.3.2 ADP induces cytokine and chemokine secretion

Since we showed up-regulation of various chemokines by microarray analysis and qRT-PCR, we aimed at investigating whether chemokine secretion is also enhanced by ADP treatment. Thus, we determined chemokine concentrations in the cell supernatants of ADP-treated P2Y12$^+$ U937 cells by ELISA. We found increased secretion of CXCL8 (IL-8), CXCL7 as well as CXCL2 in ADP-treated P2Y12$^+$ U937 cells. While CXCL2 concentration was very low (14 pg/mL), CXCL7 concentration in the supernatant was the highest among the analyzed chemokines (511 pg/mL). All these chemokines are implicated in chemotaxis of neutrophils and angiogenesis [119, 121, 414]. Whereas CXCL2 and IL-8 are predominantly secreted by monocytes and macrophages, CXCL7 is mainly released from activated platelets [415]. Several *in vitro* studies showed that CXCL7 promotes neutrophils adhesion to HUVECS and induces their transmigration [416]. Finsterbusch et al. showed that platelets directly enhance neutrophil migration via CXCL7 secretion [417]. The P2Y12 antagonist ticagrelor reduced pulmonary neutrophil infiltration in septic mice [418]. Whether the ADP-conditioned medium of P2Y12$^+$ U937 cells attracts neutrophils remains elusive.
We could not confirm increased secretion of CXCL2, CXCL7 and IL-8 in ADP-treated pBM$_{(MDI)}$. Since we also detected up-regulation of IL-1ß and TNF-α mRNA in ADP-treated pBM$_{(MDI)}$, we aimed at investigating whether secretion of these pro-inflammatory mediators is enhanced upon ADP treatment. As observed for chemokines, we failed to detect elevated cytokine concentrations in the cell supernatants of ADP-treated pBM$_{(MDI)}$. One possible explanation for the different secretory phenotype of P2Y12$^+$ U937 cells and pBM$_{(MDI)}$ is the presence of other purinergic ADP receptors including P2Y1 and P2Y13 in pBM$_{(MDI)}$ as revealed by microarray analysis. Since information about their function in macrophages are sparse, it remains elusive whether these purinergic receptors counteract the P2Y12-mediated effects. Since pBM are treated with dexamethasone and IL-4 prior to ADP stimulation, another hypothesis is that these mediators suppress the ADP-induced effects observed in P2Y12$^+$ U937 cells. Furthermore, glucocorticoids such as dexamethasone are known to inhibit protein synthesis of pro-inflammatory cytokines and chemokines [419].
Although we failed to detect increased chemokine release of ADP-treated pBM$_{(MDI)}$, ADP was shown to promote the release of several chemokines and cytokines from different cell types *in vitro*. While ADP induced the release of IL-1ß, IL-6 and TNF-α in human microglia, it induced the expression of CCL2, CCL5 as well as IL-8 in human keratinocytes [420, 421]. Interestingly, IL-8 is not only released upon ADP stimulation but also in response to TLR agonists. In macrophages, LPS and $Pam_3CSK_4$ were both shown to promote nucleotide release and subsequent IL-8 secretion by autocrine purinergic signaling via P2Y2 and P2Y6 [422-424]. Whether ADP also induces nucleotide release thereby stimulating autocrine purinergic signaling and IL-8 secretion needs to be further investigated.

To investigate whether P2Y12 blockade inhibits the ADP-induced chemokine secretion, we treated P2Y12$^+$ U937 cells with the specific and highly potent P2Y12 antagonist PSB0739. Indeed, we could abrogate the ADP-induced release of CXCL2, CXCL7 and IL-8 upon inhibition of the P2Y12 receptor. Several clinically-approved P2Y12 antagonists including clopidogrel and ticagrelor were reported to have anti-inflammatory properties besides reducing platelet

activation. Clopidogrel reduced airway inflammation associated with reduced levels of the Th2 cytokines IL-4 and IL-13 as well as IFN-γ and CCL5 in a mouse model of asthma [341]. Ticagrelor attenuated atherogenesis in *ApoE*-deficient mice accompanied by decreased expression of CCL2 and reduced accumulation of macrophages [425]. In the brain, ticagrelor treatment reduced the number of infiltrating microglia and the expression of IL-1ß, CCL2 and iNOS after cerebral artery occlusion [326]. These results fit with our finding that the P2Y12 antagonist PSB0739 abrogates ADP-induced secretion of CXCL2, CXCL7 and IL-8 in macrophages. Therefore, we hypothesize that P2Y12 antagonists can reduce inflammation by decreasing the attraction of inflammatory cells.

Since IL-8 is not present in the murine system, we were interested which chemokines are expressed in P2Y12$^+$ mouse macrophages upon ADP treatment. It has been described by others that CXCL1, CXCL2 and CXCL5 are the functional mouse homologues of IL-8 [426]. We performed a cytokine array, able to analyze the presence of 40 different cytokines and chemokines in the supernatant of ADP-treated P2Y12$^+$ Raw 264.7 cells (P2Y12 ADP). Like in human U937 cells, we detected increased concentration of CXCL2 in the supernatant of P2Y12 ADP compared to unstimulated cells. We failed to detect CXCL1 and CXCL5 in the cell supernatants of ADP-treated P2Y12$^+$ Raw 264.7 cells. Interestingly, we also found increased CCL4 and TNF-α concentrations, mediators we did not detect in human ADP-treated P2Y12$^+$ U937 cells. Since the cytokine array is not a quantitative method, we performed ELISAs to verify these results with an independent assay and to determine the exact concentrations of the mediators in the cell supernatants. Although we failed to detect elevated CCL4 levels in the supernatants of P2Y12 ADP we found significantly increased TNF-α secretion and a tendency for enhanced CXCL2 release in ADP-treated P2Y12$^+$ Raw 264.7 cells compared to untreated cells. These results suggest that ADP has similar but not 100 % overlapping biological effects in murine and human macrophages.

### 5.3.3 ADP-induced signaling pathways in P2Y12$^+$ macrophages

We went on characterizing ADP-induced signaling pathways in P2Y12$^+$ U937 cells. We detected increased ERK1/2 as well as Akt phosphorylation in ADP-treated P2Y12$^+$ cells compared to EV cells. ADP-induced signaling via P2Y12 is best characterized in platelets. Since P2Y12 is a GPCR that couples to $G_i$ proteins, the Gα subunit inhibits adenylyl cyclase while the Gßγ subunit activates PI3K and its main downstream target Akt. Various studies showed that treatment of platelets with PI3K inhibitors abrogates ADP-induced Akt phosphorylation [310]. PI3K/Akt signaling via P2Y12 is not only involved in platelet activation but also in microglial chemotaxis [427]. ATP-induced Akt phosphorylation in microglial cells can be inhibited with the PI3K inhibitor Wortmannin or with the P2Y12 antagonist AR-C69931-MX [324]. Interestingly, in microglial cells P2Y12 activation also induces p38 MAPK phosphorylation, which can be abrogated with the P2Y12 inhibitor MRS2395 [329, 428]. We failed to detect p38 MAPK phosphorylation in ADP-treated P2Y12$^+$ U937 cells and $pBM_{(MDI)}$ (data not shown) indicating that this pathway might not be as relevant for ADP-induced activation of these macrophages. In line with our results, Soulet et al. showed that besides Akt, ERK1/2 is phosphorylated upon

treatment of P2Y12$^+$ CHO cells with 2-MeSADP. Treatment with PI3K inhibitors reduced ERK1/2 as well as Akt phosphorylation, suggesting that ERK1/2 activation is downstream of PI3K/Akt signaling [306]. 2-MeSADP also induced ERK1/2 phosphorylation in human monocyte-derived DCs. Since the P2Y12 antagonist AR-C69931MX inhibited the ADP-induced ERK phosphorylation, the authors hypothesized that ERK signaling is induced via P2Y12 [429].

Besides activation of Akt and ERK1/2 signaling, we detected increased expression of the transcription factor subunits *JUN* and *FOSL1*. ERK signaling was shown to induce the expression of AP-1 transcription factor subunits [430]. We could show that treatment with specific Akt and ERK inhibitors abrogated the ADP-induced expression of *JUN* and *FOSL1*. Studies reported that the transcription factor AP-1 is important for the expression of pro-inflammatory cytokines and chemokines [431]. To investigate whether ERK and/or Akt signaling are also responsible for the ADP-induced chemokine secretion in P2Y12$^+$ U937 cells, we pre-treated the cells with Akt and ERK inhibitors prior to stimulation with ADP. Indeed, single inhibition of either Akt or ERK reduced the ADP-induced secretion of CXCL2, CXCL7 and IL-8. Similar to our results, Kawamura et al. showed that ERK1/2 inhibition abrogates the ATP-induced CXCL2 secretion from macrophages [432]. However, we showed that blockade of Akt signaling was more efficient than ERK inhibition, while co-administration of Akt and ERK inhibitors was most efficient in reducing ADP-induced chemokine release. These results suggest that both pathways act synergistically. Although many studies reported a negative crosstalk between ERK1/2 and Akt signaling, co-activation of both signaling pathways was also reported in several studies [433, 434].

To investigate whether ADP also induces the same signaling pathways in P2Y12-expressing pBM$_{(MDI)}$, we performed Western blot analysis of ADP-treated pBM$_{(MDI)}$ using anti-Akt and anti-ERK1/2 antibodies. In contrast to P2Y12$^+$ U937 cells, ADP-treated pBM$_{(MDI)}$ lacked phosphorylated Akt. However, ADP stimulation resulted in increased ERK1/2 phosphorylation and increased expression of the transcription factor subunits *FOSL1* and *JUN* in pBM$_{(MDI)}$. Pre-treatment with the ERK inhibitor did not reduce cytokine expression suggesting that ERK signaling is not responsible for the induction of these cytokines in ADP-treated pBM$_{(MDI)}$. However, the P2Y12 antagonist PSB0739 significantly inhibited ADP-induced cytokine expression. These results indicate that ADP might activate other P2Y12 downstream signaling pathways in pBM$_{(MDI)}$.

### 5.3.4 ADP promotes the migration of P2Y12$^+$ macrophages

It is well known that nucleotides released by apoptotic and necrotic cells act as find-me or danger signals and trigger the migration of phagocytic cells to the site of inflammation [260]. Therefore, we aimed to analyze whether ADP acts as a find-me signal for P2Y12$^+$ macrophages. Using a transwell migration assay we confirmed the chemoattractant effect of ADP on both, P2Y12$^+$ pBM$_{(MDI)}$ and P2Y12$^+$ Raw 264.7 cells. Various studies provided proof for the chemotactic role of ADP but also ATP for P2Y12$^+$ microglial cells [328, 355]. Concordantly, microglia from *P2y12*-deficient mice fail to migrate towards an ADP gradient [325]. ADP also enhanced the recruitment of other myeloid cells including macrophages and to a lesser extend

neutrophils to the site of bacterial infection *in vivo*, suggesting that the ADP receptors P2Y12 and P2Y13 are responsible for this effect [435]. In addition, it was shown that recruited macrophages secrete chemokines such as CXCL2 and IL-8 which attract more inflammatory cells, mostly neutrophils, to the site of infection [424, 432]. We also showed that ADP promoted IL-8 and/or CXCL2 release from human and murine P2Y12$^+$ cells indicating that P2Y12$^+$ macrophages recruit inflammatory cells to the site of inflammation.

Interestingly, we found an increased migration of P2Y12$^+$ Raw 264.7 cells not only towards ADP but also towards medium without FCS. Supplementation of medium w/o FCS with ADP potentiated the migratory capacity of P2Y12$^+$ macrophages. These results suggest that either the medium contains factors that trigger migration of P2Y12$^+$ cells or that the cells themselves release factors that promote their migration in an autocrine manner. Since the P2Y12 antagonist PSB0739 abrogated the increased migration of P2Y12$^+$ Raw 264.7 cells towards medium without FCS, we hypothesized that serum-starved cells might release nucleotides that promote their migration in an autocrine manner. Such an autocrine signaling mechanism for the migration of myeloid cells has already been shown for ATP. Chemotactic factors (IL-8, fMLP) induce ATP release of neutrophils thereby promoting their chemotaxis by autocrine purinergic signaling via P2Y2 [263]. In macrophages, complement component C5a induces ATP release, creating a positive feedback loop by purinergic signaling via P2Y2 and P2Y12 [268]. Isfort et al. showed that ATP/ADP are not chemoattractants but increase the random migration of macrophages, also known as chemokinesis [346]. These results suggest that these nucleotides act as short-range signals that are released by the immune cells themselves to stimulate their chemotaxis.

To investigate whether released nucleotides are the reason for the induced migration towards medium without FCS, we supplemented the medium in the lower chamber with the ATP/ADP-hydrolyzing enzyme apyrase. Indeed, apyrase abrogated the migration of P2Y12$^+$ Raw 264.7 cells towards medium without FCS. To investigate if the release of nucleotides depends on P2Y12, we used CM of ADP-treated and untreated transgenic Raw 264.7 cells (P2Y12$^+$ and EV cells) as chemoattractants. Like the CM of P2Y12$^+$ cells, the CM of EV cells also induced the migration of P2Y12$^+$ cells while the migratory ability of EV cells remained unaffected. These results suggest that serum-starved cells release nucleotides independently of P2Y12 expression. Interestingly, the CM of ADP-treated P2Y12$^+$ cells did not significantly increase the migration of P2Y12$^+$ Raw 264.7 cells compared to the CM of untreated P2Y12$^+$ cells, suggesting that ADP signaling via P2Y12 does not trigger nucleotide release. However, since we only assessed migration after 6 h and did not measure nucleotide concentrations in the CM, we cannot completely exclude that the CM of ADP-treated P2Y12$^+$ cells contains higher levels of nucleotides. It is possible that initial migration of P2Y12$^+$ cells is stronger induced by ADP-CM compared to CM of untreated P2Y12$^+$ cells and that differences cannot be observed at later time points when maximal migration is achieved. Since it could also be that the released nucleotides trigger chemokine secretion from P2Y12$^+$ Raw 264.7 cells which subsequently promote the migration of P2Y12$^+$ macrophages, we treated the CM of P2Y12$^+$ Raw 264.7 cells and EV cells with apyrase. The induced migration of P2Y12$^+$ cells towards CM of serum-starved cells was completely abrogated when nucleotides were hydrolyzed by apyrase, indicating that chemokines don't play a role in the ADP-induced migration of P2Y12$^+$ Raw264.7 cells. In contrast to our results, Zhang et al. showed that CCL2 release in response to ADP and not the

nucleotides themselves cause the increased migration of Raw 264.7 cells. By supplementation of the CM of ADP-treated cells with apyrase the authors found that cleavage of ADP could not abrogate the increased migration of macrophages towards ADP-CM, suggesting that released chemokines in response to ADP are the reason for the induced migration [435]. However, in contrast to our experiments with P2Y12$^+$ Raw 264.7 cells they used untransfected Raw 264.7 cells and murine peritoneal macrophages. Since we also detected down-regulation of the chemokine receptor CCR2 in ADP-treated-P2Y12$^+$ cells, it is possible that P2Y12$^+$ macrophages are mainly attracted by nucleotides and not by CCL2. Furthermore, in contrast to Zhang et al., we could not detect increased CCL2 secretion in ADP-treated transgenic Raw 264.7 cells. These results suggest that ADP promotes the migration of P2Y12$^+$ macrophages. In addition, serum-starved cells release nucleotides that trigger migration of P2Y12$^+$ macrophages via autocrine signaling.

### 5.3.5 Cell death induces the migration of P2Y12$^+$ Raw 264.7 cells

Due to inflammation, necrosis and apoptosis, the tumor microenvironment is characterized by high levels of nucleotides. Myeloid cells are recruited to the tumor microenvironment via these extracellular nucleotides but also via chemokines that are released by tumor cells and/or stromal cells [252]. To investigate whether dying tumor cells can directly induce the migration of P2Y12$^+$ macrophages, we established a co-culture with dying B16F1 melanoma cells and P2Y12$^+$ Raw 264.7 cells. B16F1 cells were seeded in the lower well of a transwell chamber and treated with puromycin for 24 h to induce cell death. Subsequently, transgenic Raw 264.7 cells were added to the transwell insert and migration towards the dying melanoma was assessed after 6 h. The migration of P2Y12$^+$ cells towards dying melanoma cells was significantly enhanced compared to untreated B16F1 cells. Cell death did not significantly promote the migration of EV cells. Addition of the P2Y12 antagonist PSB0739 to the dying B16F1 cells significantly abrogated the cell death induced migration of P2Y12$^+$ macrophages. Furthermore, addition of apyrase to the dying tumor cells also diminished the migration of P2Y12$^+$ Raw 264.7 cells. These results indicate that dying tumor cells release nucleotides that act as find-me signals for the recruitment of P2Y12$^+$ macrophages. It has been shown, that chemotherapeutic agents induce ATP release from dying tumor cells. The authors detected decreased intracellular ATP levels and increased extracellular ATP levels irrespective of the type of chemotherapeutic agent and tumor cells. ATP release occurred already from early apoptotic cells and proceeded during late apoptosis and secondary necrosis [301]. Elliott et al. showed that apoptotic cell supernatants induce the migration of THP1 monocytes *in vitro*. Moreover, macrophages were recruited to murine air pouches containing apoptotic cell supernatants. Interestingly, apoptotic cell supernatants mainly attracted macrophages, while LPS primarily attracted neutrophils indicating that extracellular nucleotides act as a paracrine signal for macrophages expressing purinergic receptors. Since they showed that apoptotic cell supernatants mainly contain ATP and UTP the authors assumed that the purinergic receptor P2Y2 is involved in sensing these nucleotides. Although macrophages of *P2y2*$^{-/-}$-mice showed impaired migration towards apoptotic cell supernatants, the migration was not completely abrogated, suggesting the involvement of other nucleotide receptors [260]. Since we showed

that P2Y12 is expressed on human and murine macrophages including TAM, and necrotic cell death induces the migration of P2Y12$^+$ macrophages, P2Y12 might also be involved in the sensing of apoptotic cells in the tumor microenvironment.

### 5.3.6 P2Y12 facilitates the adhesion and transmigration of U937 cells

Besides its role in microglial chemotaxis and platelet activation, P2Y12 enables the adhesion of platelets to leukocytes but also to tumor cells *in vitro*. Gebremeskel et al. showed that P2Y12 facilitates platelet-tumor cell interactions and promotes the adhesion of these aggregates to ECs [320]. In addition, ECs express purinergic receptors (e.g. P2Y1), which promote leukocyte recruitment and adhesion [436, 437]. We aimed at investigating whether P2Y12 over-expression alters the adhesion and transmigration of monocytes through ECs. Indeed, adhesion of P2Y12$^+$ U937 cells to HUVEC and transmigration through the endothelial monolayer were strongly enhanced when compared to EV cells. Since gene expression analysis revealed an up-regulation of the tetraspanins *TSPAN7* and *CD82* in ADP-treated P2Y12$^+$ U937 cells and tetraspanins are involved in leukocyte trafficking [407], we aimed at investigating whether these ADP-treated cells show an increased adhesion and/or transmigration. When P2Y12$^+$ cells were pre-treated with ADP for 24 h the increased adhesion to ECs was abrogated. Furthermore, transmigration across an activated HUVEC monolayer was also diminished in ADP-treated P2Y12$^+$ U937 cells. These results suggest that the tetraspanins CD82 and TSPAN7 are not involved in the adhesion and transmigration of P2Y12$^+$ monocytes. Our results suggest that P2Y12 itself and not the ADP-induced genes are important for the increased adhesion and transmigration of P2Y12$^+$ monocytes. Since we did not detect down-regulation of P2Y12 expression upon ADP treatment, there must be another explanation for the reduced adhesion and transmigration of P2Y12$^+$ cells upon ADP treatment. Hardy et al. showed that P2Y12 rapidly desensitize upon ADP treatment. This desensitization is mediated by G protein coupled receptor kinases and may also result in internalization of the receptor [438]. For GPCR including purinergic receptors it is well established that they are internalized upon activation [311]. Whether P2Y12 receptor internalization causes the reduced adhesion and transendothelial migration of ADP-treated P2Y12$^+$ monocytes has still to be determined. Another possible explanation would be that ADP competitively blocks the binding site of P2Y12 thereby blocking the adhesion to surface receptors on endothelial cells. It needs further studies to answer the question whether this competitive inhibition is the reason for the reduced adhesion of ADP-treated P2Y12$^+$ U937 cells.

## 5.4 Concluding remarks

We showed that P2Y12 is expressed in human and murine TAM of melanoma. We detected up-regulation of *P2Y12* expression upon treatment of pBM as well as BMDM with M-CSF/dexamethasone/IL-4, stimuli that promote polarization of M2 macrophages *in vitro*. Indeed, we found co-expression of P2Y12, CD68 and CD163 in macrophages of melanoma *in situ* suggesting that P2Y12 is primarily expressed by M2-like TAM. Whether presence of $P2Y12^+$ TAM correlates with overall survival of melanoma patients remains to be elucidated. P2Y12 seems not to be a specific marker for TAM since it is also expressed on a subpopulation of splenic macrophages and murine peritoneal macrophages. Since we found increased migration of $P2Y12^+$ macrophages towards extracellular nucleotides, we suggest that $P2Y12^+$ macrophages are recruited to hypoxic regions in the tumor stroma rich in apoptotic and necrotic cells. In addition, we could show that ADP signaling in monocytes induces the expression and secretion of several chemokines (CXCL2, CXCL7 and CXCL8/IL-8) that are involved in angiogenesis and chemotaxis of neutrophils. Whether the number of $P2Y12^+$ macrophages correlates with the presence of neutrophils and/or $CD31^+$ ECs in melanoma specimens remains to be determined.

In P2Y12-expressing $pBM_{(MDI)}$, ADP induces the expression of TNF-α and IL-1ß while reducing the expression of anti-inflammatory cytokines IL-10 and TGF-ß suggesting that ADP reprograms macrophages towards a pro-inflammatory phenotype. Whether $P2Y12^+$ macrophages modulate the anti-tumor immunity by inhibiting or activating T cell response needs further studies. Tumor transplantation models using mice with *P2y12*-depleted macrophages are needed to evaluate the role of $P2Y12^+$ macrophages in tumor growth and progression.

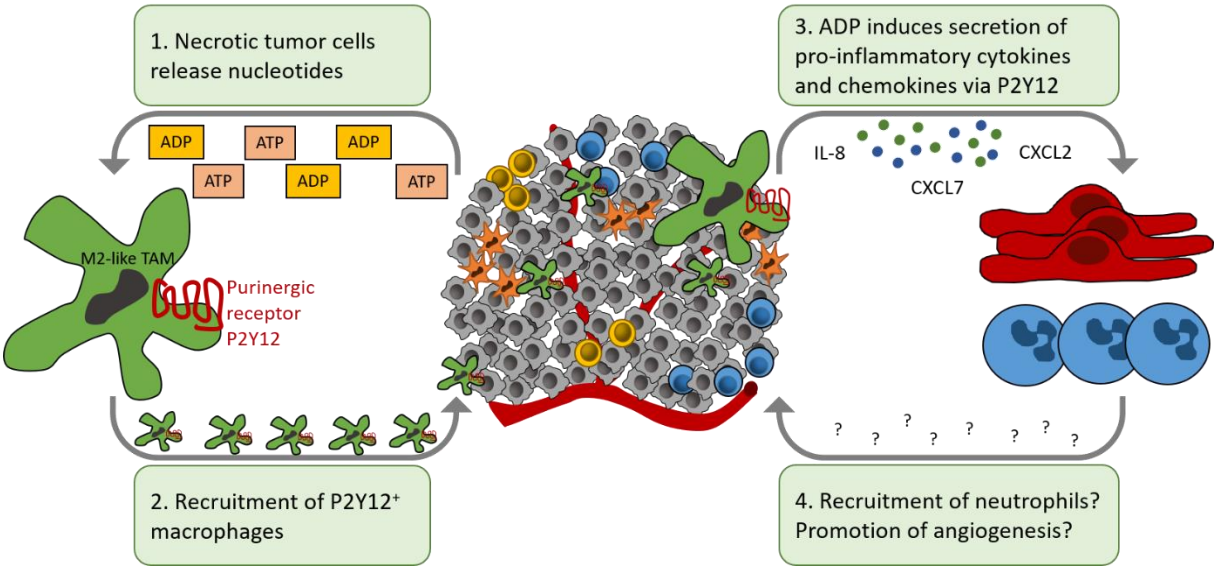


**Figure 41. Schematic overview of the function of $P2Y12^+$ macrophages.**

# References


1. Geissmann, F., et al., *Development of Monocytes, Macrophages, and Dendritic Cells.* Science, 2010. **327**(5966): p. 656-661.
2. Lavin, Y., et al., *Regulation of macrophage development and function in peripheral tissues.* Nat Rev Immunol, 2015. **15**(12): p. 731-44.
3. Wynn, T.A., A. Chawla, and J.W. Pollard, *Macrophage biology in development, homeostasis and disease.* Nature, 2013. **496**(7446): p. 445-455.
4. Varol, C., et al., *Monocytes give rise to mucosal, but not splenic, conventional dendritic cells.* J Exp Med, 2007. **204**(1): p. 171-80.
5. Yrlid, U., C.D. Jenkins, and G.G. MacPherson, *Relationships between distinct blood monocyte subsets and migrating intestinal lymph dendritic cells in vivo under steady-state conditions.* J Immunol, 2006. **176**(7): p. 4155-62.
6. Alder, J.K., et al., *Kruppel-like factor 4 is essential for inflammatory monocyte differentiation in vivo.* J Immunol, 2008. **180**(8): p. 5645-52.
7. Mildner, A., et al., *Microglia in the adult brain arise from Ly-6ChiCCR2+ monocytes only under defined host conditions.* Nat Neurosci, 2007. **10**(12): p. 1544-53.
8. Scatizzi, J.C., et al., *p21Cip1 is required for the development of monocytes and their response to serum transfer-induced arthritis.* Am J Pathol, 2006. **168**(5): p. 1531-41.
9. Dunay, I.R., et al., *Gr1(+) inflammatory monocytes are required for mucosal resistance to the pathogen Toxoplasma gondii.* Immunity, 2008. **29**(2): p. 306-17.
10. Robben, P.M., et al., *Recruitment of Gr-1+ monocytes is essential for control of acute toxoplasmosis.* J Exp Med, 2005. **201**(11): p. 1761-9.
11. Bogunovic, M., et al., *Origin of the lamina propria dendritic cell network.* Immunity, 2009. **31**(3): p. 513-25.
12. Varol, C., et al., *Intestinal lamina propria dendritic cell subsets have different origin and functions.* Immunity, 2009. **31**(3): p. 502-12.
13. Auffray, C., et al., *Monitoring of blood vessels and tissues by a population of monocytes with patrolling behavior.* Science, 2007. **317**(5838): p. 666-70.
14. Geissmann, F., S. Jung, and D.R. Littman, *Blood monocytes consist of two principal subsets with distinct migratory properties.* Immunity, 2003. **19**(1): p. 71-82.
15. Nahrendorf, M., et al., *The healing myocardium sequentially mobilizes two monocyte subsets with divergent and complementary functions.* J Exp Med, 2007. **204**(12): p. 3037-47.
16. Ajami, B., et al., *Local self-renewal can sustain CNS microglia maintenance and function throughout adult life.* Nat Neurosci, 2007. **10**(12): p. 1538-43.
17. Ginhoux, F. and M. Merad, *[Microglia arise from extra-embryonic yolk sac primitive progenitors].* Med Sci (Paris), 2011. **27**(8-9): p. 719-24.
18. Merad, M., et al., *Langerhans cells renew in the skin throughout life under steady-state conditions.* Nat Immunol, 2002. **3**(12): p. 1135-41.
19. Ginhoux, F., et al., *Fate mapping analysis reveals that adult microglia derive from primitive macrophages.* Science, 2010. **330**(6005): p. 841-5.
20. Hoeffel, G., et al., *Adult Langerhans cells derive predominantly from embryonic fetal liver monocytes with a minor contribution of yolk sac-derived macrophages.* J Exp Med, 2012. **209**(6): p. 1167-81.
21. Schulz, C., et al., *A lineage of myeloid cells independent of Myb and hematopoietic stem cells.* Science, 2012. **336**(6077): p. 86-90.
22. Ziegler-Heitbrock, L., et al., *Nomenclature of monocytes and dendritic cells in blood.* Blood, 2010. **116**(16): p. e74-80.
23. Wong, K.L., et al., *Gene expression profiling reveals the defining features of the classical, intermediate, and nonclassical human monocyte subsets.* Blood, 2011. **118**(5): p. e16-31.

24. Mukherjee, R., et al., *Non-Classical monocytes display inflammatory features: Validation in Sepsis and Systemic Lupus Erythematous.* Scientific Reports, 2015. **5**: p. 13886.
25. Cros, J., et al., *Human CD14dim monocytes patrol and sense nucleic acids and viruses via TLR7 and TLR8 receptors.* Immunity, 2010. **33**(3): p. 375-86.
26. Thomas, D.C., *The phagocyte respiratory burst: Historical perspectives and recent advances.* Immunol Lett, 2017. **192**: p. 88-96.
27. Hirayama, D., T. Iida, and H. Nakase, *The Phagocytic Function of Macrophage-Enforcing Innate Immunity and Tissue Homeostasis.* Int J Mol Sci, 2017. **19**(1).
28. Silva, M.T., *Neutrophils and macrophages work in concert as inducers and effectors of adaptive immunity against extracellular and intracellular microbial pathogens.* J Leukoc Biol, 2010. **87**(5): p. 805-13.
29. Mondino, A. and M.K. Jenkins, *Surface proteins involved in T cell costimulation.* J Leukoc Biol, 1994. **55**(6): p. 805-15.
30. Puccetti, P., M.L. Belladonna, and U. Grohmann, *Effects of IL-12 and IL-23 on antigen-presenting cells at the interface between innate and adaptive immunity.* Crit Rev Immunol, 2002. **22**(5-6): p. 373-90.
31. Kulpa, D.A., et al., *PD-1 coinhibitory signals: the link between pathogenesis and protection.* Semin Immunol, 2013. **25**(3): p. 219-27.
32. Mosser, D.M. and J.P. Edwards, *Exploring the full spectrum of macrophage activation.* Nat Rev Immunol, 2008. **8**(12): p. 958-69.
33. Erwig, L.P. and P.M. Henson, *Immunological consequences of apoptotic cell phagocytosis.* Am J Pathol, 2007. **171**(1): p. 2-8.
34. Erwig, L.P. and P.M. Henson, *Clearance of apoptotic cells by phagocytes.* Cell Death Differ, 2008. **15**(2): p. 243-50.
35. Zhang, X. and D.M. Mosser, *Macrophage activation by endogenous danger signals.* J Pathol, 2008. **214**(2): p. 161-78.
36. Kono, H. and K.L. Rock, *How dying cells alert the immune system to danger.* Nat Rev Immunol, 2008. **8**(4): p. 279-89.
37. Boyce, B.F., et al., *Bone Remodeling and the Role of TRAF3 in Osteoclastic Bone Resorption.* Front Immunol, 2018. **9**: p. 2263.
38. Pollard, J.W., *Trophic macrophages in development and disease.* Nat Rev Immunol, 2009. **9**(4): p. 259-70.
39. Nandi, S., et al., *The CSF-1 receptor ligands IL-34 and CSF-1 exhibit distinct developmental brain expression patterns and regulate neural progenitor cell maintenance and maturation.* Dev Biol, 2012. **367**(2): p. 100-13.
40. Erblich, B., et al., *Absence of colony stimulation factor-1 receptor results in loss of microglia, disrupted brain development and olfactory deficits.* PLoS One, 2011. **6**(10): p. e26317.
41. Baharom, F., et al., *Human Lung Mononuclear Phagocytes in Health and Disease*. Front Immunol, 2017. **8**: p. 499.
42. den Haan, J.M.M. and L. Martinez-Pomares, *Macrophage heterogeneity in lymphoid tissues.* Seminars in Immunopathology, 2013. **35**(5): p. 541-552.
43. Stefater, J.A., 3rd, et al., *Metchnikoff's policemen: macrophages in development, homeostasis and regeneration.* Trends Mol Med, 2011. **17**(12): p. 743-52.
44. Boulter, L., et al., *Macrophage-derived Wnt opposes Notch signaling to specify hepatic progenitor cell fate in chronic liver disease.* Nat Med, 2012. **18**(4): p. 572-9.
45. Pull, S.L., et al., *Activated macrophages are an adaptive element of the colonic epithelial progenitor niche necessary for regenerative responses to injury.* Proc Natl Acad Sci U S A, 2005. **102**(1): p. 99-104.
46. Mills, C.D., et al., *M-1/M-2 macrophages and the Th1/Th2 paradigm.* J Immunol, 2000. **164**(12): p. 6166-73.
47. Schmieder, A., et al., *Differentiation and gene expression profile of tumor-associated macrophages.* Seminars in Cancer Biology, 2012. **22**(4): p. 289-297.

48. Martinez, F.O.S.A., Mantovani A, Locati M, *Macrophage activation and polarization.* Frontiers in Bioscience, 2008. **13**: p. 453-461.
49. Doyle, A.G., et al., *Interleukin-13 alters the activation state of murine macrophages in vitro: comparison with interleukin-4 and interferon-gamma.* Eur J Immunol, 1994. **24**(6): p. 1441-5.
50. Stein, M., et al., *Interleukin 4 potently enhances murine macrophage mannose receptor activity: a marker of alternative immunologic macrophage activation.* J Exp Med, 1992. **176**(1): p. 287-92.
51. Joerink, M., H.F. Savelkoul, and G.F. Wiegertjes, *Evolutionary conservation of alternative activation of macrophages: structural and functional characterization of arginase 1 and 2 in carp (Cyprinus carpio L.).* Mol Immunol, 2006. **43**(8): p. 1116-28.
52. Schultze, J.L., A. Schmieder, and S. Goerdt, *Macrophage activation in human diseases.* Semin Immunol, 2015. **27**(4): p. 249-56.
53. Melgert, B.N., et al., *More alternative activation of macrophages in lungs of asthmatic patients.* J Allergy Clin Immunol, 2011. **127**(3): p. 831-3.
54. Gordon, S., *Alternative activation of macrophages.* Nat Rev Immunol, 2003. **3**(1): p. 23-35.
55. Ford, A.Q., et al., *Adoptive transfer of IL-4Ralpha+ macrophages is sufficient to enhance eosinophilic inflammation in a mouse model of allergic lung inflammation.* BMC Immunol, 2012. **13**: p. 6.
56. Murray, P.J. and T.A. Wynn, *Protective and pathogenic functions of macrophage subsets.* Nat Rev Immunol, 2011. **11**(11): p. 723-37.
57. Murray, P.J. and T.A. Wynn, *Obstacles and opportunities for understanding macrophage polarization.* J Leukoc Biol, 2011. **89**(4): p. 557-63.
58. Acosta-Rodriguez, E.V., et al., *Interleukins 1beta and 6 but not transforming growth factor-beta are essential for the differentiation of interleukin 17-producing human T helper cells.* Nat Immunol, 2007. **8**(9): p. 942-9.
59. Langrish, C.L., et al., *IL-23 drives a pathogenic T cell population that induces autoimmune inflammation.* J Exp Med, 2005. **201**(2): p. 233-40.
60. Hoek, R.M., et al., *Down-regulation of the macrophage lineage through interaction with OX2 (CD200).* Science, 2000. **290**(5497): p. 1768-71.
61. Gelderman, K.A., et al., *Macrophages suppress T cell responses and arthritis development in mice by producing reactive oxygen species.* J Clin Invest, 2007. **117**(10): p. 3020-8.
62. Smith, A.M., et al., *Disordered macrophage cytokine secretion underlies impaired acute inflammation and bacterial clearance in Crohn's disease.* J Exp Med, 2009. **206**(9): p. 1883-97.
63. Brancato, S.K. and J.E. Albina, *Wound macrophages as key regulators of repair: origin, phenotype, and function.* Am J Pathol, 2011. **178**(1): p. 19-25.
64. Daley, J.M., et al., *The phenotype of murine wound macrophages.* J Leukoc Biol, 2010. **87**(1): p. 59-67.
65. Meszaros, A.J., J.S. Reichner, and J.E. Albina, *Macrophage-induced neutrophil apoptosis.* J Immunol, 2000. **165**(1): p. 435-41.
66. Peters, T., et al., *Wound-healing defect of CD18(-/-) mice due to a decrease in TGF-beta1 and myofibroblast differentiation.* EMBO J, 2005. **24**(19): p. 3400-10.
67. Mirza, R. and T.J. Koh, *Dysregulation of monocyte/macrophage phenotype in wounds of diabetic mice.* Cytokine, 2011. **56**(2): p. 256-64.
68. McNelis, J.C. and J.M. Olefsky, *Macrophages, immunity, and metabolic disease.* Immunity, 2014. **41**(1): p. 36-48.
69. Wu, D., et al., *Eosinophils sustain adipose alternatively activated macrophages associated with glucose homeostasis.* Science, 2011. **332**(6026): p. 243-7.
70. Lumeng, C.N., J.L. Bodzin, and A.R. Saltiel, *Obesity induces a phenotypic switch in adipose tissue macrophage polarization.* J Clin Invest, 2007. **117**(1): p. 175-84.
71. Zeyda, M. and T.M. Stulnig, *Adipose tissue macrophages.* Immunol Lett, 2007. **112**(2): p. 61-7.

72. Martin-Fuentes, P., et al., *Individual variation of scavenger receptor expression in human macrophages with oxidized low-density lipoprotein is associated with a differential inflammatory response.* J Immunol, 2007. **179**(5): p. 3242-8.
73. Moore, K.J. and M.W. Freeman, *Scavenger receptors in atherosclerosis: beyond lipid uptake.* Arterioscler Thromb Vasc Biol, 2006. **26**(8): p. 1702-11.
74. Moore, K.J., F.J. Sheedy, and E.A. Fisher, *Macrophages in atherosclerosis: a dynamic balance.* Nat Rev Immunol, 2013. **13**(10): p. 709-21.
75. Zhu, X., et al., *Macrophage ABCA1 reduces MyD88-dependent Toll-like receptor trafficking to lipid rafts by reduction of lipid raft cholesterol.* J Lipid Res, 2010. **51**(11): p. 3196-206.
76. Aggarwal, B.B., R.V. Vijayalekshmi, and B. Sung, *Targeting inflammatory pathways for prevention and therapy of cancer: short-term friend, long-term foe.* Clin Cancer Res, 2009. **15**(2): p. 425-30.
77. Hanahan, D. and R.A. Weinberg, *Hallmarks of cancer: the next generation.* Cell, 2011. **144**(5): p. 646-74.
78. Kulbe, H., et al., *The inflammatory cytokine tumor necrosis factor-alpha generates an autocrine tumor-promoting network in epithelial ovarian cancer cells.* Cancer Res, 2007. **67**(2): p. 585-92.
79. Naugler, W.E., et al., *Gender disparity in liver cancer due to sex differences in MyD88-dependent IL-6 production.* Science, 2007. **317**(5834): p. 121-4.
80. Mantovani, A., et al., *Chemokines in the recruitment and shaping of the leukocyte infiltrate of tumors.* Semin Cancer Biol, 2004. **14**(3): p. 155-60.
81. Komohara, Y., et al., *Macrophage infiltration and its prognostic relevance in clear cell renal cell carcinoma.* Cancer Sci, 2011. **102**(7): p. 1424-31.
82. Bronkhorst, I.H., et al., *Detection of M2-macrophages in uveal melanoma and relation with survival.* Invest Ophthalmol Vis Sci, 2011. **52**(2): p. 643-50.
83. Jensen, T.O., et al., *Macrophage markers in serum and tumor have prognostic impact in American Joint Committee on Cancer stage I/II melanoma.* J Clin Oncol, 2009. **27**(20): p. 3330-7.
84. Wu, Y. and L. Zheng, *Dynamic education of macrophages in different areas of human tumors.* Cancer Microenviron, 2012. **5**(3): p. 195-201.
85. Forssell, J., et al., *High macrophage infiltration along the tumor front correlates with improved survival in colon cancer.* Clin Cancer Res, 2007. **13**(5): p. 1472-9.
86. Nagorsen, D., et al., *Tumor-infiltrating macrophages and dendritic cells in human colorectal cancer: relation to local regulatory T cells, systemic T-cell response against tumor-associated antigens and survival.* J Transl Med, 2007. **5**: p. 62.
87. Shimura, S., et al., *Reduced infiltration of tumor-associated macrophages in human prostate cancer: association with cancer progression.* Cancer Res, 2000. **60**(20): p. 5857-61.
88. Hagemann, T., et al., *Ovarian cancer cells polarize macrophages toward a tumor-associated phenotype.* J Immunol, 2006. **176**(8): p. 5023-32.
89. Condeelis, J. and J.W. Pollard, *Macrophages: obligate partners for tumor cell migration, invasion, and metastasis.* Cell, 2006. **124**(2): p. 263-6.
90. Goswami, S., et al., *Macrophages promote the invasion of breast carcinoma cells via a colony-stimulating factor-1/epidermal growth factor paracrine loop.* Cancer Res, 2005. **65**(12): p. 5278-83.
91. Patsialou, A., et al., *Invasion of human breast cancer cells in vivo requires both paracrine and autocrine loops involving the colony-stimulating factor-1 receptor.* Cancer Res, 2009. **69**(24): p. 9498-506.
92. Wyckoff, J., et al., *A paracrine loop between tumor cells and macrophages is required for tumor cell migration in mammary tumors.* Cancer Res, 2004. **64**(19): p. 7022-9.
93. Biswas, S.K., et al., *A distinct and unique transcriptional program expressed by tumor-associated macrophages (defective NF-kappaB and enhanced IRF-3/STAT1 activation).* Blood, 2006. **107**(5): p. 2112-22.

94. Muller, A., et al., *Involvement of chemokine receptors in breast cancer metastasis.* Nature, 2001. **410**(6824): p. 50-6.
95. Chen, J., et al., *CCL18 from tumor-associated macrophages promotes breast cancer metastasis via PITPNM3.* Cancer Cell, 2011. **19**(4): p. 541-55.
96. Zhu, F., et al., *Tumor-associated macrophage or chemokine ligand CCL17 positively regulates the tumorigenesis of hepatocellular carcinoma.* Med Oncol, 2016. **33**(2): p. 17.
97. Werno, C., et al., *Knockout of HIF-1alpha in tumor-associated macrophages enhances M2 polarization and attenuates their pro-angiogenic responses.* Carcinogenesis, 2010. **31**(10): p. 1863-72.
98. White, J.R., et al., *Genetic amplification of the transcriptional response to hypoxia as a novel means of identifying regulators of angiogenesis.* Genomics, 2004. **83**(1): p. 1-8.
99. Kessenbrock, K., V. Plaks, and Z. Werb, *Matrix metalloproteinases: regulators of the tumor microenvironment.* Cell, 2010. **141**(1): p. 52-67.
100. Yang, M., et al., *Cathepsin S-mediated autophagic flux in tumor-associated macrophages accelerate tumor development by promoting M2 polarization.* Mol Cancer, 2014. **13**: p. 43.
101. Mason, S.D. and J.A. Joyce, *Proteolytic networks in cancer.* Trends Cell Biol, 2011. **21**(4): p. 228-37.
102. Gocheva, V., et al., *IL-4 induces cathepsin protease activity in tumor-associated macrophages to promote cancer growth and invasion.* Genes Dev, 2010. **24**(3): p. 241-55.
103. Hildenbrand, R., et al., *Urokinase plasminogen activator receptor (CD87) expression of tumor-associated macrophages in ductal carcinoma in situ, breast cancer, and resident macrophages of normal breast tissue.* J Leukoc Biol, 1999. **66**(1): p. 40-9.
104. Meznarich, J., et al., *Urokinase plasminogen activator induces pro-fibrotic/m2 phenotype in murine cardiac macrophages.* PLoS One, 2013. **8**(3): p. e57837.
105. Duffy, M.J., et al., *uPA and PAI-1 as biomarkers in breast cancer: validated for clinical use in level-of-evidence-1 studies.* Breast Cancer Res, 2014. **16**(4): p. 428.
106. Ma, J., et al., *Overexpression of forkhead box M1 and urokinase-type plasminogen activator in gastric cancer is associated with cancer progression and poor prognosis.* Oncol Lett, 2017. **14**(6): p. 7288-7296.
107. Mahmood, N., C. Mihalcioiu, and S.A. Rabbani, *Multifaceted Role of the Urokinase-Type Plasminogen Activator (uPA) and Its Receptor (uPAR): Diagnostic, Prognostic, and Therapeutic Applications.* Front Oncol, 2018. **8**: p. 24.
108. Ma, Y.Y., et al., *Interaction of coagulation factors and tumor-associated macrophages mediates migration and invasion of gastric cancer.* Cancer Sci, 2011. **102**(2): p. 336-42.
109. Riabov, V., et al., *Role of tumor associated macrophages in tumor angiogenesis and lymphangiogenesis.* Front Physiol, 2014. **5**: p. 75.
110. Newman, A.C. and C.C. Hughes, *Macrophages and angiogenesis: a role for Wnt signaling.* Vasc Cell, 2012. **4**(1): p. 13.
111. Karayiannakis, A.J., et al., *Circulating VEGF levels in the serum of gastric cancer patients: correlation with pathological variables, patient survival, and tumor surgery.* Ann Surg, 2002. **236**(1): p. 37-42.
112. Li, L., et al., *Correlation of serum VEGF levels with clinical stage, therapy efficacy, tumor metastasis and patient survival in ovarian cancer.* Anticancer Res, 2004. **24**(3b): p. 1973-9.
113. Sanchez-Martin, L., et al., *The chemokine CXCL12 regulates monocyte-macrophage differentiation and RUNX3 expression.* Blood, 2011. **117**(1): p. 88-97.
114. Lopez, A., et al., *Targeting Angiogenesis in Colorectal Carcinoma.* Drugs, 2019. **79**(1): p. 63-74.
115. Itatani, Y., et al., *Resistance to Anti-Angiogenic Therapy in Cancer-Alterations to Anti-VEGF Pathway.* Int J Mol Sci, 2018. **19**(4).
116. Ulivi, P., G. Marisi, and A. Passardi, *Relationship between hypoxia and response to antiangiogenic therapy in metastatic colorectal cancer.* Oncotarget, 2016. **7**(29): p. 46678-46691.

117. English, B.C., D.K. Price, and W.D. Figg, *VEGF inhibition and metastasis: possible implications for antiangiogenic therapy.* Cancer Biol Ther, 2009. **8**(13): p. 1214-25.
118. Xu, L., et al., *Direct evidence that bevacizumab, an anti-VEGF antibody, up-regulates SDF1alpha, CXCR4, CXCL6, and neuropilin 1 in tumors from patients with rectal cancer.* Cancer Res, 2009. **69**(20): p. 7905-10.
119. Sarvaiya, P.J., et al., *Chemokines in tumor progression and metastasis.* Oncotarget, 2013. **4**(12): p. 2171-85.
120. Singh, S., et al., *CXCR1 and CXCR2 silencing modulates CXCL8-dependent endothelial cell proliferation, migration and capillary-like structure formation.* Microvasc Res, 2011. **82**(3): p. 318-25.
121. Giuliano, S., et al., *The ELR(+)CXCL chemokines and their receptors CXCR1/CXCR2: A signaling axis and new target for the treatment of renal cell carcinoma.* Oncoimmunology, 2014. **3**: p. e28399.
122. Sparmann, A. and D. Bar-Sagi, *Ras-induced interleukin-8 expression plays a critical role in tumor growth and angiogenesis.* Cancer Cell, 2004. **6**(5): p. 447-58.
123. Pereira, C., et al., *Wnt5A/CaMKII signaling contributes to the inflammatory response of macrophages and is a target for the antiinflammatory action of activated protein C and interleukin-10.* Arterioscler Thromb Vasc Biol, 2008. **28**(3): p. 504-10.
124. Kim, J., et al., *Wnt5a induces endothelial inflammation via beta-catenin-independent signaling.* J Immunol, 2010. **185**(2): p. 1274-82.
125. Outtz, H.H., et al., *Notch1 controls macrophage recruitment and Notch signaling is activated at sites of endothelial cell anastomosis during retinal angiogenesis in mice.* Blood, 2011. **118**(12): p. 3436-9.
126. De Palma, M., et al., *Tie2 identifies a hematopoietic lineage of proangiogenic monocytes required for tumor vessel formation and a mesenchymal population of pericyte progenitors.* Cancer Cell, 2005. **8**(3): p. 211-26.
127. Murdoch, C., et al., *The role of myeloid cells in the promotion of tumour angiogenesis.* Nat Rev Cancer, 2008. **8**(8): p. 618-31.
128. Mazzieri, R., et al., *Targeting the ANG2/TIE2 axis inhibits tumor growth and metastasis by impairing angiogenesis and disabling rebounds of proangiogenic myeloid cells.* Cancer Cell, 2011. **19**(4): p. 512-26.
129. Chen, L., et al., *Tie2 Expression on Macrophages Is Required for Blood Vessel Reconstruction and Tumor Relapse after Chemotherapy.* Cancer Res, 2016. **76**(23): p. 6828-6838.
130. Mantovani, A., et al., *Macrophage polarization: tumor-associated macrophages as a paradigm for polarized M2 mononuclear phagocytes.* Trends Immunol, 2002. **23**(11): p. 549-55.
131. Wang, Y., et al., *TGF-beta1 promoted MMP-2 mediated wound healing of anterior cruciate ligament fibroblasts through NF-kappaB.* Connect Tissue Res, 2011. **52**(3): p. 218-25.
132. Johnston, C.J., et al., *TGF-beta in tolerance, development and regulation of immunity.* Cell Immunol, 2016. **299**: p. 14-22.
133. Dennis, K.L., et al., *Current status of interleukin-10 and regulatory T-cells in cancer.* Curr Opin Oncol, 2013. **25**(6): p. 637-45.
134. Gabrilovich, D.I., S. Ostrand-Rosenberg, and V. Bronte, *Coordinated regulation of myeloid cells by tumours.* Nature Reviews Immunology, 2012. **12**(4): p. 253-268.
135. Ostrand-Rosenberg, S., et al., *Cross-talk between myeloid-derived suppressor cells (MDSC), macrophages, and dendritic cells enhances tumor-induced immune suppression.* Seminars in Cancer Biology, 2012. **22**(4): p. 275-281.
136. Deaglio, S., et al., *Adenosine generation catalyzed by CD39 and CD73 expressed on regulatory T cells mediates immune suppression.* J Exp Med, 2007. **204**(6): p. 1257-65.
137. Kobie, J.J., et al., *T regulatory and primed uncommitted CD4 T cells express CD73, which suppresses effector CD4 T cells by converting 5'-adenosine monophosphate to adenosine.* J Immunol, 2006. **177**(10): p. 6780-6.

138. Mandapathil, M., et al., *Generation and accumulation of immunosuppressive adenosine by human CD4+CD25highFOXP3+ regulatory T cells.* J Biol Chem, 2010. **285**(10): p. 7176-86.
139. Ohta, A. and M. Sitkovsky, *Extracellular adenosine-mediated modulation of regulatory T cells.* Front Immunol, 2014. **5**: p. 304.
140. Ohta, A., et al., *The development and immunosuppressive functions of CD4(+) CD25(+) FoxP3(+) regulatory T cells are under influence of the adenosine-A2A adenosine receptor pathway.* Front Immunol, 2012. **3**: p. 190.
141. Morello, S. and L. Miele, *Targeting the adenosine A2b receptor in the tumor microenvironment overcomes local immunosuppression by myeloid-derived suppressor cells.* Oncoimmunology, 2014. **3**: p. e27989.
142. Ryzhov, S., et al., *Adenosinergic regulation of the expansion and immunosuppressive activity of CD11b+Gr1+ cells.* J Immunol, 2011. **187**(11): p. 6120-9.
143. Travis, M.A. and D. Sheppard, *TGF-beta activation and function in immunity.* Annu Rev Immunol, 2014. **32**: p. 51-82.
144. Svensson, M.N., et al., *Reduced expression of phosphatase PTPN2 promotes pathogenic conversion of Tregs in autoimmunity.* J Clin Invest, 2019.
145. Romano, M., et al., *Expanded Regulatory T Cells Induce Alternatively Activated Monocytes With a Reduced Capacity to Expand T Helper-17 Cells.* Front Immunol, 2018. **9**: p. 1625.
146. Zhou, K., et al., *Regulatory T cells ameliorate intracerebral hemorrhage-induced inflammatory injury by modulating microglia/macrophage polarization through the IL-10/GSK3beta/PTEN axis.* J Cereb Blood Flow Metab, 2017. **37**(3): p. 967-979.
147. Mizukami, Y., et al., *CCL17 and CCL22 chemokines within tumor microenvironment are related to accumulation of Foxp3+ regulatory T cells in gastric cancer.* Int J Cancer, 2008. **122**(10): p. 2286-93.
148. Li, Y.Q., et al., *Tumor secretion of CCL22 activates intratumoral Treg infiltration and is independent prognostic predictor of breast cancer.* PLoS One, 2013. **8**(10): p. e76379.
149. Umansky, V., et al., *Myeloid-derived suppressor cells in malignant melanoma.* JDDG: Journal der Deutschen Dermatologischen Gesellschaft, 2014. **12**(11): p. 1021-1027.
150. Ostrand-Rosenberg, S., *Myeloid-derived suppressor cells: more mechanisms for inhibiting antitumor immunity.* Cancer Immunology, Immunotherapy, 2010. **59**(10): p. 1593-1600.
151. Umansky, V., et al., *The Role of Myeloid-Derived Suppressor Cells (MDSC) in Cancer Progression.* Vaccines (Basel), 2016. **4**(4).
152. Rodriguez, P.C., et al., *Arginase I production in the tumor microenvironment by mature myeloid cells inhibits T-cell receptor expression and antigen-specific T-cell responses.* Cancer Res, 2004. **64**(16): p. 5839-49.
153. Cassetta, L. and T. Kitamura, *Macrophage targeting: opening new possibilities for cancer immunotherapy.* Immunology, 2018. **155**(3): p. 285-293.
154. Cassetta, L. and J.W. Pollard, *Targeting macrophages: therapeutic approaches in cancer.* Nat Rev Drug Discov, 2018.
155. Dammeijer, F., et al., *Depletion of Tumor-Associated Macrophages with a CSF-1R Kinase Inhibitor Enhances Antitumor Immunity and Survival Induced by DC Immunotherapy.* Cancer Immunol Res, 2017. **5**(7): p. 535-546.
156. Lyons, Y.A., et al., *Macrophage depletion through colony stimulating factor 1 receptor pathway blockade overcomes adaptive resistance to anti-VEGF therapy.* Oncotarget, 2017. **8**(57): p. 96496-96505.
157. Strachan, D.C., et al., *CSF1R inhibition delays cervical and mammary tumor growth in murine models by attenuating the turnover of tumor-associated macrophages and enhancing infiltration by CD8(+) T cells.* Oncoimmunology, 2013. **2**(12): p. e26968.
158. Zhu, Y., et al., *CSF1/CSF1R blockade reprograms tumor-infiltrating macrophages and improves response to T-cell checkpoint immunotherapy in pancreatic cancer models.* Cancer Res, 2014. **74**(18): p. 5057-69.

159. Neubert, N.J., et al., *T cell-induced CSF1 promotes melanoma resistance to PD1 blockade.* Sci Transl Med, 2018. **10**(436).
160. Paulus, P., et al., *Colony-stimulating factor-1 antibody reverses chemoresistance in human MCF-7 breast cancer xenografts.* Cancer Res, 2006. **66**(8): p. 4349-56.
161. Loberg, R.D., et al., *Targeting CCL2 with systemic delivery of neutralizing antibodies induces prostate cancer tumor regression in vivo.* Cancer Res, 2007. **67**(19): p. 9417-24.
162. Vergunst, C.E., et al., *Modulation of CCR2 in rheumatoid arthritis: a double-blind, randomized, placebo-controlled clinical trial.* Arthritis Rheum, 2008. **58**(7): p. 1931-9.
163. Nakanishi, Y., et al., *COX-2 inhibition alters the phenotype of tumor-associated macrophages from M2 to M1 in ApcMin/+ mouse polyps.* Carcinogenesis, 2011. **32**(9): p. 1333-9.
164. van Kooten, C. and J. Banchereau, *CD40-CD40 ligand.* J Leukoc Biol, 2000. **67**(1): p. 2-17.
165. Khalil, M. and R.H. Vonderheide, *Anti-CD40 agonist antibodies: preclinical and clinical experience.* Update Cancer Ther, 2007. **2**(2): p. 61-65.
166. Hoves, S., et al., *Rapid activation of tumor-associated macrophages boosts preexisting tumor immunity.* J Exp Med, 2018. **215**(3): p. 859-876.
167. Perry, C.J., et al., *Myeloid-targeted immunotherapies act in synergy to induce inflammation and antitumor immunity.* J Exp Med, 2018. **215**(3): p. 877-893.
168. Saccani, A., et al., *p50 nuclear factor-kappaB overexpression in tumor-associated macrophages inhibits M1 inflammatory responses and antitumor resistance.* Cancer Res, 2006. **66**(23): p. 11432-40.
169. Kaneda, M.M., et al., *PI3Kgamma is a molecular switch that controls immune suppression.* Nature, 2016. **539**(7629): p. 437-442.
170. Le Mercier, I., et al., *Tumor promotion by intratumoral plasmacytoid dendritic cells is reversed by TLR7 ligand treatment.* Cancer Res, 2013. **73**(15): p. 4629-40.
171. Singh, M., et al., *Effective innate and adaptive antimelanoma immunity through localized TLR7/8 activation.* J Immunol, 2014. **193**(9): p. 4722-31.
172. Arlauckas, S.P., et al., *In vivo imaging reveals a tumor-associated macrophage-mediated resistance pathway in anti-PD-1 therapy.* Sci Transl Med, 2017. **9**(389).
173. Steggerda, S.M., et al., *Inhibition of arginase by CB-1158 blocks myeloid cell-mediated immune suppression in the tumor microenvironment.* J Immunother Cancer, 2017. **5**(1): p. 101.
174. Schadendorf, D., et al., *Melanoma.* Lancet, 2018. **392**(10151): p. 971-984.
175. Miller, A.J. and M.C. Mihm, *Melanoma.* N Engl J Med, 2006. **355**: p. 51-65.
176. Leonardi, G.C., et al., *Cutaneous melanoma: From pathogenesis to therapy (Review).* Int J Oncol, 2018. **52**(4): p. 1071-1080.
177. Parkin, D.M., D. Mesher, and P. Sasieni, *13. Cancers attributable to solar (ultraviolet) radiation exposure in the UK in 2010.* Br J Cancer, 2011. **105 Suppl 2**: p. S66-9.
178. Neale, R.E., et al., *Site-specific occurrence of nonmelanoma skin cancers in patients with cutaneous melanoma.* Br J Cancer, 2005. **93**(5): p. 597-601.
179. Zanetti, R., et al., *Comparison of risk patterns in carcinoma and melanoma of the skin in men: a multi-centre case-case-control study.* Br J Cancer, 2006. **94**(5): p. 743-51.
180. Dennis, L.K., et al., *Sunburns and risk of cutaneous melanoma: does age matter? A comprehensive meta-analysis.* Ann Epidemiol, 2008. **18**(8): p. 614-27.
181. Gandini, S., P. Autier, and M. Boniol, *Reviews on sun exposure and artificial light and melanoma.* Prog Biophys Mol Biol, 2011. **107**(3): p. 362-6.
182. Lin, J.Y. and D.E. Fisher, *Melanocyte biology and skin pigmentation.* Nature, 2007. **445**(7130): p. 843-50.
183. Scherer, D. and R. Kumar, *Genetics of pigmentation in skin cancer--a review.* Mutat Res, 2010. **705**(2): p. 141-53.
184. Kennedy, C., et al., *Melanocortin 1 receptor (MC1R) gene variants are associated with an increased risk for cutaneous melanoma which is largely independent of skin type and hair color.* J Invest Dermatol, 2001. **117**(2): p. 294-300.

185. Naysmith, L., et al., *Quantitative measures of the effect of the melanocortin 1 receptor on human pigmentary status.* J Invest Dermatol, 2004. **122**(2): p. 423-8.
186. Valverde, P., et al., *Variants of the melanocyte-stimulating hormone receptor gene are associated with red hair and fair skin in humans.* Nat Genet, 1995. **11**(3): p. 328-30.
187. Kubica, A.W. and J.D. Brewer, *Melanoma in Immunosuppressed Patients.* Mayo Clinic Proceedings, 2012. **87**(10): p. 991-1003.
188. Gandini, S., et al., *Meta-analysis of risk factors for cutaneous melanoma: I. Common and atypical naevi.* Eur J Cancer, 2005. **41**(1): p. 28-44.
189. Olsen, C.M., et al., *Nevus density and melanoma risk in women: a pooled analysis to test the divergent pathway hypothesis.* Int J Cancer, 2009. **124**(4): p. 937-44.
190. Seykora, J. and D. Elder, *Dysplastic nevi and other risk markers for melanoma.* Semin Oncol, 1996. **23**(6): p. 682-7.
191. Watt, A.J., S.V. Kotsis, and K.C. Chung, *Risk of melanoma arising in large congenital melanocytic nevi: a systematic review.* Plast Reconstr Surg, 2004. **113**(7): p. 1968-74.
192. Alexandrov, L.B., et al., *Signatures of mutational processes in human cancer.* Nature, 2013. **500**(7463): p. 415-21.
193. Hodis, E., et al., *A landscape of driver mutations in melanoma.* Cell, 2012. **150**(2): p. 251-63.
194. Omholt, K., et al., *NRAS and BRAF mutations arise early during melanoma pathogenesis and are preserved throughout tumor progression.* Clin Cancer Res, 2003. **9**(17): p. 6483-8.
195. Pollock, P.M., et al., *High frequency of BRAF mutations in nevi.* Nat Genet, 2003. **33**(1): p. 19-20.
196. Michaloglou, C., et al., *BRAFE600-associated senescence-like cell cycle arrest of human naevi.* Nature, 2005. **436**(7051): p. 720-4.
197. Ferris, L., et al., *Non-Invasive Analysis of High-Risk Driver Mutations and Gene Expression Profiles in Primary Cutaneous Melanoma.* J Invest Dermatol, 2018.
198. Sharpless, E. and L. Chin, *The INK4a/ARF locus and melanoma.* Oncogene, 2003. **22**(20): p. 3092-8.
199. Wu, H., V. Goel, and F.G. Haluska, *PTEN signaling pathways in melanoma.* Oncogene, 2003. **22**(20): p. 3113-22.
200. Felding-Habermann, B., et al., *Involvement of tumor cell integrin alpha v beta 3 in hematogenous metastasis of human melanoma cells.* Clin Exp Metastasis, 2002. **19**(5): p. 427-36.
201. Hofmann, U.B., et al., *Coexpression of integrin alpha(v)beta3 and matrix metalloproteinase-2 (MMP-2) coincides with MMP-2 activation: correlation with melanoma progression.* J Invest Dermatol, 2000. **115**(4): p. 625-32.
202. Petitclerc, E., et al., *Integrin alpha(v)beta3 promotes M21 melanoma growth in human skin by regulating tumor cell survival.* Cancer Res, 1999. **59**(11): p. 2724-30.
203. Hsu, M.Y., et al., *E-cadherin expression in melanoma cells restores keratinocyte-mediated growth control and down-regulates expression of invasion-related adhesion receptors.* Am J Pathol, 2000. **156**(5): p. 1515-25.
204. Hsu, M.Y., et al., *Shifts in cadherin profiles between human normal melanocytes and melanomas.* J Investig Dermatol Symp Proc, 1996. **1**(2): p. 188-94.
205. Gottardi, C.J., E. Wong, and B.M. Gumbiner, *E-cadherin suppresses cellular transformation by inhibiting beta-catenin signaling in an adhesion-independent manner.* J Cell Biol, 2001. **153**(5): p. 1049-60.
206. Webster, M.R., C.H. Kugel, 3rd, and A.T. Weeraratna, *The Wnts of change: How Wnts regulate phenotype switching in melanoma.* Biochim Biophys Acta, 2015. **1856**(2): p. 244-51.
207. Widlund, H.R., et al., *Beta-catenin-induced melanoma growth requires the downstream target Microphthalmia-associated transcription factor.* J Cell Biol, 2002. **158**(6): p. 1079-87.
208. McGill, G.G., et al., *Bcl2 regulation by the melanocyte master regulator Mitf modulates lineage survival and melanoma cell viability.* Cell, 2002. **109**(6): p. 707-18.

209. Garraway, L.A., et al., *Integrative genomic analyses identify MITF as a lineage survival oncogene amplified in malignant melanoma.* Nature, 2005. **436**(7047): p. 117-22.
210. Schumacher, T.N. and R.D. Schreiber, *Neoantigens in cancer immunotherapy.* Science, 2015. **348**(6230): p. 69-74.
211. Gentles, A.J., et al., *The prognostic landscape of genes and infiltrating immune cells across human cancers.* Nat Med, 2015. **21**(8): p. 938-945.
212. Umansky, V. and A. Sevko, *Melanoma-induced immunosuppression and its neutralization.* Seminars in Cancer Biology, 2012. **22**(4): p. 319-326.
213. Furudate, S., et al., *Immunomodulatory Effect of Imiquimod Through CCL22 Produced by Tumor-associated Macrophages in B16F10 Melanomas.* Anticancer Res, 2017. **37**(7): p. 3461-3471.
214. Poschke, I., et al., *Immature immunosuppressive CD14+HLA-DR-/low cells in melanoma patients are Stat3hi and overexpress CD80, CD83, and DC-sign.* Cancer Res, 2010. **70**(11): p. 4335-45.
215. Weide, B., et al., *Myeloid-derived suppressor cells predict survival of patients with advanced melanoma: comparison with regulatory T cells and NY-ESO-1- or melan-A-specific T cells.* Clin Cancer Res, 2014. **20**(6): p. 1601-9.
216. Fujimura, T., Y. Kambayashi, and S. Aiba, *Crosstalk between regulatory T cells (Tregs) and myeloid derived suppressor cells (MDSCs) during melanoma growth.* Oncoimmunology, 2012. **1**(8): p. 1433-1434.
217. Tucci, M., et al., *The immune escape in melanoma: role of the impaired dendritic cell function.* Expert Rev Clin Immunol, 2014. **10**(10): p. 1395-404.
218. Baumgartner, J., et al., *Melanoma induces immunosuppression by up-regulating FOXP3(+) regulatory T cells.* J Surg Res, 2007. **141**(1): p. 72-7.
219. Collin, M., N. McGovern, and M. Haniffa, *Human dendritic cell subsets.* Immunology, 2013. **140**(1): p. 22-30.
220. Mellman, I., *Dendritic cells: master regulators of the immune response.* Cancer Immunol Res, 2013. **1**(3): p. 145-9.
221. Failli, A., et al., *Numerical defect of circulating dendritic cell subsets and defective dendritic cell generation from monocytes of patients with advanced melanoma.* Cancer Lett, 2013. **337**(2): p. 184-92.
222. Ito, M., et al., *Tumor-derived TGFbeta-1 induces dendritic cell apoptosis in the sentinel lymph node.* J Immunol, 2006. **176**(9): p. 5637-43.
223. Zhao, F., et al., *Activation of p38 mitogen-activated protein kinase drives dendritic cells to become tolerogenic in ret transgenic mice spontaneously developing melanoma.* Clin Cancer Res, 2009. **15**(13): p. 4382-90.
224. Azimi, F., et al., *Tumor-infiltrating lymphocyte grade is an independent predictor of sentinel lymph node status and survival in patients with cutaneous melanoma.* J Clin Oncol, 2012. **30**(21): p. 2678-83.
225. Brown, I.E., et al., *Homeostatic proliferation as an isolated variable reverses CD8+ T cell anergy and promotes tumor rejection.* J Immunol, 2006. **177**(7): p. 4521-9.
226. Fregni, G., et al., *Phenotypic and functional characteristics of blood natural killer cells from melanoma patients at different clinical stages.* PLoS One, 2013. **8**(10): p. e76928.
227. Pietra, G., et al., *Melanoma cells inhibit natural killer cell function by modulating the expression of activating receptors and cytolytic activity.* Cancer Res, 2012. **72**(6): p. 1407-15.
228. Tarazona, R., E. Duran, and R. Solana, *Natural Killer Cell Recognition of Melanoma: New Clues for a More Effective Immunotherapy.* Front Immunol, 2015. **6**: p. 649.
229. Mukherji, B., *Immunology of melanoma.* Clin Dermatol, 2013. **31**(2): p. 156-65.
230. Chen, L. and D.B. Flies, *Molecular mechanisms of T cell co-stimulation and co-inhibition.* Nat Rev Immunol, 2013. **13**(4): p. 227-42.
231. Chen, L., *Co-inhibitory molecules of the B7-CD28 family in the control of T-cell immunity.* Nat Rev Immunol, 2004. **4**(5): p. 336-47.

232. Basile, M.S., et al., *Differential modulation and prognostic values of immune-escape genes in uveal melanoma.* PLoS One, 2019. **14**(1): p. e0210276.
233. Kammerer-Jacquet, S.F., et al., *Independent association of PD-L1 expression with noninactivated VHL clear cell renal cell carcinoma-A finding with therapeutic potential.* Int J Cancer, 2017. **140**(1): p. 142-148.
234. Mansh, M., *Ipilimumab and cancer immunotherapy: a new hope for advanced stage melanoma.* Yale J Biol Med, 2011. **84**(4): p. 381-9.
235. Improta, G., et al., *New developments in the management of advanced melanoma - role of pembrolizumab.* OncoTargets and Therapy, 2015: p. 2535.
236. Nakamura, M., et al., *Nivolumab in the treatment of malignant melanoma: review of the literature.* OncoTargets and Therapy, 2015: p. 2045.
237. Mariathasan, S., et al., *TGFbeta attenuates tumour response to PD-L1 blockade by contributing to exclusion of T cells.* Nature, 2018. **554**(7693): p. 544-548.
238. Chen, D.S. and I. Mellman, *Elements of cancer immunity and the cancer-immune set point.* Nature, 2017. **541**(7637): p. 321-330.
239. Ferrone, S. and F.M. Marincola, *Loss of HLA class I antigens by melanoma cells: molecular mechanisms, functional significance and clinical relevance.* Immunol Today, 1995. **16**(10): p. 487-94.
240. Cassetta, L. and T. Kitamura, *Targeting Tumor-Associated Macrophages as a Potential Strategy to Enhance the Response to Immune Checkpoint Inhibitors.* Front Cell Dev Biol, 2018. **6**: p. 38.
241. von Kugelgen, I., *Pharmacological profiles of cloned mammalian P2Y-receptor subtypes.* Pharmacol Ther, 2006. **110**(3): p. 415-32.
242. Fredholm, B.B., et al., *International Union of Pharmacology. XXV. Nomenclature and classification of adenosine receptors.* Pharmacol Rev, 2001. **53**(4): p. 527-52.
243. Sheth, S., et al., *Adenosine receptors: expression, function and regulation.* Int J Mol Sci, 2014. **15**(2): p. 2024-52.
244. Muller, C.E. and K.A. Jacobson, *Xanthines as adenosine receptor antagonists.* Handb Exp Pharmacol, 2011(200): p. 151-99.
245. Bahreyni, A., et al., *Therapeutic potential of A2 adenosine receptor pharmacological regulators in the treatment of cardiovascular diseases, recent progress, and prospective.* J Cell Physiol, 2019. **234**(2): p. 1295-1299.
246. Hasko, G., et al., *Adenosine receptor signaling in the brain immune system.* Trends Pharmacol Sci, 2005. **26**(10): p. 511-6.
247. Hasko, G. and P. Pacher, *A2A receptors in inflammation and injury: lessons learned from transgenic animals.* J Leukoc Biol, 2008. **83**(3): p. 447-55.
248. Butler, M., et al., *Impairment of adenosine A3 receptor activity disrupts neutrophil migratory capacity and impacts innate immune function in vivo.* Eur J Immunol, 2012. **42**(12): p. 3358-68.
249. Joos, G., et al., *Involvement of adenosine A3 receptors in the chemotactic navigation of macrophages towards apoptotic cells.* Immunol Lett, 2017. **183**: p. 62-72.
250. Allard, B., et al., *Immunosuppressive activities of adenosine in cancer.* Curr Opin Pharmacol, 2016. **29**: p. 7-16.
251. Habermacher, C., et al., *Molecular structure and function of P2X receptors.* Neuropharmacology, 2016. **104**: p. 18-30.
252. Cekic, C. and J. Linden, *Purinergic regulation of the immune system.* Nature Reviews Immunology, 2016. **16**(3): p. 177-192.
253. Di Virgilio, F., et al., *The P2X7 Receptor in Infection and Inflammation.* Immunity, 2017. **47**(1): p. 15-31.
254. Tuteja, N., *Signaling through G protein coupled receptors.* Plant Signal Behav, 2009. **4**(10): p. 942-7.
255. Domercq, M., N. Vazquez-Villoldo, and C. Matute, *Neurotransmitter signaling in the pathophysiology of microglia.* Front Cell Neurosci, 2013. **7**: p. 49.
256. Kunapuli, S.P., et al., *Platelet purinergic receptors.* Curr Opin Pharmacol, 2003. **3**(2): p. 175-80.

257. Jacob, F., et al., *Purinergic signaling in inflammatory cells: P2 receptor expression, functional effects, and modulation of inflammatory responses.* Purinergic Signal, 2013. **9**(3): p. 285-306.
258. Ravichandran, K.S., *Find-me and eat-me signals in apoptotic cell clearance: progress and conundrums.* J Exp Med, 2010. **207**(9): p. 1807-17.
259. Di Virgilio, F., *Purinergic mechanism in the immune system: A signal of danger for dendritic cells.* Purinergic Signal, 2005. **1**(3): p. 205-9.
260. Elliott, M.R., et al., *Nucleotides released by apoptotic cells act as a find-me signal to promote phagocytic clearance.* Nature, 2009. **461**(7261): p. 282-6.
261. Burnstock, G., *Purinergic signalling and disorders of the central nervous system.* Nat Rev Drug Discov, 2008. **7**(7): p. 575-90.
262. Praetorius, H.A. and J. Leipziger, *ATP release from non-excitable cells.* Purinergic Signal, 2009. **5**(4): p. 433-46.
263. Chen, Y., et al., *ATP release guides neutrophil chemotaxis via P2Y2 and A3 receptors.* Science, 2006. **314**(5806): p. 1792-5.
264. Woehrle, T., et al., *Pannexin-1 hemichannel-mediated ATP release together with P2X1 and P2X4 receptors regulate T-cell activation at the immune synapse.* Blood, 2010. **116**(18): p. 3475-84.
265. Yip, L., et al., *Autocrine regulation of T-cell activation by ATP release and P2X7 receptors.* FASEB J, 2009. **23**(6): p. 1685-93.
266. Schenk, U., et al., *Purinergic control of T cell activation by ATP released through pannexin-1 hemichannels.* Sci Signal, 2008. **1**(39): p. ra6.
267. Chen, Y., et al., *Purinergic signaling: a fundamental mechanism in neutrophil activation.* Sci Signal, 2010. **3**(125): p. ra45.
268. Kronlage, M., et al., *Autocrine purinergic receptor signaling is essential for macrophage chemotaxis.* Sci Signal, 2010. **3**(132): p. ra55.
269. Saez, P.J., et al., *ATP promotes the fast migration of dendritic cells through the activity of pannexin 1 channels and P2X7 receptors.* Sci Signal, 2017. **10**(506).
270. Schnurr, M., et al., *Extracellular ATP and TNF-alpha synergize in the activation and maturation of human dendritic cells.* J Immunol, 2000. **165**(8): p. 4704-9.
271. Schnurr, M., et al., *ATP gradients inhibit the migratory capacity of specific human dendritic cell types: implications for P2Y11 receptor signaling.* Blood, 2003. **102**(2): p. 613-20.
272. Gombault, A., L. Baron, and I. Couillin, *ATP release and purinergic signaling in NLRP3 inflammasome activation.* Front Immunol, 2012. **3**: p. 414.
273. Pelegrin, P., C. Barroso-Gutierrez, and A. Surprenant, *P2X7 receptor differentially couples to distinct release pathways for IL-1beta in mouse macrophage.* J Immunol, 2008. **180**(11): p. 7147-57.
274. Loomis, W.H., et al., *Hypertonic stress increases T cell interleukin-2 expression through a mechanism that involves ATP release, P2 receptor, and p38 MAPK activation.* J Biol Chem, 2003. **278**(7): p. 4590-6.
275. Yegutkin, G.G., *Nucleotide- and nucleoside-converting ectoenzymes: Important modulators of purinergic signalling cascade.* Biochim Biophys Acta, 2008. **1783**(5): p. 673-94.
276. Zimmermann, H., *Extracellular metabolism of ATP and other nucleotides.* Naunyn Schmiedebergs Arch Pharmacol, 2000. **362**(4-5): p. 299-309.
277. Ryzhov, S., et al., *Effect of A2B adenosine receptor gene ablation on adenosine-dependent regulation of proinflammatory cytokines.* J Pharmacol Exp Ther, 2008. **324**(2): p. 694-700.
278. Csoka, B., et al., *A2A adenosine receptors and C/EBPbeta are crucially required for IL-10 production by macrophages exposed to Escherichia coli.* Blood, 2007. **110**(7): p. 2685-95.
279. Moore, C.C., et al., *An A2A adenosine receptor agonist, ATL313, reduces inflammation and improves survival in murine sepsis models.* BMC Infect Dis, 2008. **8**: p. 141.
280. Ohta, A. and M. Sitkovsky, *Role of G-protein-coupled adenosine receptors in downregulation of inflammation and protection from tissue damage.* Nature, 2001. **414**(6866): p. 916-20.

281. Mizumoto, N., et al., *CD39 is the dominant Langerhans cell-associated ecto-NTPDase: modulatory roles in inflammation and immune responsiveness.* Nat Med, 2002. **8**(4): p. 358-65.
282. Hamidzadeh, K. and D.M. Mosser, *Purinergic Signaling to Terminate TLR Responses in Macrophages.* Frontiers in Immunology, 2016. **7**.
283. Sun, Y., et al., *A novel mechanism of control of NFkappaB activation and inflammation involving A2B adenosine receptors.* J Cell Sci, 2012. **125**(Pt 19): p. 4507-17.
284. Sorrentino, C., et al., *Myeloid-derived suppressor cells contribute to A2B adenosine receptor-induced VEGF production and angiogenesis in a mouse melanoma model.* Oncotarget, 2015. **6**(29): p. 27478-89.
285. Zhou, Y., et al., *Distinct roles for the A2B adenosine receptor in acute and chronic stages of bleomycin-induced lung injury.* J Immunol, 2011. **186**(2): p. 1097-106.
286. Zavialov, A.V., et al., *Human adenosine deaminase 2 induces differentiation of monocytes into macrophages and stimulates proliferation of T helper cells and macrophages.* J Leukoc Biol, 2010. **88**(2): p. 279-90.
287. Cristalli, G., et al., *Adenosine deaminase: functional implications and different classes of inhibitors.* Med Res Rev, 2001. **21**(2): p. 105-28.
288. Soler, C., et al., *Macrophages require different nucleoside transport systems for proliferation and activation.* FASEB J, 2001. **15**(11): p. 1979-88.
289. Kichenin, K., et al., *CD3 activation induces concentrative nucleoside transport in human T lymphocytes.* Eur J Immunol, 2000. **30**(2): p. 366-70.
290. Junger, W.G., *Immune cell regulation by autocrine purinergic signalling.* Nat Rev Immunol, 2011. **11**(3): p. 201-12.
291. Li, J., et al., *CD39/CD73 upregulation on myeloid-derived suppressor cells via TGF-beta-mTOR-HIF-1 signaling in patients with non-small cell lung cancer.* Oncoimmunology, 2017. **6**(6): p. e1320011.
292. Beavis, P.A., et al., *Blockade of A2A receptors potently suppresses the metastasis of CD73+ tumors.* Proc Natl Acad Sci U S A, 2013. **110**(36): p. 14711-6.
293. Stagg, J., et al., *Anti-CD73 antibody therapy inhibits breast tumor growth and metastasis.* Proc Natl Acad Sci U S A, 2010. **107**(4): p. 1547-52.
294. Allard, B., M. Turcotte, and J. Stagg, *Targeting CD73 and downstream adenosine receptor signaling in triple-negative breast cancer.* Expert Opin Ther Targets, 2014. **18**(8): p. 863-81.
295. Cekic, C., et al., *Myeloid expression of adenosine A2A receptor suppresses T and NK cell responses in the solid tumor microenvironment.* Cancer Res, 2014. **74**(24): p. 7250-9.
296. Cekic, C. and J. Linden, *Adenosine A2A receptors intrinsically regulate CD8+ T cells in the tumor microenvironment.* Cancer Res, 2014. **74**(24): p. 7239-49.
297. Zanin, R.F., et al., *Differential macrophage activation alters the expression profile of NTPDase and ecto-5'-nucleotidase.* PLoS One, 2012. **7**(2): p. e31205.
298. Ntantie, E., et al., *An adenosine-mediated signaling pathway suppresses prenylation of the GTPase Rap1B and promotes cell scattering.* Sci Signal, 2013. **6**(277): p. ra39.
299. Cekic, C., et al., *Adenosine A2B receptor blockade slows growth of bladder and breast tumors.* J Immunol, 2012. **188**(1): p. 198-205.
300. Adinolfi, E., et al., *Accelerated tumor progression in mice lacking the ATP receptor P2X7.* Cancer Res, 2015. **75**(4): p. 635-44.
301. Martins, I., et al., *Chemotherapy induces ATP release from tumor cells.* Cell Cycle, 2009. **8**(22): p. 3723-8.
302. Aymeric, L., et al., *Tumor cell death and ATP release prime dendritic cells and efficient anticancer immunity.* Cancer Res, 2010. **70**(3): p. 855-8.
303. Zhong, X., et al., *N-linked glycosylation of platelet P2Y12 ADP receptor is essential for signal transduction but not for ligand binding or cell surface expression.* FEBS Lett, 2004. **562**(1-3): p. 111-7.

304. Schöneberg, T., et al., *Structural and functional evolution of the P2Y12-like receptor group.* Purinergic Signalling, 2007. **3**(4): p. 255-268.
305. Guidetti, G.F., et al., *The Gi-coupled P2Y12 Receptor Regulates Diacylglycerol-mediated Signaling in Human Platelets.* Journal of Biological Chemistry, 2008. **283**(43): p. 28795-28805.
306. Soulet, C., et al., *Gi-dependent and -independent mechanisms downstream of the P2Y12 ADP-receptor.* Journal of Thrombosis and Haemostasis, 2004. **2**(1): p. 135-146.
307. Cattaneo, M., *P2Y12 receptors: structure and function.* J Thromb Haemost, 2015. **13 Suppl 1**: p. S10-6.
308. Gachet, C., *P2Y12 receptors in platelets and other hematopoietic and non-hematopoietic cells.* Purinergic Signalling, 2012. **8**(3): p. 609-619.
309. Brass, L.F., S.L. Diamond, and T.J. Stalker, *Platelets and hemostasis: a new perspective on an old subject.* Blood Adv, 2016. **1**(1): p. 5-9.
310. Hardy, A.R., *Reciprocal cross-talk between P2Y1 and P2Y12 receptors at the level of calcium signaling in human platelets.* Blood, 2004. **104**(6): p. 1745-1752.
311. Cunningham, M.R., S.P. Nisar, and S.J. Mundell, *Molecular mechanisms of platelet P2Y(12) receptor regulation.* Biochem Soc Trans, 2013. **41**(1): p. 225-30.
312. Andre, P., et al., *P2Y12 regulates platelet adhesion/activation, thrombus growth, and thrombus stability in injured arteries.* J Clin Invest, 2003. **112**(3): p. 398-406.
313. Foster, C.J., et al., *Molecular identification and characterization of the platelet ADP receptor targeted by thienopyridine antithrombotic drugs.* J Clin Invest, 2001. **107**(12): p. 1591-8.
314. Gawaz, M., H. Langer, and A.E. May, *Platelets in inflammation and atherogenesis.* J Clin Invest, 2005. **115**(12): p. 3378-84.
315. Steinhubl, S.R., et al., *Clinical evidence for anti-inflammatory effects of antiplatelet therapy in patients with atherothrombotic disease.* Vasc Med, 2007. **12**(2): p. 113-22.
316. Abele, S., et al., *Attenuation of transplant arteriosclerosis with clopidogrel is associated with a reduction of infiltrating dendritic cells and macrophages in murine aortic allografts.* Transplantation, 2009. **87**(2): p. 207-16.
317. Paruchuri, S., et al., *Leukotriene E4-induced pulmonary inflammation is mediated by the P2Y12 receptor.* J Exp Med, 2009. **206**(11): p. 2543-55.
318. Nonaka, Y., T. Hiramoto, and N. Fujita, *Identification of endogenous surrogate ligands for human P2Y12 receptors by in silico and in vitro methods.* Biochem Biophys Res Commun, 2005. **337**(1): p. 281-8.
319. Wang, Y., et al., *Platelet P2Y12 Is Involved in Murine Pulmonary Metastasis.* PLoS ONE, 2013. **8**(11): p. e80780.
320. Gebremeskel, S., et al., *The reversible P2Y12 inhibitor ticagrelor inhibits metastasis and improves survival in mouse models of cancer.* International Journal of Cancer, 2015. **136**(1): p. 234-240.
321. Suzuki, T., et al., *Production and release of neuroprotective tumor necrosis factor by P2X7 receptor-activated microglia.* J Neurosci, 2004. **24**(1): p. 1-7.
322. Monif, M., et al., *The P2X7 receptor drives microglial activation and proliferation: a trophic role for P2X7R pore.* J Neurosci, 2009. **29**(12): p. 3781-91.
323. Koizumi, S., et al., *UDP acting at P2Y6 receptors is a mediator of microglial phagocytosis.* Nature, 2007. **446**(7139): p. 1091-5.
324. Ohsawa, K., et al., *Involvement of P2X4 and P2Y12 receptors in ATP-induced microglial chemotaxis.* Glia, 2007. **55**(6): p. 604-16.
325. Haynes, S.E., et al., *The P2Y12 receptor regulates microglial activation by extracellular nucleotides.* Nature Neuroscience, 2006. **9**(12): p. 1512-1519.
326. Gelosa, P., et al., *Microglia is a key player in the reduction of stroke damage promoted by the new antithrombotic agent ticagrelor.* Journal of Cerebral Blood Flow & Metabolism, 2014. **34**(6): p. 979-988.

327. Charolidi, N., T. Schilling, and C. Eder, *Microglial Kv1.3 Channels and P2Y12 Receptors Differentially Regulate Cytokine and Chemokine Release from Brain Slices of Young Adult and Aged Mice.* PLoS ONE, 2015. **10**(5): p. e0128463.
328. De Simone, R., et al., *TGF-β and LPS modulate ADP-induced migration of microglial cells through P2Y1 and P2Y12 receptor expression.* Journal of Neurochemistry, 2010. **115**(2): p. 450-459.
329. Kobayashi, K., et al., *P2Y12 Receptor Upregulation in Activated Microglia Is a Gateway of p38 Signaling and Neuropathic Pain.* Journal of Neuroscience, 2008. **28**(11): p. 2892-2902.
330. Amadio, S., et al., *Oligodendrocytes express P2Y12 metabotropic receptor in adult rat brain.* Neuroscience, 2006. **141**(3): p. 1171-80.
331. Amadio, S., et al., *P2Y12 receptor protein in cortical gray matter lesions in multiple sclerosis.* Cereb Cortex, 2010. **20**(6): p. 1263-73.
332. Amadio, S., et al., *P2Y12 Receptor on the Verge of a Neuroinflammatory Breakdown.* Mediators of Inflammation, 2014. **2014**: p. 1-15.
333. Zrzavy, T., et al., *Loss of 'homeostatic' microglia and patterns of their activation in active multiple sclerosis.* Brain, 2017. **140**(7): p. 1900-1913.
334. Diehl, P., et al., *Clopidogrel affects leukocyte dependent platelet aggregation by P2Y12 expressing leukocytes.* Basic Res Cardiol, 2010. **105**(3): p. 379-87.
335. Rudolph, T.K., et al., *Prasugrel as opposed to clopidogrel improves endothelial nitric oxide bioavailability and reduces platelet-leukocyte interaction in patients with unstable angina pectoris: A randomized controlled trial.* Int J Cardiol, 2017. **248**: p. 7-13.
336. Sexton, T.R., et al., *Ticagrelor Reduces Thromboinflammatory Markers in Patients With Pneumonia.* JACC Basic Transl Sci, 2018. **3**(4): p. 435-449.
337. Kim, T.J., et al., *Clopidogrel may decrease the risk of post-stroke infection after ischaemic stroke.* Eur J Neurol, 2019. **26**(2): p. 261-267.
338. Wang, L., et al., *P2 receptor mRNA expression profiles in human lymphocytes, monocytes and CD34+ stem and progenitor cells.* BMC Immunol, 2004. **5**: p. 16.
339. Qin, C., et al., *Critical Role of P2Y12 Receptor in Regulation of Th17 Differentiation and Experimental Autoimmune Encephalomyelitis Pathogenesis.* J Immunol, 2017. **199**(1): p. 72-81.
340. Muniz, V.S., et al., *Purinergic P2Y12 Receptor Activation in Eosinophils and the Schistosomal Host Response.* PLoS One, 2015. **10**(10): p. e0139805.
341. Suh, D.H., et al., *P2Y12 antagonist attenuates eosinophilic inflammation and airway hyperresponsiveness in a mouse model of asthma.* J Cell Mol Med, 2016. **20**(2): p. 333-41.
342. Feng, C., et al., *Adenine nucleotides inhibit cytokine generation by human mast cells through a Gs-coupled receptor.* J Immunol, 2004. **173**(12): p. 7539-47.
343. Ben Addi, A., et al., *Role of the P2Y12 receptor in the modulation of murine dendritic cell function by ADP.* J Immunol, 2010. **185**(10): p. 5900-6.
344. Liao, L., et al., *Immunosuppressive Effect of Ticagrelor on Dendritic Cell Function: A New Therapeutic Target of Antiplatelet Agents in Cardiovascular Disease.* J Biomed Nanotechnol, 2018. **14**(9): p. 1665-1673.
345. Lattin, J.E., et al., *Expression analysis of G Protein-Coupled Receptors in mouse macrophages.* Immunome Res, 2008. **4**: p. 5.
346. Isfort, K., et al., *Real-time Imaging Reveals That P2Y2 and P2Y12 Receptor Agonists Are Not Chemoattractants and Macrophage Chemotaxis to Complement C5a Is Phosphatidylinositol 3-Kinase (PI3K)- and p38 Mitogen-activated Protein Kinase (MAPK)-independent.* Journal of Biological Chemistry, 2011. **286**(52): p. 44776-44787.
347. Liu, O., et al., *Clopidogrel, a platelet P2Y12 receptor inhibitor, reduces vascular inflammation and angiotensin II induced-abdominal aortic aneurysm progression.* PLoS One, 2012. **7**(12): p. e51707.
348. Martinez, F.O., et al., *Transcriptional Profiling of the Human Monocyte-to-Macrophage Differentiation and Polarization: New Molecules and Patterns of Gene Expression.* The Journal of Immunology, 2006. **177**(10): p. 7303-7311.

349. Myrtek, D., et al., *Activation of human alveolar macrophages via P2 receptors: coupling to intracellular Ca2+ increases and cytokine secretion.* J Immunol, 2008. **181**(3): p. 2181-8.
350. Dollt, C.B., K., et al., *The shedded ectodomain of Lyve-1 expressed on M2-like tumor-associated macrophages inhibits melanoma cell proliferation.* Oncotarget, 2017. **8**(61): p. 103682-103692.
351. Komohara, Y., M. Jinushi, and M. Takeya, *Clinical significance of macrophage heterogeneity in human malignant tumors.* Cancer Sci, 2014. **105**(1): p. 1-8.
352. Dollt, C., et al., *The novel immunoglobulin super family receptor SLAMF9 identified in TAM of murine and human melanoma influences pro-inflammatory cytokine secretion and migration.* Cell Death Dis, 2018. **9**(10): p. 939.
353. Schmieder, A., et al., *Synergistic activation by p38MAPK and glucocorticoid signaling mediates induction of M2-like tumor-associated macrophages expressing the novel CD20 homolog MS4A8A.* International Journal of Cancer, 2011. **129**(1): p. 122-132.
354. Schmieder, A., et al., *The CD20 homolog Ms4a8a integrates pro- and anti-inflammatory signals in novel M2-like macrophages and is expressed in parasite infection.* Eur J Immunol, 2012. **42**(11): p. 2971-82.
355. Moore, C.S., et al., *P2Y12 expression and function in alternatively activated human microglia.* Neurol Neuroimmunol Neuroinflamm, 2015. **2**(80).
356. Hohenhaus, D.M., et al., *An mRNA atlas of G protein-coupled receptor expression during primary human monocyte/macrophage differentiation and lipopolysaccharide-mediated activation identifies targetable candidate regulators of inflammation.* Immunobiology, 2013. **218**(11): p. 1345-53.
357. Martinez, F.O. and S. Gordon, *The M1 and M2 paradigm of macrophage activation: time for reassessment.* F1000Prime Reports, 2014. **6**.
358. Lacey, D.C., et al., *Defining GM-CSF- and macrophage-CSF-dependent macrophage responses by in vitro models.* J Immunol, 2012. **188**(11): p. 5752-65.
359. Salmi, S., et al., *The number and localization of CD68+ and CD163+ macrophages in different stages of cutaneous melanoma.* Melanoma Res, 2018.
360. Shaykhiev, R., et al., *Smoking-dependent reprogramming of alveolar macrophage polarization: implication for pathogenesis of chronic obstructive pulmonary disease.* J Immunol, 2009. **183**(4): p. 2867-83.
361. Yang, L., Y. Pang, and H.L. Moses, *TGF-beta and immune cells: an important regulatory axis in the tumor microenvironment and progression.* Trends Immunol, 2010. **31**(6): p. 220-7.
362. Moore, K.W., et al., *Interleukin-10 and the interleukin-10 receptor.* Annu Rev Immunol, 2001. **19**: p. 683-765.
363. Cuenda, A. and S. Rousseau, *p38 MAP-kinases pathway regulation, function and role in human diseases.* Biochim Biophys Acta, 2007. **1773**(8): p. 1358-75.
364. Jimenez-Garcia, L., et al., *Critical role of p38 MAPK in IL-4-induced alternative activation of peritoneal macrophages.* Eur J Immunol, 2015. **45**(1): p. 273-86.
365. Kobayashi, K., et al., *Multiple P2Y subtypes in spinal microglia are involved in neuropathic pain after peripheral nerve injury.* Glia, 2012. **60**(10): p. 1529-39.
366. Bhattacharyya, S., et al., *Macrophage glucocorticoid receptors regulate Toll-like receptor 4-mediated inflammatory responses by selective inhibition of p38 MAP kinase.* Blood, 2007. **109**(10): p. 4313-9.
367. Kadmiel, M. and J.A. Cidlowski, *Glucocorticoid receptor signaling in health and disease.* Trends Pharmacol Sci, 2013. **34**(9): p. 518-30.
368. Vogel, D.Y., et al., *Human macrophage polarization in vitro: maturation and activation methods compared.* Immunobiology, 2014. **219**(9): p. 695-703.
369. Taves, M.D., C.E. Gomez-Sanchez, and K.K. Soma, *Extra-adrenal glucocorticoids and mineralocorticoids: evidence for local synthesis, regulation, and function.* Am J Physiol Endocrinol Metab, 2011. **301**(1): p. E11-24.

370. Rauch, B.H., et al., *Regulation of functionally active P2Y12 ADP receptors by thrombin in human smooth muscle cells and the presence of P2Y12 in carotid artery lesions.* Arterioscler Thromb Vasc Biol, 2010. **30**(12): p. 2434-42.
371. Franklin, R.A., et al., *The cellular and molecular origin of tumor-associated macrophages.* Science, 2014. **344**(6186): p. 921-5.
372. Ferenbach, D. and J. Hughes, *Macrophages and dendritic cells: what is the difference?* Kidney Int, 2008. **74**(1): p. 5-7.
373. Ruffell, B., N.I. Affara, and L.M. Coussens, *Differential macrophage programming in the tumor microenvironment.* Trends Immunol, 2012. **33**(3): p. 119-26.
374. Fabriek, B.O., C.D. Dijkstra, and T.K. van den Berg, *The macrophage scavenger receptor CD163.* Immunobiology, 2005. **210**(2-4): p. 153-60.
375. Martinez, F.O., et al., *Genetic programs expressed in resting and IL-4 alternatively activated mouse and human macrophages: similarities and differences.* Blood, 2013. **121**(9): p. e57-69.
376. Jablonski, K.A., et al., *Novel Markers to Delineate Murine M1 and M2 Macrophages.* PLoS One, 2015. **10**(12): p. e0145342.
377. Barbera-Cremades, M., A. Baroja-Mazo, and P. Pelegrin, *Purinergic signaling during macrophage differentiation results in M2 alternative activated macrophages.* Journal of Leukocyte Biology, 2015. **99**(2): p. 289-299.
378. Lechner, M.G., et al., *Immunogenicity of murine solid tumor models as a defining feature of in vivo behavior and response to immunotherapy.* J Immunother, 2013. **36**(9): p. 477-89.
379. Tozaki-Saitoh, H., et al., *P2Y12 receptors in primary microglia activate nuclear factor of activated T-cell signaling to induce C-C chemokine 3 expression.* J Neurochem, 2017. **141**(1): p. 100-110.
380. Laverty, H.G., et al., *TGF-beta3 and cancer: a review.* Cytokine Growth Factor Rev, 2009. **20**(4): p. 305-17.
381. Wu, H., et al., *The angiogenic responses induced by release of angiogenic proteins from tumor cell-activated platelets are regulated by distinct molecular pathways.* IUBMB Life, 2015. **67**(8): p. 626-633.
382. Zhao, G., et al., *Activation of Epidermal Growth Factor Receptor in Macrophages Mediates Feedback Inhibition of M2 Polarization and Gastrointestinal Tumor Cell Growth.* J Biol Chem, 2016. **291**(39): p. 20462-72.
383. Rigo, A., et al., *Macrophages may promote cancer growth via a GM-CSF/HB-EGF paracrine loop that is enhanced by CXCL12.* Mol Cancer, 2010. **9**: p. 273.
384. Carroll, M.J., et al., *M2 macrophages induce ovarian cancer cell proliferation via a heparin binding epidermal growth factor/ matrix metalloproteinase 9 intracellular feedback loop.* Oncotarget, 2016. **7**(52): p. 86608-86620.
385. Ongusaha, P.P., J.C. Kwak, and A.J. Zwible, *HB-EGF is a potent inducer of tumor growth and angiogenesis.* Cancer Research, 2004. **64**: p. 5283-5290.
386. Stawowczyk, M., et al., *Matrix Metalloproteinase 14 promotes lung cancer by cleavage of Heparin-Binding EGF-like Growth Factor.* Neoplasia, 2017. **19**(2): p. 55-64.
387. Koshikawa, N., et al., *Membrane type 1-matrix metalloproteinase cleaves off the NH2-terminal portion of heparin-binding epidermal growth factor and converts it into a heparin-independent growth factor.* Cancer Res, 2010. **70**(14): p. 6093-103.
388. Kivisaari, A.K., et al., *Matrix metalloproteinase-7 activates heparin-binding epidermal growth factor-like growth factor in cutaneous squamous cell carcinoma.* Br J Dermatol, 2010. **163**(4): p. 726-35.
389. Pahwa, S., M.J. Stawikowski, and G.B. Fields, *Monitoring and Inhibiting MT1-MMP during Cancer Initiation and Progression.* Cancers (Basel), 2014. **6**(1): p. 416-35.
390. Vlodavsky, I. and Y. Friedmann, *Molecular properties and involvement of heparanase in cancer metastasis and angiogenesis.* J Clin Invest, 2001. **108**(3): p. 341-7.
391. Andreasen, P.A., R. Egelund, and H.H. Petersen, *The plasminogen activation system in tumor growth, invasion, and metastasis.* Cell Mol Life Sci, 2000. **57**(1): p. 25-40.

392. Carlson, S., et al., *Cardiac macrophages adopt profibrotic/M2 phenotype in infarcted hearts: Role of urokinase plasminogen activator.* J Mol Cell Cardiol, 2017. **108**: p. 42-49.
393. Hu, J., et al., *uPAR induces expression of transforming growth factor beta and interleukin-4 in cancer cells to promote tumor-permissive conditioning of macrophages.* Am J Pathol, 2014. **184**(12): p. 3384-93.
394. Schroder, W.A., et al., *A physiological function of inflammation-associated SerpinB2 is regulation of adaptive immunity.* J Immunol, 2010. **184**(5): p. 2663-70.
395. Kubala, M.H., et al., *Plasminogen Activator Inhibitor-1 Promotes the Recruitment and Polarization of Macrophages in Cancer.* Cell Rep, 2018. **25**(8): p. 2177-2191 e7.
396. Cooke, N.M., et al., *Aspirin and P2Y12 inhibition attenuate platelet-induced ovarian cancer cell invasion.* BMC Cancer, 2015. **15**(1).
397. Egan, K., et al., *Platelet adhesion and degranulation induce pro-survival and pro-angiogenic signalling in ovarian cancer cells.* PLoS One, 2011. **6**(10): p. e26125.
398. von Kugelgen, I. and A. Wetter, *Molecular pharmacology of P2Y-receptors.* Naunyn Schmiedebergs Arch Pharmacol, 2000. **362**(4-5): p. 310-23.
399. Adrian, K., et al., *Expression of purinergic receptors (ionotropic P2X1-7 and metabotropic P2Y1-11) during myeloid di¡erentiation of HL60 cells.* Biochimica et Biophysica Acta (BBA) - Reviews on Cancer, 2000. **1492**: p. 127-138.
400. Bernhard, M.K. and K. Ulrich, *RT-PCR study of purinergic P2 receptors in hematopoietic cell lines.* Biochemistry (Moscow), 2006. **71**(6): p. 607-611.
401. Chu, H.X., et al., *Role of CCR2 in inflammatory conditions of the central nervous system.* J Cereb Blood Flow Metab, 2014. **34**(9): p. 1425-9.
402. Phillips, R.J., M. Lutz, and B. Premack, *Differential signaling mechanisms regulate expression of CC chemokine receptor-2 during monocyte maturation.* J Inflamm (Lond), 2005. **2**: p. 14.
403. Creery, D., et al., *Differential regulation of CXCR4 and CCR5 expression by interleukin (IL)-4 and IL-13 is associated with inhibition of chemotaxis and human immunodeficiency Virus (HIV) type 1 replication but not HIV entry into human monocytes.* Viral Immunol, 2006. **19**(3): p. 409-23.
404. Pushkareva, M.Y., et al., *Increased cell-surface receptor expression on U-937 cells induced by 1-O-octadecyl-2-O-methyl-sn-glycero-3-phosphocholine.* Cancer Immunol Immunother, 2000. **48**(10): p. 569-78.
405. Lebel-Binay, S., et al., *CD82, member of the tetra-span-transmembrane protein family, is a costimulatory protein for T cell activation.* J Immunol, 1995. **155**(1): p. 101-10.
406. Lebel-Binay, S., et al., *CD82, tetra-span-transmembrane protein, is a regulated transducing molecule on U937 monocytic cell line.* J Leukoc Biol, 1995. **57**(6): p. 956-63.
407. Yeung, L., M.J. Hickey, and M.D. Wright, *The Many and Varied Roles of Tetraspanins in Immune Cell Recruitment and Migration.* Front Immunol, 2018. **9**: p. 1644.
408. Kwon, J.O., et al., *Tetraspanin 7 regulates sealing zone formation and the bone-resorbing activity of osteoclasts.* Biochem Biophys Res Commun, 2016. **477**(4): p. 1078-1084.
409. Sugo, T., et al., *Identification of a lysophosphatidylserine receptor on mast cells.* Biochem Biophys Res Commun, 2006. **341**(4): p. 1078-87.
410. Makide, K., et al., *Novel lysophosphoplipid receptors: their structure and function.* J Lipid Res, 2014. **55**(10): p. 1986-95.
411. Schoneberg, T., et al., *The G protein-coupled receptor GPR34 - The past 20years of a grownup.* Pharmacol Ther, 2018. **189**: p. 71-88.
412. Liebscher, I., et al., *Altered immune response in mice deficient for the G protein-coupled receptor GPR34.* J Biol Chem, 2011. **286**(3): p. 2101-10.
413. Preissler, J., et al., *Altered microglial phagocytosis in GPR34-deficient mice.* Glia, 2015. **63**(2): p. 206-15.
414. Owen, J.L. and M. Mohamadzadeh, *Macrophages and chemokines as mediators of angiogenesis.* Front Physiol, 2013. **4**: p. 159.
415. Gleissner, C.A., P. von Hundelshausen, and K. Ley, *Platelet chemokines in vascular disease.* Arterioscler Thromb Vasc Biol, 2008. **28**(11): p. 1920-7.

416. Schenk, B.I., et al., *Platelet-derived chemokines CXC chemokine ligand (CXCL)7, connective tissue-activating peptide III, and CXCL4 differentially affect and cross-regulate neutrophil adhesion and transendothelial migration.* J Immunol, 2002. **169**(5): p. 2602-10.
417. Finsterbusch, M., et al., *Platelet retention in inflamed glomeruli occurs via selective prolongation of interactions with immune cells.* Kidney Int, 2019. **95**(2): p. 363-374.
418. Rahman, M., et al., *Ticagrelor reduces neutrophil recruitment and lung damage in abdominal sepsis.* Platelets, 2014. **25**(4): p. 257-63.
419. Pace, T.W. and A.H. Miller, *Cytokines and glucocorticoid receptor signaling. Relevance to major depression.* Ann N Y Acad Sci, 2009. **1179**: p. 86-105.
420. Liu, P.W., et al., *P2Y12 and P2Y13 receptors involved in ADPbetas induced the release of IL-1beta, IL-6 and TNF-alpha from cultured dorsal horn microglia.* J Pain Res, 2017. **10**: p. 1755-1767.
421. Pastore, S., et al., *Stimulation of purinergic receptors modulates chemokine expression in human keratinocytes.* J Invest Dermatol, 2007. **127**(3): p. 660-7.
422. Warny, M., et al., *P2Y(6) nucleotide receptor mediates monocyte interleukin-8 production in response to UDP or lipopolysaccharide.* J Biol Chem, 2001. **276**(28): p. 26051-6.
423. Kukulski, F., et al., *Extracellular nucleotides mediate LPS-induced neutrophil migration in vitro and in vivo.* J Leukoc Biol, 2007. **81**(5): p. 1269-75.
424. Ben Yebdri, F., et al., *Concomitant activation of P2Y(2) and P2Y(6) receptors on monocytes is required for TLR1/2-induced neutrophil migration by regulating IL-8 secretion.* Eur J Immunol, 2009. **39**(10): p. 2885-94.
425. Ganbaatar, B., et al., *Ticagrelor, a P2Y12 antagonist, attenuates vascular dysfunction and inhibits atherogenesis in apolipoprotein-E-deficient mice.* Atherosclerosis, 2018. **275**: p. 124-132.
426. Hol, J., L. Wilhelmsen, and G. Haraldsen, *The murine IL-8 homologues KC, MIP-2, and LIX are found in endothelial cytoplasmic granules but not in Weibel-Palade bodies.* J Leukoc Biol, 2010. **87**(3): p. 501-8.
427. Irino, Y., et al., *Akt activation is involved in P2Y12 receptor-mediated chemotaxis of microglia.* J Neurosci Res, 2008. **86**(7): p. 1511-9.
428. Tatsumi, E., et al., *RhoA/ROCK pathway mediates p38 MAPK activation and morphological changes downstream of P2Y12/13 receptors in spinal microglia in neuropathic pain.* Glia, 2015. **63**(2): p. 216-228.
429. Marteau, F., *Involvement of multiple P2Y receptors and signaling pathways in the action of adenine nucleotides diphosphates on human monocyte-derived dendritic cells.* Journal of Leukocyte Biology, 2004. **76**(4): p. 796-803.
430. Vial, E. and C.J. Marshall, *Elevated ERK-MAP kinase activity protects the FOS family member FRA-1 against proteasomal degradation in colon carcinoma cells.* J Cell Sci, 2003. **116**(Pt 24): p. 4957-63.
431. Rajasekaran, S., et al., *Expression profiling of genes regulated by FRA-1/AP-1 transcription factor during bleomycin-induced pulmonary fibrosis.* BMC Genomics, 2013. **14**.
432. Kawamura, H., et al., *Extracellular ATP-stimulated macrophages produce macrophage inflammatory protein-2 which is important for neutrophil migration.* Immunology, 2012. **136**(4): p. 448-58.
433. Liu, C., et al., *Coactivation of the PI3K/Akt and ERK signaling pathways in PCB153-induced NF-kappaB activation and caspase inhibition.* Toxicol Appl Pharmacol, 2014. **277**(3): p. 270-8.
434. Neilson, L.M., et al., *Coactivation of janus tyrosine kinase (Jak)1 positively modulates prolactin-Jak2 signaling in breast cancer: recruitment of ERK and signal transducer and activator of transcription (Stat)3 and enhancement of Akt and Stat5a/b pathways.* Mol Endocrinol, 2007. **21**(9): p. 2218-32.
435. Zhang, X., et al., *Extracellular ADP facilitates monocyte recruitment in bacterial infection via ERK signaling.* Cell Mol Immunol, 2016. **15**(1): p. 58-73.

436. Zerr, M., et al., *Major contribution of the P2Y(1)receptor in purinergic regulation of TNFalpha-induced vascular inflammation.* Circulation, 2011. **123**(21): p. 2404-13.
437. Cardoso, T.C., T.E. Pompeu, and C.L.M. Silva, *The P2Y1 receptor-mediated leukocyte adhesion to endothelial cells is inhibited by melatonin.* Purinergic Signal, 2017. **13**(3): p. 331-338.
438. Hardy, A.R., *P2Y1 and P2Y12 receptors for ADP desensitize by distinct kinase-dependent mechanisms.* Blood, 2005. **105**(9): p. 3552-3560.

# Appendix

## List of Figures

# List of Tables

# List of Abbreviations

| | |
|---|---|
| Ab | antibody |
| ADA | adenosine deaminase |
| ADP | adenosine diphosphate |
| AEC | 3-amino-9-ethylcarbazole |
| Ag | antigen |
| AMP | adenosine monophosphate |
| AMPA | 4-Aminophenylmercuric acetate |
| ANG-2 | angiopoietin |
| AP1 | activator protein 1 |
| APC | antigen-presenting cell |
| APS | ammonium persulfate |
| ARF | alternative reading frame |
| Arg1 | arginase-1 |
| ATP | adenosine triphosphate |
| BAD | Bcl-2 antagonist of cell death |
| Bcl-2 | B cell lymphoma 2 |
| BMDM | bone-marrow derived macrophages |
| BrdU | 5-bromo-2'-deoxy-uridine |
| BSA | bovine serum albumin |
| C5a | complement component 5a |
| CD | cluster of differentiation |
| CDK | cyclin-dependent kinase |
| CNS | central nervous system |
| CSF1 | colony stimulating factor 1 |
| CSF1R | colony stimulating factor 1 receptor |
| CFSE | carboxyfluorescein succinimidyl ester |
| CIAP | calf intestinal alkaline phosphatase |
| CM | conditioned medium |
| COPD | chronic obstructive pulmonary disease |
| COX | cyclooxygenase |
| CTLA4 | cytotoxic T lymphocyte-associated protein 4 |
| CTRL | control |
| DAF-2DA | 4,5-Diaminofluorescein, diacetate |
| DAMP | danger associated molecular patterns |
| DC | dendritic cell |
| dexa | dexamethasone |
| $dH_2O$ | distilled water |
| $ddH_2O$ | double-distilled water |
| DMEM | Dulbecco's Modified Eagle's Medium |
| DMSO | dimethyl sulfoxide |
| DNA | deoxyribonucleic acid |
| dNTP | nucleoside triphosphate |
| EC | endothelial cell |
| ECM | extracellular matrix |
| EDTA | ethylenediaminetetraacetic acid |

| | |
|---|---|
| EF1α | elongation factor 1 α |
| EGF | epidermal growth factor |
| EGM | endothelial cell growth medium |
| ELISA | enzyme-linked immunosorbent assay |
| EMT | epithelial mesenchymal transition |
| ENPP | ectonucleotide pyrophosphatase/phosphodiesterase |
| ENTPD | ectonucleoside triphosphate diphosphohydrolase |
| ERK | extracellular signal regulated kinase |
| EtOH | ethanol |
| EV | empty vector |
| FACS | fluorescence activated cell sorting |
| $F_cR$ | $F_c$ receptor |
| FCS | fetal calf serum |
| FDA | US Food and Drug Administration |
| FFPE | formalin-fixed paraffin embedded |
| FGF | fibroblast growth factor |
| FITC | fluorescein isothiocyanate |
| fMLP | N-Formylmethionyl-leucyl-phenylalanine |
| FOSL1 | FOS like 1 |
| FSC | forward scatter |
| fw | forward |
| GAPDH | glycerinaldehyd-3-phosphat-dehydrogenase |
| GC | glucocorticoid |
| GDP | guanosine diphosphate |
| GM-CSF | granulocyte-macrophage colony stimulating factor |
| GPCR | G protein coupled receptor |
| GPR34 | G protein coupled receptor 34 |
| GRE | glucocorticoid response element |
| GR | glucocorticoid receptor |
| GTP | guanosine triphosphate |
| HB-EGF | heparin-binding epidermal growth factor |
| HCl | hydrogen chlorine |
| HGF | hepatocyte growth factor |
| HIF | hypoxia inducible factor |
| HIV | human immunodeficiency virus |
| HLA-DR | human leucocyte antigen-antigen D related |
| HPF | hydroxyphenyl fluorescein |
| HRP | horse radish peroxidase |
| hs | homo sapiens |
| HUVEC | human umbilical vein endothelial cells |
| ICAM | intercellular adhesion molecule |
| ICC | immunocytochemistry |
| IDO | indolamine-2,3-dioxygenase |
| IF | immunofluorescence |
| IFN | interferon |
| Ig | immunoglobulin |
| IHC | immunohistochemistry |
| IL | interleukin |

| | |
|---|---|
| INK4A | inhibitor of cyclin-dependent kinase 4a |
| iNOS | inducible nitric oxide synthase |
| IRES | internal ribosomal entry site |
| JNK | c-Jun N-terminal kinase |
| KLH | keyhole limpet hemocyanin |
| LB | lysogeny broth |
| LFA-1 | lymphocyte function-associated antigen 1 |
| LLC | Lewis lung carcinoma |
| LPS | lipopolysaccharide |
| LTD4 | leukotriene D4 |
| LTE4 | leukotriene E4 |
| Ly6C | lymphocyte antigen 6 C |
| Lyve-1 | lymphatic vessel endothelial hyaluronan receptor |
| M-CSF | macrophage-colony stimulating factor |
| MACS | magnetic activated cell sorting |
| MAPK | mitogen activated protein kinase |
| MC1R | melanocortin 1 receptor |
| MCP-1 | monocyte chemoattracting protein-1 |
| MCS | multiple cloning site |
| mDC | myeloid DC |
| MDI | M-CSF/dexamethasone/IL-4 |
| MDM | monocyte-derived macrophages |
| MDSC | myeloid derived suppressor cell |
| MFI | median fluorescence intensity |
| MHC | major histocompatibility complex |
| MITF | microphthalmia-associated transcription factor |
| mm | mus musculus |
| M-MDSC | monocytic MDSC |
| MMM | marginal metallophilic macrophages |
| MMP | matrix metalloproteinase |
| MRC1 | mannose receptor C-type 1 |
| mRNA | messenger RNA |
| MS | multiple sclerosis |
| MSH | melanocyte-stimulating hormone |
| MT-MMP | membrane-type matrix metalloproteinase |
| MZM | marginal zone macrophages |
| NEAA | non-essential amino acids |
| NF-κB | nuclear factor κ-light-chain-enhancer of activated B cells |
| NK cell | natural killer cell |
| NO | nitric oxide |
| NOS | nitric oxide synthase |
| ns | not significant |
| OD | optical density |
| P | P2Y12 |
| PAGE | polyacrylamide gelelectrophoresis |
| PAI | plasminogen activator inhibitor |
| PAMP | pathogen associated molecular patterns |
| pBM | peripheral blood monocytes |

| | |
|---|---|
| PBMC | peripheral blood mononuclear cells |
| PBS | phosphate buffered saline |
| PBST | PBS tween |
| PCR | polymerase chain reaction |
| PD1 | programmed cell death 1 |
| pDC | plasmacytoid DC |
| PD-L1 | programmed cell death-ligand 1 |
| PDGF | platelet derived growth factor |
| PFA | paraformaldehyde |
| PGD2 | prostaglandin D2 |
| PGE2 | prostaglandin E2 |
| PI3K | phosphatidylinositol 3-kinase |
| PLC | phospholipase C |
| PMA | phorbol 12-myristate 13-acetate |
| PMN-MDSC | polymorphonuclear MDSC |
| PPBP | pro platelet basic protein |
| PRR | pattern recognition receptor |
| PTEN | phosphatase and tensin homolog |
| puro | puromycin |
| PVDF | polyvinylidenfluorid |
| qRT-PCR | quantitative real-time PCR |
| rev | reverse |
| RFP | red fluorescent protein |
| RFU | relative fluorescence units |
| RNA | ribonucleic acid |
| ROS | reactive oxygen species |
| RT | room temperature |
| SDS | sodium dodecyl sulphate |
| SSC | side scatter |
| STAT | signal transducer and activator of transcription |
| TAE | Tris-acetate-EDTA |
| TAM | tumor-associated macrophages |
| TCR | T cell receptor |
| TEMED | tetramethylethylenediamine |
| TEM | TIE2-expressing macrophages |
| TERT | telomerase reverse transcriptase |
| TGF | transforming growth factor |
| TGS | Tris-Glycine-SDS |
| Th 1 / 2 / 17 | T helper 1 / 2 / 17 |
| TIL | tumor infiltrating lymphocytes |
| TLR | toll-like receptor |
| TNF | tumor necrosis factor |
| TNFSF | tumor necrosis factor superfamily |
| Treg | regulatory T cell |
| TSPAN7 | tetraspanin 7 |
| U | units |
| UDP | uridine diphosphate |
| uPA | urokinase/plasminogen activator |

| | |
|---|---|
| uPAR | urokinase/plasminogen activator receptor |
| UT | untreated |
| UTP | uridine triphosphate |
| UV | ultraviolet |
| VEGF | vascular endothelial growth factor |
| WB | Western blot |
| WT | wild type |

# Acknowledgements

My highest appreciation goes to Prof. Dr. Viktor Umansky for being my first supervisor, for reviewing this thesis and for his excellent scientific advice. The fruitful discussions in the lab meetings not only helped me to broaden my scientific knowledge but also to advance this PhD project.

I would like to express my gratitude to Prof. Dr. Sergij Goerdt for giving me the opportunity to perform my PhD at the Dermatology Department at the UMM and to become a member of the RTG 2099 Hallmarks of Skin Cancer. Joining this RTG enabled me to strengthen my personal and scientific skills and provided an excellent scientific atmosphere.

My sincerest gratitude goes to PD Dr. Astrid Schmieder for the opportunity to perform my PhD in her lab and for being the second supervisor of this thesis. I want to thank her not only for the supervision but also for her encouragement as well as for her constant intellectual, practical and personal support. Astrid, thank you very much for your positive attitude and for always being supportive and motivating.

I would like to thank Prof. Dr. Adelheid Cerwenka for her valuable scientific input during the annual Thesis Advisory Committee meetings.

I would like to thank our London cooperation partner Prof. Dr. Sergio Quezada for giving me the chance to visit his lab at the UCL Cancer Institute in London. There I got the chance to work in an excellent scientific atmosphere, develop new techniques and get in touch with great researchers.

I want to thank Dr. Calin Manta, Dr. Kai Schledzewski, Hilltrud Schönhaber, Jochen Weber and Sayran Arif-Said for their excellent scientific advice and technical assistance.

My warmest thank goes to all the former lab members of AG Schmieder: Claudia Dollt, Andreas Krewer and Susanne Melchers. Thank you for your experimental and personal support, I really enjoyed working with you.

I would like to thank all the current and former members of the Umansky lab for their experimental help, the lively scientific discussions and for always being supportive.

Of course, I also want to thank all my colleagues from AG Goerdt and AG Geraud for the pleasant working atmosphere as well as for their practical support.

My deepest thank goes to my colleagues Sina Kürschner, Theresa Staniczek, Bianca Dietsch, Celine Weller, Calin Manta, Verena Häfele and Ana Olsavszky. I really had a wonderful time with you. Thank you, guys, for your open ears, for the laughter we shared and for the funny times we spent together, not only at work but also outside work. Without you it wouldn't have been the same. Thank you for not only being colleagues but for becoming friends!

Thank you Sina for always offering a place to sleep, for being so welcoming, lovely and positive. I really enjoyed spending time with you!

My deepest gratitude goes to my family who has always believed in me and constantly supported and encouraged me. Mum, Dad, Leni, Alex and Isabella, I love you!